LATE HOLOCENE ENVIRONMENTAL RECONSTRUCTIONS USING POLLEN: FROM MORPHOLOGICAL SPECTRA TO STABLE ISOTOPES

Doctoral thesis
submitted in fulfilment of the
requirements for the academic degree
Doctor rerum naturalium (Dr. rer. nat.)
to the Department of Earth Sciences of the
FREIE UNIVERSITÄT BERLIN

by
M.Sc.
Carolina Müller

Berlin, June 2020

1^{st} **Reviewer:** **Prof. Dr. Frank Riedel**
Freie Universität Berlin

2^{nd} **Reviewer:** **Prof. Dr. Ulrich Struck**
Museum für Naturkunde Berlin
& Freie Universität Berlin

Date of defence: 08. September 2020

Abstract

Pollen are widespread and abundant microspores that are resistant against decay. Their frequent appearance in climate archives gives the opportunity to study vegetation cover changes and past environmental characteristics. Morphology-based pollen analysis focus on the taxonomic identification of pollen grains extracted out of sediment cores or other archives. The prime advantage of this approach is a worldwide applicability enabling temperature and precipitation reconstructions through quantitative methods. Stable isotope analysis is another approach using pollen in climate studies. Due to the immediate physiological responses of plants to environmental change, isotope values of pollen potentially provide high-resolution palaeoclimate information. Because this method for studying environmental changes is still in the need of a general assessment of its spectrum of applicability and limitations, this thesis focusses mainly on preliminary investigations of species-specific pollen-isotope variability and applicability in environmental studies.

A case study of climate and vegetation reconstruction on the north-eastern Qinghai-Tibetan Plateau using classical morphology-based palynology is included in this dissertation as a first research topic. Pollen assemblages extracted out of the Daotang Pond record reveal environmental changes over the last 1200 years. The Medieval Warm Period occurred on the Qinghai-Tibetan Plateau between CE 850 and 1400. This climate anomaly was accompanied by regular East Asian Summer Monsoon penetrations and moisture input from the eastern lowland. Dry spells with diminished precipitation during the Medieval Warm Period are detectable out of the deposited pollen assemblages, but they have not been as severe as reported from other regions on the Qinghai-Tibetan Plateau. This is most likely caused by a humid micro-climate in the vicinity of the Qinghai Lake drainage basin. Features of the Little Ice Age (CE 1450 to 1950) can also be traced by analysing the pollen assemblages of the samples. Although the Little Ice Age is characterized by a weakened East Asian Summer Monsoon, the pollen record does not display a particularly dry environment during this time period, probably due to generally lower temperatures and diminished evapotranspiration. However, long distance transport of pollen is known

to falsify pollen assemblages and its impact on the reconstruction of past environmental conditions cannot be ruled out. Additionally, the Qinghai-Tibetan Plateau is a pastoral region and its vegetation composition has been affected by grazing herds, diminishing the climate information which can be drawn from a quantitative morphology-based pollen analysis.

The second part of this dissertation focusses on comprehensive investigations about species-specific isotope variability of modern pollen to promote the application of isotope analysis of fossil pollen in palaeoclimate reconstructions. Modern pollen of nine abundant tree species were sampled during the consecutive vegetation periods of 2015 and 2016 in seven national and nature parks in central and northern Europe. The investigation of various non-climate impact factors on the pollen-isotopes helps to assess sampling strategies in future studies and supports the interpretation of fossil pollen-isotope values. The results suggest that each species has specific δ^{13}C and δ^{18}O patterns and ranges within their pollen-isotope values and their spectra reveal gradients between maritime and continental study sites. The altitudinal effect, an increase in the isotope values with elevation, can be traced within the δ^{13}C but not within the δ^{18}O values of *Picea abies* pollen. The $\delta^{13}C_{pollen}$ and $\delta^{18}O_{pollen}$ values of broad-leaved species flowering before leaf proliferation (January to March) were significantly lower than the isotope values of broad-leaved trees flowering later in spring (April to May). Pollen-isotope values of early flowering species are believed to reflect environmental conditions of the previous autumn and winter, whereas the isotope values of spring-flowering species reflect conditions of the ongoing season after the reoccurrence of growth. These findings indicate, that seasonal weather reconstructions using pollen-isotope values of different species are feasible. Pollen-isotope values of all species varied within the sampling sites. They even varied significantly between different flower positions on a tree and also within single branches. The circumferential variability within trees was up to 3.5‰ for $\delta^{13}C_{pollen}$ and 2.1‰ for $\delta^{18}O_{pollen}$. Species-specific pollen-isotope variation between the two consecutive years was on average 1.0‰ for δ^{13}C and 1.6‰ for δ^{18}O and oxygen pollen-isotopes even changed significantly during the last stages of pollen maturation. Regarding palaeoclimate investigations, these results emphasize the need for a taxonomic separation of fossil pollen and the analysis of a sufficient amount of pollen material to avoid interpretation errors due to outliers caused by flowering positions or an unusual origin of the pollen.

A chemical purification protocol of modern and fossil pollen samples needs to be established to advance reproducibility of the analytical results when fossil pollen-isotopes

are used to reconstruct climate conditions. Therefore, the impact of four chemicals on the $\delta^{13}C$ and $\delta^{18}O$ values of modern pollen sampled from eight abundant tree species were assessed and evaluated. The results suggested species-specific alterations of the pollen-isotope values. Potassium hydroxide, hydrofluoric acid and sodium hypochlorite alter the carbon and oxygen isotope values of pollen to an assessable degree and therefore their usage to purify pollen samples can be rated as unproblematic in future palaeoclimate studies. The application of sulfuric acid on the other hand should generally be avoided, because the chemical alters the $\delta^{13}C_{pollen}$ and $\delta^{18}O_{pollen}$ values with a highly variable offset.

The outcome of the comprehensive research on pollen-isotope variability and influencing factors is a contribution towards a regular usage of stable isotope analysis of pollen in palaeoecological investigations. Open research questions on the topic of amplifying pollen-isotope analysis in palaeoclimate research remain. An actual application of the method requires additional analytical tests, in particular an improved separation technique to extract fossil pollen using a minimal amount of chemicals. Also, the determination of important climatological impact factors defining the carbon and oxygen isotope values of pollen is necessary. The possibility to use multiple approaches of fossil pollen to reconstruct climate conditions of the past is valuable and worthy of further intensive investigations.

Kurzfassung

Pollen sind weit verbreitete, zahlreich vorhandene und sehr resistente Mikrosporen. Ihr häufiges Auftreten in Klimaarchiven bietet die Möglichkeit, Veränderungen der Vegetationsdecke und vergangene Umweltmerkmale zu untersuchen. Morphologie-basierte Pollenanalysen konzentrieren sich auf die taxonomische Identifizierung von Pollenkörnern, die aus Sedimentbohrkernen oder anderen Archiven extrahiert wurden. Der Hauptvorteil dieses Ansatzes ist eine weltweite Anwendbarkeit, die verlässliche Temperatur- und Niederschlagsrekonstruktionen durch etablierte quantitative Methoden ermöglicht. Die Analyse stabiler Isotope ist ein weiterer Ansatz, bei dem Pollen in Klimastudien verwendet werden können. Aufgrund der unmittelbaren physiologischen Reaktionen von Pflanzen auf Umweltveränderungen können Isotopenwerte von Pollen hochauflösende Paläoklimainformationen liefern. Da diese neuere Methode zur Untersuchung von Umweltveränderungen noch einer generellen Einschätzung ihres Anwendungsspektrums und ihrer Grenzen bedarf, konzentriert sich diese Arbeit hauptsächlich auf Voruntersuchungen zur artspezifischen Pollenisotopenvariabilität und Anwendbarkeit in Umweltstudien.

Eine Fallstudie zur Klima- und Vegetationsrekonstruktion auf dem Qinghai-Tibetischen Plateau unter Verwendung der klassischen Morphologie-basierten Palynologie ist als erstes Forschungsthema in dieser Dissertation enthalten. Die wechselnde Zusammensetzung der Pollentypen, die aus den Proben des Daotang Ponds extrahiert wurden, zeigen die Umweltveränderungen der letzten 1200 Jahre auf dem nord-östlichen Qinghai-Tibetischen Plateau. Die mittelalterliche Warmzeit fand in der Region zwischen 850 und 1400 n. Chr. statt. Diese Klimaanomalie ist am Daotang Pond gekennzeichnet von regelmäßigen Einbrüchen des ostasiatischen Sommermonsuns und Feuchtigkeitseinträgen aus dem östlichen Tiefland. Trockenperioden mit vermindertem Niederschlag während des mittelalterlichen Klimaoptimums sind aus den abgelagerten Pollenansammlungen nachweisbar, aber sie waren nicht so schwerwiegend wie in anderen Regionen auf dem Qinghai-Tibetischen Plateau, was vermutlich auf ein bestehendes feuchtes Mikroklima durch den nahegelegenen Qinghai See zurückzuführen ist. Die Kleine Eiszeit (1450 bis 1950 n. Chr.) kann

auch durch die Morphologie-basierte Analyse der Pollenansammlungen in den Daotang Proben zurückverfolgt werden. Obwohl die Kleine Eiszeit durch einen abgeschwächten ostasiatischen Sommermonsun gekennzeichnet ist, zeigt der Pollenflug in diesem Zeitraum keine besonders trockene Umgebung. Vermutlich war in der Region aufgrund allgemein niedrigerer Temperaturen auch die Evapotranspiration deutlich vermindert. Es ist jedoch bekannt, dass der Langstreckentransport von Pollen die Pollenansammlungen verfälscht, und sein Einfluss auf die Rekonstruktion vergangener Umweltbedingungen kann nicht ausgeschlossen werden. Darüber hinaus ist das Qinghai-Tibetische Plateau eine Hirtenregion und die Vegetationszusammensetzung wurde stark durch weidende Herden beeinträchtigt, wodurch die Klimainformationen, die aus einer quantitativen Morphologie-basierten Pollenanalyse gewonnen werden können, vermindert sind.

Der zweite Teil dieser Dissertation konzentriert sich auf umfassende Untersuchungen zur artspezifischen Isotopenvariabilität moderner Pollen, um die Anwendung der Isotopenanalyse fossiler Pollen bei Paläoklima-Rekonstruktionen zu fördern. In sieben National- und Naturparks in Mittel- und Nordeuropa wurden während zwei aufeinanderfolgender Vegetationsperioden 2015 und 2016 moderne Pollen von neun weit verbreiteten Baumarten beprobt. Die Untersuchung verschiedener nicht-klimatischer Einflussfaktoren auf die Pollenisotope hilft bei der Beurteilung von Beprobungsstrategien in zukünftigen Studien und unterstützt die Interpretation der Isotopenwerte fossiler Pollen. Die Ergebnisse deuten darauf hin, dass jede Art spezifische δ^{13}C- und δ^{18}O-Muster und Spannweiten innerhalb ihrer Pollenisotopenwerte aufweist und ihre Spektren zeigen Gradienten zwischen maritimen und kontinentalen Untersuchungsgebieten. Der Höheneffekt, eine Zunahme der Isotopenwerte mit der Höhe über NN, kann innerhalb der δ^{13}C-, aber nicht innerhalb der δ^{18}O-Werte von *Picea abies* Pollen nachgewiesen werden. Die $\delta^{13}C_{pollen}$- und $\delta^{18}O_{pollen}$-Werte von Laubbaumarten, die vor dem Blattaustrieb blühten (Januar bis März), waren signifikant niedriger als die Isotopenwerte von Laubbäumen, die später im Frühjahr blühen (April bis Mai). Man geht davon aus, dass die Pollenisotopenwerte früh blühender Arten die Umweltbedingungen des vorangegangenen Herbstes und Winters widerspiegeln, während die Isotopenwerte anderer Arten die Bedingungen der laufenden Saison nach dem Wiederauftreten des Wachstums aufzeigen. Diese Ergebnisse deuten darauf hin, dass saisonale Wetterrekonstruktionen mit den Pollenisotopenwerten verschiedener Arten durchführbar sind. Die Pollenisotopenwerte aller Arten variierten innerhalb der Sammelorte, und sie variierten auch signifikant zwischen verschiedenen Blütenpositionen an einem Baum und sogar innerhalb eines einzelnen Zweiges. Die zirkum-

ferentielle Variabilität betrug bis zu 3.5‰ für $\delta^{13}C_{pollen}$ und 2.1‰ für $\delta^{18}O_{pollen}$. Die artenspezifische Pollenisotopenvariation zwischen den beiden aufeinanderfolgenden Jahren betrug durchschnittlich 1.0‰ für $\delta^{13}C$ und 1.6‰ für $\delta^{18}O$ und die Sauerstoffisotopenwerte änderten sich sogar signifikant während der letzten Stadien der Pollenreifung in der Blüte. Im Hinblick auf paläoklimatische Untersuchungen unterstreichen diese Ergebnisse die Notwendigkeit einer taxonomischen Trennung fossiler Pollen und der Analyse einer ausreichenden Menge an Pollenmaterial, um Interpretationsfehler als Folge von Ausreißern aufgrund der Blühposition oder einer ungewöhnlichen Herkunft der Pollen zu vermeiden.

Ein standardisiertes chemisches Aufbereitungsprotokoll für moderne und fossile Pollenproben ist notwendig um die Reproduzierbarkeit der analytischen Ergebnisse zu verbessern, wenn fossile Pollenisotope zur Rekonstruktion der Klimabedingungen verwendet werden. Daher wurden die Auswirkungen von vier Chemikalien auf die $\delta^{13}C$- und $\delta^{18}O$-Werte moderner Pollenproben von acht häufig vorkommenden Baumarten untersucht und bewertet. Die Ergebnisse deuteten auf artspezifische und substanzspezifische Veränderungen der Pollenisotopenwerte hin. Kaliumhydroxid, Flusssäure und Natriumhypochlorit verändern die Kohlenstoff- und Sauerstoffisotopenwerte von Pollen in einem abschätzbaren Maße, sodass ihre Verwendung zur Aufbereitung von Pollenproben in zukünftigen Paläoklimastudien als unproblematisch eingestuft werden kann. Der Einsatz von Schwefelsäure hingegen sollte generell vermieden werden, da die Chemikalie die $\delta^{13}C_{pollen}$- und $\delta^{18}O_{pollen}$-Werte mit einem sehr variablen Offset verändert.

Das Ergebnis der umfangreichen Forschung zur Pollen-Isotopenvariabilität und zu deren Einflussfaktoren ist ein Beitrag zu der zukünftigen etablierten Anwendung der stabilen Isotopenanalyse von Pollen in paläoökologischen Untersuchungen. Offene Forschungsfragen zur Pollenisotopenanalyse in der Paläoklimaforschung bleiben bestehen. Eine tatsächliche Anwendung der Methode erfordert zusätzliche analytische Tests, insbesondere eine verbesserte Trenntechnik zur Extraktion fossiler Pollen mit einem minimalen Chemikalieneinsatz. Auch die Bestimmung wichtiger klimatologischer Einflussfaktoren, die die Kohlenstoff- und Sauerstoffisotopenwerte von Pollen definieren, ist notwendig. Die Möglichkeit, mehrere Methoden zur Analyse fossiler Pollen für eine Rekonstruktion von Klimabedingungen anwenden zu können, ist wertvoll. Daher verdient das Vorranbringen der Pollenisotopie-Methode weitere intensive Untersuchungen.

Acknowledgements

Many colleagues, friends and family members supported me along the way of gaining my PhD and I would like to express my gratitude to them. First of all, my very special thanks go to my supervisor Prof. Dr. Frank Riedel (FU Berlin). I benefitted from his support in many ways and I am grateful for all the advice, encouraging words, constructive feedback and his novel and insightful ideas of tackling various research questions. I would also like to thank Dr. Gerhard Helle (GFZ Potsdam) for his valuable ideas and contributions to the success of the pollen-isotope project and additionally on conducting the pollen-isotope measurements and his great support during analysis and interpretation.

Many thanks go to Dr. Manja Hethke (FU Berlin) and Prof. Dr. Pavel Tarasov (FU Berlin) for constructive discussions, encouragement, critical assessment and valuable suggestions of improvement on my manuscripts. I also like to thank Dr. Georg Stauch (RWTH Aachen) and Dr. Birgit Plessen (GFZ Potsdam), who both have helped me in many ways, personally and scientifically, during the completion of this thesis. I am also very thankful for the support of Franziska Pritzke (HU Berlin), Alena Zippel (UP), Julian Hennig (FU Berlin), Vanessa Skiba (FU Berlin) and Hendrik Schultz (HU Berlin), who helped with the fieldwork and contributed to the general knowledge of pollen-isotopes by writing their bachelor or master thesis in the pollen-isotope project. Also, Robert Wiese and Maike Glos supported me with the laboratory work and Jan Evers helped relentlessly with professional figures for the publications, thanks!

Many thanks go to other colleagues and friends of the institute, especially to Mareike Schmidt, Franziska Slotta, Steffi Hildebrandt and Kim Kühne, for many chats, celebrations and hilarious lunch breaks.

I am utmost grateful for the support of my family. My parents, who stood by my side in all moments while finishing my dissertation, Ludo and my greatest joy Phineas, who was not particularly helpful in finishing my PhD, but owns the most important place in my heart.

Contents

List of Figures

List of Tables

Chapter 1

Introduction

1.1 Pollen as a proxy for environmental reconstruction

Palynology, the study of organic microfossils found in geological archives, can provide information about past vegetation cover changes and palaeoclimate patterns (Birks and Birks, 1980; Traverse, 2007). Pollen grains are highly resistant palynomorphs, protected against decay by a strong outer pollen wall (e.g. Faegri *et al.*, 1989; Moore *et al.*, 1991). They have been deposited in sediments dating back millions of years and the approach can be applied in most regions worldwide (e.g. Traverse, 2007; Speer, 2010). Conventional palynological studies are based on the accuracy of identifying fossilized pollen grains and assigning family, genus or even species affiliation (Figure 1.1). Due to the high resistance of the outer pollen wall, morphological characteristics are at least partially preserved in fossil archives (Seppä and Bennett, 2003). The identification of the affiliation allows conclusions to be drawn about typical environmental traits of the host plant and thus facilitates inferences about environmental changes in the past (Traverse, 2007). The interpretation of fossil pollen assemblages is often supported by the modern analogue technique (Delcourt and Delcourt, 1985) and the biomization method (Prentice *et al.*, 1996), both quantitative approaches that compare fossil to modern pollen spectra and assign the knowledge gained through the investigation of modern plant communities to palaeoenvironments. Another frequently used quantitative method is the determination of the ratio of *Artemisia* to Chenopodiaceae pollen. This method enables the reconstruction of the predominance of either desert or steppe environments in semi arid Central Asia and thus holds information about long term precipitation amounts (El-Moslimani, 1990). Analysing and comparing pollen assemblages out of fossil sediment samples can thus provide references to different climate environmental parameters, but most reliably to local summer temperatures and

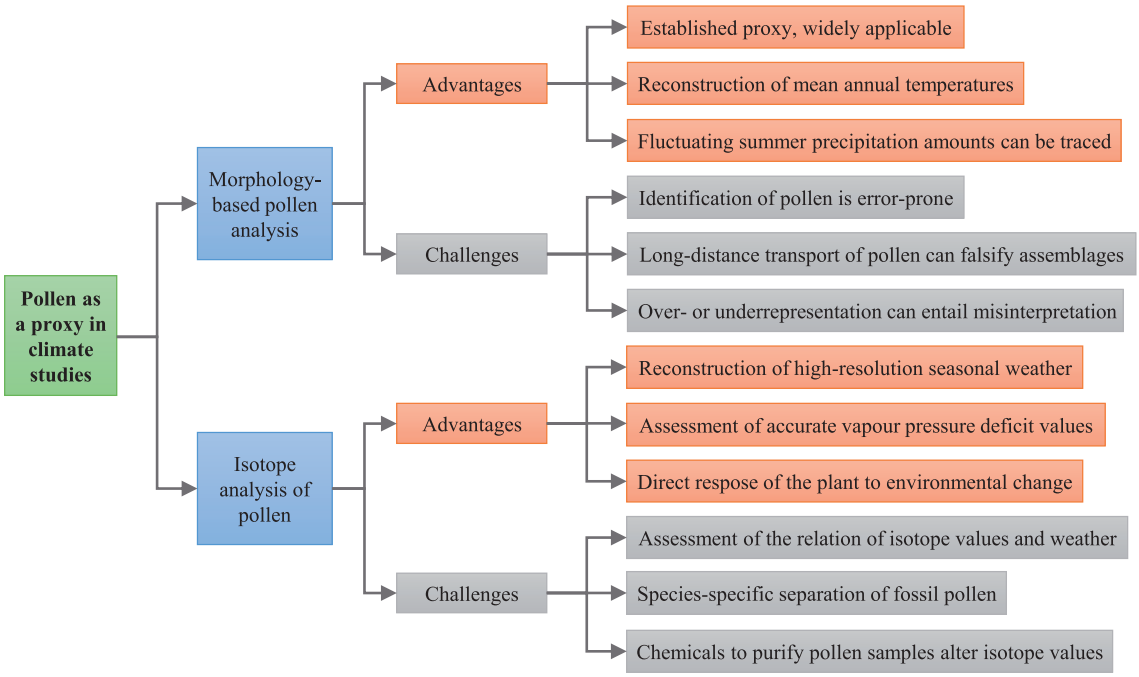

Figure 1.1: Flowchart showing ways to use pollen as a proxy in climate studies. Most important advantages and challenges of the two usage approches morphology-based palynology and stable isotope analysis of pollen, are visualised in grey and red.

annual precipitation amounts (Traverse, 2007). However, morphology-based methods are vulnerable to errors on numerous levels (Figure 1.1). The identification of fossilized pollen grains is rarely feasible up to the species level, especially if the pollen wall is decomposed, which may hinder the reconstruction of more specific climate factors (Schwarz, 2016). Long-distance transport of pollen can falsify the interpretation of the local vegetation composition and over- or under-representation of pollen types may lead to a misinterpretation of the environmental conditions. Additionally, the resolution of sediment samples is often low and a time lack between climatic changes and the actual vegetation response might be problematic, especially when reconstructions with a very high-resolution are desired (Loader and Hemming, 2000).

Another pollen-based method to reconstruct past environmental changes is the relatively new approach of stable carbon and oxygen isotope analysis of pollen (Bell, 2018). In general, plant material, such as leaf tissue, tree-rings and pollen is directly connected to ongoing climate parameters through the process of photosynthesis (Loader and Hemming, 2000). Stable relationships between isotope values of plant tissue and various environmental parameters, e.g. temperature and drought indexes, have been recognized and allow climate reconstructions using isotope ratios (e.g. Saurer and Siegenthaler 1989; Walcroft *et al.*, 1997; Bell *et al.*, 2019). This approach's prime advantage is its potential for reconstructions on a high-resolution time scale due to the direct response of the plant to changes

in the environment (Figure 1.1). Even short-term events, which may not affect the general vegetation composition and are therefore not be traceable by traditional palynological methods, can be recorded in the isotope values of plant tissue and pollen. Also, the reconstruction of seasonal temperatures and precipitation amounts is possible by analysing pollen of species with different flowering periods. In general, a species-specific analysis of the pollen-isotope values enables detailed environmental reconstructions, as long as the relationship of the pollen-isotopes of the modern analogue (the species or closely related genus) with the the environment has already been examined. Due to the significantly different $\delta^{13}C_{pollen}$ values of plants with C3 and C4 photosynthetic pathways, isotope analysis of bulk pollen samples from one plant community can easily provide information about the aridness of the environment (Nelson *et al.*, 2006; Descolas-Gros and Schölzel, 2007; Urban *et al.*, 2016). For a routine application of pollen-isotope analysis in climate research the approach is still in need of basic research about the impact of climate and non-climate factors on the isotope values (Schwarz, 2016).

The key priority is still the understanding of the species-specific response to environmental changes and the linkage of the pollen-isotope values to actual weather conditions during plant growth and pollen maturation (Bell, 2018). Besides the necessity of basic research, technical procedures for the isotope analysis of fossil pollen require improvements (Figure 1.1). Current sample preparation methods involve a manual separation of pollen grains at the lowest possible taxonomic affiliation level, which is very labor-intensive. (Bell *et al.*, 2017). Additionally, fossil samples need to be treated chemically to purify the pollen from sediment and other debris. Due to a variety in origin and constitution, different fossil samples require different treatment protocols and chemicals. Therefore, standardisation of protocols is mandatory to enable accurate comparisons across different studies.

1.2 Research framework and motivation

This doctoral thesis is a combination of two scientific approaches that use pollen as a proxy in palaeoclimate investigations and are designed to answer similar research questions regarding past environmental change, each with its own significant advantages and limitations (Figure 1.1). Morphology-based pollen analysis is already an established approach, whereas pollen-isotope analysis, which is more suited to answer questions regarding a direct and high-resolution response of the plant to environmental changes, is still new. The need for a better understanding of the interaction between climate and the isotope values

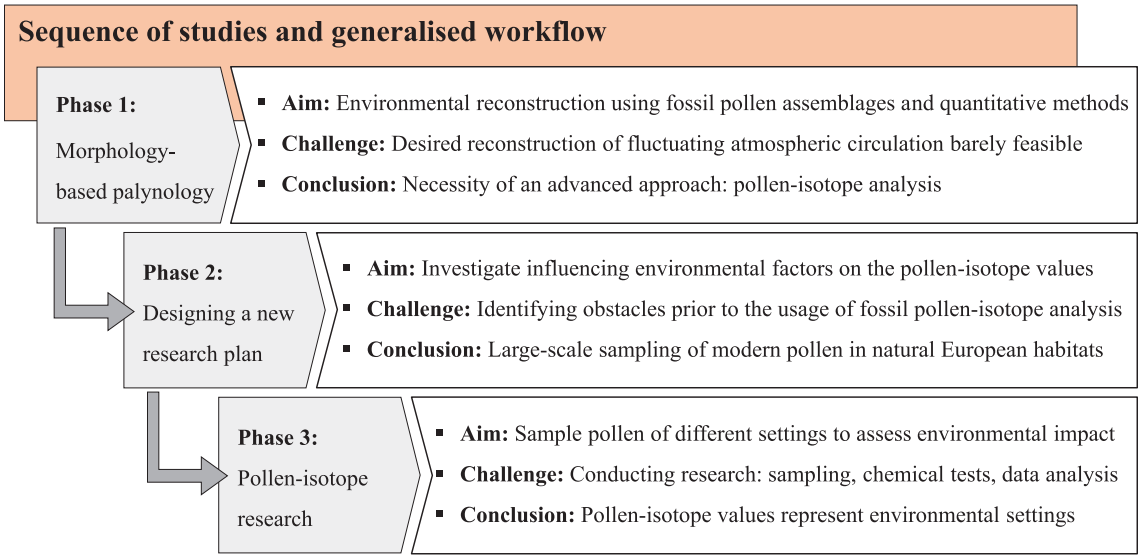

Figure 1.2: Overview of the sequence of studies and research framework consisting of three separate research phases. The generalised workflow of each phase contains the aim, challenges and drawn conclusion of the research episode.

of pollen lead to designing a research plan that aimed at advancing the general knowledge about pollen-isotopes and their application in climate and palaeoecological studies (Figure 1.2).

The first part of the research workflow contains a morphology-based palynological study. Challenges that occurred during the research lead to the conclusion that advanced analyses are necessary to cover upcoming research questions regarding high-resolution environmental changes and fluctuations within the source of moisture. Therefore, another research plan was designed (Figure 1.2, phase 2; Figure 1.3). The newly designed research plan contains preparative thoughts about conducting comprehensive pollen-isotope investigations by the identification of missing knowledge and possible obstacles prior to the actual study (Figure 1.4). The last step (Figure 1.2) of the research workflow (phase 3) is to conduct comprehensive pollen-isotope research, including sampling, measuring and interpreting isotope data as well as methodological improvements of chemical preparation protocols prior to pollen-isotope analysis. This comprehensive research is done as a first contribution towards an intensive amplification of the application of pollen-isotopes in palaeoclimate studies.

1.2.1 Morphology-based palynological study at Daotang Pond, China

The classic morphology-based palynological approach (Figure 1.2) is applied as a case study of climate and vegetation reconstruction of the past 1200 years on the northeastern Qinghai-Tibetan Plateau (QTP). It is a contribution to comprehensive research projects of the palaeontological working group of the FU Berlin aiming for many years to advance knowledge about the climate history in Central Asia (e.g. Demske *et al.*, 2009; Taft *et al.*, 2012; Leipe *et al.*, 2014). The study site Daotang Pond is situated on the Eastern margin of the QTP (36°57'35.4 N, 100°74'48.4 E; Figure 2.1, *pp.* 24). Contemporary climate at the site is characterised by a high seasonality with summer rainfall and semi-arid climate conditions (Coleman *et al.*, 2007; An *et al.*, 2012; Liu *et al.*, 2015). The aim of this study was to reconstruct high-resolution temperature and precipitation changes using the morphology-based palynological approach. Changes within the vegetation composition roughly every 20 years are assessed and quantitative methods, e.g. the *Artemisia*/Chenopodiaceae ratio, support the reconstruction of long-term moisture input (Figure 1.2). In the study area, climate and vegetation are frequently impacted by alternating dominance of atmospheric forcing: the East Asian Summer Monsoon (EASM), the Indian Summer Monsoon (ISM), the Asian Winter Monsoon (AWM) and the Westerly Winds (Figure 2.1; Wischnewski *et al.*, 2011) and in general, the QTP environment is sensitive to short term shifts within these atmospheric forcing systems (Zan *et al.*, 2015).

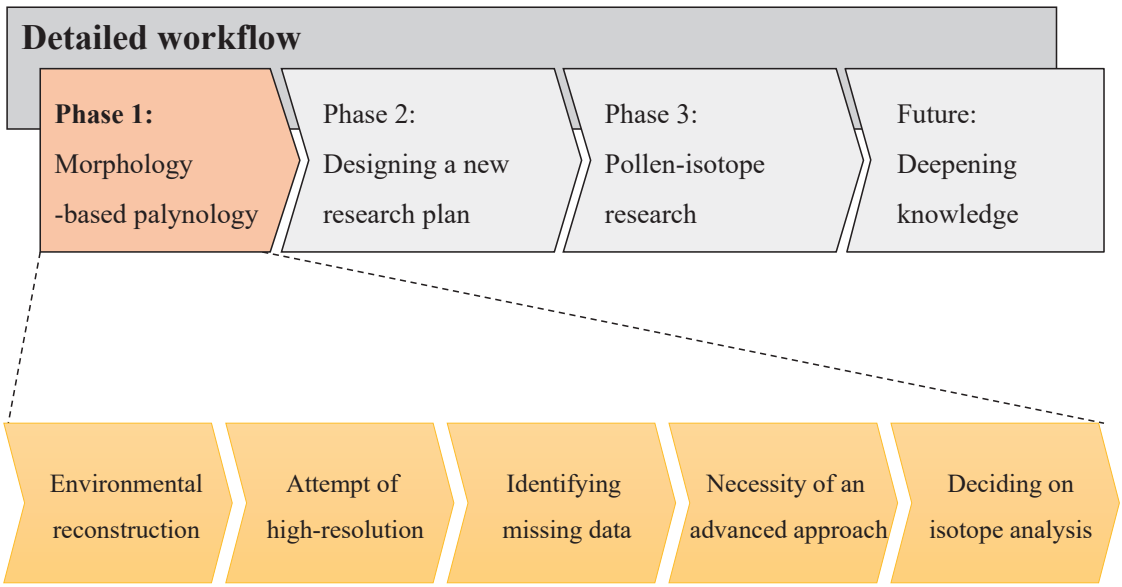

Figure 1.3: Detailed workflow of research phase 1: morphology-based palynology. This phase contains the application of classic palynology and quantitative methods for environmental reconstruction. The attempt to reconstruct high-resolution climate fluctuations on the northeastern Qinghai-Tibetan Plateau lead to identifying uncertainties in the outcome of the research and the realisation of the necessity of an advanced method to answer desired research questions.

Nowadays, the expansion of the critical rainfall boundary (400 mm) lies roughly within the region of Daotang Pond (New *et al.*, 2002). However, fluctuations of monsoonal strength are common and summer precipitation is particularly important for the dry mountainous region of the QTP. Thus, understanding and predicting these shifts is crucial for many people living in the vicinity of the plateau.

High-resolution pollen analysis on the QTP can provide information about sudden changes of intensity within the predominant wind system (Herzschuh, 2006). However, if the strength of the EASM and ISM are similar, quantitative pollen analysis cannot reveal the source of the summer rainfall. Thus, aiming a more detailed reconstruction of the predominant wind system requires other or additional analytical techniques (Figure 1.3, 1.4). Isotope analysis of various proxy records investigating the climate history of the Tibetan Plateau are available on a high-resolution: e.g. tree ring analysis (Yang *et al.*, 2014), ice core records (Thompson *et al.*, 1997), speleothem analysis (Zhang *et al.*, 2008), isotope analysis of mollusk shells (Taft *et al.*, 2013) and isotope hydrology (Henderson *et al.*, 2010). Stable carbon and oxygen isotopes in plant tissue are newly incorporated on a yearly basis through plant physiological processes during plant growth (section 1.4). Hence, stable isotope analysis of pollen may open possibilities within the field of revealing the climate histories of the Tibetan Plateau and elsewhere. The desire to answer questions about the vegetation changes of the QTP more fully lead to explore and evaluate the second approach: stable isotope analysis of pollen.

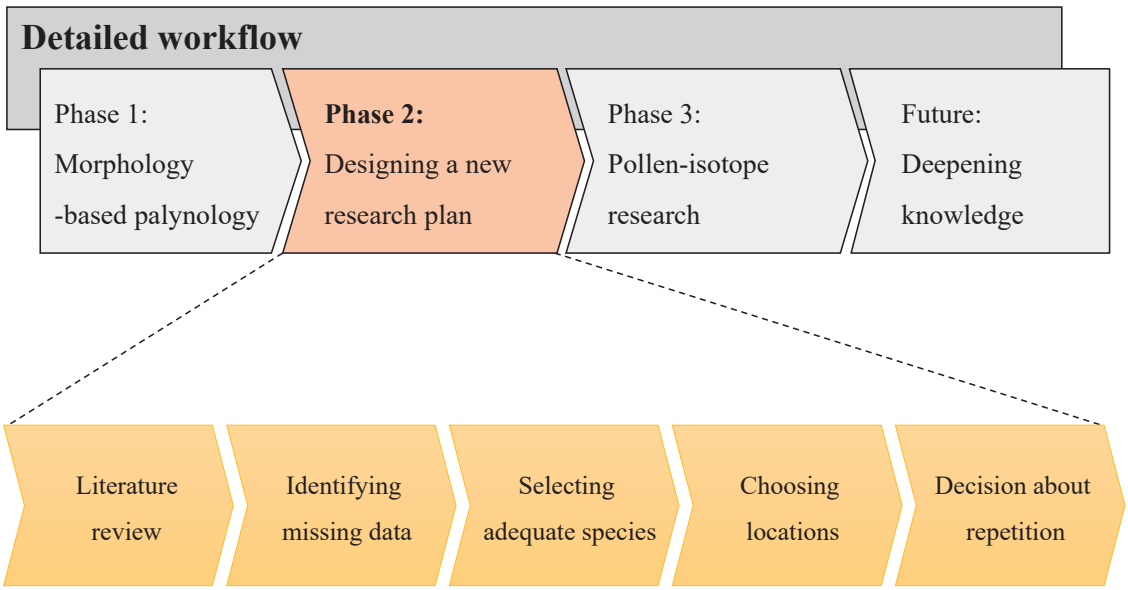

Figure 1.4: Detailed workflow of research phase 2: designing an advanced research plan. Preparations prior to conducting research on pollen-isotope variability include literature review, identifying missing knowledge, the selection of investigated species and locations and the decision about repetitions of sampling.

1.2.2 Stable isotope analysis of pollen from European nature parks

The second part of this thesis contains the advancement of stable carbon and oxygen isotope analysis of pollen as another proxy for palaeoclimate reconstructions. This approach is a new method for studying high-resolution environmental change and is still in the need of a general assessments of its spectrum of applicability and limitations (Figure 1.4). Intensive investigations of the impact of various climate and non-climate environmental parameters on the pollen-isotope values need to be executed, since reference values of modern pollen-isotopes are mandatory to interpret fossil pollen-isotope values. These climate and non-climate parameters are, for example, temperatures during pollen formation, precipitation amounts and vapor pressure deficit, location of the individual tree within a forest (availability of water and surrounding vegetation composition), the type of soil, slope angle of the forest ground, maturity of the inflorescence during the time of sampling and general effect of the geographic location, a combination of longitude, latitude and altitude.

A few general investigations about modern carbon and oxygen pollen-isotope spectra of different species have already been conducted (e.g. Amundson *et al.*, 1997; Jahren, 2004; Loader and Hemming, 2004; King *et al.*, 2012; Schwarz, 2016) and the values of modern pollen-isotopes have also successfully been linked to ongoing environmental traits, such as moisture availability (Bell *et al.*, 2017) and temperature during pollen formation (Loader and Hemming, 2002). However, knowledge about spectra, species and temporal variability of modern pollen-isotopes is still limited (Schwarz, 2016) and due to that, only very few studies using fossil pollen-isotopes to infer past climate conditions are available (e.g. Urban *et al.*, 2016; Bell *et al.*, 2019). Additionally, since the structure and composition of a pollen grain wall varies widely across species (e.g. Moore *et al.*, 1991; Stanley and Linskens, 2012) and the carbon and oxygen pollen-isotope values differ significantly within genera and plant families (Jahren, 2004), more general background knowledge about the relation of species-specific pollen-isotope values and environmental conditions is required.

Gaining profound knowledge about isotope variability prior to the actual usage of pollen-isotopes to reconstruct environmental changes, e.g. of the QTP, is inevitable and this study is designed to cover multiple research question regarding pollen-isotope variability. Since intensive sampling is required, this study takes place in Europe for practical reasons (Table 1.1; Figure 3.1, *pp.* 46). Nine abundant tree species (Table 3.2, *pp.* 48) are selected for their abundance under variable environmental settings and the recurring appearance of their pollen in fossil records, so that pollen of these species can directly be

used as reference material in future studies measuring fossil pollen-isotopes. The inter- and intraspecific variability of pollen sampled at seven different natural habitats enable the investigation of spatial effects on the isotope values (Table 3.1, *pp.* 47). The selected species flower during three different time periods within one vegetation period: early flowering species flower before leaf proliferation (*Corylus avellana* and *Alnus glutinosa*), spring flowering species flower during April and May (*Acer pseudoplatanus*, *Betula pendula*, *Carpinus betulus*, *Fagus sylvatica* and *Quercus robur*) and the coniferous species *Picea abies* and *Pinus sylvestris* flower in June at the beginning of summer. The investigation of several species is necessary to evaluate species-specific applicability of pollen-isotope analysis in climate research and analysing pollen which are formed during different flowering periods enable even seasonal weather reconstructions in future palaeoclimate studies. The whole spectrum of pollen-isotope variability within individual trees is evaluated by sampling pollen from different cardinal directions and different heights within trees of several species. To test temporal variability of pollen-isotope values, samples of two consecutive vegetation periods (2015 and 2016) were collected (Table 1.1; Figure 1.5). The sampling areas are located in central and northern Europe where high-resolution weather records to investigate the weather-isotope relation are available (Figure 3.1; Table 3.1). The most important criteria for selection of the locations are the presence of a natural setting with minimal human impact and a natural occurrence of at least two of the selected tree species chosen for this study (Figure 1.5).

1.2.3 Impact of chemical treatments on pollen

A major part of advancing the approach of pollen-isotope analysis in palaeoenvironmental research is the investigation of the impact of chemicals on the isotope values (Figure 1.5). In general, there are three different reasons for the application of chemical substances on pollen. First, to prepare fossil pollen samples for morphology-based environmental investigations. Second, to prepare fossil pollen samples for pollen-isotope analysis and third, to perform an artificial diagenesis to extract sporopollenin of the modern pollen grain wall and obtain reference values for fossil pollen-isotopes. This last application is done to enhance the comparability of modern and fossil pollen-isotope values, since fossilised pollen already underwent natural diagenetic processes leaving only the resistant parts of the pollen wall, the exine consisting of sporopollenin, intact (section 1.5; Figure 1.6). Hence, the third study of this thesis examines different pollen preparation and purification protocols and tests the impact of chemical substances on the carbon and

oxygen isotope values.

Fossil samples for morphology-based pollen analysis are treated chemically to extract the pollen, remove clastic debris and small organic parts (Table 1.2). Additionally, chemicals are applied to accentuate morphological features of the pollen wall through staining of the exine to support the identification. Chemical purification of fossil pollen from lake sediment material for morphology-based palynological analysis generally follows the standard protocols of Erdman (1969) and Faegri *et al.* (1989). The slightly adjusted protocol to extract fossil pollen from the Daotang Pond sediment samples contains hydrogen chloride (HCl) to remove carbonates, potassium hydroxide (KOH) to digest humic acids, hydrofluoric acid (HF) to degenerate clastic debris and an acetolysis with acetic anhydride ($C_4H_6O_3$) and sulfuric acid (H_2SO_4; Table 1.2, Protocol P 1) to extract sporopollenin and stain the exine.

Fossil pollen used for isotope analysis also need to be extracted chemically from the sample, but some of the chemicals used in purification protocols for morphology-based analysis alter the isotope values of pollen (Jahren, 2004). Hence, preparation protocols to purify pollen from clastic debris and small organic parts have to be adjusted prior to pollen-isotope analysis. Acetolysis is known to affect the carbon isotope values of pollen and therefore needs to be avoided (Amundson *et al.*, 1997). Some protocols to purify

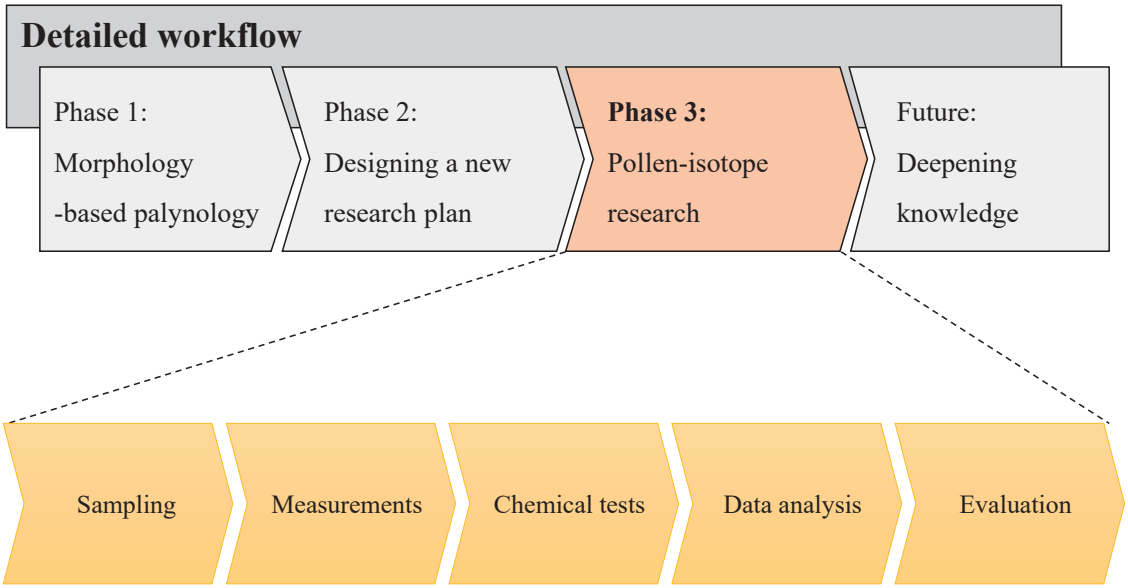

Figure 1.5: Detailed workflow of phase 3: conducting pollen-isotope research. This phase contains the workflow advancing the general knowledge on pollen-isotopes. Sampling refers to collection of pollen on 19 sampling trips to European national and nature parks; measurements refer to the laboratory work of preparing pollen samples and measuring carbon and oxygen isotope values; chemical tests include the test of isotope-altering effects of chemicals used in pollen purification protocols; data analysis contains all statistical tests and evaluation refers to the drawn conclusions of this state of research.

pollen as a preparation for carbon isotope analysis of pollen have already been tested (e.g. Loader and Hemming, 2000; Jahren, 2004; Nelson *et al.*, 2006, Bell *et al.*, 2017). These protocols contain HCl, KOH, HF, NaClO (sodium hypochloride), NaOH (sodium hydroxite) and H_2O_2 (hydrogen peroxide) in different combinations. As a result, all of the protocols lead to a variable, but species-specific carbon isotope offset compared to untreated pollen material. Neither the single effect of the chemicals on pollen-isotope values, nor the impact of chemicals on oxygen isotopes of pollen have been examined so far. Hence, to be able to adjust purification protocols according to the requirements of the source material, the impact of single chemicals on the carbon and oxygen pollen-isotope values need to be investigated.

H_2SO_4 is mostly applied on modern pollen to perform an artificial diagenesis by removing cellulose and other organic material from the pollen grain (intine, cell organelles and pollen wall coating; Figure 1.6) to standardise the pollen material and enhance comparability of fossil and modern sporopollenin-isotope values. The effect of H_2SO_4 on the carbon isotope values of modern pollen have already been examined (e.g. Loader and Hemming, 2000; Descolas-Gros and Schölzel, 2007; Bell *et al.*, 2017). The offsets are highly species-specific and vary between -0.6‰ (Bell *et al.*, 2017) and -3.55‰ (Loader and Hemming, 2000). Hence, the specific impact of H_2SO_4 needs to be tested for all species used in future palaeoclimate investigations.

1.3 Objectives of this thesis

The overarching aim of this thesis is to explore ways and limitations of using pollen as a proxy for palaeoenvironmental reconstruction. A confident application of traditional morphology-based palynology is fundamental and thus, broad knowledge about pollen remains in lake sediment archives and their implication for environmental reconstruction shall be gained prior to an advancement of pollen-isotopes in climate research. The focus of this study lies on advancing the relatively unexplored application of pollen-isotope analysis in palaeoclimate research by starting with necessary preliminary research on modern pollen-isotope patterns and ranges, which can later be assigned to studies on fossil pollen-isotopes. The key objectives are:

1. Determine high-resolution changes in the vegetation cover by using morphology-based palynological methods. This shall be done in an area impacted by different atmospheric systems fluctuation over time, where stable isotope analysis of other

proxies has already been applied and brought benefit to local climate reconstruction approaches.

2. Determine non-climate related causes for variability of species-specific carbon and oxygen pollen-isotope ranges and patterns from different sites and different years and advance basic knowledge about plant physiology reactions that can affect the geochemistry of pollen.

3. Examine the effect of various chemical substances on the isotope values of raw pollen which are usually applied in palaeoclimate to extract fossil pollen from lake sediment and develop a treatment protocol with minimized impact for isotope analysis of fossil pollen.

1.4 Background knowledge

1.4.1 Pollen: morphology, composition and formation

Pollen are the male microspores of angiosperms and gymnosperms. Even though they differ in shape and size among species, pollen grains of all plants share similar characteristics. The structure can morphologically be divided into the inner cell and the protective outer layers, called the pollen wall (Figure 1.6). The inner cell contains the living proportion of the grain with a generative nucleus, cell organelles and vegetative cytoplasm. The pollen wall functions mainly as protection and can further be divided into inner wall layers (together called intine) and outer wall layers (together called exine). The outermost layer is the ektexine, an additional morphological division of the exine holing either connected columnar structures (the tectum) or unconnected ones (in case of intectate pollen; Figure 1.6). Additionally, the surface of the exine is often sculptured and the ornamentation accounts for species- or genus-specific morphological features allowing taxonomic identification of the pollen grains. The size of pollen varies between 5 and 200 μm, depending on species, origin and condition of the pollen grains (Faegri *et al.*, 1989). Another morphological feature which is often found in angiosperm and gymnosperm pollen is the presence of apertures in variable numbers and shapes. Apertures are thin openings allowing pollen tube growth during germination. They can be present as furrows (colpi) or pores (pori) (Beug, 2004).

Pollen are formed within the anthers inside the inflorescences by meiotic divisions of a mother cell (Jarzen and Nichols, 1996). The microspores already develope up to the quartet stage in the vegetation period prior to the year of pollination (Brett, 1964; Ducousso *et al.*, 1993). During winter dormancy of the host plant, the pollen remain at the quartet pollen-mother-cell stage inside the premature anther (Kupila-Ahvenniemi and Pihakaski, 1966). Further meiosis and maturation of pollen starts with early bud swell in the subsequent spring (Stairs, 1964). The tapetum, a layer of nutritive cells inside the anther, forms the outer pollen wall consisting mostly of sporopollenin (Figure 1.6; Moore *et al.*, 1991). Detailed synthesis of sporopollenin on a molecular basis is mostly unknown (Dickinson and Bell, 1976; Bell *et al.*, 2017; Li *et al.*, 2019). Inner pollen wall layers are deposited during the whole process of pollen maturation. In general, molecules are exchanged during resumed pollen development in spring and a major exchange of nutrients takes place directly before pollination (Rowley *et al.*, 2000; Blackmore *et al.*, 2007).

The pollen wall of raw (or modern) pollen consist of several layers of pectin, cellulose and hemicellulose (Marquez *et al.*, 1997; Fan *et al.*, 2019). The inner pollen wall (intine) is mainly composed of cellulose $(C_6H_{10}O_5)_n$ and some additional proteins (Fang *et al.*, 2008), whereas the main component of the outer pollen wall (exine) is sporopollenin. Sporopollenin is a highly resistant biopolymer consisting of approximately of $C_{90}H_{150}O_{33}$ (Loader und Hemming, 2004; Fraser *et al.*, 2014; Li *et al.*, 2019), which is formed by oxidative polymerisation of carotene and carotene esters (Brooks and Shaw, 1978). The degree of sporopollenin-polymerisation determines the relative strength and resistance of the exine (Faegri *et al.*, 1989). The structure and composition of a pollen grain wall varies highly with species (e.g. Moore *et al.*, 1991; Stanley and Linskens, 2012), but the average proportion of sporopollenin within pollen grains ranges between 55% and 85% (Nelson, 2012). The resistant exine is the most important protection-layer for the reproductive cell inside the pollen grains (Figure 1.6), but it functions additionally as a storage layer for various pollen coat substances (Wiermann and Gubatz, 1992). Additional to several inner and outer pollen wall layers, raw pollen hold cell organelles, vegetative cytoplasm and species-specific pollen wall coatings of lipids, protein and carbohydrates under the form of nectar and pollenkitt (Kuang and Musgrave, 1996; Marquez *et al.*, 1997). Fossil pollen differ from raw pollen due to the occurrence of diagenetic processes during fossilisation (Figure 1.6). The inner pollen wall layers, the coating and the cell organelles are highly susceptible to degradation and therefore only the outer pollen wall elements consisting of sporopollenin remain present in fossil pollen (Figure 1.6; Faegri *et al.*, 1989).

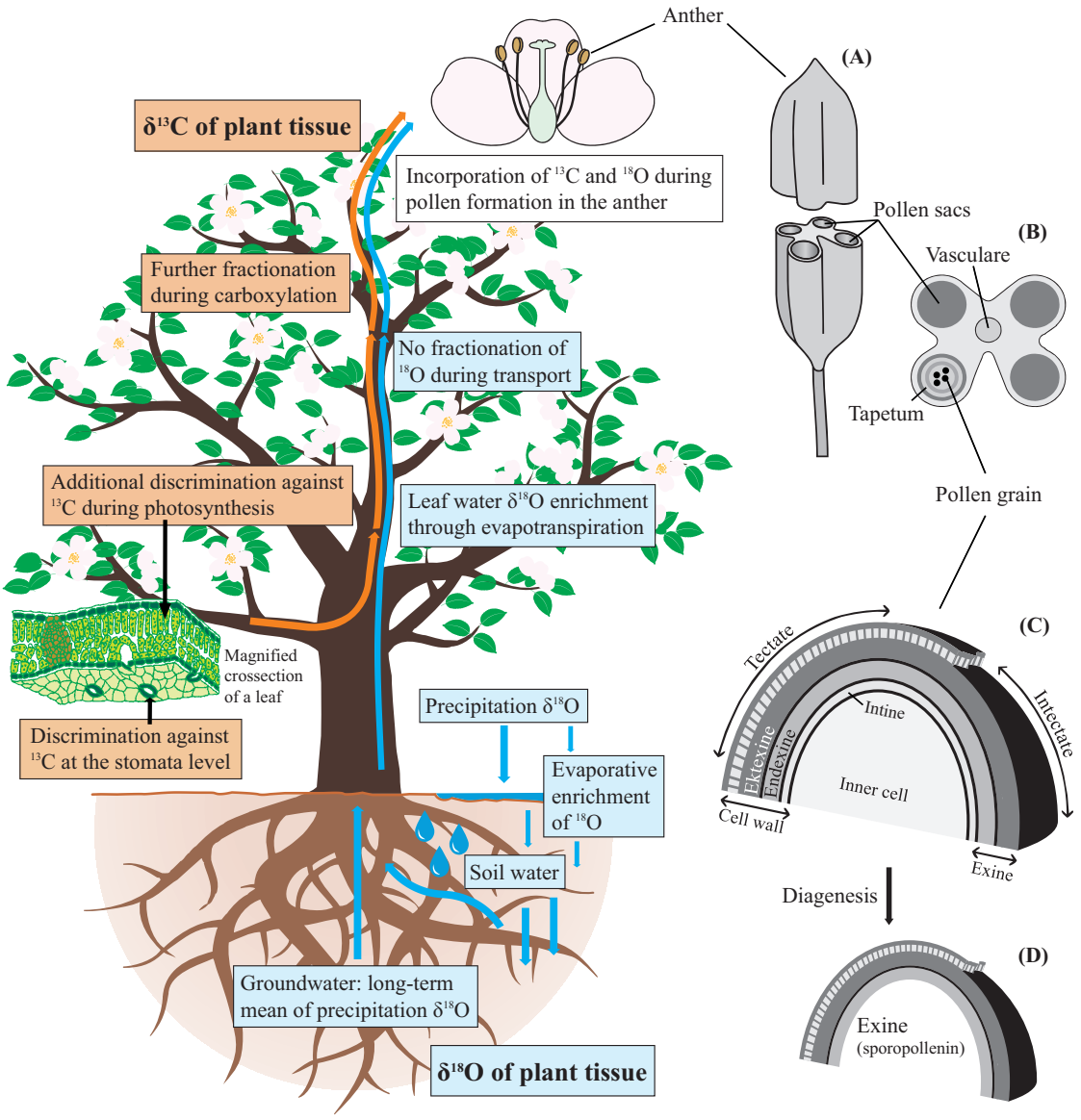

Figure 1.6: Simplified tree showing the carbon (orange) and oxygen (blue) isotope pathways and influencing processes that occur during uptake and transport from source (leaf and soil water) to sink (location of plant tissue formation). (A) Enlarged depiction of the anther and insight into four pollen sacs. (B) Cross section of the anther and details of a pollen sac with tapetum layer and pollen grains. (C) Simplified cross section of a pollen grain and detailed depiction of the pollen wall layers. The inner cell contains the living portion of the pollen and the intine, a cellulose pollen wall layer. The outer cell wall (exine) is divided into ektexine and endexine. (D) Pollen grain after diagenetic processes: only the exine consisting of sporopollenin remains present.

1.4.2 Isotope composition of plant material

The carbon isotope composition of plant material is determined by several steps of discrimination against ^{13}C and fractionation during carbon fixation in the leaf, hence stable carbon isotope values of plant material are lower than isotope values of atmospheric carbon dioxide (e.g. Farquhar *et al.*, 1989). The amount of discrimination against heavy ^{13}C to lighter ^{12}C during stomatal CO_2 uptake and photosynthesis has thoroughly been investigated and identified as the prime reason for the varying stable carbon isotope composition of plant material (e.g. O'Leary, 1988; Farquhar *et al.*, 1989). Therefore, isotopic ratios of plant tissue are controlled by local environmental conditions and plant-physiological reactions to those conditions (Loader and Hemming, 2000). Single environmental factors, such as temperature, humidity, irradiance and soil water availability, have successfully been linked to isotopic discrimination during photosynthesis (Wilson and Grinstedt, 1977; Leavitt and Long, 1984 and 1986; Saurer and Siegenthaler, 1989; Walcroft *et al.*, 1997). In detail, discrimination of ^{13}C against ^{12}C occurs at first at the stomata, the leaf-openings where atmospheric CO_2 enters the leaf (Figure 1.6). Due to a higher molecule mass, $^{13}CO_2$ diffuses slower across the epidermis of the plant than $^{12}CO_2$. Additionally, ^{13}C forms stronger chemical bonds and is therefore generally less accessible (O'Leary, 1988). The first discrimination at the stomata level leads to kinetic fractionation processes and an approximate change of -4.4‰ of the $\delta^{13}C$ values (Farquhar *et al.*, 1989). Subsequent fractionation processes occur during carbon fixation in the leaf. Carbon molecules are fractionated depending on environmental factors as well as the photosynthetic pathway of the plant, being either C3 or C4. Within the C3 photosynthetic pathway, the additional fractionation and discrimination alters the $^{13}C/^{12}C$ ratio further by approximately -25‰ (Farquhar *et al.*, 1989). Plants with a C3 cycle are common in temperate climates (Ehleringer *et al.*, 1997) and use an enzyme called Rubisco (ribulose bisphosphate carboxylase-oxygenase) to bind the CO_2 in a first step of the photosynthesis onto a 5-carbon sugar called RuBP (ribulose bisphosphate). In contrast to C3 plants, C4 plants are common in hot and arid environments (Pearcy and Ehleringer, 1984) and use the enzyme PEP (phosphoenolpyruvate) to fixate CO_2 first onto a 4-carbon acid before starting the same cycle of C3 plants using Rubisco and RuBP. Both cycles involve different steps leading to a variable number of ^{13}C fractionations and thus result in different averages of the $\delta^{13}C$ values of plant tissue. In general, $\delta^{13}C$ values of C3 plants range from -35‰ to -26‰, whereas the $\delta^{13}C$ values of C4 plants range between -14‰ and -12‰ (O'Leary, 1988; Cerling, 1999).

Variations of δ^{13}C values within a species can be linked to the geographic location of the individual plants. The rate of discrimination of ^{13}C against ^{12}C is linearly related to the ratio of intercellular to ambient CO_2 partial pressures (Körner *et al.*, 1991). At high altitudes, the CO_2 partial pressure inside the leaf is lower than outside, limiting the amount of available carbon for photosynthesis. Thus, discrimination of ^{13}C decreases with altitude and higher δ^{13}C values occur in plant tissues from high altitudes (Körner *et al.*, 1991). The same mechanism is responsible for the occurrence of a latitudinal effect. The amount of ^{13}C in CO_2 increases approximately 5‰ along the latitudinal gradient from the tropics to the tundra (Lancaster, 1990) and the latitudinal effect accounts for higher δ^{13}C values at high latitudes (Hultine and Marshall, 2000). Also, differences in sunlight availability and CO_2 recycling close to forest floors lead to an intra-tree variability of δ^{13}C values of leaf tissue up to 10‰. The latter is known as the canopy effect (Lockheart *et al.*, 1997; Graham *et al.*, 2014).

The usage of stored carbon for building new plant tissue after the reoccurrence of growth in spring has been recognized for winter deciduous tree species, affecting the carbon isotope values of plant tissues to a varying degree (Loescher*et al.*, 1990; Schwarz, 2016). The allocated and remobilized carbon molecules differ in age between 0.7 and 10 years (Gaudinski *et al.*, 2009; Richardson *et al.*, 2013)

The carbon isotope composition of pollen highly correlates with the carbon compositions of other plant tissues, such as leafs, twigs and tree rings of the same individual (Jahren, 2004; Bell *et al.*, 2017). Just as any other plant material, pollen are also primarily built out of the products of photosynthesis when aerial CO_2 is breathed by the plant and molecules are incorporated during basic plant tissue formation (Figure 1.6; Loader and Hemming, 2000). Hence, sporopollenin has a direct connection to ongoing environmental conditions in the weeks of pollen formation and maturation (Loader and Hemming, 2000; Schwarz, 2016; Bell *et al.*, 2017). The specific δ^{13}C values of pollen are mainly determined by the species identity, timing of pollen formation and local environmental factors during seasonal plant growth (Jahren, 2004; Loader and Hemming, 2004). The exact timing and the process of pollen development on a molecular basis in the anther are decisive for the composition of the pollen-isotopes. Unfortunately, relatively little is known about exact molecular processes, chemical composition and changes of the tapetum during male microspore development (Datta *et al.*, 2002). Additionally, information about the timing of the process varies (e.g. Luomajoki, 1986; Blackmore *et al.*, 2007). Some researchers state that plants only use storage molecules for building new plant tissue in spring and

early summer (Luomajoki, 1986; Schwarz, 2016), whereas a direct correlation of various plant tissues to environmental processes of the ongoing season have already been proven by others (Loader and Hemming, 2001; Blackmore *et al.*, 2007).

The oxygen isotope composition of plant material is mostly determined by three important factors, which need to be considered when interpreting the $\delta^{18}O$ values of fossil plant material (Barbour and Farquhar, 2000). These factors are the composition of the source water, the evaporative enrichment in the leaves during transpiration and biochemical fractionation during sugar and starch formation (Figure 1.6; Helle and Schleser, 2004). No fractionation processes occur during water uptake from the roots and transport in the stem (Ehleringer and Dawson, 1992; Baker, 1996), and therefore the isotopic signal of plant tissue is highly dependent on the composition of the source water. Main water sources for plants are soil water or groundwater and the preference depends on the species-specific root system (Helle und Schleser, 2004). Soil water $\delta^{18}O$ reflects the isotope values of precipitation of the ongoing season, whereas the groundwater displays a long-term isotope mean of past rainfall (Helle und Schleser, 2004). In general, source water originating from precipitation can be affected by evaporative enrichment before seeping into the soil (Figure 1.6; Hoefs, 2009). After transport to the leaves and depending on the ambient air humidity, evapotranspiration through open stomata may occur changing the isotopic composition of the source water (Helle and Schleser, 2004). Different vapor pressures outside and inside the leaf determine kinetic equilibrium processes that may lead to leaf water enrichment: lighter and more mobile ^{16}O molecules diffuse faster, which leads to enriched intercellular ^{18}O values (Farquhar and Gan, 2003; Farquhar *et al.*, 2007). Additionally, water undergoes fractionation processes during photosynthetic activities in the leaves. Source or soil water signals might therefore be altered severely by processes masking the original signal in the isotope record (Helle and Schleser, 2004). Furthermore, leaf water $\delta^{18}O$ values change over the course of a day, which complicates the assessment of the relationship of source water, leaf water and stored oxygen isotopes. The analysis of oxygen isotopes from fossil plant material gives insights into climate variations of the past. Especially the amount of precipitation and air temperature during plant tissue formation are related to the $\delta^{18}O$ values of e.g. tree ring cellulose, leaf cellulose and phytoliths (Yapp and Epstein, 1982; Saurer *et al.*, 1995; Webb and Longstaff, 2000; Helle and Schleser, 2004). However, $\delta^{18}O$ values of plant tissue are difficult to interpret, since physiological reactions to environmental parameters are species and site specific (Helle and Schleser, 2004).

So far, the oxygen isotope composition of pollen and its relation to climate parameters such as precipitation and temperatures is still poorly understood (Schwarz, 2016). In general, the oxygen pollen-isotope composition is mostly determined by $\delta^{18}O$ of precipitation, but the degree of dependence is different amongst species and related to plant type and physiology (Schwarz, 2016). Tree and grass pollen $\delta^{18}O$ are highly influenced by leaf water enrichment during evapotranspiration (Schwarz, 2016). Oxygen pollen-isotopes have already been applied to determine the provenance of honey, but no significant relationship of the $\delta^{18}O$ of pollen and precipitation could be detected in the same study (Chesson *et al.*, 2013). A negative relationship between $\delta^{18}O_{pollen}$ and $\delta^{18}O$ of precipitation during the time of pollen formation was recognized by Loader and Hemming (2004). This result is contrary to already established positive relationships between $\delta^{18}O$ of precipitation and other plant material, e.g. wood and leaves (Loader and Hemming, 2004).

1.5 Material and methods

1.5.1 Fieldwork and sampling

For the morphology-based palynological analysis a 136 cm long sediment core was taken in August 2013 from Daotang Pond (36°57'35.4 N, 100°74'48.4 E), 2 km southeast of Lake Qinghai (Figure 3.1, *pp.* 24). The core was retrieved with an UWITEC short coring system (60 mm diameter) at approximately 50 cm water depth. It was subsampled in 1 cm steps and immediately stored in numbered plastic boxes to prevent contamination with modern airborne pollen.

The collection of modern pollen samples for stable isotope analysis was executed in natural habitats in central and northern Europe (between 46.6 °N to 60.7 °N and 5.7 °E to 23.9 °E; Figure 3.1, *pp.* 46) during the vegetation periods from February to June 2015 and 2016 (Figure 3.2, *pp.* 48). Male inflorescences were collected during the respective flowering periods, which are variable for species and sites due to specific phenology and weather conditions of spring and the previous winter (Table 3.1, *pp.* 47, and Table 3.2, *pp.* 48). In total, 19 sampling trips were conducted in two consecutive years (Table 1.1). The flowers were cut or plucked directly from the trees and bulk pollen samples of each individual tree consisted of several inflorescences from various positions in the canopy (Figure 3.3, *pp.* 49). Some trees were additionally subsampled to infer intra-tree variability of the pollen-isotope values.

1.5.2 Morphological pollen analysis

The Daotang Pond sediment core war sampled in 1 cm steps and pollen of every second sample were extracted, summing up to a total of 62 analysed pollen samples. The pollen were extracted in the laboratory out of 3 g material following the standard procedure (Table 1.2, P1). Prior to the laboratory treatment, a *Lycopodium* spore tablet was added to each sample in order to calculate the pollen concentration after counting. Pollen were counted up to a minimum number of 300 pollen grains using a Meiji Techno (MT 4300L) microscope at 400× and 600× magnification. The pollen percentages of each

Table 1.1: Nine sampling trips have been executed in seven localities throughout the vegetation periods of 2015 (left column) and 10 sampling trips took place in 2016 (right column). Weeks refers to calendar weeks in 2015 and 2016. Details of the sampling sites are listed in Table 3.1.

	2015		2016	
Week	**Sampling Site**	**Collected species**	**Sampling site**	**Collected species**
8	–	–	Müritz Nationalpark	*Alnus glutinosa* *Corylus avellana*
11	Parc Naturel Forêt d'Anlier	*Alnus glutinosa* *Corylus avellana*	Parc Naturel Forêt d'Anlier	*Alnus glutinosa* *Corylus avellana*
12	–	–	Gorczanski Park Narodowy	*Alnus glutinosa* *Corylus avellana*
14	Gorczanski Park Narodowy	*Alnus glutinosa* *Corylus avellana*	–	–
17	–	–	Müritz Nationalpark	*Betula pendula*
18	–	–	Steigerwald Nationalpark	*Acer pseudoplatanus* *Betula pendula* *Carpinus betulus* *Fagus sylvatica* *Quercus robur* *Picea abies*
19	Parc Naturel Forêt d'Anlier	*Betula pendula* *Carpinus betulus* *Quercus robur* *Picea abies* *Pinus sylvestris*	Parc Naturel Forêt d'Anlier	*Acer pseudoplatanus* *Betula pendula* *Carpinus betulus* *Fagus sylvatica* *Quercus robur* *Picea abies* *Pinus sylvestris*
20	Parco Naturale Tre Cime	*Acer pseudoplatanus* *Picea abies* *Pinus sylvestris*	Parco Naturale Tre Cime	*Acer pseudoplatanus* *Betula pendula* *Fagus sylvatica* *Picea abies* *Pinus sylvestris*
20	Müritz Nationalpark	*Pinus sylvestris*	–	–
21	Gorczanski Park Narodowy	*Acer pseudoplatanus* *Fagus sylvatica* *Picea abies* *Pinus sylvestris*	Gorczanski Park Narodowy	*Acer pseudoplatanus* *Fagus sylvatica* *Picea abies* *Pinus sylvestris*
21	–	–	Tatrzanski Park Narodowy	*Picea abies*
22	Steigerwald Nationalpark	*Picea abies* *Pinus sylvestris*	Liesjärvi kansallispuisto	*Picea abies* *Pinus sylvestris*
23	Gorczanski Park Narodowy	*Pinus sylvestris*	–	–
23	Tatrzanski Park Narodowy	*Picea abies*	–	–

sample were calculated based on all present pollen types. Identification of the taxonomic affiliation was supported by a reference collection at FU Berlin and by pollen atlases (Reille, 1992–1998; Beug, 2004). Visualisation of the pollen record was done with the TILIA, TILIA Graph and TG View Software 1.7.16 (Grimm, 2011). Included in the diagram are only pollen types exceeding 1% of the total pollen sum in at least one samples. The dataset of the pollen counts is available on the open access platform PANGAEA at https://doi.pangaea.de/10.1594/PANGAEA.919329.

1.5.3 Chemical treatment of pollen

The chemical purification of fossil pollen from lake sediment material followed a standard protocol (Erdman 1969 and Faegri *et al.*, 1989). Hence, the protocol to extract fossil pollen from the Daotang Pond sediment samples contained hydrogen chloride (HCl), applied in a water bath for 15 minutes to dissolute carbonates, potassium hydroxide (KOH), applied in a water bath for 20 minutes to digest humic acids, and hydrofluoric acid (HF), applied for 24 hours to degenerate clastic debris. These steps were followed by two washings with acetic acid ($C_2H_4O_2$) to dehydrate the samples and an acetolysis step with acetic anhydride ($C_4H_6O_3$) and sulfuric acid (H_2SO_4; Table 1.2, P 1), which dissolute remaining cellulose and stains the exine of the pollen. Each treatment followed thorough and repeated rinsing with deionised water.

The chemical treatment protocol of modern pollen followed the same standard protocol

Table 1.2: Protocol 1 (P1) is a standard chemical purification method of fossil pollen from lake sediment material including steps of HCl (hydrogen chloride), KOH (potassium hydroxide), HF (hydrofluoric acid) and acetolysis, whose proportion (v/v 9:1) of $C_4H_6O_3$ and H_2SO_4 (sulfuric acid) is given in percentage by volume. Protocol 2 (P2) indicates chemicals used to purify pollen prior to stable isotope analysis. H_2SO_4 is applied to extract sporopollenin and enhance the comparability of fossil and modern pollen-isotope values. NaClO (sodium hypochlorite) is added in the end of P2 to dissolute remaining small organic components. The purity of the chemicals is indicated in % and the type of treatment describes the detailed execution of the protocol step. The effect gives information about the changes within the pollen sample after application of chemicals. Both protocols follow the standard treatments of Faegri *et al.* (1989) and Erdman (1969).

Chemical	P1	P2	Purity	Type of treatment	Duration	Effect
HCl	X		10%	Water bath at 90 °C	15 min	Dissolution of carbonates
KOH	X	X	10%	Water bath at 70 °C	20 min	Digestion of humic acids
HF	X	X	38%	Resting, room temperature	24 h	Degeneration of clastic debris
$C_2H_4O_2$	X		100%	Two processes of washing	–	Dehydration of the sample
$C_4H_6O_3$	X		100%	With H_2SO_4 96% (v/v 9:1), water bath at 70 °C	2 min	Dissolution of cellulose remains and staining the sporopollenin
H_2SO_4	X	X	96%	Constantly on a shaker	5 h	Extraction of sporopollenin
NaClO		X	3%	Stirring, room temperature	90 s	Dissolution of organic contents

(Table 1.2, P 2) to imitate a purification process and to assess the specific effect of the chemicals on the carbon and oxygen pollen-isotope values. Hence, modern pollen samples of eight species were treated separately with potassium hydroxide (KOH), hydrofluoric acid (HF) and sodium hypochlorite (NaClO; Table 1.2 and Table 4.2, *pp.* 88) to test the species-specific effect of the chemicals on the pollen-isotope values. Sulfuric acid (H_2SO_4) was applied to isolate sporopollenin from modern pollen material and compare the isotope values of raw and diagenetically changed pollen grains. All samples were cleaned from chemical remains by repeated rinsing with deionised water.

1.5.4 Stable isotope measurements

The pollen was weighed into silver capsules using a high-precision scale (Mettler Toledo AX 26 Delta Range). Prior to stable isotope measurements, the samples were vacuum dried for at least 12 hours in a Thermo Scientific Heraeus VT 6060 P at 100 °C. The coupling of a High Temperature Conversion Elemental Analyzer (TC/EA; 1400 °C; Thermo Fisher ScientificTM, Bremen) to an IRMS (DELTA V isotope ratio mass spectrometer, Thermo Fisher Scientific^{TM}, Bremen) enabled a simultaneous attainment of the carbon and oxygen isotope ratios through reduction to CO. The measurements of 220 μg $\pm$ 10% raw pollen material were usually repeated three times for each sample. The isotope ratios are expressed relative to VPDB (Vienna Pee Dee Belemnite) for δ^{13}C and to VSMOW (Vienna Standard Mean Ocean Water) for δ^{18}O and the data was compared to international and lab-internal reference material (IAEA-CH3, IAEA-CH6 and IAEA 601 and 602). The normalisation followed Paul *et al.* (2007) using two reference standards with a wide isotopic composition to obtain a single-point normalisation (detailed information is provided in chapters 3 and 4).

1.6 Integrated manuscripts

This dissertation in a cumulative from consists of three separate manuscripts (chapters 2-4). Two manuscripts have already been peer reviewed and published in international scientific journals, whereas the third is submitted and currently under review. Each publication represents a self-contained research article on connected topics, therefore repetitions in methodology and regional settings are unavoidable. Table 1.3 contains information about title, authorship, journal and actual publication status of each manuscript.

Carolina Müller is the lead author of all individual manuscripts presented in this dissertation. Frank Riedel and Bernd Wünnemann carried out the fieldwork in manuscript I, but C. Müller planned the fieldwork of manuscripts II and III entirely, reviewed relevant literature and wrote all three publications. Laboratory work was mostly done by Carolina Müller, as well as generating and assembling the figures (Table 1.3).

Table 1.3: Overview of the manuscripts presented in this thesis, their current publication status and own contribution to the conceptualisation (C), execution (E) and publishing (P) to manuscript I, II and III (in %).

Manuscript no./chapter	**Manuscript title, author list and publication status**	**Own contribution (%)**		
		C	**E**	**P**
I/2	Bi-decadal climate reconstruction derived from a 1200-year long pollen record from the NE Qinghai-Tibet Plateau and its implications for discussion of the late Holocene environmental dynamics *Carolina Müller* Published in *Quaternary International* 444 (2017), *pp.* 1–10 doi.org/10.1016/j.quaint.2017.05.058	80	70	100
II/3	Inter- and intra-tree variability of carbon and oxygen stable isotope ratios of modern pollen from nine European tree species *Carolina Müller*, *Manja Hethke*, *Frank Riedel*, *Gerhard Helle* Published in *PLoS ONE* (2020) 15(6):e0234315 doi.org/10.1371/journal.pone.0234315	70	80	85
III/4	Quantifying the impact of chemicals on stable carbon and oxygen isotope values of raw pollen *Carolina Müller*, *Julian Hennig*, *Frank Riedel*, *Gerhard Helle* Under review at *Journal of Quaternary Sciences* (number: JQS-20-0020)	100	90	95

Chapter 2

Bi-decadal climate reconstruction derived from a 1200-year long pollen record from the NE Qinghai-Tibet Plateau and its implications for discussion of the late Holocene environmental dynamics

Carolina Müller[a]

[a] Institute of Geological Sciences, Freie Universität Berlin, Malteserstraße 74-100, Building D, 12249 Berlin, Germany

Published in *Quaternary International* 444 (15 July 2017) pp. 1–10
https://doi.org/10.1016/j.quaint.2017.05.058

Keywords: Lake Qinghai drainage basin; vegetation cover changes; atmospheric circulation system; Medieval Warm Period; Little Ice Age

Abstract

This study presents bi-decadal scale pollen record of climate change from the Daotang Pond (36°57'35.4 N, 100°74'48.4 E; 3205 m a.s.l.). The pollen record, situated 2 km south-east of Lake Qinghai in the north-eastern part of the Qinghai-Tibet Plateau (QTP), reveals a pattern of consequent changes in the alpine meadow and steppe vegetation throughout the last 1200 years. Due to its location at the interface of the East Asian Summer Monsoon (EASM) and the North Atlantic Westerlies, the Daotang record reacts sensitively

even to minor changes in precipitation. Consequently, impact of both these major atmospheric circulation systems on the regional environments can be analysed and discussed along with the other climatic proxies from the region. The EASM impact was generally strong throughout the Medieval Warm Period (MWP), which lasted from the beginning of the record at CE 850 up to roughly CE 1400. This time interval was characterised by a favorable warm and rather moist climate with a precipitation peak around CE 950. However, two dry spells indicating irregular EASM weakening occurred around CE 1050-1150 and CE 1250-1400. Westerlies dominated the atmospheric circulation during the Little Ice Age (LIA). This cold phase started around CE 1450 and lasted roughly until CE 1950. It was characterised by a drier regional climate compared to the humid MWP, though lower evaporation due to decreased summer temperatures helped in keeping locally wet environment at the study site. Three dry and cold intervals are detected in the Daotang record at CE 1450-1550, CE 1650-1700 and CE 1800-1850, based on an exceptionally low *Artemisia*/Chenopodiaceae (A/C) pollen ratio and a generally low pollen concentration. After CE 1950 a shift towards a warmer and wetter climate occurred interrupted by a pronounced dry spell during the recent years

2.1 Introduction

Climate warming of past decades has affected the Qinghai-Tibet Plateau (QTP) and neighbouring Gansu province enormously. Lately, the whole region was plagued again by drought and heat waves, which evoked an existential threat to the 6.2 million inhabitants and their livestock. Thus it is of great importance to investigate causes and mechanisms of the recent weather extremes and to search for possible analogues in the recent past (Global Times (China), Xinhua Press, 2016/09/04).

The high mountainous area of the QTP (Chang *et al.*, 1989) provides various proxy records to analyse past climate changes. Thus numerous climate reconstruction studies covering great areas of the QTP are available nowadays (e.g. Gasse *et al.*, 1991; Thompson *et al.*, 1997; Liu *et al.*, 1998; Yu and Kelts, 2002). Recent investigations have shown that the interplay of several driving forces, including the Asian monsoon circulation system, the complex geomorphology of the QTP, solar irradiance as well as authentic micro-climate of each individual site and accuracy of each individual record's age model, may lead to a divergence in duration and strength of reconstructed climate optima and short term changes (An *et al.*, 2006; Chen *et al.*, 2008; Wischnewski *et al.*, 2011). The crucial step

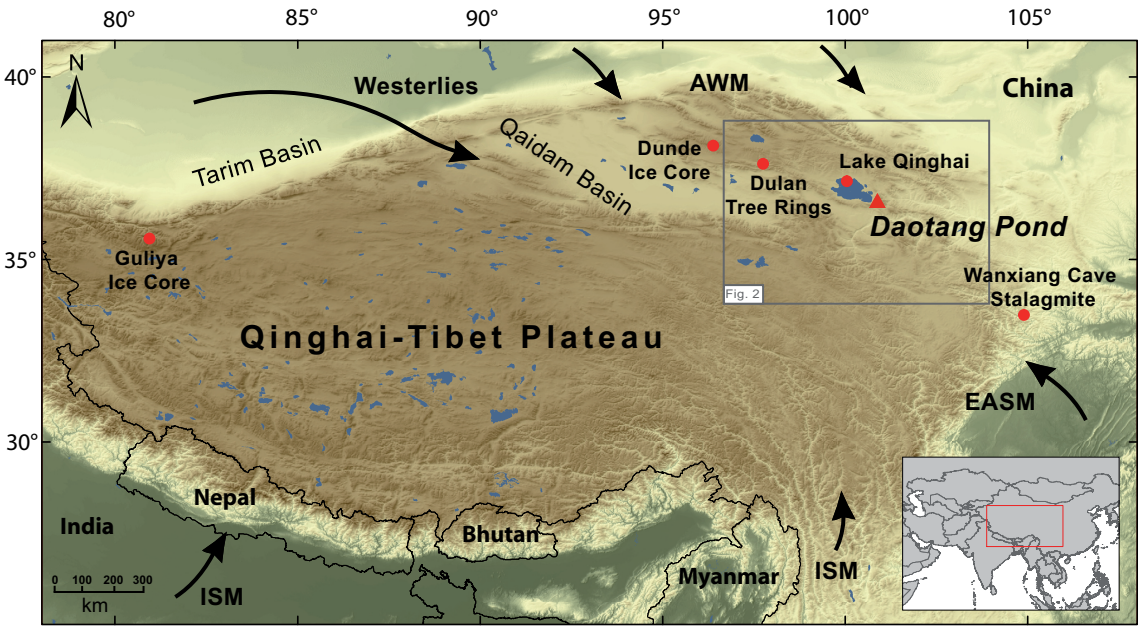

Figure 2.1: Overview map showing locations of the Qinghai-Tibet Plateau (QTP), the Daotang study area (grey square, enlarged in Figure 2.2), and the published reference records, i.e. Guliya Ice Core (Thompson *et al.*, 1997), Dunde Ice Core (Thompson *et al.*, 1990), Dulan Tree Rings (Yang *et al.*, 2014), Lake Qinghai (Henderson *et al.*, 2010) and Wanxiang Cave Stalagmite (Zhang *et al.*, 2008), discussed in the text. Black arrows indicate contemporary atmospheric circulation system including the Indian Summer Monsoon (ISM), East Asian Summer Monsoon (EASM), Westerlies and Asian Winter Monsoon (AWM).

towards accurate local and regional climate reconstruction is to find inter-links amongst patterns, localities and deviating reconstruction approaches. It is essential to regard each locality under the implication of various individual factors and focus especially on human induced changes within recent times (Tian *et al.*, 2013).

Landmass heating of the QTP area is considered to be the main driving factor for the East Asian Summer Monsoon (EASM) and the Indian Summer Monsoon (ISM) (Thompson *et al.*, 1997; Kumar *et al.*, 1999; An *et al.*, 2000; Clift and Plumb, 2008; Wang *et al.*, 2015). Nowadays, the westernmost limit of the EASM lies along the north-eastern QTP (An *et al.*, 2012; Zan *et al.*, 2015). The atmospheric circulation system over China is rather complex. The main players, including EASM, ISM, Asian Winter Monsoon (AWM) and all-year-round Westerly stream, have their conjunction zone in the region centred over Lake Qinghai (Figure 2.1).

Therefore, this area is sensitive to short-term shifts in monsoonal strength, temperature and atmospheric circulation. Especially the relation of Westerly winds and the EASM are in the focus of ongoing research (e.g. Xu *et al.*, 2007; Zan *et al.* 2015). The Westerlies dominate the climate in the arid Central Asian regions permanently (Chen *et al.*, 2010), whereas the interplay of Westerlies and EASM in the QTP region in sum-

mer remains variable in strength over long time periods and on a short term basis (Li *et al.*, 2016). This makes the area particularly suitable for high resolution climate reconstructions (Henderson *et al.*, 2010; Liu *et al.*, 2015) and allows better understanding of the atmospheric-circulation-induced climate patterns. Tree ring based climate reconstructions are one of the common approaches applied at the QTP (Zhang *et al.*, 2003; Bräuning and Mantwill, 2004; Sheppard *et al.*, 2004; Shao *et al.*, 2010; Huang and Zhang, 2007; Zhang *et al.*, 2008; Yang *et al.*, 2014), followed by ice core analyses (Yao *et al.*, 1996, 1997; Thompson *et al.*, 1997; Wang *et al.*, 2002; Bao *et al.*, 2003; Yao *et al.*, 2008) and various proxy based reconstructions derived from the archives stored in lacustrine sediments, such as diatoms (Wischnewski *et al.*, 2011), ostracods (Henderson *et al.*, 2003; Mischke *et al.*, 2005), chironomids (Chen *et al.*, 2009), and geochemical properties (Xu*et al.*, 2006, 2007, 2008, 2010; He *et al.*, 2013; Pu *et al.*, 2013). Another commonly applied method for reconstructing past climate variability is the analysis of fossil pollen and non-pollen palynomorphs (e.g. Liu *et al.*, 2002; Herzschuh, 2006). It allows detecting shifts in the local and regional vegetation cover with a high temporal/spatial resolution. Nonetheless, until now there are no available high resolution pollen records from the Lake Qinghai drainage basin.

A frequently raised question of recent climate investigations on the north-eastern QTP concerns the cause and effect of a fluctuating strength of the EASM on the regional environments (e.g. Sheppard *et al.*, 2004; Xu *et al.*, 2008; Henderson and Holmes, 2009) and its link to the larger scale climate phenomena, such as the Medieval Warm Period (MWP; approximately CE 800-1400 in central China) and the Little Ice Age (LIA; approximately CE 1450-1900 in the north-eastern QTP; He *et al.*, 2013). Several studies found a direct response of monsoonal strength to solar forcing and standardised Northern Hemisphere Temperatures (NHT; e.g. Zhang *et al.*, 2008; Liu *et al.*, 2014), explaining an enhanced precipitation during the MWP and a weakened EASM during the LIA. In the latter case, an enlarged sphere of influence of the North Atlantic Westerlies and a greater southward extension of the AWM controlled the Lake Qinghai area (Liu *et al.*, 2009). Even if the total amount of annual precipitation was less during the LIA than during the MWP, colder temperatures lead to lower evapotranspiration losses (Henderson *et al.*, 2010; Yang *et al.*, 2014) and thus potentially to an equal amount of available moisture at one location (An*et al.*, 2006). This phenomenon causes further difficulties for the interpretation of climate variability, because cause and effect are sometimes hardly distinguishable. Whether or not the ISM reaches the Daotang area is debated (Zhang *et al.*, 2011; He *et al.*, 2013).

The aim of this study is to catch bi-decadal scale climate variability in a pollen record from the Daotang Pond near Lake Qinghai. The site located in the semi-arid region at the interface of the EASM and Westerlies should react sensitively to the regional climate changes controlled by these two major atmospheric circulation systems. An advantage of Daotang against the nearby Lake Qinghai (e.g. Yang *et al.*, 2009a, Hou *et al.*, 2012) lies in the smaller size and pollen catchment area of the site, which makes the record easier to understand. A rather high sedimentation rate at Daotang enables the analysis in high temporal resolution. Furthermore, a thorough comparison of an annual precipitation reconstruction derived from Dulan juniper tree rings reflecting Westerly and convective rainfalls (Yang *et al.*, 2014; Figure 2.1) and a stalagmite isotope record of the EASM precipitation from Wanxiang Cave (Zhang *et al.*, 2008; Figure 2.1) with the centrally located Daotang record presented in this study has been performed.

2.2 Regional setting

2.2.1 Contemporary climate

The Daotang site belongs to the Lake Qinghai drainage basin which occupies a large intermountain depression with prevailingly cold and semi-arid climate conditions (Liu *et al.*, 2015, Wang *et al.*, 2016). Mean annual atmospheric precipitation averaged from three meteorological stations (Gangcha, 37°19'N, 100°10'E; Tianjun, 37°17'N, 99°2'E; Haiyan, 36°53'N, 100°59'E) located in the Lake Qinghai drainage area is 373 mm. Recently, about 65% of the annual precipitation falls during the summer months (June-August), indicating a strong contribution of the EASM (An *et al.*, 2012). Due to high insolation the mean annual evaporation is about 800 mm (Coleman *et al.*, 2007). During the winter months, the region is primarily influenced by a combination of the constantly streaming Westerlies and by the AWM originating from a very cold high pressure zone over Siberia and Mongolia (An *et al.*, 2012). The cold mountainous environment has a mean annual temperature of -0.7 °C with daily averages of 10.4 °C to 15.2 °C in July and -10.4 °C to -14.7 °C in January (Henderson *et al.*, 2010), reflecting a rather high degree of seasonality (Coleman *et al.*, 2007).

Figure 2.2: (A) Overview map showing the regional vegetation distribution pattern around Lake Qinghai and Daotang Pond in the north-eastern QTP (after Hou, 2001). A forb meadow/*Kobresia meadow* is directly adjoining to the study site (red triangle). Northern and western dry lowlands are covered by a temperate semi-shrubby and shrubby desert, south-eastern regions are characterised as alpine meadow, Qilian Mountain forest scrub and in the south alpine steppe vegetation communities are distributed. (B) Photo of the coring site location environments at Daotang, north-eastern QTP. (C) Detail map showing the area around Daotang Pond, with the Daotang River as the major inflow. Coring site location (36°57'35.4 N, 100°74'48.4 E) is indicated by the red triangle

2.2.2 Vegetation

The Daotang area is surrounded by a high mountainous dry adapted alpine meadow, alpine steppe and desert vegetation (Figure 2.2., a and b), which nowadays is highly impacted by grazing of cattle, sheep and goats (Miehe *et al.*, 2008). Directly adjoined to the Daotang River and Daotang site is a forb meadow vegetation with prominent Iridaceae (*Iris lactea*), which transits into a temperate needle grass steppe, dominated by *Achnatherum splendens*, and further into widespread high-cold *Kobresia* sedge meadows, mainly consisting of *Kobresia pygmaea*. These temperate forms covering the vast plains around Daotang and Lake Qinghai are known as an indicator of permanent and severe human impact (Miehe *et al.*, 2008, 2011). In more distant regions to the north and west the vegetation changes into shrubby and semi-shrubby deserts associated with prevailing drier conditions and lower elevations. In the northern vicinity, where the elevation decreases towards Inner Mongolia, these landscapes are characterised by the dominant occurrence of several Tamaricaceae and Chenopodiaceae species (e.g. *Reaumuria soongoria-Ceratiodes latens* desert) as temperate shrubby and semi-shrubby desert zones. *Ephedra-Tamarix-Nitraria* desert in the dry Qaidam Basin occurs in the west (Hou, 2001), whereas in the Qilian Mountain valleys at lower elevations east of Daotang a forest/scrub and alpine meadow steppe district with *Potentilla fruticosa* and several *Picea* and *Carex* species is established (Wang *et al.*, 2002). Further in the south, mountainous steppe and meadow vegetation with *Potentilla* scrubs and diverse *Kobresia* mats dominate the landscape (Kürschner *et al.*, 2005).

2.2.3 Human impact

The history of human activity on the north-eastern QTP is rather complex, thus the type and degree of human impact on the vegetation cover change through time and micro-regions. The human behaviour and migrations of sedentary and herdsmen populations in the Lake Qinghai region is linked to prevailing weather conditions (Putnam *et al.*, 2016). During the last two millennia the region was inhabited mainly by pastoral nomads herding livestock and performing hunting and gathering, though sedentary population became more numerous during the strong Chinese central power associated with the Han, Tang and Ming dynasty (Sheppard *et al.*, 2004). The first significant increase of archaeological sites in the Lake Qinghai region is dated to the second millennium BC (Hosner *et al.*, 2016), but became more evident during the historical dynastic period.

Economic and climatological instability forced settlers and nomads to move frequently, causing continuous shifts in human land use and the impact on the vegetation cover. Since the Sui and particularly during the Tang dynasty, horse breeding became widespread in the western regions of China (Wertmann *et al.*, 2016). This activity continued markedly through the Mongol time (CE 1244-1368) and further, thus it can be assumed, that wood being used for fencing is the reason for a continuous decline of forests and tree stands on the north-eastern QTP which lead to a general enlargement of the nowadays vast grasslands (Gernet, 1997).

2.2.4 Study site

The Daotang coring site (36°57'35.4 N, 100°74'48.4 E; 3205 m a.s.l.) is situated approximately 2 km southeast of Lake Qinghai on the QTP (Figure 2.1). The pond and surrounding wetland is part of the catchment of the Daotang River, whose outflow contributes to Lake Erhai, a beach-wall pond bordering Lake Qinghai (Figure 2.2, c). The shallow water covers an area of roughly 4 km^2. The maximum water depth was not investigated, but in August 2013, the water was about half a meter deep at the coring location near the outflow.

2.3 Material and methods

2.3.1 Core background information and dating

A 136 cm long sediment core (QW14) was retrieved in August 2013 with an UWITEC short coring system (60 mm diameter) from approximately 50 cm water depth (Figure 2.2, b). It was sub-sampled in the field in 1 cm steps and transferred to FU Berlin, Germany, for further investigation. The sediment throughout the core mostly consists of homogenous dark-grey organic gyttja with no visible lamination. Some parts differ only slightly in the amount of siliciclastic components and an associated lighter mid-grey colour. Organic bulk material from four samples (QW14 8-9, QW14 35-36, QW14 80-81, QW14 133-134), containing organic bulk material, were sent to be dated in the Poznan Radiocarbon Laboratory. The accelerator mass spectrometry (AMS) radiocarbon dates provided in Table 2.1 were converted into calendar dates (cal. CE) with the help of CALPAL-2007 (Weninger and Jöris, 2008; Weninger *et al.*, 2015) and further used for constructing the age model of the QW14 record. Table 2.1 also provides uncertainty intervals of calendar age, where the true ages of the samples encompass with the probability of 68.2% and 95.4%. These uncertainty intervals were calculated using the OxCal software (OxCal v4.1.5, Ramsey *et al.* (2010); r:5; https://c14.arch.ox.ac.uk/oxcal/OxCal.html) and atmospheric data from Reimer *et al.* (2009).

The third point in the age model is the date CE 2013 assigned to the core top. This initial suggestion obtained by visual investigation during the coring campaign has been later approved by the recent analysis of the topmost sediment layer at the study site using the 210Pb (lead-210) method (Yan *et al.*, 2017).

2.3.2 Pollen analysis

Pollen and spores were extracted out of 3 g soggy sediment. A *Lycopodium* spore tablet (Batch no. 177745, spore content in each tablet: 18,584±372) was added to each sample prior to the laboratory treatment in order to evaluate the pollen and spore concentration after counting. The laboratory treatment followed the basic method of Faegri *et al.* (1989), including an overnight step in HF (hydrofluoric acid, 39%) followed by acetolysis and 7 μm ultrasonic fine sieving. Samples in 2 cm steps were further processed and analysed. Each sample contains 1 cm material and is thus labelled after its average depth in half-cm steps. In total 62 samples were counted up to a minimum number of 300 pollen grains using a

Table 2.1: AMS radiocarbon dates processed on samples from the QW14 core, which were used in the age-depth model for the Daotang record presented in this study. The dates were generated in the Radiocarbon Dating Laboratory at Poznan, Poland. The dates expressed in ^{14}C BP (radiocarbon years before 1950 CE) were converted to calendar dates (CE) using CALPAL-2007 (Weninger and Jöris, 2008; Weninger *et al.*, 2013). The 2 sigma (95.4%) and one sigma (68.2%) confidence intervals are calculated using OxCal v4.1.5 calibration software (Ramsey *et al.*, 2010; https://c14.arch.ox.ac.uk/oxcal/OxCal.html) and atmospheric data from Reimer *et al.* (2009). The two dates from the upper part of the core show unrealistically older ages and therefore are not considered in the final age model. The core top in the age model is assigned to the date CE 2013. Analysis of the topmost sediment layer at the study site using the 210Pb (lead-210) method confirmed this assumption (Figure 2.3).

Sample name	Laboratory number	Core depth (cm)	Radiocarbon age (^{14}C yr BP)	Cal. age (yr CE)	68.2% confidence interval (yr CE)	95.4% confidence interval (yr CE)
Pb/Cs*	–	0.0	-63	2013	–	–
QW 8-9	Poz-58700	8.5	310 ± 30	1569 ± 52	1521-1643	1485-1650
QW 35-36	Poz-58703	35.5	715 ± 25	1275 ± 8	1270-1290	1259-1380
QW 80-81	Poz-58701	80.5	540 ± 25	1374 ± 40	1331-1426	1320-1435
QW 133-134	Poz-58702	133.5	1165 ± 25	863 ± 52	782-937	777-963

Meiji Techno (MT 4300L) microscope at 400× and 600× magnification. Pollen identification was supported by published pollen atlases (e.g. Reille, 1992–1998; Beug, 2004) and the reference collection of modern pollen taxa at FU Berlin. The pollen percentages were calculated based on all present pollen types excluding spores, algae and hypha. The diagram is generated using TILIA, TILIA Graph and TG View Software 1.7.16 (Grimm, 2011). Six subzones (PSZ a-f) within the pollen diagram can be defined based on the results of the CONISS cluster analysis (Grimm, 2011). For clarity only pollen taxa which exceed 1% of the total pollen sum in at least one sample are shown in the diagram. Except for pollen, remains of the green algae (*Pediastrum* sp. and *Botryococcus* sp.) colonies, as well as hyphae of the fungi genus *Glomus*, were counted and their percentages were calculated based on the total pollen sum. Complete data set is deposited at the Open Access information system PANGAEA (https://doi.pangaea.de/10.1594/PANGAEA.919329)

2.3.3 Interpretation methods

The *Artemisia*/Chenopodiaceae (A/C) pollen percentage ratio (El-Moslimany, 1990) has been calculated for further interpretation. The ratio has been applied to distinguish between steppe and desert vegetation, particularly of arid central Asia (e.g. Van Campo, 1996; Demske and Mischke, 2003) and China (Herzschuh *et al.*, 2004). When used for interpreting past climate conditions (e.g. Herzschuh *et al.*, 2004; Leipe *et al.*, 2014) the generalised assumption is that Chenopodiaceae plant taxa are more common in desert-like environments, whereas *Artemisia* prefer less dry steppe environments. The calculated pollen concentration, the pollen accumulation rate (PAR) and the ratio of arboreal pollen

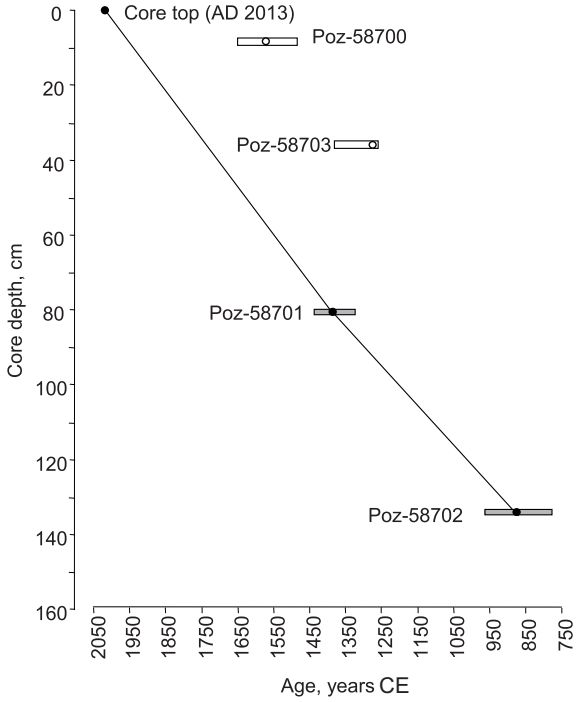

Figure 2.3: Age-depth model of the Daotang QW14 core record used in the current study. Three fixed points indicate the core top and the two AMS measurements converted into calendar years. White rectangles indicate 95.4% confidence interval of the radiocarbon date (see Table 2.1 for details).

(AP) to non-arboreal pollen (NAP) are also used to discuss vegetation composition, density and the influx amount of pollen out of long-distance transport, and to interpret changes in the regional climate (Cour *et al.*, 1999; Yu *et al.*, 2001; Herzschuh *et al.*, 2006).

2.4 Results

2.4.1 Age-depth model

The age-depth-model for the investigated core QW14 suggests that the record covers approximately 1200 years, starting from about CE 850 (Figure 2.3). Linear interpolation between the dates has been used demonstrating relatively stable sedimentation rate of about 1 mm per year.

2.4.2 Fossil pollen record

In total, 60 pollen taxa have been identified in 62 examined samples of the QW14 profile from Daotang (https://doi.pangaea.de/10.1594/PANGAEA.919329). In the simplified percentage diagram (Figure 2.4) 41 pollen taxa are shown. The pollen types are grouped based on the growth form and edaphic conditions of the pollen producing plants into trees and shrubs, herbs and grasses and aquatics, respectively, whereas the group herbs and grasses contains most of the identified pollen types. A CONISS cluster analysis calcu-

lating constrained incremental sum of squares helped to define 6 pollen sub-zones (PSZ a-f, Figure 2.4) reflecting changes in pollen composition and percentages. Furthermore, counted remains of the green algae colonies of *Pediastrum* sp. and *Botryococcus* sp., as well as hyphae of the fungi genus *Glomus*, are shown in the diagram (Figure 2.4) are used to interpret local environmental conditions.

2.4.3 Brief description of the pollen record

PSZ f (135.5–128.5 cm, CE 850–910) consists of four samples (59-62) from the lowest part of the core and is characterised by an increase in *Artemisia* pollen percentages towards the uppermost sample, accompanied by a decrease in Poaceae, whereas Chenopodiaceae and Ranunculaceae pollen percentages throughout this zone are rather high. Noticeable is the generally low amount of Cyperaceae accompanied by an apparent sparse amount of the aquatic pollen taxa *Hippuris* and *Myriophyllum*. The pollen concentration is low in this subzone.

PSZ e (samples 56-58, 126.5–122.5 cm, CE 930–970) is compositionally very close to PSZ f. However, it reveals an extraordinary peak of *Myriophyllum* pollen and almost complete absence of *Hippuris*, accompanied by low *Botryococcus* and *Glomus* percentages. Grass pollen percentages are low, whereas *Artemisia* and Chenopodiaceae still remain high. The regional pollen input is represented by a *Carpinus* pollen peak and frequent appearances of *Pinus*, *Nitraria*, *Hippophae* and *Salix*.

PSZ d (samples 41-55, 120.5–91.5 cm, CE 990-1270) shows some fluctuations within the three most prominent pollen types accounting for the local pollen signal, i.e. *Artemisia*, Cyperaceae and Poaceae. Otherwise percentages are relatively stable. The regional pollen signal is characterised by *Pinus* and *Carpinus*, which are more abundant in the lower part of this subzone, whereas *Quercus* and *Nitraria* are more prominent in the upper part. The frequent occurrence of Saxifragaceae pollen and a high abundance of *Helianthemum* and Ranunculaceae are also noticeable. In the samples with high percentages of Ranunculaceae increasing *Bortyococcus* and *Hippuris* and a higher amount of *Glomus* also occur.

PSZ c (samples 34-40, 89.5–72.5 cm, CE 1290-1440) is characterised by a high amount of *Pediastrum*, increasing *Botryococcus* and a stable *Myriophyllum* contents. The overall highest percentages of *Artemisia* and Chenopodiaceae pollen, accompanied by low Cyper-

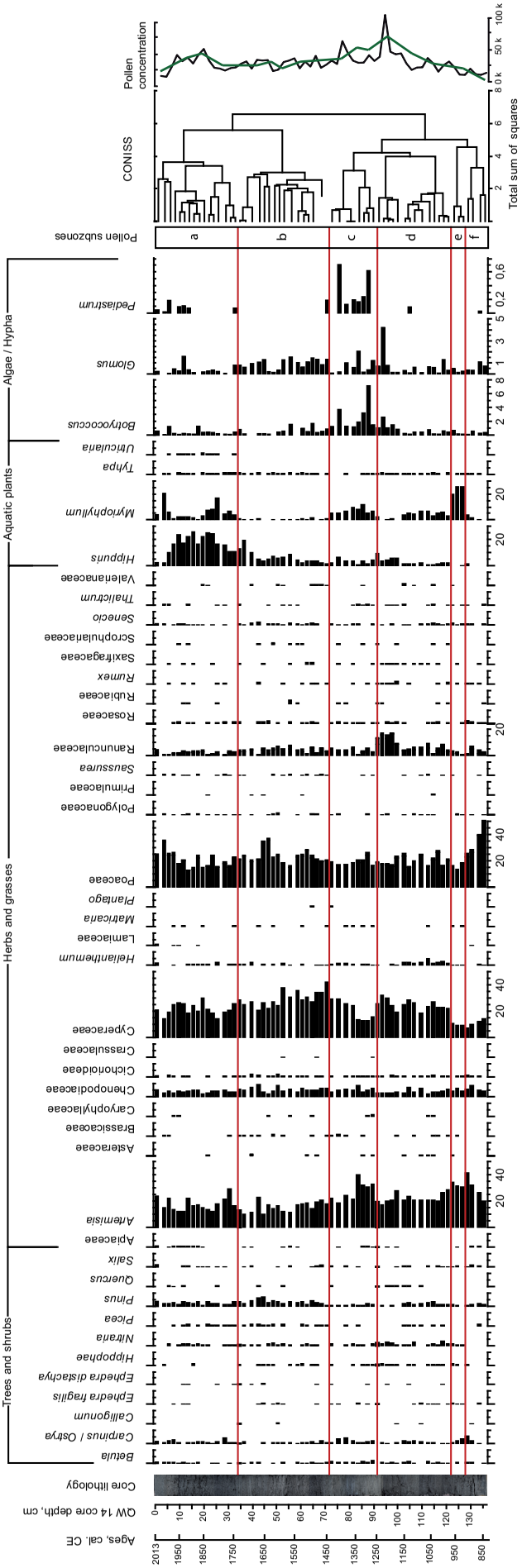

Figure 2.4: Simplified percentage diagram presenting the results of the palynological analysis of the Daotang core record plotted together with the lithology column along the depth and age axes.

aceae percentages, are observed in the lower part of this subzone. The regional pollen signal is characterised by frequent *Carpinus*, *Betula* and *Quercus* pollen grains and relatively few *Pinus* pollen.

PSZ b (samples 17-33, 70.5–34.5 cm, CE 1450–1740) is characterised by the highest values of *Pinus* pollen, accompanied by *Nitraria*, *Picea* and *Hippophae*. In contrast, *Carpinus* and *Betula* pollen percentages are low. The local climate is displayed in the high grass pollen values of Poaceae and Cyperaceae. Additionally, the *Artemisia* abundance is lowest in this part of the record, whereas *Senecio*, Cichorioideae, Brassicaceae as well as other entomophilous plant taxa are frequently present and the highest percentages of Chenopodiaceae occur. The aquatic pollen taxa percentages are greatly diminished. *Hippuris* appears only in low amounts and *Myriophyllum*, as well as *Pediastrum*, are almost absent. However, a steady input of *Glomus* should be noticed.

PSZ a (samples 1-16, 32.5–0.5 cm, CE 1750–2013). In the upper part of the core the percentages of *Hippuris*, *Utricularia* and *Myriophyllum* pollen increase and *Pediastrum* appears in the upper part. The lowest percentages of Ranunculaceae and Chenopodiaceae pollen occur. Whereas Apiaceae pollen grains frequently appear and more Lamiaceae pollen can be found, Brassicaceae and Cichorioideae pollen percentages are low. Regional pollen taxa are represented by increased values of *Carpinus*, *Salix* and *Quercus*, whereas *Pinus* and *Hippophae* pollen decrease in abundance.

2.4.4 The A/C pollen ratio

The A/C ratio (Figure 2.5) is fluctuating between 1.6 and 11 in the Daotang record with a decreasing trend throughout the core from the bottom to the top. PSZ d-f have an average A/C value between 6 and 8 with minor fluctuations, except for a period around CE 1050, when the highest value is followed by a sudden drop to below 4. In PSZ a-c the values are gradually decreasing with an average of 4 to 5, though two peaks (up to 8) occur around CE 1600 and CE 1750. Lowest A/C ratio values appear around CE 1700.

2.4.5 Pollen concentration and AP/NAP ratio

The pollen concentrations (between 1785 and 106939) throughout the record show an increasing trend from PSZ f to the end of PSZ d (Figure 2.5), with highest value around CE 1250. Except for another two peaks in the middle of PSZ a, the values are decreasing

again and show minor fluctuations. The ratio of arboreal pollen to non-arboreal pollen is characterised by two prolonged minima in the lower part of the core (PSZ f-d, CE 950-1000 and CE 1150-1200) and short term fluctuations in the upper part PSZ c-a with a peak of arboreal pollen around CE 1650.

2.5 Discussion

The Daotang pollen record begins at CE 850 within the favourable and rather wet climate phase often attributed to the MWP. Corresponding studies suggest that it started in the 9-10 century CE on the north-eastern QTP (Yang *et al.*, 2002; Shi *et al.*, 1999; Paulsen *et al.*, 2003) and ended sometime during the 13-14 century CE (Xu *et al.* 2008). The north-eastern QTP is dominated by strong monsoonal winds and constant moisture input from the EASM (Wernicke *et al.*, 2015). Therefore, the environment around Daotang Pond is highly impacted by a changing EASM strength (Figure 2.5).

A short-term dry event which appears within the generally humid MWP around CE 850-890 in the Daotang record is not mentioned by any other climate reconstruction from the Lake Qinghai area. However, several high-resolution records, including the Guliya Ice Core record in the western Kunlun Mountains (Thompson *et al.*, 1997; Yang *et al.*, 2009b), the central Chinese Wanxiang Cave stalagmite record (Zhang *et al.*, 2008) and a lacustrine climate reconstruction from western Inner Mongolia (Chen *et al.*, 2010) also report a short warm and dry interval during this time.

Another slightly dry phase in the Daotang record occurred CE 1050-1150. Zhang *et al.* (2004) suggested a phase of high salinity in Lake Qinghai with a little offset to that in Daotang Pond, dated from CE 1100 to CE 1160. In the Pond, the dry phase was followed by an exceptionally wet phase with a high water stand from CE 1160 to CE 1290. In this timeframe, reconstructed salinity in Lake Qinghai was also low indicating a wet period (Zhang *et al.*, 2004). Henderson *et al.* (2010) also noticed an earlier onset of a rather strong EASM between CE 1100 and 1250 in the region.

Often mentioned is a warm and dry phase, which affected the north-eastern QTP towards the end of the MWP from CE 1250 to CE 1400 (e.g. Ji *et al.*, 2005; Henderson and Holmes, 2009; He *et al.*, 2013). Thus, Ji *et al.* (2005) reported the driest interval around Lake Qinghai at CE 1150-1350, which is not in phase with the reconstruction from Daotang, where the dry period began as late as at CE 1290. Supporting our interpretation, Henderson and Holmes (2009) referred to a dry and warm period around the time of the

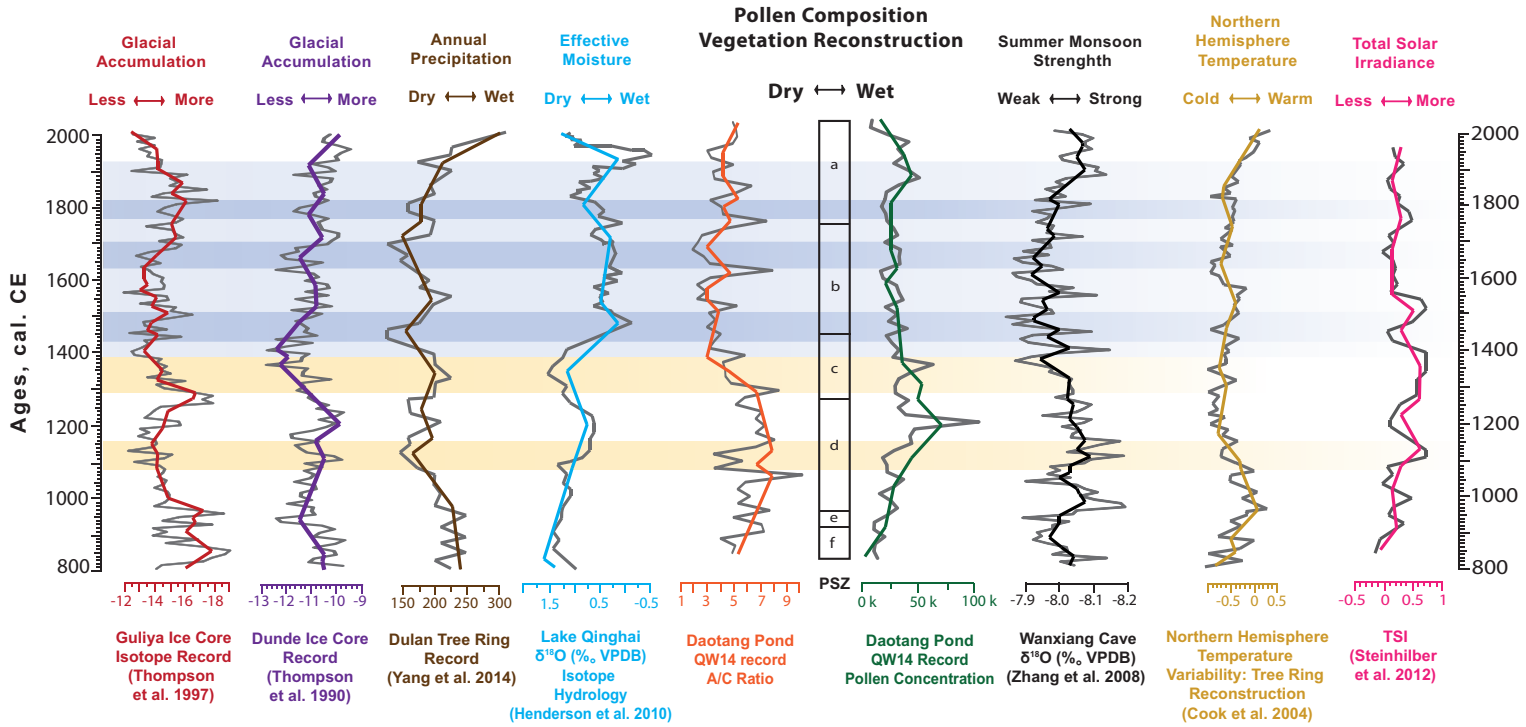

Figure 2.5: Summary chart showing changes in the Daotang A/C ratio and pollen concentration in comparison to published environmental records from several locations, arranged from West (left) to East (right): Guliya Ice Core (Thompson *et al.*, 1997), Dunde Ice Core (Thompson *et al.*, 1990), Dulan Tree Rings (Yang *et al.*, 2014), Lake Qinghai (Henderson *et al.*, 2010) and Wanxiang Cave Stalagmite (Zhang *et al.*, 2008). Additionally, Northern Hemisphere Temperature (Cook *et al.*, 2004) and Total Solar Irradiance (Steinhilber *et al.*, 2012) are shown. Yellow bars indicate dry phases, and light blue bars indicate colder than average phases, and dark blue bars indicate very cold phases in the QTP region.

Mongol reign (CE 1244-1368). However, Zhang *et al.* (2004) reconstructed low salinity in Lake Qinghai between CE 1330 and 1410, thus suggesting a moist climate interval.

There are several possible explanations for the leads and lags in the reconstructed climatic events in the records from the same region. Inadequate dating control is one of the common problems for the sedimentary-based climate archives representing QTP and the Lake Qinghai region (see Henderson and Holmes, 2009; Yang *et al.*, 2009a; Hou *et al.*, 2012 for discussion and references). Another problem could be an inadequate sensitivity of the different proxy records to the climate change. The climatic archive derived from the Dulan juniper tree rings (Yang *et al.*, 2014) is located outside the zone of EASM precipitation and reflects convective rains originating from evaporation over the QTP. Yang *et al.* (2014) state that increasing temperatures and landmass-heating in summer caused enhanced evaporation on the plateau and thus the available atmospheric moisture for the Dulan juniper trees was higher during the MWP. Additionally, Yang *et al.* (2014) reported a direct correlation between the Dulan precipitation and the Northern Hemisphere Temperature (NHT; Cook *et al.*, 2004) during recent millennia (Figure 2.5). Correlations to the Total Solar Irradiance (TSI; Steinhilber *et al.*, 2012) and NHT (Cook *et al.*, 2004), as major factors driving monsoon circulation, can be seen in the Daotang Pond pollen record as well as in the record from the western QTP (Guliya Ice Core, Figure 2.5).

Evapotranspiration represents an important factor, which influences moisture availability in the Lake Qinghai drainage basin (Henderson *et al.*, 2010) and may complicate the pollen and vegetation based climate reconstructions. However, the EASM represents the most important moisture source for the north-eastern QTP environments (Henderson *et al.*, 2003, 2010). This is also suggested by the Daotang pollen record, in which arboreal pollen taxa representing eastern (more humid) regions more frequently appear during the intervals of stronger EASM, such as MWP. Henderson *et al.* (2010) pointed out, that in the Lake Qinghai region the EASM precipitation was more important during the MWP than during the LIA. However, the vegetation communities during the LIA could locally profit from the decreased temperatures and evapotranspiration. This seems to be true for the Daotang area, as the pollen record suggests that during the LIA decreased EASM precipitation was likely compensated by lower evaporation and did not destroy surrounding wetland and meadow vegetation (An *et al.*, 2006).

A gradual shift to colder conditions on the north-eastern QTP marks the onset of the LIA period beginning roughly at CE 1450. This phase is mostly influenced by strong

Westerly winds, therefore more *Pinus* and *Picea* pollen, as well as *Ephedra* out of the western steppe regions occur in the Daotang record. The local pollen taxa composition indicates a moderately wet LIA with only two short term dry events (around CE 1700 and CE 1800) and generally colder temperatures than during the MWP. Henderson *et al.* (2010) reconstructed an overall dry LIA due to a retreat of EASM, which is barely seen in the isotope record from Lake Qinghai (Figure 2.5). A short dry episode reconstructed from the Lake Qinghai sedimentary archives around 1500 CE (e.g. Zhang *et al.*, 2004; Huang and Zhang, 2007; Xu *et al.*, 2007) within the Spörer Minimum cannot be seen in the Daotang pollen record, suggesting the local vegetation did not undergo severe changes related to the colder climate. This might be due to locally wet environments, but also because the colder temperatures are not as restrictive a factor as lack of moisture for the most of the local plants. The coldest period of the LIA around the Dalton Minimum (CE 1790 to CE 1830) is expressed by increased regional dryness in the Daotang record. This exceptionally cold period affected the vegetation more than previous colder phases, because also runoff in summer was restricted and evaporation over the QTP diminished due to lower solar irradiance, causing a lack of convective summer rainfall. This result is consistent with most other published climate records from the north-eastern QTP. Nowadays, increased summer temperatures triggers strengthened monsoon activity. Therefore, the EASM penetrates the north-eastern QTP regularly (e.g. Jiang *et al.*, 2015) and summer precipitation is mostly brought by the EASM.

The data comparison (Figure 2.5) suggests that the EASM influence in the Daotang area was stronger during the MWP and Westerly influence prevailed during the LIA, interrupted by short term episodes of stronger monsoon. However, some inconsistencies mentioned in the discussion also should be noted as a target for future investigations. In the north-eastern QTP changes in vegetation could be at least partly caused by humans (Wischnewski *et al.*, 2014). However, our record does not indicate direct human impact at and around the study site prior to the industrial period, i.e. before CE 1950. Therefore, reconstructed changes likely reflect natural climatic and environmental variability in a highly sensitive wetland, which potential as a regional paleoclimatic archive remains underexploited to date.

2.6 Conclusions

1. The Daotang record, located at the interface of EASM and Westerly winds, reveals the possibility to detect even minor changes in the vegetation cover caused by fluctuating strength and weaknesses of the prevailing wind system. Local and regional climate differ at times, but both can be attributed to the widespread climate anomalies of the MWP, which occurs in the Daotang record at CE 850-1400, and the LIA around CE 1450-1950.

2. Regular EASM penetration around Lake Qinghai drainage basin during a generally humid and warm MWP occurs. Due to a moist micro-climate around Daotang Pond, dry periods during the MWP are not as severe and thorough as recognised in other regional EASM influenced records drier phases during the MWP can be detected around CE 850-890, CE 1050-1150 and CE 1290-1400.

3. General fewer moisture input into lacustrine systems on the north-eastern QTP caused by weaker EASM winds during the LIA is balanced through lower insolation and, thus, lower temperature and diminished evapotranspiration. During a generally humid LIA only two shortterm dry events (around CE 1700 and CE 1800) and one event around the Dalton Minimum (CE 1790 to CE 1830) can be detected in the Daotang record.

4. Deviating temporal appearance of dry or wet phases reconstructed from QTP records are caused by each unique local setting and investigated systems, such as local geomorphology, catchment size, elevation (m a.s.l.) and the applied approach for reconstruction. additionally, difficulties of accurate dating obstruct comparisons at a high resolution.

5. Habitation and pastoral use as rangeland imprinted on the environment of the NE-QTP. Human landuse started much earlier than the oldest part of the Daotang Pond pollen record, thus the vegetation has already extensively been changed and further human impact cannot be detected.

2.7 Acknowledgements

I am highly grateful for outstanding support of Frank Riedel, whose suggestions and support were vital to this manuscript. I am also deeply thankful to Pavel Tarasov, who helped to interpret the pollen data and contributed greatly to this manuscript with intensive discussions. Many thanks to Steffi Hildebrandt, Stefanie Müller and Dieter Demske (all FU Berlin) for the help with rare pollen types identification, to Christian Leipe and Jan Evers (both FU Berlin) for drafting the overview maps and picture processing and to Robert Wiese (FU Berlin) for the laboratory treatment of the sediment samples. I also like to thank Mayke Wagner (DAI Berlin) for paying the radiocarbon dating and Tomasz Goslar (Poznan Radiocarbon Laboratory) for handling the samples in the laboratory and providing the age determination. I also gratefully thank Bernd Wünnemann and his working group at Nanjing University for comments and suggestions regarding the core chronology. Thanks a lot to the participants of a field course training of FU Berlin and Nanjing University for their active support in retrieving the QW14 core. The field trip was jointly funded by the Nanjing University, FU Berlin and the German Academic Exchange Service (DAAD).

Chapter 3

Inter- and intra-tree variability of carbon and oxygen stable isotope ratios of modern pollen from nine European tree species

Carolina Müller[1,2], *Manja Hethke*[1], *Frank Riedel*[1], *Gerhard Helle*[1,2]

[1]Institute of Geological Sciences, Palaeontology, Freie Universität Berlin, Berlin, Germany
[2]GFZ German Research Centre for Geoscience, Section 4.3 Climate Dynamics and Landscape Evolution, Potsdam, Germany

Published in *PLoS ONE* 15(6): e0234315 (9 June 2020)
https://doi.org/10.1371/journal.pone.0234315

Abstract

Stable carbon and oxygen isotope ratios of raw pollen sampled from nine abundant tree species growing in natural habitats of central and northern Europe were investigated to understand the intra- and inter-specific variability of pollen-isotope values. All species yielded specific $\delta^{13}C_{pollen}$ and $\delta^{18}O_{pollen}$ values and patterns, which can be ascribed to their physiology and habitat preferences. Broad-leaved trees flowering early in the year before leaf proliferation (*Alnus glutinosa* and *Corylus avellana*) exhibited on average 2.6‰ lower $\delta^{13}C_{pollen}$ and 3.1‰ lower $\delta^{18}O_{pollen}$ values than broad-leaved and coniferous trees flowering during mid and late spring (*Acer pseudoplatanus*, *Betula pendula*, *Carpinus betulus*, *Fagus sylvatica*, *Picea abies*, *Pinus sylvestris* and *Quercus robur*). Mean species-specific $\delta^{13}C_{pollen}$ values did not change markedly over time, whereas $\delta^{18}O_{pollen}$ values of

two consecutive years were often statistically distinct. An intra-annual analysis of *B. pendula* and *P. sylvestris* pollen revealed increasing $\delta^{18}O_{pollen}$ values during the final weeks of pollen development. However, the $\delta^{13}C_{pollen}$ values remained consistent throughout the pollen-maturation process. Detailed intra-individual analysis yielded circumferential and height-dependent variations within carbon and oxygen pollen-isotopes and the sampling position on a tree accounted for differences of up to 3.5‰ for $\delta^{13}C_{pollen}$ and 2.1‰ for $\delta^{18}O_{pollen}$. A comparison of isotope ranges from different geographic settings revealed gradients between maritime and continental as well as between high and low altitudinal study sites. The results of stepwise regression analysis demonstrated, that carbon and oxygen pollen-isotopes also reflect local non-climate environmental conditions.

A detailed understanding of isotope patterns and ranges in modern pollen is necessary to enhance the accuracy of palaeoclimate investigations on $\delta^{13}C$ and $\delta^{18}O$ of fossil pollen. Furthermore, pollen-isotope values are species-specific and the analysis of species growing during different phenophases may be valuable for palaeoweather reconstructions of different seasons.

3.1 Introduction

Stable carbon and oxygen isotope ratios of plant material are generally determined to understand the relationship between plants and their surrounding environment (Dawson *et al.*, 2002). The continuously deepening knowledge of stable isotope patterns in plants of natural habitats finds applications in, for example, plant ecology, phytochemistry, genetic research and reconstructions of past environmental changes (Helle and Schleser 2004; McCarroll and Loader, 2004; Jones *et al.*, 2009; Gessler *et al.*, 2014; van der Sleen *et al.*, 2017). Plant physiological reactions to environmental factors, such as temperature, moisture availability and density of the surrounding vegetation, are known to affect the stable carbon and oxygen isotope composition of plant material (Lockheart *et al.*, 1997; Dawson *et al.*, 2002; Graham *et al.*, 2014). Carbon isotope ratios ($\delta^{13}C$) of plant material are mostly determined by the factor-dependent amount of discrimination against ^{13}C during CO_2 uptake and by subsequent photosynthetic processes (e.g. O'Leary, 1988; Farquhar *et al.*, 1989), while oxygen isotope ratios ($\delta^{18}O$) are often linked with the isotopic composition of environmental source water (Ehleringer and Dawson, 1992; Flanagan and Farquhar, 2014; Schwarz, 2016).

In general, the stable carbon isotope composition of stem material, leaves and pollen

of the same plant individual highly correlate with one another (Jahren, 2004; Schwarz, 2016; Bell *et al.*, 2017). Research on stable carbon isotope ratios of modern pollen focused mainly on species-specific patterns and ranges (Amundson *et al.*, 1997; King *et al.*, 2012; Nelson, 2012; Bell *et al.*, 2017;) and has been applied to investigate predominant photosynthetic pathways within grasslands (Nelson *et al.*, 2006; Descolas-Gros and Schölzel, 2007; Urban *et al.*, 2013). Loader and Hemming (2001) analysed $\delta^{13}C_{pollen}$ of *Pinus sylvestris* from 28 sites across Europe and identified a positive linear correlation between $\delta^{13}C$ values and the prevailing temperature during pollen formation. Also, Jahren (2004) detected positive correlations of $\delta^{13}C_{pollen}$ values with temperature for nine out of 14 plant species. Studies focussing on the determination of influencing climate factors on the isotope values of modern pollen include Bell *et al.* (2017), who showed that $\delta^{13}C_{pollen}$ of *Cedurs atlantica* (Atlas cedar) correlates with precipitation and a long-term annual and summer scPDSI (self-calibrating Palmer Drought Severity Index). Schwarz (2016) suspected a relationship between $\delta^{13}C_{pollen}$ and relative humidity, but no significant correlation of $\delta^{13}C_{pollen}$ of *Pinus retinosa* (Red pine), *Pinus sylvestris* (Scots pine) and *Quercus rubra* (Northern red oak) could be detected at North American sampling sites. However, all correlations were highly species-dependent and several plants strongly reacted to other untested environmental factors, superimposing the climate signal archived in the pollen (Jahren, 2004).

Little is known about the variability within modern oxygen pollen-isotope values. Nonetheless, they have already been successfully applied to determine the provenance of honey (e.g. Chesson *et al.*, 2011 and 2013). Loader and Hemming (2004) identified a negative relationship of $\delta^{18}O_{pollen}$ values with the $\delta^{18}O$ values of precipitation during pollen formation, contrasting $\delta^{18}O$ of wood and leaves that is typically positively related to the $\delta^{18}O$ of precipitation (e.g. Saurer and Siegenthaler, 1989; Saurer *et al.*, 1997). Even if the $\delta^{18}O_{pollen}$ is highly determined by the $\delta^{18}O$ of local precipitation, the degree of dependence seems to vary with plant type and physiology (Schwarz, 2016). Hence, $\delta^{13}C_{pollen}$ and $\delta^{18}O_{pollen}$ values are influenced by local climate conditions during pollen formation (Loader and Hemming, 2001; Bell *et al.*, 2017), but not all variability within pollen-isotope values can be ascribed to climate-related environmental factors alone. Morphology-based analysis of fossil pollen is frequently used to reconstruct palaeovegetation, since fossil pollen are often well preserved, widespread and abundant in various Cenozoic archives (Birks and Birks, 1980; Moore *et al.*, 1991; Traverse, 2007; Bezrukova *et al.*, 2010; Speer, 2010; Demske *et al.*, 2013; Müller, 2017). A combination of traditional pollen analysis and stable isotope analysis of fossil pollen might enhance environmental reconstructions

in a high spatio-temporal resolution. Due to plant-specific timings in pollen production and pollen shedding, even intra-annual weather signals may be recorded in the $\delta^{13}C_{pollen}$ and $\delta^{18}O_{pollen}$ (Schwarz, 2016). Some studies have already applied $\delta^{13}C$ analysis to fossil pollen in an attempt to reconstruct past environmental changes (Nelson *et al.*, 2008; Kamenik *et al.*, 2009; Urban *et al.*, 2016). A fossil $\delta^{13}C_{pollen}$ record of *C. atlantica* from Morocco revealed the feasibility of reconstructing a long-term trend of increasing aridity by analysing species-specific pollen-isotopes (Bell *et al.*, 2019). Also, fossil *Nothofagus* (Southern beech) $\delta^{13}C_{pollen}$ indicated different moisture availability in Antarctica during the early and middle Eocene (Griener *et al.*, 2013).

However, interpretation of fossil pollen-isotopes are based on observations of modern $\delta^{13}C_{pollen}$ and $\delta^{18}O_{pollen}$ patterns and ranges. In addition to climate conditions during pollen formation, non-climate impact factors may need to be considered when interpreting the $\delta^{13}C_{pollen}$ and $\delta^{18}O_{pollen}$ values. These factors include site-specific environmental parameters such as type of soil, plant associations, position on slopes, and the proximity of the individual tree to perennial waterbodies. A comparison of several abundant tree species growing at different sites under the same environmental conditions, intra-tree differences and fluctuations over several vegetation periods helps to assess the impact of non-climate environmental factors on the pollen-isotope values.

In the present study, we address the species-specific natural variability of pollen-isotopes of nine abundant tree species across seven European sites ranging from Belgium to Poland and Finland to Italy, sampled during the years 2015 and 2016. The species have been chosen based on their widespread abundance in natural European forests and the frequency of their pollen in fossil records.

Inter- and intra-tree $\delta^{13}C_{pollen}$ and $\delta^{18}O_{pollen}$ isotope variabilities were assessed and tested for relationships with non-climate environmental factors by stepwise regression analysis. In doing so, we aimed to advance our understanding of pollen stable isotope signals for future palaeoclimate reconstructions. In detail we investigated:

1. Species-specific $\delta^{13}C_{pollen}$ and $\delta^{18}O_{pollen}$ patterns of selected tree taxa and the variability of their pollen-isotopes between two consecutive vegetation periods (2015/2016).

2. $\delta^{13}C_{pollen}$ and $\delta^{18}O_{pollen}$ at different stages of the pollen maturation process.

3. Variability of $\delta^{13}C_{pollen}$ and $\delta^{18}O_{pollen}$ at different heights and cardinal directions of individual trees.

4. $\delta^{13}C_{pollen}$ and $\delta^{18}O_{pollen}$ along a gradient of continentality (W – E transect) and along a gradient in day length (N – S transect).

3.2 Material and methods

3.2.1 Sampling locations, sample collection and preparation

We sampled modern pollen from 658 individual trees of nine selected tree species growing in seven national and nature parks, which we consider natural habitats (Figure 3.1; Table 3.1 and 3.2).

None of the species sampled in this study is endangered or protected and sampling followed generally a non-invasive scheme of few inflorescences per individual tree. Therefore, after contacting and consulting with the national park authorities of each sampling site, no specific permissions were required for these locations and activities. Pollen were collected during two consecutive vegetation periods (February to June of 2015 and 2016) within the species-specific flowering periods (Figure 3.2; Table 3.2). The schedule for sampling followed individual phenology and thus roughly the geographic distribution and climate conditions of west-east and south-north gradients in Europe (Ahas *et al.*, 2002). All selected tree species use the C3 photosynthetic pathway. In principle, 20 flowering individuals were sampled per site and per species (Table 3.2). In case of dense forests, trees close to hiking trails, forestry roads or glades were sampled because sunlight illuminating the full height of tree crowns allows the development of lower branches with inflorescences. Samples were taken with a pruning device and an extendable stick from branches at positions of one metre up to seven metres above ground. Male inflorescences were cut off and placed in plastic bags. Bulk -samples of an individual tree were composed of several inflorescences of different branches from various heights. In the field, the samples were kept in a cooling box. Later, they were stored in a refrigerator at 6 °C to prevent mould infestation. In the laboratory, the samples were dried in a drying oven at a maximum temperature of 45 °C for seven to nine days. Dry samples were kept in a freezer at -16 °C until further processing. The separation of pollen from other flower tissue was achieved by thorough rinsing with deionised water using sieves with mesh sizes from 10 μm to 200 μm. Following rinsing and sieving the pollen were freeze-dried for 48–72 hours until fully dehydrated, transferred into Eppendorf (2 ml) safe lock tubes and frozen at -16 °C for preservation.

To investigate intra-tree isotope patterns, an additional 152 intra-tree sub-samples were

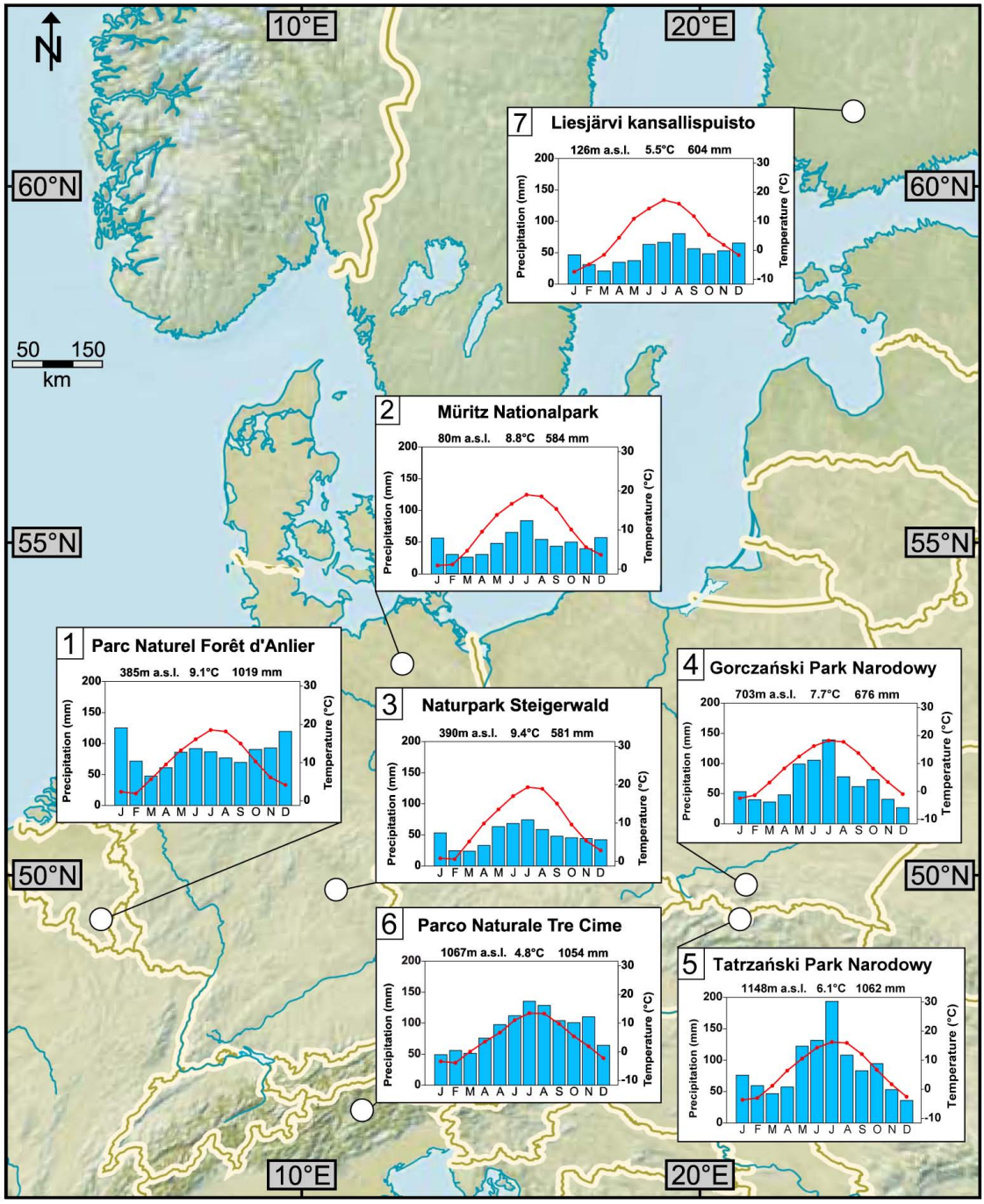

Figure 3.1: Study region (46.6°N – 53.3°N/5.7°E – 23.7°E). Topographic map of central Europe showing the sites (Nature Parks or National Parks) for pollen sampling (white dots) and respective climate diagrams with average seasonal temperature and precipitation. Refer to Table 3.1 for sampling site numbers and further details. Map modified from https://www.cia.gov/library/publications/the-world-factbook/index.html.

Site No.	Site name	Park authority address	Forest type and location characteristics (soil type after WRB-FULL)	Coordinates Altitude (masl) MAT (°C; min/max) MAP (mm)
1	Parc naturel Foret d'Anlier	Federation des PN de Wallonie Rue de Coppin 20 5100 Jambes Belgium ☎ +32 81 30 21 81 ✉ info@fpnw.be	Mesophytic deciduous broad-leaved and mixed coniferous-broad-leaved forest; beech and mixed beech forest, montane to altimontane type, partly with fir and spruce (Dystric Cambisol)	49.7899° N, 5.6829° E 385 9.1 (-0.1/16.1) 1019
2	Müritz Nationalpark	Nationalparkamt Müritz Schlossplatz 3 17237 Hohenzieritz Germany ☎ +49 39 82 42 52 0 ✉ npoststelle@npa-mueritz.de	Mesophytic deciduous broad-leaved and mixed coniferous-broad-leaved forest; beech and mixed beech forest, lowland to submontane type (Haplic Luvisol)	53.3268° N, 13.1925° E 80 8.8 (-0.9/17.2) 584
3	Naturpark Steigerwald	Naturpark Steigerwald e.V. Hauptstraße 1 91443 Scheinfeld Germany ☎ +49 91 61 92 15 23 ✉ info@steigwald-naturpark.de	Mesophytic deciduous broad-leaved and mixed coniferous-broad-leaved forest; mixed oak-hornbeam forest (Dystric Cambisol)	49.8616° N, 10.5241° E 390 9.4 (-1.2/17.5) 581
4	Gorczanski Park Narodowy	Gorczanski Park Narodowy Poręba Wielka 590 34-735 Niedzwiedz Poland ☎ +48 33 17 20 7 ✉ gpn@gorcepn.pl	Mesophytic deciduous broad-leaved and mixed coniferous-broad-leaved forest; beech and mixed beech forest, montane to altimontane type, partly with fir and spruce (Haplic Leptosol/Dystric Cambisol)	49.5608° N, 20.1614° E 703 7.7 (-3.8/17.5) 676
5	Tatrzanski Park Narodowy	Tatrzanski Park Narodowy Kuznice 134-500 Zakopane ☎ +48 18 20 23 20 0 ✉ sekretariat@tpn.pl	Mesophytic and hygromesophytic coniferous and mixed broad-leaved-coniferous forest; montane to altimontane, partly submontane fir and spruce forests in the nemoral zone (Calcaric Leptosol/Dystric Leptosol)	49.2571° N, 19.9691° E 1148 6.1 (-5.3/15.3) 1062
6	Parco Naturale Tre Cime	Amt für Natur Landhaus 11 Rittner Straße 4 39100 Bozen Italy ☎ +39 47 14 17 77 0 ✉ natur.bozen@provinz.bz.it	Mesophytic deciduous broad-leaved and mixed coniferous-broad-leaved forest; beech and mixed beech forest, montane to altimontane type, partly with fir and spruce (Rendzic Leptosol)	46.6412° N, 12.3374° E 1067 4.8 (-5.8/15.0) 1054
7	Liesjärvi kansallispuisto	Metsähallitus P.O. Box 94 (Ratatie 11) FI-01301 Vantaa Finland ☎ +358 20 63 94 00 0	Mesophytic and hygromesophytic coniferous and mixed broad-leaved-coniferous forest; southern boreal type (Haplic Podzol)	60.6633° N, 23.8797° E 126 5.5 (-7.1/16.0) 604

Table 3.1: Sampling site overview including park authority address with contact details for sampling permissions, geographic coordinates, average elevation above sea level, forest and soil classification, average temperatures and mean annual precipitation. Forest classifications follow the "General Map of the Natural Vegetation of Europe" (Federal Agency for Nature Conservation, Bonn 2001). Soil classifications according to the European Soil Data Centre (Panagos *et al.*, 2012); MAP (mean annual precipitation) and MAT (mean annual temperature; including the mean temperature of the coldest and warmest month) have been calculated based on the high-resolution gridded dataset CRU TS at http://www.cru.uea.ac.uk/data.

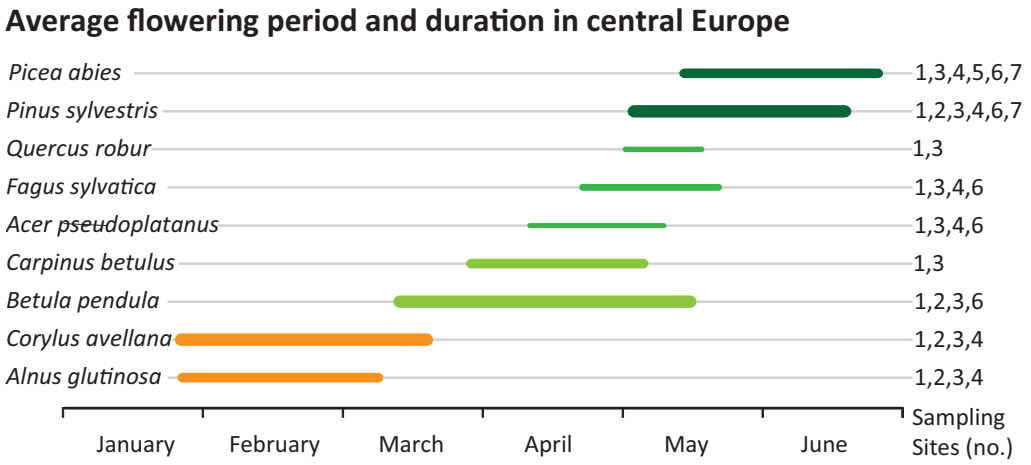

Figure 3.2: Average seasonal timing and duration of flowering periods in central Europe. Relative amount of pollen released by the nine examined species of this study indicated by line thickness in three steps (summarised from http://www.pollenstiftung.de and personal observation). Colours classify species according to their average blossoming time (orange: early blossoming, January to March; green colour saturation level indicates spring to early summer). The duration is an estimated average of species from central European locations. Sampling site (no.) indicates the sites where the various species have been sampled according to Table 3.1 and Figure 3.1

Table 3.2: Taxonomic classification of the nine investigated tree species including their common names and specific flowering periods. The number of individuals sampled represents the sum of trees sampled at all sites in 2015 and 2016, respectively.

Taxonomy		Common name	Flowering period	Individuals 2015	Individuals 2016
Coniferophyta					
Pinaceae					
	Picea abies (L.) H. KARST.	Norway spruce	May/June	63	65
	Pinus sylvestris (L.)	Scots pine	May/June	69	59
Magnoliopsida					
Sapindaceae					
	Acer pseudoplatanus (L.)	Sycamore	April/May	9	24
Betulaceae					
	Alnus glutinosa (L.) GAERTN.	Black alder	January/March	43	49
	Betula pendula ROTH	Silver birch	April/May	33	38
	Carpinus betulus (L.)	European hornbeam	April/May	1	18
	Corylus avellana (L.)	Common hazel	January/March	43	49
Fagaceae					
	Fagus sylvatica (L.)	European beech	May	11	46
	Quercus robur (L.)	Pendunculate oak	May	16	22

taken at different heights and cardinal directions from 22 trees of eight species (Figure 3.3). In addition, individual inflorescences were collected separately in plastic bags to allow a high-resolution intra-tree variance analysis.

Intra-annual analyses at different stages of the pollen maturation process were carried out for *B. pendula* and *P. sylvestris*, which were sampled twice at the same location within one vegetation period. *Betula pendula* was collected at Forêt d'Anlier on 10 March and 5 May 2015, whereas *P. sylvestris* was sampled twice in Gorczański National Park on the 20 May and 1 June 2015. The individual trees sampled for the intra-annual analysis grew within a small assessable area with similar habitat conditions. Due to minimal individual offsets in flower development and senescence, only some tree individuals could be sampled

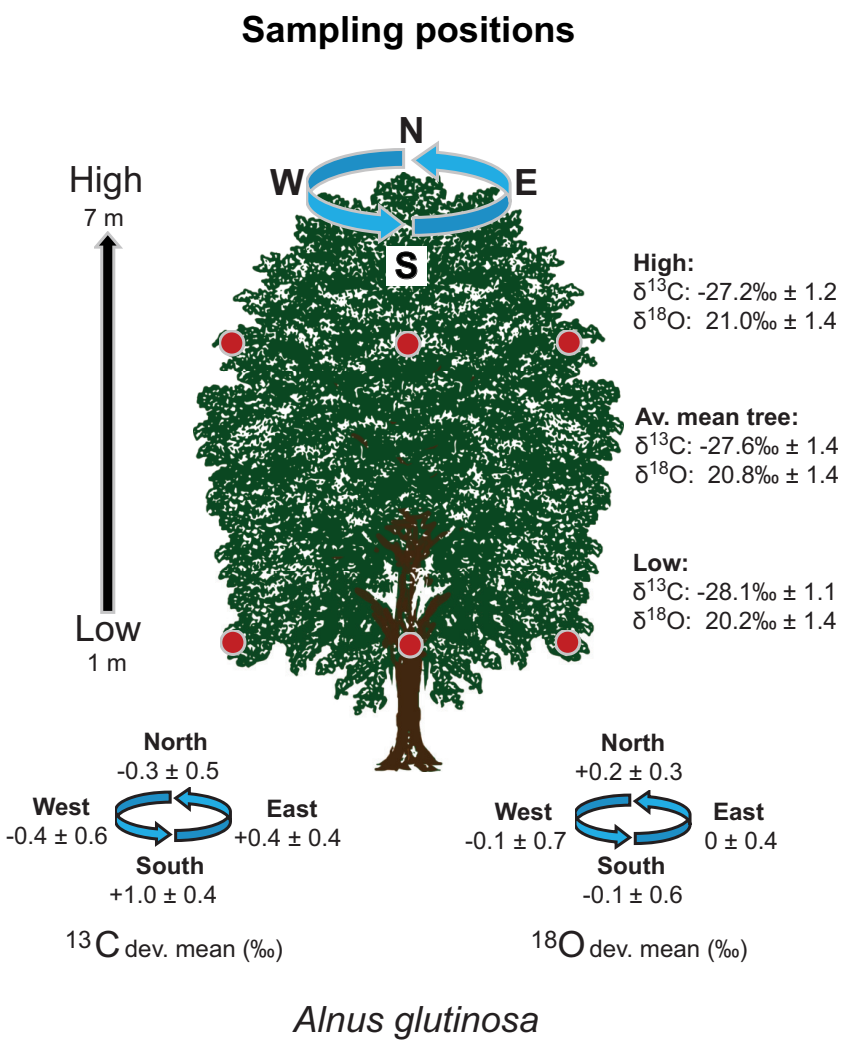

Figure 3.3: Intra-tree pollen-isotope variability of Alnus glutinosa. The sampling scheme for intra-tree pollen-isotope analysis comprises the sampling of pollen from each cardinal direction at a low and a high position in a tree (1 m and 7 m above ground; red dots). Average isotope values (Av. mean tree) as well as the values of both the high and low positions are given for one exemplary Alnus glutinosa tree. ^{13}C and ^{18}O dev. mean = average deviation from the mean isotope value of the tree.

and analysed twice. Seven of the *P. sylvestris* individuals were identical (total number of samples at first sampling: 12; total number of samples at second sampling: 16) and eight *B. pendula* trees were samples twice (total number of samples at first sampling: 11; total number of samples at second sampling: 22). An elevation transect in the Tatrzański Mountains National Park extends from 1053 m a.s.l. to 1345 m a.s.l. on a north-facing slope. Along the gradient of roughly 300 m, 15 individual trees of *Picea abies* were sampled at five different elevations in 2015 and 2016.

3.2.2 Stable isotope analysis

For each measurement, the amount of 220 μg $\pm$ 10% of chemically untreated pollen material was weighed directly into silver capsules using a high-precision scale (Mettler Toledo AX 26 Delta Range). δ^{13}C and δ^{18}O were determined using a DELTA V isotope ratio mass spectrometer (IRMS; Thermo Fisher ScientificTM, Bremen) at the dendrochronological laboratory, section 4.3, GFZ Potsdam, Germany. To exclude potential water contamination from air humidity, all samples were vacuum dried at 100 °C for at least 12 hours in a Thermo Scientific Heraeus VT 6060 P prior to measurement. The pollen material was reduced to CO for simultaneous IRMS analysis of carbon and oxygen isotope ratios in a High Temperature Conversion Elemental Analyzer (TC/EA; 1400 °C; Thermo Fisher ScientificTM, Bremen) coupled to the IRMS. All isotope ratios are expressed relative to VPDB for δ^{13}C and VSMOW for δ^{18}O. Isotope data were compared against international and lab-internal reference material (IAEA-CH3, IAEA-CH6 and IAEA 601 and 602) using two reference standards with widespread isotopic compositions for a single-point normalisation (Paul *et al.*, 2007). Most of the 809 individual pollen samples were weighed and measured with two or three repetitions. In total, we conducted 2132 measurements of stable isotopes. The pollen-isotope dataset is deposited at Pangea Database (https://doi.org/10.1594/PANGAEA.910977).

3.2.3 Stepwise regression analysis

Variables influencing the stable isotope composition in pollen (δ^{13}C, δ^{18}O) were explored by means of stepwise regression as implemented by the JMP Pro 13.1.0 software. Stepwise regression reduces variance to a linear model by eliminating insignificant predictors and was performed (1) by species (to investigate the most important influencing factors for each species over several sites) and (2) by site (to evaluate possible location-dependent

environmental factors for the pollen-isotopes). For the analysis by species eight potential predictors entered our models, the categorical variables *year* (of sampling: 2015 and 2016), *month* (of sampling: February to June), *maturity* (of the pollen at the time of sampling: -1 = immature, 0 = mature, 1 = withered inflorescence), *slope* (steepness: 0 = flat, 1 = minimal incline, up to 10°, 2 = moderate incline, more than 10°), *water* (proximity to water body: 0 = none in the direct vicinity, 1 = one between 10 and 20 m away, 2 = one up to ten metres away), *water classification* (type of water body, e.g. river, lake, wetland), *soil* (type of soil; Table 3.1) and the predictor *site* as a site-specific combination of latitude, longitude and altitude. For the second analysis (by site) the continous variable *altitude* was additionally included to the categorial variables *year*, *month*, *maturity*, *slope*, *water*, *water classification*, *soil* and *species* and thus, nine potential predictors entered the second model. The factors were noted for each individual tree during field work. For all analyses, we deleted singletons by having a look at column variation (< 5 values in a column), hence, several analyses were performed using a subset of the predictors mentioned above.

Categorical variables were hierarchically coded by maximizing the sum of squares between groups. Therefore, the analysis also informs about how levels in categorical predictors are associated with each other. For example, a notation such as site{FAN & STE & GOR & LIE-TAT & TRE} (SI Dataset 1 and 2; availiable online at: https://doi.org /10.1371/journal.pone.0234315) contrasts sites Forêt d'Anlier, Steigerwald, Gorczański, and Liesjärvi against Tatrzański and Tre Cime. Variables revealing the highest statistical significance were added to the model in a stepwise process. As a stopping rule for adding terms we used the minimum Bayesian Information Criterion. Subsequently, the model parameters were estimated using least squares regression.

3.3 Results

$\delta^{13}C_{pollen}$ and $\delta^{18}O_{pollen}$ of 809 samples of 658 individual trees from nine common tree species have been analysed (Table 3.3). The samples were taken at seven locations across Europe during three different time periods of flowering (January to March, April to May and May to June).

Table 3.3: Stable isotope values of $\delta^{13}C_{pollen}$ and $\delta^{18}O_{pollen}$ (min., max., standard deviation) differentiated by sample location (site name and assigned number), species and year. Flowering periods (Time) are indicated by letters: (A) January to March, (B) April to May and (C) May to June. The number of samples (No.) includes bulk samples of individual trees and sub-samples of different positions within a tree. Missing data is denoted as NA.

Site name (no.)	Species	Year	Time	No.	$\delta^{13}C$ mean	$\delta^{13}C$ min.	$\delta^{13}C$ max.	$\delta^{13}C$ sd	$\delta^{18}O$ mean	$\delta^{18}O$ min.	$\delta^{18}O$ max.	$\delta^{18}O$ sd
Parc	*Acer pseudoplatanus*	2016	B	6	-25.2	-27.1	-22.5	1.7	25.7	25.0	26.7	0.6
Naturel	*Alnus glutinosa*	2015	A	25	-28.6	-30.9	-25.9	1.5	22.0	21.0	23.1	0.6
Forêt	*Alnus glutinosa*	2016	A	33	-29.3	-32.3	-25.5	2.0	22.0	21.1	22.6	0.4
d'Anlier	*Betula pendula*	2015/1	B	11	-25.6	-26.9	-23.9	0.9	20.9	19.9	21.4	0.7
(1)	*Betula pendula*	2015/2	B	22	-25.7	-28.5	-23.3	1.5	24.9	22.2	26.5	1.2
	Betula pendula	2016	B	15	-24.1	-25.8	-21.4	1.1	24.2	22.5	25.6	0.9
	Carpinus betulus	2015	B	1	-25.2	NA	NA	NA	29.0	NA	NA	NA
	Carpinus betulus	2016	B	8	-26.1	-29.3	-23.4	2.2	26.3	25.3	27.5	0.6
	Corylus avellana	2015	A	27	-29.0	-30.7	-27.6	0.8	22.8	22.1	23.4	0.4
	Corylus avellana	2016	A	30	-28.6	-32.2	-26.3	1.5	22.0	20.7	23.6	0.7
	Fagus sylvatica	2016	B	23	-27.3	-29.3	-24.7	1.6	23.2	22.4	24.3	0.5
	Picea abies	2015	C	15	-26.2	-29.0	-23.5	1.3	24.0	23.1	25.4	0.8
	Picea abies	2016	C	22	-25.8	-28.0	-23.9	1.4	25.1	23.7	26.2	0.7
	Pinus sylvestris	2015	C	12	-27.8	-29.4	-26.3	1.0	25.2	21.1	28.7	2.7
	Pinus sylvestris	2016	C	20	-25.7	-27.8	-23.9	1.2	29.2	26.8	30.8	1.2
	Quercus robur	2015	B	16	-26.4	-29.0	-25.6	0.9	26.2	24.0	29.0	1.4
	Quercus robur	2016	B	21	-25.7	-27.4	-22.8	1.5	27.4	25.1	29.2	1.1
Tre Cime	*Acer pseudoplatanus*	2015	B	3	-25.5	-27.3	-24.6	1.6	24.7	23.9	25.1	0.7
Parco	*Acer pseudoplatanus*	2016	B	4	-26.1	-26.7	-25.0	0.8	23.1	21.8	24.3	1.0
Naturale	*Betula pendula*	2016	B	4	-24.8	-26.1	-23.8	1.0	23.9	22.9	25.2	1.0
(6)	*Fagus sylvatica*	2016	B	4	-27.6	-28.1	-27.2	0.4	24.1	23.1	26.1	1.4
	Picea abies	2015	C	9	-23.8	-25.7	-22.3	1.1	23.5	21.0	26.0	1.5
	Picea abies	2016	C	31	-23.2	-24.6	-22.0	0.9	21.6	20.0	23.2	0.9
	Pinus sylvestris	2015	C	20	-26.3	-27.7	-25.1	0.7	26.0	24.4	26.9	0.8
		2016	C	14	-27.0	-29.1	-25.3	1.1	23.6	21.2	26.0	1.9
Gorczański	*Acer pseudoplatanus*	2015	B	6	-25.5	-28.3	-23.2	1.7	18.0	16.2	19.7	1.1
Park	*Acer pseudoplatanus*	2015	B	11	-24.8	-27.9	-23.3	1.4	18.5	16.9	20.2	1.0
Narodowy	*Alnus glutinosa*	2015	A	26	-27.4	-29.6	-25.2	1.4	18.1	16.9	19.2	0.6
(4)	*Alnus glutinosa*	2016	A	26	-26.4	-29.9	-22.3	1.9	19.1	17.6	21.7	1.1
	Corylus avellana	2015	A	29	-27.8	-30.4	-24.6	1.2	18.5	16.0	21.9	1.4
	Corylus avellana	2016	A	27	-26.5	-30.4	-24.4	1.6	19.2	17.5	21.2	1.3
	Fagus sylvatica	2015	B	10	-27.9	-28.9	-26.4	0.8	18.6	17.4	20.5	0.9
	Fagus sylvatica	2016	B	13	-27.4	-29.5	-24.9	1.8	19.5	17.4	22.1	1.3
	Picea abies	2015	C	17	-25.6	-27.8	-23.2	1.23	24.8	22.5	26.5	1.0
	Picea abies	2016	C	26	-25.8	-26.8	-24.1	0.8	21.5	20.5	22.4	0.6
	Pinus sylvestris	2015/1	C	12	-26.3	-27.5	-25.2	0.7	25.7	24.2	26.7	0.8
	Pinus sylvestris	2015/2	C	52	-26.3	-27.9	-23.9	1.3	26.9	25.6	28.4	0.8
	Pinus sylvestris	2016	C	13	-26.9	-28.9	-25.6	1.1	25.0	22.0	27.4	1.4
Liesjärvi	*Picea abies*	2016	C	10	-25.6	-27.4	-24.3	0.7	22.7	21.7	24.0	0.7
kan. (7)	*Pinus sylvestris*	2016	C	20	-27.9	-29.6	-26.5	0.8	23.6	21.6	24.6	0.7
Müritz	*Alnus glutinosa*	2016	A	5	-31.0	-32.3	-30.0	1.0	22.5	22.2	23.2	0.4
National	*Betula pendula*	2016	B	13	-23.9	-26.4	-22.1	1.7	24.1	25.2	25.1	0.6
Park (2)	*Corylus avellana*	2016	A	6	-25.3	-27.6	-23.0	1.7	23.9	23.7	24.1	0.1
	Pinus sylvestris	2015	C	6	-26.9	-28.8	-26.2	0.9	28.8	28.1	29.4	0.5
Steigerwald	*Acer pseudoplatanus*	2016	B	9	-23.7	-24.8	-23.0	1.0	24.6	24.0	25.4	0.7
National	*Alnus glutinosa*	2016	A	2	-26.6	-28.1	-25.2	2.1	22.9	22.9	22.9	0.0
Park (3)	*Carpinus betulus*	2016	B	10	-25.6	-27.1	-23.5	1.4	26.1	24.7	27.3	0.9
	Corylus avellana	2016	A	2	-27.0	-27.6	-26.4	0.8	23.8	23.7	23.9	0.1
	Betula pendula	2016	B	9	-22.9	-25.0	-21.1	1.3	24.8	24.0	25.6	0.6
	Fagus sylvatica	2016	B	10	-25.5	-27.1	-23.6	1.1	23.4	22.4	24.9	0.8
	Picea abies	2015	C	7	-26.1	-28.8	-24.9	1.3	25.2	22.6	26.9	1.6
	Picea abies	2016	C	5	-25.8	-27.4	-23.6	1.5	21.7	19.6	22.9	1.3
	Pinus sylvestris	2015	C	5	-26.0	-27.3	-23.9	1.4	27.6	26.3	28.7	1.0
	Quercus robur	2016	B	3	-23.3	-23.6	-22.8	0.4	26.3	26.2	26.5	0.1
Tatrzańsk	*Picea abies*	2015	C	18	-24.3	-26.4	-22.1	1.1	22.6	21.1	23.9	0.8
PN (5)	*Picea abies*	2016	C	5	-26.3	-26.6	-26.0	0.3	21.3	21.0	21.9	0.5

3.3.1 $\delta^{13}C_{pollen}$ values of broad-leaved and coniferous tree species

Flowering period January to March: *Alnus glutinosa* and *Corylus avellana*

The range of mean $\delta^{13}C_{pollen}$ values from *A. glutinosa* for all sites and both years is 4.6‰ (-31.0‰ to -26.4‰; Table 3.3). With the exception of the Gorczański site (2015) the $\delta^{13}C_{pollen}$ values of two consecutive years yield comparable medians at p(sm)=0.26 and 0.17 (Figure 3.4). Mean $\delta^{13}C_{pollen}$ values of *C. avellana* pollen range from -29.1‰ to -25.3‰ (3.8‰; Table 3.3) and are normally distributed. Similar medians for both years are suggested for Forêt d'Anlier at p(sm)=0.07, while the null hypothesis of equal medians was rejected at Gorczański at p(sm)=0.004.

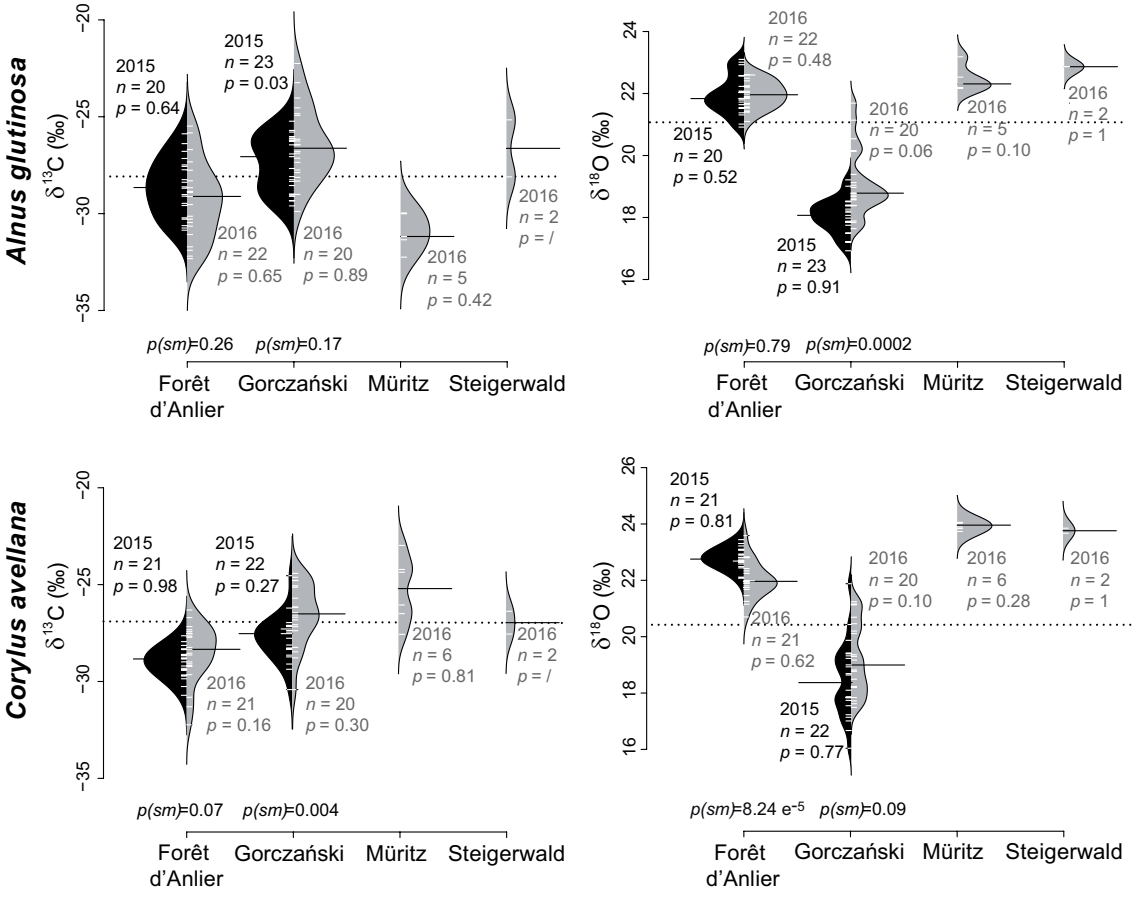

Figure 3.4: Pollen-isotopes of broad-leaved species flowering January to March: *Alnus glutinosa* and *Corylus avellana*. The bean plots show the values of $\delta^{13}C_{pollen}$ and $\delta^{18}O_{pollen}$ of the two species, *Alnus glutinosa* and *Corylus avellana*, from four different locations (Figure 3.1) sampled in 2015 (black) and 2016 (grey). Localities Steigerwald and Müritz were only sampled in 2016. n indicates the number of trees sampled on each occasion (i.e. year). p-values indicate whether the pollen-isotope values of one year are normally distributed, whereas p(sm) represents the probability for equal medians in samples of two consecutive years. The dotted line represents the mean over all localities and both years. The means of each sampling are indicated by a black bar.

Flowering period April to May: *Acer pseudoplatanus*, *Betula pendula*, *Carpinus betulus*, *Fagus sylvatica* and *Quercus robur*

Mean $\delta^{13}C_{pollen}$ values of *A. pseudoplatanus* range from -26.1‰ to -23.7‰ (2.4‰; Table 3.3, Figure 3.5). With one exception at Tre Cime (2015, p=0.02), the $\delta^{13}C_{pollen}$ values of all sites are normally distributed and they yield similar medians for both vegetation periods. $\delta^{13}C_{pollen}$ values of *B. pendula* are also normally distributed. Their mean ranges from -25.7‰ to -22.9‰ (2.8‰; Table 3.3, Figure 3.5), but the distributions yield unequal medians for both years at the site Forêt d'Anlier (p(sm)=0.0005). Mean $\delta^{13}C_{pollen}$ of *C. betulus* range between -26.1‰ and -25.6‰ (0.5‰) and the values reveal a normal distribution at each site (Table 3.3, Figure 3.5).

The range of *F. sylvatica* mean $\delta^{13}C_{pollen}$ values is -27.9‰ to -25.5‰ (2.4‰) and the values are normally distributed with similar medians for both years at the site Gorczański (Table 3.3, Figure 3.6). Mean $\delta^{13}C_{pollen}$ values of *Q. robur* range from -26.4‰ to -23.3‰ (3.1‰). The $\delta^{13}C_{pollen}$ values are not normally distributed at Forêt d'Anlier (2015: p=0.003; 2016: p=0.02), but the carbon isotope values of both years are similar at this site (p(sm)=0.40).

Flowering period May to June: *Pinus sylvestris* and *Picea abies*

Pinus sylvestris mean $\delta^{13}C_{pollen}$ values range between -27.9‰ and -26.0‰ (1.9‰; Table 3.3, Figure 3.7) and the values are normally distributed with one exception at Müritz (2015; p=0.02). Medians of both years are mostly comparable, only Forêt d'Anlier yields statistically distinct medians at p(sm)=0.001. The mean $\delta^{13}C_{pollen}$ values of *P. abies* range from -26.3‰ to -23.2‰ (3.1‰; Table 3.3) and only the samples from Steigerwald (2015; p=0.03) are not normally distributed. Between-year equal medians are present for all locations except Tatrzański (p(sm)=0.02).

3.3.2 Intra-tree variability, intra-annual variability and variability with elevation of $\delta^{13}C_{pollen}$

Intra-tree variability of $\delta^{13}C_{pollen}$

64% of $\delta^{13}C_{pollen}$ values of samples taken at lower branches of the broad-leaved species *A. pseudoplatanus*, *A. glutinosa* and *C. avellana* are more negative in comparison to the branches higher up in the same individuals (Figure 3.3, Table 3.4). The isotopic values

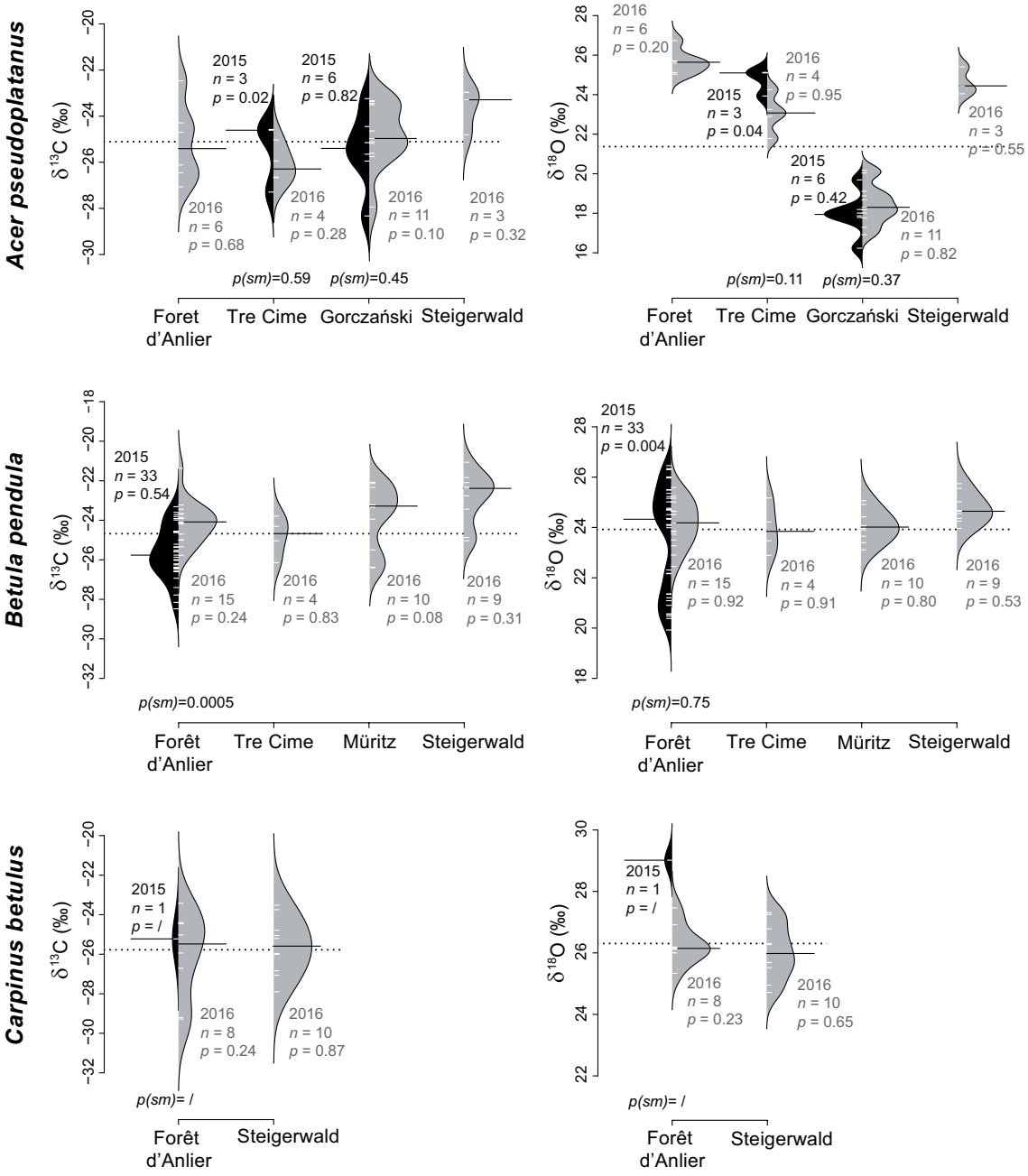

Figure 3.5: Pollen-isotopes of broad-leaved species flowering April to May: *Acer pseudoplatanus*, *Betula pendula* and *Carpinus betulus*. The broad-leaved species were sampled at two to four locations. The bean plots show $\delta^{13}C_{pollen}$ values (left) and $\delta^{18}O_{pollen}$ values (right) of 2015 (black) and 2016 (grey). n indicates the number of individuals. p-values indicate whether pollen-isotope values of a single year are normally distributed (sign. level = 0.05), whereas p(sm) represents the probability for equal medians in samples of two consecutive years. The dotted line represents the mean over all localities and both years. The means of each sampling are indicated by a black bar.

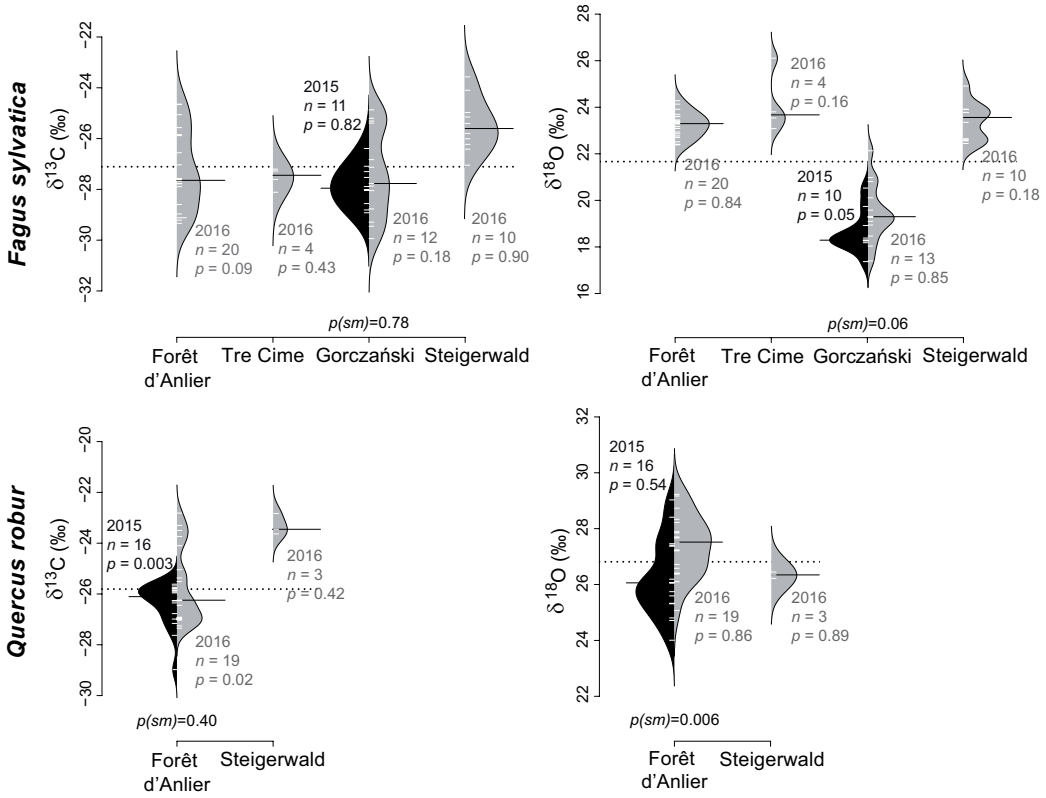

Figure 3.6: Pollen-isotopes of broad-leaved species flowering April to May: *Fagus sylvatica and Quercus robur*. The broad-leaved species *Fagus sylvatica* and *Quercus robur* were sampled at two to four locations. The bean plots show $\delta^{13}C_{pollen}$ values (left) and $\delta^{18}O_{pollen}$ values (right) of 2015 (black) and 2016 (grey). *n* indicates the number of individuals. *p*-values indicate whether the pollen-isotope values of a single year are normally distributed (sign. level = 0.05), whereas *p*(sm) represents the probability for equal medians in samples of two consecutive years. The dotted line represents the mean over all localities and both years. The means of each sampling are indicated by a black bar.

of the samples taken at different positions within the canopy are mostly ranging within one or two standard deviations from the mean isotope value of the tree. $\delta^{13}C_{pollen}$ values from pollen growing at the east side of a tree are likely to be higher, whereas values of the west tend to show lower $\delta^{13}C_{pollen}$ values in comparison to the mean isotope value of the trees. Deviations from the mean at northern and southern positions appear to be species-specific. The $\delta^{13}C_{pollen}$ value of *A. pseudoplatanus* is lower in the North (-0.7‰ from the mean value) and *A. glutinosa* yields lower values in the North in two out of three samples (Table 3.4). The carbon isotope depletion in the North averages at -0.4‰ for *A. glutinosa*. In contrast, *C. avellana* exhibits higher pollen-isotope values in the North (+0.5‰) compared to the intra-tree average of this species. Twenty samples taken at different positions within the canopy of a single *P. abies* tree show higher $\delta^{13}C_{pollen}$ values at eastern and western positions and lower values at the southern exposition (Table 3.5). The analysis of 34 individual inflorescences from low and high positions demonstrates the

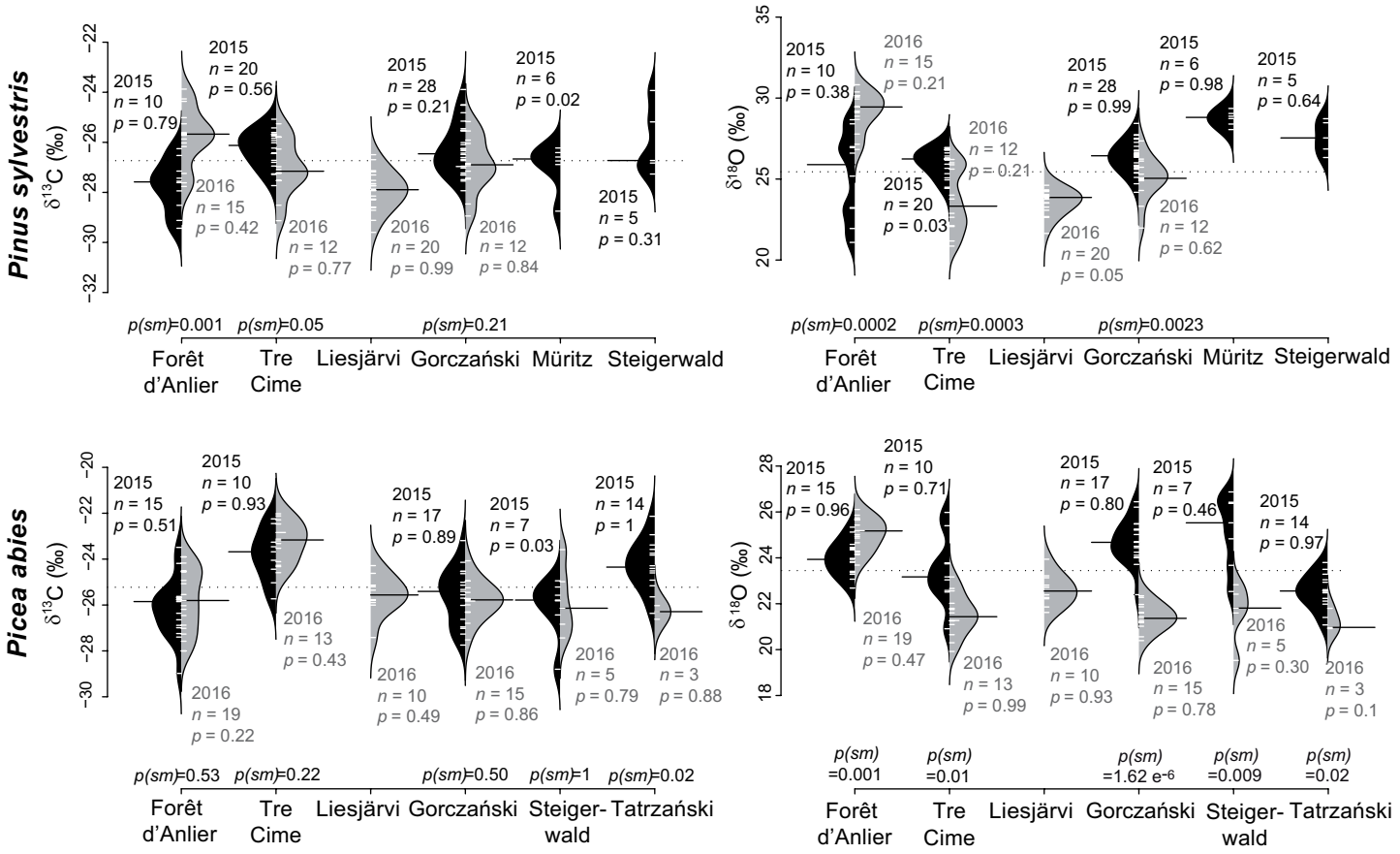

Figure 3.7: Pollen-isotopes of coniferous species flowering May to June: *Pinus sylvestris* and *Picea abies*. *Pinus sylvestris* and *Picea abies* were sampled at six locations. The bean plots show $\delta^{13}C_{pollen}$ values (left) and $\delta^{18}O_{pollen}$ values (right) of 2015 (black) and 2016 (grey). n indicates the number of individuals, p represents the probability of normally distributed pollen-isotopes within one year and p(sm) indicates the probability for similar medians in samples of two consecutive years. The dotted line represents the mean over all localities and both years. The means of each sampling are indicated by a black bar.

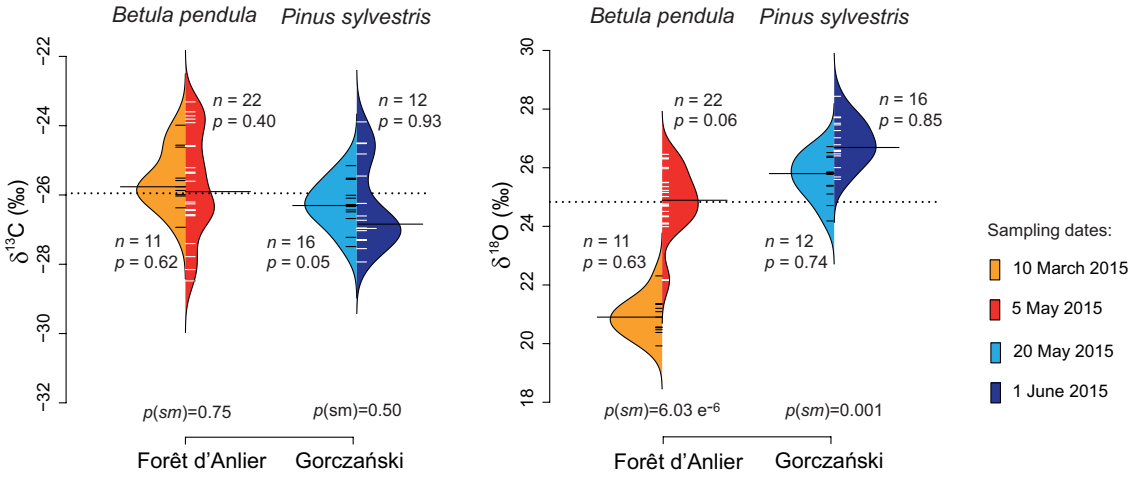

Figure 3.8: Intra-annual comparison of $\delta^{13}C_{pollen}$ and $\delta^{18}O_{pollen}$ values of *Betula pendula* (Forêt d'Anlier) and *Pinus sylvestris* (Gorczański). Both species were sampled twice in 2015. The bean plots show $\delta^{13}C_{pollen}$ values (left) and $\delta^{18}O_{pollen}$ values (right). Colours indicate the sampling date (orange = 10 March 2015; red = 5 May 2015; light blue = 20 May 2015; dark blue = 1 June 2015). n is the number of individuals sampled. The p-values indicate whether the pollen-isotope values of one year are normally distributed (sign. level = 0.05), whereas p(sm) represents the probability for equal medians in samples of the same year. The dotted line represents the mean over all localities and both years. The means of each sampling are indicated by a black bar.

intra-branch variability in pollen-isotopes of six neighbouring *P. sylvestris* trees (Table 3.6). $\delta^{13}C_{pollen}$ values from the same branch of one individual tree differ in a range of 0‰ to 1.2‰ (Table 3.6). The average $\delta^{13}C_{pollen}$ difference between inflorescences from the same branch is 0.3‰.

$\delta^{13}C_{pollen}$ values at different stages of pollen maturation

The $\delta^{13}C_{pollen}$ values of *B. pendula* collected in March (-25.6‰) and May (-25.7‰) 2015 and of *P. sylvestris* collected in May (-26.3‰) and June (-26.3‰) 2015 are normally distributed and the statistical test reveals similar medians of the isotope values for both samplings of *B. pendula* and *P. sylvestris* (Figure 3.8).

Isotope variability of $\delta^{13}C_{pollen}$ with elevation

The $\delta^{13}C_{pollen}$ values of *P. abies* at Tatrzański Park Narodowy increase with altitude from 26.6‰ (1053 m a.s.l) up to 22.1‰ (1344 m a.s.l.) (Figure 3.9). The coefficient R^2 of 0.52 reveals a weak linear correlation with elevation.

Table 3.4: Isotope analysis of pollen samples from eight individual trees of three species (*Acer pseudoplatanus*, *Alnus glutinosa* and *Corylus avellana*) taken at each cardinal direction and from two different positions on each tree. ID = individual identification (including species, sample number and site identity number); Dir. = cardinal direction; Pos. = position on the tree (L = low; H = high); V = variance; A = average; D = deviation from the mean value. The mean isotope values of the tree are noted in the black box (A_{tree}).

ID	Dir.	Pos.	δ^{13}C (‰)	δ^{18}O (‰)	V[δ^{13}C] (L-H)	V[δ^{18}O] (L-H)	A[δ^{13}C] (‰)	A[δ^{18}O] (‰)	D[δ^{13}C] (‰)	D[δ^{18}O] (‰)
*Acer*_1 (3)	North	L	-25.7	25.8	-	-	-25.7	25.8	N-0.7 / W+0.0 / -24.8 (A_{tree}) / E+0.3 / S+0.4	N+0.4 / W-0.1 / 25.4 (A_{tree}) / E+0.3 / S-0.5
		H	-	-						
	South	L	-24.8	25.1	-0.4	0.2	-24.6	25.0		
		H	-24.3	24.8						
	East	L	-25.2	25.3	-1.1	-1.0	-24.6	25.7		
		H	-24	26.2						
	West	L	-25.4	25.0	-1	-0.8	-24.9	25.3		
		H	-24.4	25.7						
*Alnus*_1 (1)	North	L	-	-	-	-	-26.4	21.4	N+0.3 / W-1.4 / -26.7 (A_{tree}) / E+0.2 / S+1.1	N-0.2 / W+0.1 / 21.6 (A_{tree}) / E -0.2 / S+0.3
		H	-26.4	21.4						
	South	L	-	-	-	-	-25.8	21.9		
		H	-25.8	21.9						
	East	L	-	-	-	-	-26.5	21.4		
		H	-26.5	21.4						
	West	L	-28.1	21.6	-	-	-28.1	21.6		
		H	-	-						
*Alnus*_9 (1)	North	L	-29.9	21.6	-2.3	-1.3	-28.8	22.3	N-0.5 / W+0.4 / -28.3 (A_{tree}) / E+0.6 / S +0.7	N+0.4 / W-0.7 / 21.8 (A_{tree}) / E+0.4 / S -0.2
		H	-27.6	22.9						
	South	L	-27.6	21.7	-	-	-27.6	21.7		
		H	-	-						
	East	L	-	-	-	-	-29.0	22.2		
		H	-29.0	22.2						
	West	L	-27.5	21.1	0.9	-0.1	-27.9	21.1		
		H	-28.4	21.2						
*Alnus*_11 (1)	North	L	-28.7	19.0	-0.9	-0.7	-28.3	19.4	N-0.9 / W-0.1 / -27.3 (A_{tree}) / E-0.2 / S+1.2	N+0.3 / W+0.3 / 19.1 (A_{tree}) / E-0.1 / S-0.5
		H	-27.8	19.8						
	South	L	-26.5	18.5	-0.6	-0.2	-26.2	18.6		
		H	-25.9	18.7						
	East	L	-27.6	19.1	-	-	-27.6	19.1		
		H	-	-						
	West	L	-27.6	19.5	-0.3	0.2	-27.5	19.4		
		H	-27.3	19.3						
*Corylus*_11 (4)	North	L	-24.6	19.1	0.8	-0.3	-25.0	19.3	N+0.7 / W+0.1 / -25.1 (A_{tree}) / E+1.4 / S-2.2	N-0.0 / W +0.1 / 19.3 (A_{tree}) / E+0.3 / S-0.3
		H	-25.3	19.4						
	South	L	-25.4	18.9	0.9	-0.3	-27.8	19		
		H	-26.2	19.1						
	East	L	-24.2	20.1	0.1	1.0	-24.3	19.6		
		H	-24.3	19.1						
	West	L	-25.1	19.3	0.8	-0.1	-25.5	19.4		
		H	-25.9	19.4						
*Corylus*_19 (4)	North	L	-27.0	20.3	-2.5	-0.5	-25.7	20.5	N+1.4 / W-1.0 / -27.2 (A_{tree}) / E-0.0 / S -0.5	N+1.1 / W -0.4 / 19.4 (A_{tree}) / E-0.2 / S -0.5
		H	-24.5	20.8						
	South	L	-27.5	18.9	0.3	-0.1	-27.6	18.9		
		H	-27.8	19.0						
	East	L	-27.7	19.6	-1.1	0.7	-27.2	19.2		
		H	-26.6	18.9						
	West	L	-28.6	18.4	-0.9	-1.2	-28.1	19.0		
		H	-27.7	19.6						
*Corylus*_7 (1)	North	L	-29.6	23.4	-0.9	-0.1	-29.2	23.5	N+0.2 / W-0.5 / -29.2 (A_{tree}) / E+0.9 / S -0.5	N+1.0 / W-1.2 / 22.7 (A_{tree}) / E +0.4 / S -0.3
		H	-28.7	23.5						
	South	L	-30.4	22.2	-1.1	-0.1	-29.8	22.3		
		H	-29.3	22.3						
	East	L	-29.9	23.0	-2.9	0.0	-28.4	23.0		
		H	-27.0	23.0						
	West	L	-29.8	21.4	-	-	-29.8	21.4		
		H	-	-						
*Corylus*_21 (1)	North	L	-29.0	23.1	-0.7	0.1	-28.6	23.1	N-0.4 / W -1.3 / -28.4 (A_{tree}) / E+1.3 / S +0.4	N+0.5 / W-0.3 / 22.6 (A_{tree}) / E-0.2 / S-0.1
		H	-28.3	23.0						
	South	L	-27.0	22.3	1.5	-0.5	-27.7	22.5		
		H	-28.5	22.7						
	East	L	-	-	-	-	-26.9	22.4		
		H	-26.9	22.4						
	West	L	-29.2	22.5	0.5	0.4	-29.5	22.3		
		H	-29.7	22.1						

Table 3.5: Isotope analysis of pollen samples from three cardinal directions (south, east and west; the northern side was not flowering), different sampling heights (low/high) and the comparison of individual inflorescences from each sampling position. ID = individual identification (including species, number and site); Dir. = cardinal direction; Pos. = position on the tree (L = low; H = high); Inf._ID = inflorescence identification per branch; V = variance; A = average; D = deviation from the mean value. The mean isotope values of the tree are noted in the black box (A_{tree}).

ID	Dir.	Pos.	Inf._ID	$\delta^{13}C_{pollen}$ (‰)	$\delta^{18}O_{pollen}$ (‰)	A[δ^{13}C] (‰)	A[δ^{18}O] (‰)	V[δ^{13}C] (L-H)	V[δ^{18}O] (L-H)	D (‰)
Picea_12 (Tre Cime)	South	L	-	-22.4	23.4	-22.5	23.1	-0.1	1.9	δ^{13}C: W+0.1 / N / S-0.4 / E+0.2; δ^{18}O: W+0.3 / N / S-0.8 / E+0.5; A_{tree} = -22.2 (δ^{13}C), 22.9 (δ^{18}O)
			S_low_1	-22.5	23.4					
			S_low_2	-22.8	21.6					
			S_low_3	-22.2	23.9					
		H	-	-22.5	21.1	-22.3	21.3			
			S_high_1	-22.3	20.6					
			S_high_2	-22.8	21.9					
			S_high_3	-21.7	21.5					
	East	L	-	-22.6	22.9	-22.5	23.2	-1.0	-0.4	
			E_low_1	-21.3	22.6					
			E_low_2	-23.6	24.2					
		H	-	-21.2	23.5	-21.5	23.7			
			E_high_1	-21.8	23.7					
			E_high_2	-21.4	23.8					
	West	L	-	-22.3	23	-21.7	23.1	0.6	-0.5	
			W_low_1	-21.8	22.6					
			W_low_2	-21.1	23.6					
		H	-	-21.8	23.2	-22.3	23.5			
			W_high_1	-22.4	24.3					
			W_high_2	-22.8	23					

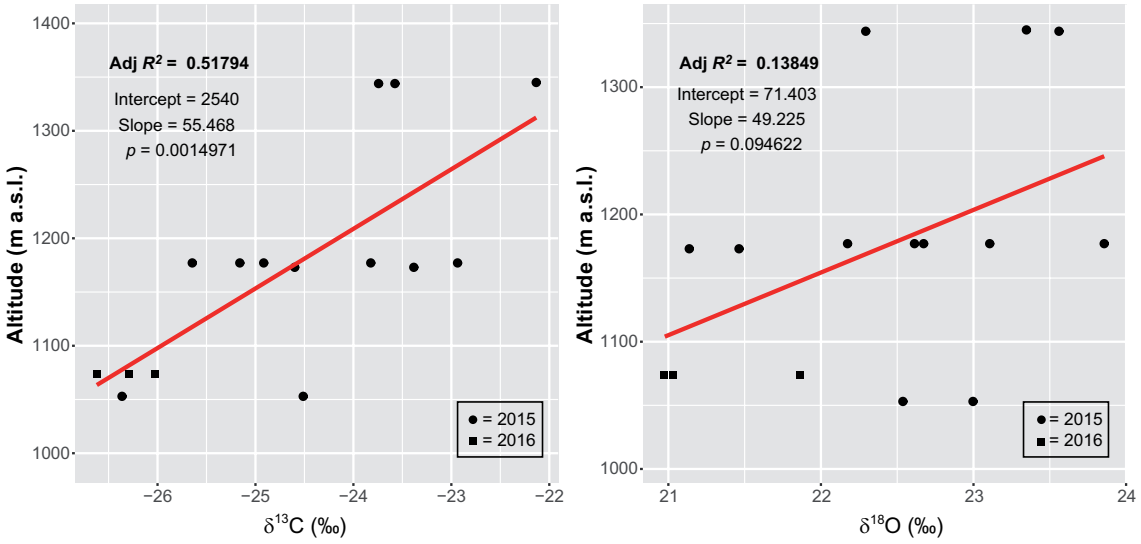

Figure 3.9: 300 m altitudinal transect of *Picea abies* at Tatrzański Park Narodowy. The plots show the linear regression analysis of $\delta^{13}C_{pollen}$ values and altitude (left) and $\delta^{18}O_{pollen}$ values and altitude (right). Samples were taken in 2015 (black dots) and 2016 (black squares). The red line indicates the slope of the linear regression model. Adjusted R^2 indicates the proportion of variance explained by the linear association of isotopes and elevation.

Table 3.6: The samples of six individual *Pinus sylvestris* trees from the same location represent single inflorescences from different positions (low/high) on the tree. The isotopic difference between the inflorescences shows the variability of $\delta^{13}C_{pollen}$ and $\delta^{18}O_{pollen}$ values (in ‰) on branches and within trees at a high resolution. Tree ID = individual identification, (including species, number and site); Position = position on the tree (L = low; H = high); Branch ID = branch identification at each tree; Inf. ID = inflorescence identification of each branch; D[] = deviation from the mean value.

Tree ID	**Position**	**Branch ID**	**Inf. ID**	$\delta^{13}\mathbf{C}_{pollen}$	$\delta^{18}\mathbf{O}_{pollen}$	$\mathbf{D}[\delta^{13}\mathbf{C}_{pollen}]$	$\mathbf{D}[\delta^{18}\mathbf{O}_{pollen}]$
Pinus 1	L	low_1	1	-25.3	27.0	0.7	0.8
	L	low_1	2	-26.0	27.8		
	L	low_2	1	-24.8	28.0	0.4	0.4
	L	low_2	2	-25.2	28.4		
	H	high_1	1	-25.7	27.2	0.1	1.4
	H	high_1	2	-25.6	28.6		
	H	high_2	1	-25.4	27.3	0.2	0.1
	H	high_2	2	-25.2	27.2		
Pinus 2	L	low_1	1	-23.7	26.4	0.0	0.2
	L	low_1	2	-23.7	26.6		
	L	low_2	1	-24.0	26.5	0.3	0.7
	L	low_2	2	-23.7	27.2		
	H	high_1	1	-24.5	26.1	0.1	0.2
	H	high_1	2	-24.4	26.3		
	H	high_2	1	-23.8	26.4	0.0	0.7
	H	high_2	2	-23.8	27.1		
Pinus 3	L	low_1	1	-23.3	27.4	1.2	0.1
	L	low_1	2	-24.5	27.5		
	L	low_2	1	-24.7	26.7	0.2	0.2
	L	low_2	2	-24.9	26.9		
	H	high_1	1	-24.8	26.9	0.0	0.8
	H	high_1	2	-24.8	27.7		
	H	high_2	1	-25.0	26.6	0.2	0.4
	H	high_2	2	-25.2	26.2		
Pinus 4	L	low_1	1	-25.4	27.6	0.8	0.5
	L	low_1	2	-24.6	27.1		
	H	high_1	1	-24.6	27.5	0.0	0.3
	H	high_1	2	-24.6	27.8		
Pinus 5	L	low_1	1	-26.4	26.3	0.2	0.7
	L	low_1	2	-26.6	27.0		
Pinus 6	L	low_1	1	-27.8	27.2	0.6	0.3
	L	low_1	2	-27.2	26.9		
	H	high_1	1	-27.0	27.4	0.9	0.1
	H	high_1	2	-27.9	27.3		
Average:						**0.3**	**0.5**

3.3.3 Stepwise regression analysis for $\delta^{13}C_{pollen}$

By species

The most relevant factor influencing $\delta^{13}C_{pollen}$ values for several species is *site* with very high probability values of Prob > F = <0.0001* (Table 3.7; S1 Dataset available at: https://doi.org/10.1371/journal.pone.0234315.s001). The *year* of sampling influenced $\delta^{13}C_{pollen}$ of *B. pendula*, *C. avellana Q. robur*. The factor *soil* and the factor *maturity* of the pollen are important for *A. glutinosa* and *P. sylvestris*. The other factors *proximity to water* and *water classification* occur only once in the analytical outcome.

By site

The site-specific statistical evaluation of the deviation of $\delta^{13}C_{pollen}$ values from the means reveals the factor *species* as the most important one (Table 3.8; S2 Dataset available at: https://doi.org/10.1371/journal.pone.0234315.s002). Species are often hierarchically

Table 3.7: Relevant environmental impact factors on $\delta^{13}C_{pollen}$ and $\delta^{18}O_{pollen}$ values for each species. Prob > F gives the probability value after Levene´s test (Schönwiese, 2013). The factor site groups locations by similarity. Abbreviations for locations: FAN (Forêt d'Anlier); GOR (Gorczański); MUR (Müritz); STE (Steigerwald); TAT (Tatrzański); TRE (Tre Cime); LIE (Liesjärvi).

Plant species	Influencing factor on $\delta^{13}C_{pollen}$	Prob <F	Influencing factor on $\delta^{18}O_{pollen}$	Prob <F
A. pseudoplatanus	proximity to water	0.0266*	site {GOR - FAN&DOL&STE}	0.0012*
	–	–	site {DOL&STE FAN}	0.0019*
A. glutinosa	soil	0.0097	year	0.0034*
	maturity	0.0012*	site {GOR-FAN&MUR&STE}	<0.0001*
	–	–	site {FAN-MUR&STE}	0.0162*
	–	–	site {MUR-STE}	0.0009*
	–	–	maturity	<0.0001*
B. pendula	year	0.0001*	year	0.0165*
	–	–	month {mar-apr&may}	<0001*
C. betulus	water classification	0.0186*	proximity to water	0.0048*
C. avellana	year	0.0043*	site {GOR-FAN&STE&MUR}	<0001*
	site {FAN - GOR&STE&MUR}	<0.0001*	site {FAN-STE&MUR}	0.0003*
F. sylvatica	site {GOR&TRE&FAN - STE}	0.0001*	site {GOR-FAN&STE&TRE}	<0001*
	–	–	maturity	<0.0001*
P. abies	site {FAN&STE&GOR-&LIE -TAT&TRE}	0.0001*	site {TRE&TAT&LIE&GOR STE&FAN	0.0055*
	site {TAT-TRE}	0.0022*	year	<0.0001*
	–	–	site {TRE&TAT&LIE-GOR}	0.0204*
	–	–	water_classification	<0.0001*
P. sylvestris	maturity	0.0009*	site {LIE&TRE&GOR -	<0.0001*
	soil	0.0018*	STE&FAN&MUR}	
	–	–	month	0.0124*
	–	–	maturity	<0.0001*
Q. robur	year	0.0240*	year	0.0164*

Table 3.8: Relevant environmental factors on $\delta^{13}C_{pollen}$ values and $\delta^{18}O_{pollen}$ for each site. Prob > F gives the probability value after Levene´s test (Schönwiese, 2013). Hierarchical clusters follow statistical similarity of the $\delta^{13}C_{pollen}$ and $\delta^{18}O_{pollen}$ values within the factor species. The significance level lies at 0.05.

Site	**Influencing factor on $\delta^{13}C_{pollen}$**	**Prob <F**	**Influencing factor on $\delta^{18}O_{pollen}$**	**Prob <F**
PN Forêt d'Anlier	species {*A. glutinosa* & *C. avellana* – *F. sylvatica* & *P. sylvestris* & *Q. robur* & *P. abies* & *C. betulus* & *A. pseudoplatanus* & *B. pendula*}	<.0001*	species {*A. glutinosa* & *C. avellana* & *F. sylvatica* & *B. pendula* & *P. abies* – *A. pseudoplatanus* & *C. betulus* & *Q. robur* & *P. sylvestris*}	<.0001*
	species {*F. sylvatica* & *P. sylvestris* - *Q. robur* & *P. abies* & *C. betulus* & *A. pseudoplatanus* & *B. pendula*}	<.0001*	species {*A. glutinosa* & *C. avellana* - *F. sylvatica* & *B. pendula* & *P. abies*}	0.0189*
	species {*Q. robur* & *P. abies* & *C. betulus* - *A. pseudoplatanus* & *B. pendula*}	0.0001*	species {*F. sylvatica* & *B.pendula* – *P.abies*}	0.0002*
	year	0.0020*	species {*F. sylvatica* - *B. pendula*}	<.0001*
	–	–	species {*A. pseudoplatanus* & *C. betulus* & *Q. robur* - *P. sylvestris*}	<.0001*
	–	–	species {*A. pseudoplatanus* – *C. betulus* & *Q. robur*}	0.0042*
	–	–	year	0.0004*
	–	–	month	<.0001*
	–	–	maturity	0.0017*
	–	–	water classification	0.0013*
PN Tre Cime	species {*F. sylvatica* & *P. sylvestris* & *A. pseudoplatanus* - *B. pendula* & *P. abies*}	<.0001*	species {*P. abies* - *A. pseudoplatanus* & *B. pendula* & *F. sylvatica* & *P. sylvestris*}	<.0001*
	species {*B. pendula* - *P. abies*}	0.0010*	year	<.0001*
	maturity	0.0085*	–	–
Liesjärvi k.	species	<.0001*	species	0.0028*
Gorczański	species {*F. sylvatica* & *C. avellana* & *A. glutinosa* & *P. sylvestris* - *P. abies* & *A. pseudoplatanus*}	<.0001*	species {*A. pseudoplatanus* & *A. glutinosa* & *C. avellana* & *F. sylvatica* - *P. abies* & *P. sylvestris*}	<.0001*
Park Narodowy	year	0.0179*	species {*P. abies* - *P. sylvestris*}	<.0001*
	soil	<.0006*	altitude	0.0204*
	–	–	month	0.0021*
Müritz NP	species {*A. glutinosa* - *P. sylvestris* & *C. avellana* & *B. pendula*}	<.0001*	species {*A. glutinosa* & *C. avellana* & *B. pendula* - *P. sylvestris*}	<.0001*
	–	–	species {*A. glutinosa* - *C. avellana* & *B. pendula*}	<.0001*
Steigerwald NP	species {*C. avellana* & *A. glutinosa* & *P. sylvestris* & *P. abies* & *C. betulus* & *F. sylvatica* – *A. pseudoplatanus* & *Q. robur* & *B. pendula*}	<.0001*	species {*A. glutinosa* & *F. sylvatica* & *C. avellana* & *P. abies* & *A. pseudoplatanus* & *B. pendula* - *C. betulus* & *Q. robur* & *P. sylvestris*}	0.0017*
	–	–	species {*A. glutinosa* & *F. sylvatica* & *C. avellana* & *P. abies* –*A. pseudoplatanus* & *B. pendula*}	<.0001*
	–	–	year	<.0001*
	–	–	altitude	0.0028*
Tatrzański PN	year	0.0324*	year	0.0127*
	longitude	0.0027*	–	–

grouped by statistical similarity. The *year* of sampling influences the pollen variability at two sites (Forêt d'Anlier and Gorczański) and also *maturity* occurs twice (Tre Cime and Tatrzański). *Soil* (Gorczański) and *altitude* (Tatrzański) are once listed as influencing factors.

3.3.4 $\delta^{18}O_{pollen}$ values of broad-leaved and coniferous tree species

Flowering period January to March: *Alnus glutinosa* and *Corylus avellana*

Mean $\delta^{18}O_{pollen}$ values of *A. glutinosa* range from 18.1‰ to 22.9‰ (4.8‰; Table 3.3). Values of each year are normally distributed (Figure 3.4). However, their medians are statistically distinct for site Gorczański at p(sm)=0.0002. Mean *C. avellana* $\delta^{18}O_{pollen}$ values range from 18.5‰ to 23.9‰ (5.4‰, Table 3.3). The pollen-isotope values are normally distributed but years 2015 and 2016 yield statistically distinct medians for Forêt d'Anlier.

Flowering period April to May: *Acer pseudoplatanus*, *Betula pendula*, *Carpinus betulus*, *Fagus sylvatica* and *Quercus robur*

Mean $\delta^{18}O_{pollen}$ values of *A. pseudoplatanus* range between 18.0‰ and 25.7‰ (7.7‰; Table 3.3, Figure 3.5). Values of each year are normally distributed except for site Tre Cime (2015, at p=0.04). The statistical test reveals similar medians between years. Mean *B. pendula* $\delta^{18}O_{pollen}$ values range from 23.5‰ to 24.8‰ (1.3‰) and are normally distributed with one exception (Forêt d'Anlier 2015, p=0.004; Figure 3.5). The $\delta^{18}O_{pollen}$ values of 2015 and 2016 yield similar medians (p(sm)=0.75). Mean $\delta^{18}O_{pollen}$ values of *C. betulus* range from 26.1‰ to 26.3‰ (0.2‰; Table 5.3) and are also normally distributed (Figure 3.5). The comparatively low mean $\delta^{18}O_{pollen}$ values of *F. sylvatica* range from 18.6‰ to 24.1‰ (5.5‰; Table 3.3) and the values are normally distributed with similar medians for both years from Gorczański (Figure 3.6). Mean *Q. robur* $\delta^{18}O_{pollen}$ values range between 26.2‰ and 27.4‰ (1.2‰; Table 3.3) and are normally distributed but statistically distinct between both years at p(sm)=0.006 (Figure 3.6).

Flowering period May to June: *Pinus sylvestris* and *Picea abies*

Mean $\delta^{18}O_{pollen}$ values of *P. sylvestris* range from 23.6‰ to 29.2‰ (5.6‰; Table 3.3) and the values are normally distributed except for the samples at Tre Cime collected in 2015 (p=0.03). All comparisons between the two vegetation periods are statistically distinct. Mean *P. abies* $\delta^{18}O_{pollen}$ values range between 21.3‰ and 25.2‰ (3.9‰; Table 3.3). The values are normally distributed within each sampling (Figure 3.7) but comparisons between 2015 and 2016 are statistically distinct for all sites.

3.3.5 Intra-tree variability, intra-annual variability and variability with elevation of $\delta^{18}O_{pollen}$

Intra-tree variability of $\delta^{18}O_{pollen}$

68% of the $\delta^{18}O_{pollen}$ values of samples from *A. pseudoplatanus*, *A. glutinosa* and *C. avellana* taken at the lower branches are more negative in comparison to the values of the higher branches from the same individual (Figure 3.3, Table 3.4). The $\delta^{18}O_{pollen}$ values were often lower at southern and western positions, whereas values from the northern position seem to be generally higher for all species (Table 3.4). Twenty samples taken at different positions within the canopy of a *P. abies* tree show higher $\delta^{18}O_{pollen}$ at eastern and western positions, and lower values at the southern exposition (Table 3.5). Similar to the broad-leaved species, $\delta^{18}O_{pollen}$ values from lower branches of *P. abies* tend to be lower than those from higher branches (Table 3.5). The analysis of individual inflorescences demonstrates an intra-branch variability ranging between 0‰ and 1.4‰ (Table 3.6). The average deviation for inflorescences from the same branch is 0.5‰ for $\delta^{18}O_{pollen}$.

$\delta^{18}O_{pollen}$ values at different stages of pollen maturation

The $\delta^{18}O_{pollen}$ values of *B. pendula* are normally distributed (Figure 3.8), but the medians are statistically distinct. The mean $\delta^{18}O_{pollen}$ values increase by 4‰ within 11 weeks (from 20.9‰ on 10 March to 24.9‰ on 5 May). $\delta^{18}O_{pollen}$ values of *P. sylvestris* are also normally distributed for each sampling (Figure 3.8). However, they increase by 1.2‰ within 12 days: $\delta^{18}O_{pollen}$ were at 25.7‰ on 20 May and at 26.9‰ on 1 June and the medians are statistically distinct.

Isotope variability of $\delta^{18}O_{pollen}$ with elevation

$\delta^{18}O_{pollen}$ values of *P. abies* at Tatrzański Park Narodowy (Figure 3.9) are scattered throughout the elevation transect and do not correlate with elevation (R^2= 0.14). The values range from 21.0‰ (1074 m a.s.l.) to 23.9‰ (1177 m a.s.l.).

3.3.6 Stepwise Regression Analysis of $\delta^{18}O_{pollen}$

By species

$\delta^{18}O_{pollen}$ values were found to be affected by variable factors. The most important factor was *site*, which impacts the $\delta^{18}O_{pollen}$ variability in six species (Table 3.7). The *year* of sampling influences the $\delta^{18}O_{pollen}$ variability in four species, whereas the *maturity* of the pollen determines the $\delta^{18}O_{pollen}$ variability in three species and the factor *month* of sampling occurs twice. The factors *proximity to water* and *water classification* are rarely influential and, if significant, they were species-specific.

By site

$\delta^{18}O_{pollen}$ value variability within sites is mostly determined by the factor *species* (Table 3.8). The *year* of sampling is important in four cases and the *month* of sampling and *altitud* occur twice in the analytical outcome. The factors *maturity* of the pollen and *water classification* are each listed once.

3.4 Discussion

3.4.1 $\delta^{13}C_{pollen}$ values of broad-leaved species flowering January to March

Alnus glutinosa and *Corylus avellana*

Like other winter-deciduous tree species, *A. glutinosa* and *C. avellana* (both family Betulaceae) have a similar timing of leaf unfolding and senescence, i.e. a similar duration of the photosynthetically active period in one year (McVean, 1953; Kikuzawa, 1995; Kramer, 1996; Vitasse *et al.*, 2009a; Črepinšek *et al.*, 2012; Gallinat *et al.*, 2015). Nonetheless, their $\delta^{13}C_{pollen}$ values are generally low compared to tree species flowering April to June (*A. glutinosa*: -28.2‰, *C. avellana*: -27.4‰; Table 3.3). Catkins of both species occur before the leaf buds emerge (Figure 3.2), thus the pollen can only be polymerized from stored fatty and amino acids, phenols and other precursors of sporopollenin predominately accumulated during previous vegetation periods. *Alnus glutinosa* and *C. avellana* pollen are present and fully developed in shape before winter dormancy, but the size of maturing pollen grains increases in early spring until a few days before pollen shedding (Krizo and

Slobodnik, 1997). This indicates that some biopolymers are still added to the pollen grains and possibly exchanged right before pollination.

Ambient air temperatures shortly before the onset of flowering affect the catkin development of both species and the onset date for trees flowering in early spring is highly variable, even between consecutive years (Myszkowska *et al.*, 2010). However, the responsiveness of the plant to favorable weather conditions does not seem to have any marked effect on its $\delta^{13}C_{pollen}$ values. The measurements indicate similar medians for consecutive years for *A. glutinosa* (p(sm)=0.26 and 0.17; Figure 3.4), although flowering started roughly two weeks earlier at all sites sampled in 2016 (personal observation). *Corylus avellana* $\delta^{13}C_{pollen}$ values deviate more strongly between the two years (p(sm)=0.07 and 0.004; Figure 3.4). But even though both species react differently over two vegetation periods, they show similar patterns between particular sites (Figure 3.4): The signals of the western sampling location of Forêt d'Anlier are similar to the signals of the eastern sampling location of Gorczański (Figure 3.1). Especially noticeable are the low values of $\delta^{13}C_{pollen}$ for *A. glutinosa* from Müritz (2016) compared to those of other sites. The mean $\delta^{13}C_{pollen}$ value is -31.0‰ and thus 2.8‰ lower than the average *A. glutinosa* pollen-isotope value of -28.2‰ from all sampling sites. However, all values lie within the range of a normal distribution (p=0.81; Figure 3.4), so we can exclude measurement errors or tree-individual outliers to have caused the observed low mean $\delta^{13}C_{pollen}$ value. Additionally, *C. avellana* from the same site and year (Müritz 2016) does not show exceptionally low values in comparison to data of that species measured at other sites. At the moment, we do not have a valid explanation for the unusual deviation of $\delta^{13}C_{pollen}$ values of *A. glutinosa* sampled at Müritz (2016).

3.4.2 $\delta^{13}C_{pollen}$ values of broad-leaved species flowering April to May

Acer pseudoplatanus

Mean $\delta^{13}C_{pollen}$ values of *A. pseudoplatanus* (Sapindaceae; -25.1‰) are intermediate compared to other broad-leaved species in this study. Depending on location and year of sampling, the $\delta^{13}C_{pollen}$ values of *A. pseudoplatanus* are closest to *Q. robur* (-25.7‰, Forêt d'Anlier 2016) and *B. pendula* (-24.8‰, Tre Cime 2016), but they show no consistent offset or similarity to any other species examined. In general, *Acer* ssp. are not dependent on prevailing spring temperatures to start seasonal development but instead require a specific amount of daylight (Vitasse *et al.*, 2009). Their leaves emerge early in the season

and immediately exhibit a high rate of photosynthesis (Sparks and Carey, 1995). However, *Acer* ssp. are easily affected by short-term weather events and under unfavourable conditions, their carbon fixation during photosynthesis is rather ineffective, up to 50% less compared to the genus *Quercus* under the same conditions (Morecroft and Roberts, 1999). Additionally, *A. pseudoplatanus* is very sensitive to cold air inversions in spring and autumn (Schuster *et al.*, 2014). Inter-annual variations in leaf senescence are highly correlated with precipitation: in dry years, high respiration rates cause early senescence and even premature leaf fall (Archetti *et al.*, 2013). Therefore, photosynthetically active periods of *Acer* ssp. are highly variable even between consecutive years. Hence, their pollen-isotope values may be challenging to interpret.

Fagus sylvatica* and *Quercus robur

$\delta^{13}C_{pollen}$ values of *Q. robur* show a mean of -25.1‰, whereas the mean value of *F. sylvatica* is 2‰ lower (-27.1‰). Deviations between the species of the family Fagaceae can be explained by plant physiology and individual phenology. Both were examined at two locations in 2016: Forêt d'Anlier and Steigerwald (Figure 3.6 and Table 3.3). Catkins of the genera *Quercus* and *Fagus* emerge during the same period in late April or early May, simultaneously with their first leaves and twigs. This happens roughly two weeks before anthesis is complete and the pollen starts to shed (Lejoly-Gabriel and Leuschner, 1983). They both carry winter-dormant leaf and flower buds (Brett, 1964), but the spring ontogeny is genus-specific (Vitasse *et al.*, 2009b). *Quercus robur* shows a high sensitivity to favourable spring temperatures regarding bud burst, whereas *F. sylvatica* needs twelve hours of daylight to start developing (Schuster *et al.*, 2014). Trees of the genus *Quercus* are slow in leaf unfolding and it takes about two months until full performance of carbon fixation in the leaves (Morecroft *et al.*, 2003). Thus, the length of the vegetation period in which carbon can be fixated and stored out of a positive net productivity from photosynthesis is shorter for *Quercus* in comparison to *Fagus*. In general, warmer spring temperatures tend to increase carbon uptake, whereas warmer summer and autumn temperatures decrease the uptake due to larger respiration rates (Piao *et al.*, 2008). The impact of prevailing temperature on pollen-isotope values during different stages of a vegetation period has yet to be examined in detail.

Betula pendula and *Carpinus betulus*

Mean $\delta^{13}C_{pollen}$ values of *B. pendula* (-24.3‰) are on average 1.3‰ less negative than the mean values of *C. betulus* (-25.6‰), even though they belong to the same family (Betulaceae), flower during the same period from mid-April to mid-May and prefer similar habitats (Figure 3.2, 3.5; Lejoly-Gabriel and Leuschner, 1983). The total phase of pollen development spans early September to early April, and the size of *B. pendula* pollen grains still increases two to three weeks before pollen release (Krizo and Slobodnik, 1997), which implies a continuous addition and exchange of biomolecules during pollen maturation. Stach *et al.* (2008) reported a positive correlation of aerial pollen counts of *B. pendula* with temperature and rainfall of the year before pollination. Thus, plant physiological reactions to prevailing environmental conditions can be assumed for *B. pendula*. *Carpinus betulus* is known to be particularly sensitive to frost damage and tends to prolong catkin proliferation when temperatures in spring are low. That affects the positive net productivity of photosynthesis in early spring (Chuine *et al.*, 2000) and leads to a shift of pollen development and maturation, which may have an effect on the $\delta^{13}C_{pollen}$ values.

Differences in pollen-isotopes within families and subfamilies

$\delta^{13}C_{pollen}$ deviate much less within one plant family than between families (Jahren, 2004). However, our findings show that this result does not apply to European taxa of the Betulaceae family. Four tree taxa of this family have been examined in this study (*A. glutinosa*, *C. avellana*, *B. pendula* and *C. betulus*). Taxonomically and genetically, the family is divided into two subfamilies: Coryloideae (including *Corylus* and *Carpinus*) and Betuloideae (including *Betula* and *Alnus*). Pollen grains of the members within the subfamilies are almost similar in shape and size (Beug, 2004). However, due to their different flowering periods from January to March (*A. glutinosa* and *C. avellana*) and April to May (*B. pendula* and *C. betulus*), they are isotopically very different. We found that isotopic differences within these subfamilies were higher than between-family differences (Table 3.9; differences within the Betuloideae $\delta^{13}C_{pollen}$ 3.9‰ and within the Coryloideae $\delta^{13}C_{pollen}$ 1.8‰). Analysing all Betulaceae pollen together would imply a loss of information in the isotope signal.

Table 3.9: Mean $\delta^{13}C_{pollen}$ and $\delta^{18}O_{pollen}$ pollen isotope values (in ‰) and standard deviations of the plant families and of the species within the two subfamilies of the Betulaceae. Mean values for each species include all sites and samplings of 2015 and 2016.

Plant Family	Subfamily	Species	$\delta^{13}C_{pollen}$	$\delta^{18}O_{pollen}$
Betulaceae	–	–	-26.4 ± 2.3	22.8 ± 2.7
	Betuloideae	*A. glutinosa*	-28.2 ± 1.9	21.1 ± 2.1
	Betuloideae	*B. pendula*	-24.3 ± 1.6	24.1 ± 1.6
	Coryloideae	*C. avellana*	-27.4 ± 1.7	21.7 ± 2.2
	Coryloideae	*C. betulus*	-25.6 ± 1.7	24.5 ± 1.0
Fagaceae	–	–	-26.2 ± 1.6	23.5 ± 3.2
Pinaceae	–	–	-26.0 ± 1.5	24.5 ± 2.3
Sapindaceae	–	–	-25.1 ± 1.5	22.4 ± 2.5

3.4.3 $\delta^{13}C_{pollen}$ values of coniferous trees flowering May to June

Picea abies and *Pinus sylvestris*

Even though both species of the family Pinaceae prefer similar habitats (George *et al.*, 1997), the mean carbon isotope offset between the two species is 1.5‰. The mean $\delta^{13}C_{pollen}$ value of *P. abies* is -25.3‰ (2015: -25.2‰; 2016: -25.4‰), that of *P. sylvestris* lies at -26.8‰ (2015: -26.6‰; 2016: -26.9‰). Thus, analysing bulk coniferous pollen would reduce the environmental information incorporated in the plant material. However, comparison of the mean $\delta^{13}C_{pollen}$ values of *P. sylvestris* and *P. abies* within the sampling sites reveals almost equal signals for both species between 2015 and 2016. Between-year mean $\delta^{13}C_{pollen}$ values of *P. abies* deviate by 0.2‰ and that of *P. sylvestris* by 0.3‰. Schwarz (2016) reported low $\delta^{13}C_{pollen}$ ranges between four consecutive years for *Pinus retinosa* (0.53‰) and between three years for *Pinus strobus* (1.03‰). Carbon molecules (mostly soluble sugars from the previous vegetation periods) can be allocated in the individuals (Richardson *et al.*, 2013) and are remobilized directly after the resumption of growth in spring (Schwarz, 2016; Loescher *et al.*, 1990). Thus, the usage of stored carbon as basic modules for the pollen might compensate seasonal variations in the $\delta^{13}C_{pollen}$. Hence, between-year median $\delta^{13}C_{pollen}$ values (p(sm); Figure 3.7) of most sites cannot be statistically distinguished for both species. The stored carbon differs in age between 0.7 years (Gaudinski *et al.*, 2009) and up to ten years (Richardson *et al.*, 2013).

Tree growth and photosynthetic activity of *P. sylvestris* starts approximately 40 days prior to budburst (Michelot *et al.*, 2012). *Pinus sylvestris* $\delta^{13}C_{pollen}$ values are found to correlate with temperature four to six weeks prior to pollen release (Loader and Hemming, 2004). Hence, it can be assumed that the plant uses newly fixated carbon in substantial portions to finish pollen maturation. There is no support for a correlation between North American *Pinus*-species $\delta^{13}C_{pollen}$ and temperature (Schwarz, 2016). Thus, this correlation might be species-specific to *P. sylvestris* (Loader and Hemming, 2001).

Intra-site pollen-isotope variability of the $\delta^{13}C_{pollen}$ values of *P. abies* range between 0.6‰ and 5.5‰ and that of *P. sylvestris* range between 2.5‰ and 4.0‰. Factors determining the intra-site isotope variability of *C. atlantica* and herbaceous species are microclimate, physiological differences between the individuals, water and nutrient availability and the number of trees in the direct vicinity (King *et al.*, 2012; Bell *et al.*, 2017). These factors may also account for the isotope variability of *P. abies* and *P. sylvestris*. Compared to *P. abies*, *P. sylvestris* has a broader physiological tolerance range to a variety of environmental conditions (Ingestad, 1979; George *et al.*, 1997). Hence, with larger plasticity, physiological reactions turn out smaller and their pollen-isotope values fluctuate less within one location. In general, the pollen-isotope ranges of both species are broader in pollen sampled in 2015 than in samples of 2016.

3.4.4 Intra-tree variability of $\delta^{13}C_{pollen}$

$\delta^{13}C_{pollen}$ values vary between 1.1‰ and 3.5‰ within an individual tree (Table 3.4). In most cases the values are higher at the eastern exposed side than at the southern and western sides. With less insolation, open stomata do not discriminate as much against the heavy aerial $\delta^{13}C$ isotopes (Schleser, 1999). That phenomenon is also expressed by circumferential variations of 1–3‰ in leaf-tissue $\delta^{13}C$ (Schleser, 1999) and Leavitt (2010) mentioned an average of 0.5–1.5‰ deviation from the mean within a circumferential tree ring cellulose analysis. In addition, the difference between mean $\delta^{13}C_{pollen}$ values can be up to 3‰ within a height difference of 6 m (Table 3.4). For 64% of the individuals, $\delta^{13}C_{pollen}$ values of the lower samples of a tree are lower compared to the upper ones (Table 3.4). These results agree with Schleser (1999) who described an enrichment of ^{13}C in leaf-tissue of 1–4‰ from bottom to top within one tree. The intra-tree variability between several inflorescences within one branch can be as high as 1.2‰ for $\delta^{13}C_{pollen}$ (Table 3.6). However, average differences of pollen-isotope values in neighbouring inflorescences of *P. sylvestris* are as little as 0.3‰ ($\delta^{13}C_{pollen}$, Table 3.6). Due to different carbon and oxygen sources the $\delta^{13}C_{pollen}$ shows a higher intra-tree variability than $\delta^{18}O_{pollen}$ (Table 3.6). Carbon is fixated in the leaves as the product of photosynthesis. The rate of photosynthesis varies in relation to the position of the leaf on the tree, which leads to isotopic differences between the cardinal directions. Stable isotopes of tree ring cellulose and other plant material vary in one individual (Leavitt and Long, 1984 and 1986) and it is generally suggested to pool several cores/samples in order to get the average representative isotope weight for the tree/year relation (McCarroll and Loader, 2004).

3.4.5 $\delta^{13}C_{pollen}$ values at different stages of pollen maturation

Betula pendula

Mean $\delta^{13}C_{pollen}$ values of *B. pendula* do not vary much over the flowering period and both samplings (11 weeks apart) cannot be statistically distinguished (-25.6‰ and -25.7‰; Figure 3.8, black bar). Pollen primordia are already built by the end of the previous year and the pollen maturation continues after a winter dormancy. In spring, the catkins emerge at the same time as the first leaf buds. Photosynthesis is not yet profitable this early in the year, thus the trees use stored and pooled carbon molecules to build new plant tissue in the beginning of the vegetation period (Luomajoki, 1986). This explains why the carbon composition of the pollen remained constant.

Pinus sylvestris

Mean $\delta^{13}C_{pollen}$ values of *P. sylvestris* did not change within 12 days (-26.3‰ and -26.3‰; Figure 3.8). Comparatively little is known about timing, exact molecular processes and chemical compositions during pollen development (Datta *et al.*, 2002; Blackmore *et al.*, 2007). Plants may use only storage molecules to build plant tissue in spring and early summer (Luomajoki, 1986; Schwarz, 2016). However, Loader and Hemming (2001) reported a correlation between $\delta^{13}C_{pollen}$ and temperature approximately six weeks prior to pollen release. Thus, at least in parts, *P. sylvestris* uses newly accumulated carbon molecules to build pollen. Perhaps we detected no change in the $\delta^{13}C_{pollen}$ of *P. sylvestris* because the sporopollenin of the grain wall had already been synthesised during the previous weeks.

3.4.6 $\delta^{13}C_{pollen}$ values of the elevation transect

$\delta^{13}C_{pollen}$ values of *P. abies* increase by 3.4‰ (mean value at 1053 m a.s.l: -26.6‰; mean value at 1344 m a.s.l.: -23.2‰) within the elevation transect covering roughly 300 m at the Tatrzański Mountains. The values correlate with elevation (Adj R^2=0.52; Figure 3.9). Although the increase of 3.4‰ is statistically distinct, it cannot be exclusively attributed to an altitudinal effect. In general, the discrimination of $\delta^{13}C$ is linearly related to the ratio of intercellular to ambient CO_2 partial pressures, and thus $\delta^{13}C$ values increase with increasing altitude (Körner *et al.*, 1991). Hultine and Marshall (2000) found a linear relationship between $\delta^{13}C$ from *Picea* ssp. needle tissue and elevation where the values of the $\delta^{13}C_{needle}$ increase by approximately 0.5‰ per 300 m in altitude, whereas Warren *et al.* (2001) reported an increase of 2.5‰ over 1000 m of $\delta^{13}C_{wood}$ from 14 different coniferous species. The *P. abies* individuals chosen for the elevation transect were all located on the

same slope facing north, thus ensuring comparable environmental conditions of e.g. wind, insolation and precipitation. However, the inflorescences from higher elevations were still immature, whereas they were already flowering at lower altitude. Flowering of *P. abies* starts with a delay of three days with every additional 100 m of elevation (Rötzer and Chmielewski, 2001). Bell *et al.* (2017) found that local environmental constraints mask the effect of altitude. They concluded that the source of air masses and moisture input seem to determine the pollen-isotopic weight more than the actual altitude in the mountains. In addition, Treydte *et al.* (2001) pointed out, that an existing temperature signal of *P. abies* in $\delta^{13}C_{tree-ring}$ was independent of elevation. Influencing factors on pollen-isotope values are very variable in mountainous areas. Which combination of factors caused the high 3.4‰ isotope offset over 300 m remains uninvestigated for now.

3.4.7 Stepwise Regression Analysis

Factors influencing $\delta^{13}C_{pollen}$ of each species

$\delta^{13}C_{pollen}$ values of all species are determined by several variable factors, and the outcome of the statistical analysis is sometimes inconclusive (Table 3.7). The factor site strongly influences *C. avellana* (Prob > F = <0.0001), where the maritime site (Forêt d'Anlier) contrasts the continental sites (Gorczański, Steigerwald, Müritz). *Picea abies* $\delta^{13}C_{pollen}$ values seem to be grouped by altitude, where the mountainous sites of Tre Cime and Tatrzański are contrasting the lower-altitude sites (Forêt d'Anlier, Steigerwald, Gorczański and Liesjärvi). However, these groupings could also be caused by genetic predispositions affecting phenological responses (Chuine *et al.*, 2000; Willis *et al.*, 2008; Wilczek *et al.*, 2010). *Pinus sylvestris* is known to have different haplotypes in Europe, one of which is restricted to the Southern Alps. Another haplotype of *P. sylvestris* spreads throughout central Europe (Cheddadi *et al.*, 2006) and can be found at all other sites of this study. *Pinus sylvestris* has distinct $\delta^{13}C_{pollen}$ values at northern and southern European sites, which seems to be caused by a different reaction to local temperatures due to their genetic background (Loader and Hemming, 2001).

Factors influencing $\delta^{13}C_{pollen}$ at each site

$\delta^{13}C_{pollen}$ values are mostly determined by the factor species which largely overprints other local non-climatic factors (e.g. the proximity of the tree to the next water body,

type of soil, slope angle; Table 3.8). Species groupings of the factor species at each site are variable and do not seem to follow plant family affiliation or flowering period. In addition, the factor *maturity* is important for the mountainous sites Tre Cime and Tatrzański.

3.4.8 General considerations for the usage of $\delta^{13}C_{pollen}$ in palaeoclimate studies

Species-specific isotope values and patterns display susceptibility to different environmental factors due to their phenology and physiology (Table 3.3; Figures 3.4–3.7). Therefore, the pollen must be separated by species prior to isotope analysis. Without separation, the individual isotope signal within the pollen will be lost and the method cannot be applied in palaeoclimate studies (Jahren, 2004; Nelson *et al.*, 2008). To date, the separation process is done manually which makes it very time-consuming to pick a sufficient amount of pollen for stable-isotope analysis (Nelson *et al.*, 2008; van Roij *et al.*, 2017). The amount of pollen needed to obtain representative average isotopic values is variable. Bell *et al.* (2019) suggest to use a sample size of at least 30 µg carbon when using standard stable-isotope measuring techniques. New technology makes it feasible to decrease this amount. Nelson *et al.* (2008) developed an isotope measuring technique using single pollen grains in order to estimate their photosynthetic pathway and Roij *et al.* (2017) even measured as little as 0.042 µg carbon with a precision better than 0.5‰. However, we identified significantly different pollen-isotope values within one site and even within one tree and therefore suggest using a higher amount of carbon/pollen depending on the pollen type to obtain significant mean pollen-isotope values.

Furthermore, mostly sporopollenin of the pollen wall is preserved in fossil pollen (Loader and Hemming, 2004). The analysis of raw pollen material, as reported by this study, shows the general variability between species and sites, but patterns and ranges cannot directly be compared to fossil pollen-isotope values (Jahren, 2004). To accomplish that, extant pollen will have to be treated chemically prior to analysis. The method of sporopollenin-extraction with sulfuric acid has been tested for several species and a consistent offset between raw and the chemically treated pollen material was found (Loader and Hemming, 2004; Bell *et al.*, 2017). The same accounts for the species of this study: treatment with sulfuric acid resulted in a stable but species-specific offset when compared to raw pollen material (unpublished data).

3.4.9 $\delta^{18}O_{pollen}$ values of broad-leaved species flowering January to March

Alnus glutinosa and *Corylus avellana*

Mean $\delta^{18}O_{pollen}$ values of *A. glutinosa* (21.1‰) and *C. avellana* (21.5‰) of the family Betulaceae are exceptionally low (Table 3.3). The trees sampled for this study grew on saturated soils with ample water supply out of consistent precipitation throughout the winter months and snowmelt in February and March. Therefore, both species did not face water stress during times of sampling, which may explain the observed low $\delta^{18}O_{pollen}$ values. *Alnus glutinosa* and *C. avellana* generally prefer areas with aggravated or missing drainage close to a streamside (Bennett and Birks, 1990). In case of insufficient water supply, riparian trees are able to switch sources and especially *A. glutinosa* is drought resistant (McVean, 1953). In general, there is no fractionation of oxygen isotopes during water uptake by the roots (Dongmann *et al.*, 1974). The xylem water remains unaltered during transport until it reaches evaporative tissue or is used to build plant tissue, such as flower primordia and pollen grains (Ehleringer and Dawson, 1992). Since *A. glutinosa* and *C. avellana* flower before leaf proliferation, the water is not passing transpiring leaf tissue, where the isotopes would be altered by evaporative ^{18}O enrichment. Mean $\delta^{18}O_{pollen}$ values of *A. glutinosa* and *C. avellana* from Gorczański are exceptionally low, but display broader ranges than the $\delta^{18}O_{pollen}$ values from Forêt d'Anlier (Figure 3.4). We expect variable interactions of non-climate environmental influences, e.g. elevation, slope and density of the surrounding vegetation, to have caused the wider distribution of $\delta^{18}O_{pollen}$ values at Gorczański.

3.4.10 $\delta^{18}O_{pollen}$ of broad-leaved species flowering April to May

Acer pseudoplatanus

Mean $\delta^{18}O_{pollen}$ values of *A. pseudoplatanus* (Sapindaceae) are highly variable between the sites (range of 18.0‰ to 25.7‰). Mean isotope values are comparable to *B. pendula* and *F. sylvatica*, depending on the location and year of sampling (Table 3.3). Noteworthy are the pollen-isotope values at Gorczański, where *A. pseudoplatanus* exhibits the lowest $\delta^{18}O_{pollen}$ values of all samplings in this study (2015: 18.0‰, 2016: 18.5‰). Although *A. pseudoplatanus* is flowering in May after leaf proliferation, the values are even lower than $\delta^{18}O_{pollen}$ of *A. glutinosa* and *C. avellana*.

Fagus sylvatica* and *Quercus robur

$\delta^{18}O_{pollen}$ of *Q. robur* are on average 3‰ higher than the values of *F. sylvatica* at those sites where both species from the family Fagaceae occur (Forêt d'Anlier and Steigerwald). This likely results from the developmental delay in spring. *Quercus robur* is slower in leaf unfolding, water uptake and in establishing a positive net productivity out of photosynthesis (Morecroft *et al.*, 2003; Schuster *et al.*, 2014). Oxygen isotope values of precipitation are enriched by evaporation before seeping into the soil, especially during summer months. An increased activity of *Q. robur* in summer and the uptake of water enriched in ^{18}O might explain the differences in $\delta^{18}O_{pollen}$ between the two species. The $\delta^{18}O_{pollen}$ values of *F. sylvatica* from Gorczański are exceptionally low (2015: 18.6‰; 2016: 19.5‰). This was also recognized in the May-flowering species *A. pseudoplatanus* (Table 3.3). However, we do not have a valid explanation for this site-specific phenomenon at the moment.

Betula pendula* and *Carpinus betulus

Mean $\delta^{18}O_{pollen}$ values of species of the Betuloideae deviate by more than 3‰ where *C. betulus* (27.1‰) yields higher values than *B. pendula* (24.1‰). In general, the mean $\delta^{18}O_{pollen}$ values within the species are very similar between the investigated sites and do not deviate much from the overall mean (Figure 3.5, dotted line). In particular the 2016 oxygen isotope values of *B. pendula* are very similar (Figure 3.5, black bar), implying that the $\delta^{18}O_{pollen}$ values of these two species are less affected by local environmental events but rather by trans-regional trends. Isotope values of other species deviate more between sites per year (Figure 3.4, 3.6, 3.7).

3.4.11 $\delta^{18}O_{pollen}$ values of coniferous trees flowering May to June

Picea abies* and *Pinus sylvestris

Mean $\delta^{18}O_{pollen}$ values of *P. abies* and *P. sylvestris* (both Pinaceae) are significantly different, even within the same site (p(sm); Figure 3.7). Schwarz (2016) pointed out that oxygen pollen-isotopes are highly sensitive to environmental conditions. We expect the varying interaction of all local conditions (e.g. micro-climate at the sampling site and water availability) to have caused the different $\delta^{18}O_{pollen}$ values between the vegetation periods 2015 and 2016. However, all European sites compared, both species show similar pollen-isotope patterns. The year-to-year differences between mean $\delta^{18}O_{pollen}$ values of *P. abies* from all sites is 1.7‰ (2015: 24.0‰; 2016: 22.3‰), whereas the differences between

P. sylvestris pollen-isotopes is 1.4‰ (2015: 26.8‰; 2016: 25.4‰). With an offset of only 0.3‰ between both, the species seem to react to regional environmental conditions in a similar way. Nevertheless, their species-specific isotope values are still very distinct. *Picea abies* (overall average: 23.2‰) and *P. sylvestris* (overall average: 26.1‰) yield an average offset of 2.9‰

The $\delta^{18}O_{pollen}$ values at Forêt d'Anlier are higher for 2016 compared to 2015, whereas the $\delta^{18}O_{pollen}$ values at all other locations in this study are higher for 2015 (Figure 3.7). Both species display the same patterns, therefore weather conditions, which were not investigated further in this study, are expected to have caused the $\delta^{18}O_{pollen}$ inversions. The North Atlantic Oscillation (NAO) is known to influence phenology and temporal variability of seasonal tree development in Europe (Scheifinger *et al.*, 2002). The site of Forêt d'Anlier lies closest to the Atlantic Ocean and is therefore more strongly influenced by the NAO than more inland-located sites.

In general, $\delta^{18}O$ values of precipitation become more negative with increasing altitude and latitude. The $\delta^{18}O_{cellulose}$ of coniferous trees shows a clear latitudinal pattern at a transect in North America covering the area between 65° N and 33° N (Burk and Stuiver, 1981). Our study covers an area from 60° N to 46° N, but the pollen-isotopes do not show any pattern resembling this latitudinal effect. The northernmost site (Liesjärvi) yields low $\delta^{18}O_{pollen}$ values for *P. sylvestris* (23.6‰), but average values of $\delta^{18}O_{pollen}$ for *P. abies* (22.7‰). The southernmost site (Tre Cime, 1067 m a.s.l.) should yield the highest $\delta^{18}O_{pollen}$ values. However, compared to other central European sites the $\delta^{18}O_{pollen}$ values at Tre Cime are overprinted by an additional altitudinal effect leading to comparatively low $\delta^{18}O_{pollen}$ values for both species (*P. abies*: 22.6‰, *P. sylvestris*: 24.8‰; Figure 3.7). All sites of this study are influenced by a variety of location-dependent factors, such as longitude, proximity to the ocean and altitude that overprint the latitudinal effect.

3.4.12 Intra-tree variability of $\delta^{18}O_{pollen}$

$\delta^{18}O_{pollen}$ values differ between 0.6‰ and 2.1‰ between different cardinal directions in a single tree. Increasing tree height from 1 m to 7 m accounts for a statistically distinct increase in $\delta^{18}O_{pollen}$ of 1.3‰ (Table 3.4). In general, lower samples yield lower isotope values than upper samples. In addition, the southern and western samples yield lower isotope values than the northern samples (Table 3.4). The $\delta^{18}O_{pollen}$ intra-branch variability can be as high as 1.4‰ (Table 3.6), but the average difference between neighbouring inflorescences is 0.5‰, which can be considered to lie within a natural tolerance range.

3.4.13 $\delta^{18}O_{pollen}$ values at different stages of pollen maturation

Betula pendula

$\delta^{18}O_{pollen}$ values (20.9‰ and 24.9‰; Figure 3.8) are dependent on floral development. Oxygen molecules within the pollen tissue are exchanged until pollination. Rowley *et al.* (2000) reported pollen alteration on the exact day of pollen shedding, where last cells from the pollen developmental tissue are removed and a nutritional transfer takes place. The coating of the outer grain wall contains mostly lipids and proteins and the inside holds cell organelles which develop only late in the pollen maturation process. Therefore, we assume that the variability of the $\delta^{18}O_{pollen}$ values is caused by alteration and exchange of volatile components of the outer and inner pollen grains. Another reason for the highly variable $\delta^{18}O_{pollen}$ of both samplings might be oxidation of the grain wall. The catkins of *B. pendula* on 10 March were very young and tightly closed. The ones sampled on 5 May were mostly open, dry and some catkins already exceeded the time of pollination. Therefore, pollen in open catkins may have been oxidized subsequent to air exposure changing the $\delta^{18}O_{pollen}$ values.

Pinus sylvestris

Mean $\delta^{18}O_{pollen}$ noticeably changes (25.7‰ and 26.9‰; Figure 3.8, black bar) over a time period of 12 days. On 20 May the *P. sylvestris* inflorescences were still closed, whereas on 1 June the flowers were open and pollinating. Thus, as with *B. pendula*, the difference of $\delta^{18}O_{pollen}$ might result from changes of attached nutrients and volatile grain wall components. In addition, the immature sacculae of coniferous pollen contain a liquid that is only reabsorbed a few days before pollination (Rowley *et al.*, 2000). The isotope composition of that liquid remains unknown.

3.4.14 $\delta^{18}O_{pollen}$ values of the elevation transect

$\delta^{18}O_{pollen}$ values do not correlate with altitude (Adj.R^2=0.14; Figure 3.9). The mean $\delta^{18}O_{pollen}$ value increases by 1.2‰ over 300 m elevation. However, considering the different maturity of the inflorescences at the time of sampling, the isotopic weight of immature pollen grains on the mountaintop was most likely affected by further maturation.

3.4.15 Stepwise Regression Analysis

Factors influencing $\delta^{18}O_{pollen}$ of each species

$\delta^{18}O_{pollen}$ values are especially dependent on the geographic location, hence the factor *site* (a combination of latitude, longitude and altitude) is particularly important for all species. The broad-leaved trees *A. glutinosa* and *C. avellana* as well as *F. sylvatica* mostly differ between the western sites (Forêt d'Anlier, Steigerwald and Müritz) in relation to the eastern site of Gorczański. The sampling sites for the coniferous pollen are separated in a similar way compared to the broad-leaved species, apart from Gorczański, which is also grouped with the high-latitude site of Liesjärvi and the mountainous site of Tre Cime (Table 3.7). These groupings indicate differences between maritime and continental (and high-altitude) sampling sites. The factor maturity makes a noticeable difference for *A. glutinosa*, *F. sylvatica* and *P. sylvestris* (Table 3.7), because volatile components and cell organelles increase in size and volume until the end of the pollen maturation process.

Factors influencing $\delta^{18}O_{pollen}$ at each site

$\delta^{18}O_{pollen}$ values are also often determined by species. However, the statistical groupings are even more variable than those of $\delta^{13}C_{pollen}$. At most of the sites where pollen of the same species were sampled in two consecutive years (Forêt d'Anlier, Tre Cime, Steigerwald and Tatrańzki), the factor year significantly affects the pollen-isotope values, reflecting comparative results of Figures 3.4 to 3.7 (Table 3.8).

3.5 Conclusions

1. Most of the $\delta^{13}C_{pollen}$ and $\delta^{18}O_{pollen}$ are normally distributed and all examined species yield specific pollen-isotope patterns, even if the isotope ranges of the species partly overlap.

2. $\delta^{13}C_{pollen}$ and $\delta^{18}O_{pollen}$ ranges show gradients between maritime and continental study sites (W – E transect) as well as between those which differ in day length (N – S transect).

3. Mean species-specific pollen-isotope values vary inter-annually, on average 1.0‰ for $\delta^{13}C_{pollen}$ and 1.6‰ for $\delta^{18}O_{pollen}$. Due to storage of carbon molecules for building new plant tissue, the variation within $\delta^{13}C_{pollen}$ is lower than the variation within $\delta^{18}O_{pollen}$.

4. Broad-leaved tree species flowering before leaf proliferation (January to March; *Alnus glutinosa* and *Corylus avellana*) yield significantly lower $\delta^{13}C_{pollen}$ and $\delta^{18}O_{pollen}$ values than broad-leaved species flowering later in spring (April to May).

5. The coniferous species *Pinus sylvestris* and *Picea abies* show similar reactions to local environmental conditions, but their specific $\delta^{13}C_{pollen}$ and $\delta^{18}O_{pollen}$ values are significantly different.

6. Intra-annual pollen-isotope analysis reveals that $\delta^{13}C_{pollen}$ values do not significantly change during the last stages of the pollen maturation process, whereas $\delta^{18}O_{pollen}$ can be altered during that time.

7. $\delta^{13}C_{pollen}$ and $\delta^{18}O_{pollen}$ differ between sampling positions on trees. Samples from lower positions yield lower isotopic weights than samples from upper positions. Isotope values of single inflorescences can vary within branches up to 1.2‰ for $\delta^{13}C_{pollen}$ and 1.4‰ for $\delta^{18}O_{pollen}$. There is also a circumferential variability of pollen-isotopes at different cardinal directions of up to 3.5‰ for $\delta^{13}C_{pollen}$ and 2.1‰ for $\delta^{18}O_{pollen}$. Because of that variability, an appropriate amount of pollen is needed for stable isotope analysis to enhance the precision of the measured mean $\delta^{13}C_{pollen}$ and $\delta^{18}O_{pollen}$ values.

8. $\delta^{13}C_{pollen}$ values increase with elevation by 3.4‰ over 300 m. Even though the two variates are significantly correlated, the difference is too high to be explained by altitude alone. Thus, additional unknown factors must have influenced the isotopic trend. $\delta^{18}O_{pollen}$ values do not change linearly with elevation.

9. Stepwise regression analysis reveals that the most important factor determining pollen-isotope values of any species in this study is their geographic location (factor site). In addition, the statistical analysis shows that the pollen-isotopes within one site are mostly determined by the factor species.

Stable carbon and oxygen isotope analysis of fossil pollen can improve the precision of palaeoenvironmental investigations. The applicability of different pollen types in palaeoclimate research relies on the specific plant physiological traits as well as on the pollen abundance in fossil archives. However, due to species-specific pollen-isotope ranges and patterns, fossil pollen should be separated by species as thoroughly as possible. After separation, varying vegetation periods and ecological preferences of the host-plant will allow climate reconstructions on an intra-seasonal scale.

3.6 Acknowledgements

We are thankful to the students who helped during fieldwork and sample preparation in the laboratory: Julian Hennig, Camilla Brunello, Franziska Pritzke, Alena Zippel, Hendrik Schultz and Vanessa Skiba. Also, we thank Maike Glos (Freie Universität Berlin) for discussion, support and consultations concerning laboratory methods. We also acknowledge Raffella Dibona and all colleagues from the Centro Studi Ambiente Alpino in San Vito Di Cadore for accommodation during fieldwork in Italy and discussions about the biogeography in the adjoining Dolomite Mountains. Additionally, we are very grateful to Vincent Duponcheel (Forêt d'Anlier), Nils Altvater, Ralf Pauli (both Müritz NP) and Pawel Czarnota (Gorczański NP) for regional information about the national parks, local phenology and seasonality as well as pollinator behaviour. We also thank two anonymous reviewers for many positive comments and suggestions to improve an earlier version of the manuscript.

Chapter 4

Quantifying the impact of chemicals on stable carbon and oxygen isotope values of raw pollen

Carolina Müller[1], *Julian Hennig*[1], *Frank Riedel*[1], *Gerhard Helle*[1,2]

[1]Institute of Geological Sciences, Palaeontology, Freie Universität Berlin, Berlin, Germany
[2]GFZ German Research Centre for Geoscience, Section 4.3 Climate Dynamics and Landscape Evolution, Potsdam, Germany

Submitted to *Journal of Quaternary Science* (under review)

Keywords: Pollen; stable carbon and oxygen isotopes; chemical treatment; pollen purification protocol

Abstract

Purification protocols to extract pollen from lake sediments contain chemicals, which alter the carbon and oxygen pollen-isotope values according to pollen characteristics and family affiliation. Modern (raw) pollen of broad-leaved (*Alnus glutinosa*, *Betula pendula*, *Carpinus betulus*, *Corylus avellana*, *Fagus sylvatica* and *Quercus robur*) and coniferous tree species (*Picea abies* and *Pinus sylvestris*) have been treated with potassium hydroxide (KOH), hydrofluoric acid (HF), sodium hypochlorite (NaClO) and sulfuric acid (H_2SO_4) to test the individual impact on $\delta^{13}C_{pollen}$ and $\delta^{18}O_{pollen}$. Alterations of $\delta^{13}C_{pollen}$ values vary between +1.0‰ (*B. pendula*, NaClO treatment) and -5.0‰ (*P. sylvestris*, H_2SO_4 treatment), but raw and treated mean $\delta^{13}C_{pollen}\delta^{13}C_{pollen}$ values correlate for KOH, NaClO

and H_2SO_4. The general impact of chemicals on $\delta^{18}O_{pollen}$ values are more diverse. The offset ranges between +1.1‰ (*C. avellana*, NaClO treatment) and -17.9‰ (*P. sylvestris*, H_2SO_4 treatment). However, raw and treated $\delta^{18}O_{pollen}$ correlate for KOH, NaClO and HF, but not for H_2SO_4. Even though the overall offset is higher for treated $\delta^{18}O_{pollen}$ values, species-specific response patterns are generally alike for carbon and oxygen. After treatments with KOH, NaClO and HF coherences between raw and treated pollen are still apparent, whereas application of H_2SO_4 leads to inconsistent changes on the different pollen types.

4.1 Introduction

Stable carbon and oxygen isotope analysis of modern pollen find various fields of application, e.g. the investigation of predominant photosynthetic pathways within grasslands (Nelson *et al.*, 2006; Descolas-Gros and Schölzel, 2007; Urban *et al.*, 2016), determining the provenance of honey (e.g. Chesson *et al.*, 2011 and 2013) and tracing ongoing climate conditions such as moisture availability (Bell *et al.*, 2017) and local temperatures during pollen formation (Loader and Hemming, 2002). Some studies investigated the relationship of fossil pollen-isotopes to climate conditions in the past (Nelson *et al.*, 2008; Kamenik *et al.*, 2009; Urban *et al.*, 2016; Bell *et al.*, 2019) and used pollen for age dating (e.g. Zhou *et al.*, 1997; Fletcher *et al.*, 2017). But most available research on modern pollen-isotopes focused on species-specific patterns and ranges (e.g. Amundson *et al.*, 1997; Jahren, 2004; Loader and Hemming, 2004; King *et al.*, 2012; Nelson, 2012; Schwarz, 2016; Müller *et al.*, 2020). The structure and composition of a pollen grain wall varies highly with species (e.g. Moore *et al.*, 1991; Stanley and Linskens, 2012) and the carbon and oxygen pollen-isotope values differ significantly within genera and plant families (Müller *et al.*, 2020). The main component of a pollen wall is sporopollenin, a highly resistant biopolymer approximately consisting of $C_{90}H_{150}O_{33}$ (Brooks and Shaw, 1978; Loader und Hemming, 2004; Fraser *et al.*, 2014; Li *et al.*, 2019; Mikhael *et al.*, 2019). The average proportion of sporopollenin within raw pollen of different species is 55-85% (Nelson, 2012).

Applying a method of stable carbon and oxygen isotope analysis on fossil pollen may lead to an enhancement of paleoclimate reconstructions, since the spatio-temporal resolution can be very high and thus even intra-annual weather signals may be recorded in $\delta^{13}C_{pollen}$ and $\delta^{18}O_{pollen}$ due to plant-specific timings in pollen production and shedding (Schwarz, 2016; Bell *et al.*, 2019; Müller *et al.*, 2020). However, prior to the interpreta-

tion of fossil pollen-isotopes, some obstacles need to be overcome. First, raw (or modern) pollen differ from fossil pollen (Loader and Hemming, 2000). Additional to sporopollenin, the outer wall of raw pollen contains lipids, proteins and in some cases pollenkitt and the inner pollen wall is composed of pectin, cellulose and hemicellulose (Fan *et al.*, 2019). Chemical substances (mostly H_2SO_4) can be applied to extract sporopollenin and imitate diagenetic processes, as they occur during fossilisation of pollen in lakes. Sporopollenin extraction generally promotes the comparability of isotope values from raw and fossil pollen. Second, pollen samples from lake sediments contain various types of pollen, other organic matter and clastic debris. Therefore, pollen samples need to be chemically purified prior to isotope analysis. Testing the impact of chemicals on raw pollen-isotopes needs to be executed in order to interpret the values of fossil pollen accurately.

Some chemicals are traditionally used to extract and purify pollen from lake sediments for paleoclimate studies (Faegri *et al.*, 1989; Nelson *et al.*, 2006; Griener *et al.*, 2013). These are mainly: Hydrochloric acid (HCl) to remove inorganic carbon particles, potassium hydroxide (KOH) to digest humic acids, hydrofluoric acid (HF) to dissolve siliciclastic components and a glacial acetic acid used for an acetylation technique. These chemicals lead to substance-dependent carbon-isotopic contamination of the pollen grain wall, especially, when an acetolysis is part of the protocol (Amundson *et al.*, 1997). It was found, that any protocol containing acetolysis needs to be avoided due to its major impact on the carbon pollen-isotopes (Amundson *et al.*, 1997; Descolas-Gros and Schölzel, 2007). However, the impact of most of the chemical substances used to purify pollen samples have not been tested yet and only a few purification-protocols have been examined especially for their influence on pollen-isotope alterations. To prevent contamination of the $\delta^{13}C_{pollen}$, Loader and Hemming (2000) tested an acid digestion method avoiding chemicals affecting the carbon isotope composition of the pollen. They used solely sulfuric acid (H_2SO_4) to remove all organic components from raw pollen grains (cellulose, hemicellulose, cell organelles and pollen wall coating of lipids and pollenkit) except sporopollenin. A stable and species-specific offset of the $\delta^{13}C_{pollen}$ from *Pinus sylvestris* (-2.18‰), *Zea mais* (-1.81‰) and *Popolus tricoparca* (-3.55‰) was detected and all species yield strong linear correlations between raw and chemically treated pollen-isotope values ($R^2 = 0.93$; Loader and Hemming, 2000). When Descolas-Gros and Schölzel (2007) applied H_2SO_4 on raw pollen to investigate reflections of the C3 and C4 photosynthetic pathway in $\delta^{13}C_{pollen}$, they detected offsets of -1.18‰ (*Sorghum vulgare*) and -0.91‰ (*Platanus* sp.). Another test of the method using H_2SO_4 to extract sporopollenin revealed an average offset of

-1.5‰ between raw and treated $\delta^{13}C_{pollen}$ of *Cedrus atlantica* (range between -0.6‰ and -2.1‰; Bell *et al.* 2017).

Nelson *et al.* (2006) established a protocol containing HCl, KOH, HF, NaClO and H_2SO_4. Applied to raw pollen of grass species, it led to depletions ranging between -1.2‰ and -3.7‰ in the $\delta^{13}C_{pollen}$. The average depletion within raw pollen $\delta^{13}C$ from *Artemisia* and *Ambrosia* (family Asteraceae) following the same treatment is -1.45‰ (range -0.15 to -2.71; Nelson 2012). Griener *et al.* (2013) used this protocol on raw and fossil *Nothofagus* pollen and detected an average depletion of -1.7‰ within the $\delta^{13}C_{pollen}$ (range between -0.9‰ and -3.6‰). Overall, treatments including sulfuric acid leads to depleted carbon pollen-isotope values, but the impact seems to be highly species-specific.

Less impact on carbon pollen-isotopes of several species had chemicals tested by Jahren (2004): sodium hydroxide (NaOH) led to enrichments of 0.79‰ to 1.55‰, hydrogen peroxide (H_2O_2) altered the pollen on average by -0.15‰ to -0.68‰ and a modified Schulze´s solution (which contains HF) depleted the pollen-isotopes by -0.04‰ to -0.52‰. These treatments are suggested to simulate the effect of diagenesis avoiding acetolysis and H_2SO_4 and additionally to be used for the isolation of isotopically unaltered pollen. Most recently, Bell *et al.* (2019) successfully used a dense-media separation technique to extract fossil pollen from lake sediment avoiding H_2SO_4 and other carbon isotope altering chemicals.

However, lake sediment samples vary in composition. Each sediment core requires the application of different chemicals due to its unique features and hence, individual protocols should be created prior to each study. In general, applying fewer chemicals lessens pollen isotopic alterations. However, if the sediment material requires the application of chemicals which are known to have a strong impact on the $\delta^{13}C_{pollen}$ values, it may in some cases still be beneficial (Jahren, 2004).

There is little suggestion about a method to avoid oxygen-isotope alteration of the pollen wall components available and the impact of certain chemicals on the oxygen pollen-isotope values have not been tested yet. A published technique including ethanol dilution to separate pollen from honey for oxygen pollen-isotope analysis revealed a large but consistent impact on the $\delta^{18}O_{pollen}$ values (depletion of -3.3‰ to -5.6‰; Chesson *et al.*, 2013). Different drying methods led to alterations of the oxygen isotope values of raw sunflower pollen (oven-dried: -2.8‰; freeze-dried: -5.8‰; air-dried: -4.0‰). Since the temperature during a drying procedure impacted the pollen-isotope values, Chesson *et al.* (2013) generally advise to investigate the impact of microclimate on $\delta^{18}O_{pollen}$ values more

thoroughly before drawing of the provenance of honey through pollen-isotope values.

The approach of fossil pollen-isotopes can only be applied in paleoclimate reconstructions when the species-specific impact of chemical substances on $\delta^{13}C_{pollen}$ and $\delta^{18}O_{pollen}$ has thoroughly been investigated. Therefore, we test the particular effect of four chemical substances (KOH, NaClO, HF and H_2SO_4) and a successive treatment including all chemicals on raw pollen of eight different tree species. We want to assess general alterations of pollen-isotope values after exposure to different chemical substances to promote the compilation of a treatment protocol minimizing the impact on fossil pollen-isotopes. Additionally, species-specific variations of the carbon and oxygen pollen-isotopes after a chemical treatment are investigated.

4.2 Material and Methods

4.2.1 Sample location, collection and preparation

Modern pollen samples of seven abundant tree species (*Alnus glutinosa*, *Betula pendula*, *Corylus avellana*, *Fagus sylvatica*, *Picea abies*, *Pinus sylvestris* and *Quercus robur*; Table 4.1) were collected in March and May 2016 within their respective flowering period in Parc naturel Forêt d'Anlier (Belgium: 49.7899° N, 5.6829° E; average elevation: 385 m a.s.l.). The mean yearly temperature (MAT) at this location is 9.1 °C (mean temperature of coldest month: -0.1 °C; mean temperature of warmest month: 16.1 °C). The mean annual precipitation (MAP) amounts to 1019 mm (based on the high-resolution gridded dataset CRU TS at http://www.cru.uea.ac.uk/data). Pollen of *Carpinus betulus* (Table 4.1) was collected in May 2016 at Nationalpark Steigerwald (Germany: 49.8616° N, 10.5241° E; average elevation: 390m a.s.l.; MAT: 9.4 °C; mean temperature of coldest month: -1.2 °C; mean temperature of warmest month: 17.5 °C; MAP: 581 mm).

Table 4.1: Overview of species, taxonomic classification and pollen characteristics (Beug, 2004) of eight tree species examined in this study including their common names and family affiliation.

Family	Species	Common name	Size of pollen	Shape of pollen
Betulaceae	*Alnus glutinosa* (L.) GAERTN.	Black alder	24 - 34 μm	Stephanoporatae, pentagonal
	Betula pendula ROTH	Silver birch	26 - 32 μm	Triporatae, triangular
	Carpinus betulus (L.)	European hornbeam	38 - 48 μm	Stephanoporatae, roundish
	Corylus avellana (L.)	Common hazel	28 - 33 μm	Triporatae, triangular
Fagaceae	*Fagus sylvatica* (L.)	European beech	28 - 39 μm	Tricolporatae, roundish
	Quercus robur (L.)	Pendunculate oak	31 - 40 μm	Tricolpatae, oval
Pinaceae	*Picea abies* (L.) H. KARST.	Norway spruce	110 - 148 μm	Vesiculatae
	Pinus sylvestris (L.)	Scots pine	62 - 84 μm	Vesiculatae

Collected inflorescences were kept in a customary refrigerator during fieldwork and dried afterwards in a drying oven with a maximum temperature of 45 °C for seven days. Dry samples were kept frozen at -16 °C until further processing. The pollen were separated from the rest of the flower tissue through rinsing and sieving using sieves with mesh sizes of 10-200 μm. Afterwards, the pollen were transferred into safe lock tubes, freeze-dried until fully dehydrated and kept frozen for preservation.

4.2.2 Chemical treatment procedure

Three samples of each species were treated separately with potassium hydroxide (KOH 10%; 20 min., ca. 70 °C water bath), sulphuric acid (H_2SO_4 96%; 5h on a shaker), hydrofluoric acid (HF 38%; 24 h) and sodium hypochlorite (NaClO 3%; 90 sec.; Table 4.2). Repeated and thorough rinsing of the pollen samples with deionised water followed each chemical treatment. To test add-up effects of the chemicals, as it occurs following a standard protocol for fossil pollen sample preparation, three samples of each species underwent all chemical treatments in the same order and length. All samples were visually inspected after each chemical treatment using a Meiji MT4300L microscope at 400x and 600x magnification.

4.2.3 Stable isotope and statistical analysis

220 μg $\pm$ 10% of pollen material was weighed directly into silver capsules using a high precision scale (Mettler Toledo AX 26 Delta Range) at the dendrochronological laboratory, section 4.3, GFZ Potsdam. The carbon and oxygen isotope values were determined using a DELTA V isotope ratio mass spectrometer (IRMS; Thermo Fisher ScientificTM, Bremen). Each sample was weighed and measured with three repetitions and vacuum dried for at least 12 hours in a Thermo Scientific Heraeus VT 6060 P at 100°C prior to measurement. The pollen material was reduced to CO for simultaneous IRMS analysis of carbon and

Table 4.2: Details of the chemical treatment procedure used to prepare pollen for stable carbon and oxygen isotope analysis including the common names and purity of the chemicals, the specifications of each treatment, the time for each treatment and the effect on the pollen sample.

Chemical	Common name	Purity	Type of treatment	Duration	Effect
KOH	Potassium hydroxide	10%	Water bath at 70 °C	20 min.	Digestion of humic acids
H_2SO_4	Sulfuric acid	96%	Constantly on a shaker	5 hours	Extraction of sporopollenin
HF	Hydrofluoric acid	38%	Resting	24 hours	Degeneration of clastic debris
NaClO	Sodium hypochlorite	3%	Gentle stirring	90 sec.	Dissolution of organic contents

oxygen isotope ratios in a High Temperature Conversion Elemental Analyzer (TC/EA; 1400°C; Thermo Fisher ScientificTM, Bremen) coupled to the IRMS. Isotope ratios are expressed relative to VPDB for δ^{13}C and VSMOW for δ^{18}O. The isotope values were compared against lab-internal and international reference material (IAEA-CH3, IAEA-CH6 and IAEA 601 and 602). For a single-point normalisation two reference standards with widespread isotopic compositions were used (Paul *et al.*, 2007). In total, we conducted 296 measurements of chemically treated pollen and 72 measurements of untreated (referred to as raw) pollen of the same individuals (supplementary material, Table 7.3). Simple linear correlations (Adj.R^2 values, range 0-1) were applied for testing relationship of isotope values from raw and chemically treated pollen of individual trees. The hypothesis of linear correlation was rejected, if the probability p was smaller than the significance level (range: 0-1; significance level: p=0.05). All calculations and the graphic depiction were made using the programmes R (RCore Team, 2017) and RStudio (RStudio Team, 2015).

4.3 Results

4.3.1 $\delta^{13}C_{pollen}$ after chemical treatment

Mean $\delta^{13}C_{pollen}$ values are mostly depleted after chemical treatment procedures compared to raw pollen-isotope values (Table 4.3; Figure 4.1). The depletion of mean $\delta^{13}C_{pollen}$ values after KOH exposure ranges from -0.3‰ (*F. sylvatica*) to -4.0‰ (*C. avellana*). The HF treatment results in a depletion ranging between -0.4‰ (*P. abies*) and -1.4‰ (*C. avellana*) and the impact of sulfuric acid (H_2SO_4) on mean $\delta^{13}C_{pollen}$ values results in a depletion ranging from -1.2‰ (*F. sylvatica*) to -5.0‰ (*P. sylvestris*). A successive treatment with all chemicals (*all*) has the highest impact on $\delta^{13}C_{pollen}$ values compared to the untreated pollen material. The depletions range between -1.6‰ (*F. sylvatica*) and -6.4‰ (*P. sylvestris*). Enriched mean $\delta^{13}C_{pollen}$ values occur only after NaClO treatment for *B. pendula* (+1.0‰) and *C. betulus* (+0.8‰). Pollen-isotope values of other species are depleted after exposure to NaClO and range between -0.3‰ (*P. sylvestris*) and -1.4‰ (*C. avellana*). There was no effect on *P. abies* pollen measurable for NaClO (Table 4.3; Figure 4.1).

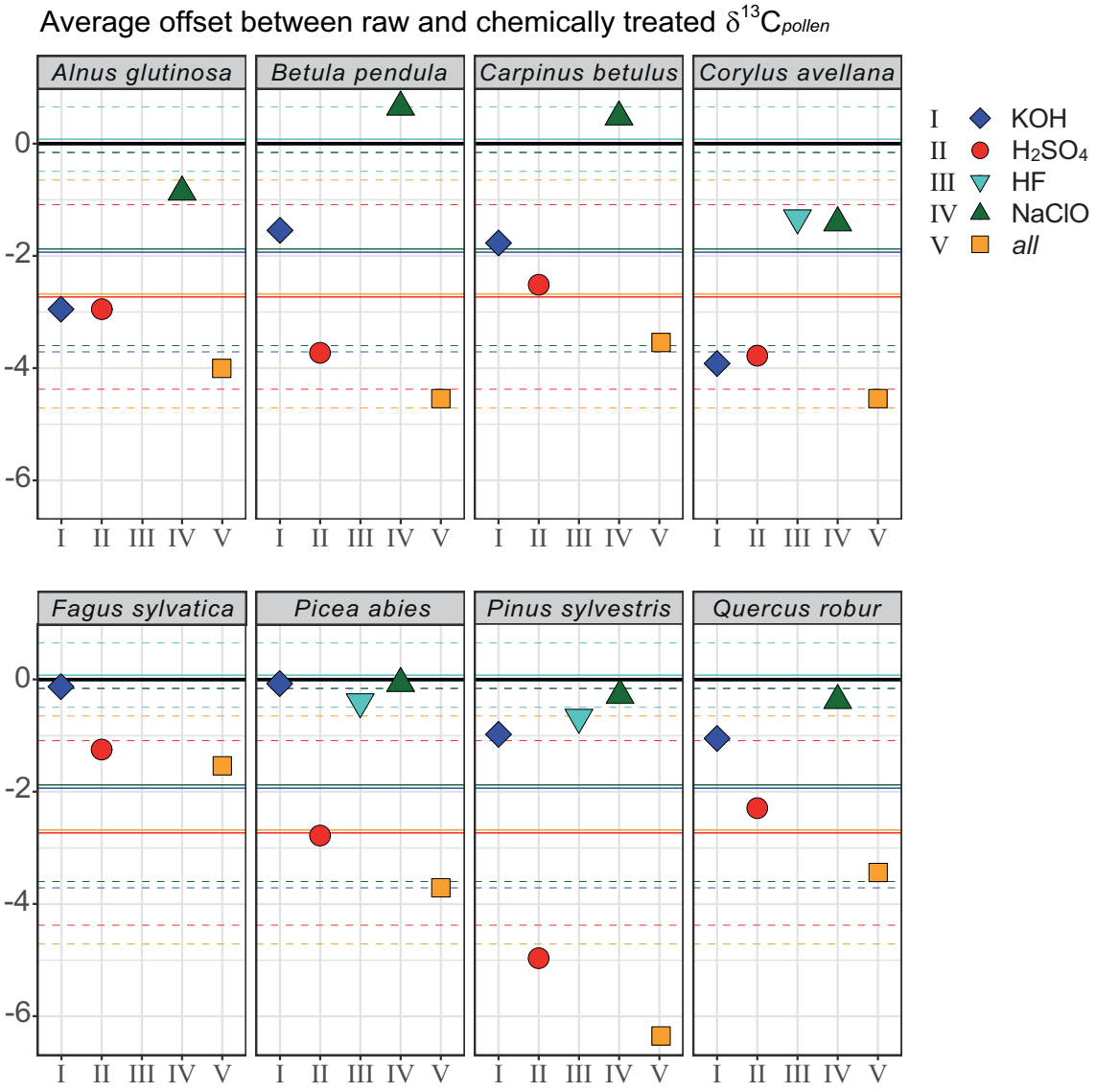

Figure 4.1: Average offset between untreated (raw) and chemically treated $\delta^{13}C_{pollen}$ values (vs. VPDB). Three pollen samples from individual trees of eight species were treated with four different chemicals (KOH (I), H_2SO_4/all (II), HF (III) and NaClO (IV); HF was applied to three species and NaClO is missing for *F. sylvatica*). Three samples each underwent a full chemical treatment procedure (*all* (V)). Coloured symbols indicate the mean value of three repetitions for each species and chemical. Horizontal solid lines show the mean deviation of each chemical for all species compared to the mean isotope values of the raw material. Dashed lines represent the corresponding first standard deviation to the overall mean isotope values for each chemical.

Table 4.3: Mean $\delta^{13}C_{pollen}$ values (expressed in ‰) and standard deviation after chemical treatment with KOH, HF, NaClO, H_2SO_4 and *all* (successive treatment procedure following the protocol of four chemicals applied consecutively; see text). Raw $\delta^{13}C_{pollen}$ values refer to chemically untreated pollen of the same individuals. Isotope ratios are expressed relative to VPDB for ^{13}C. Dev. H_2SO_4/*all* refers to the difference between values after treatment solely with H_2SO_4 and after the successive treatment (*all*, expressed in ‰).

Plant species	δ^{13}**C raw**	δ^{13}**C KOH**	δ^{13}**C HF**	δ^{13}**C NaClO**	δ^{13}**C H_2SO_4**	δ^{13}**C all**	**Dev. δ^{13}C: H_2SO_4/all**
A. glutinosa	-30.6 ± 0.3	-33.6 ± 1.4	–	-31.3 ± 0.2	-33.6 ± 0.7	-34.6 ± 0.4	1.0
B. pendula	-24.6 ± 0.1	-26.2 ± 0.2	–	-23.6 ± 0.1	-28.5 ± 0.3	-29.2 ± 0.2	0.7
C. betulus	-26.0 ± 0.1	-27.7 ± 0.3	–	-25.2 ± 0.2	-28.6 ± 0.3	-29.5 ± 0.3	0.9
C. avellana	-28.4 ± 0.3	-32.4 ± 0.2	-29.8 ± 0.3	-29.8 ± 0.1	-32.1 ± 0.7	-33.0 ± 0.1	0.9
F. sylvatica	-28.2 ± 0.1	-28.5 ± 0.2	–	–	-29.4 ± 0.5	-29.8 ± 0.1	0.4
Q. robur	-26.1 ± 0.3	-27.2 ± 0.6	–	-26.5 ± 0.2	-28.4 ± 0.3	-29.5 ± 0.2	1.1
P. abies	-27.4 ± 0.3	-27.5 ± 0.2	-27.8 ± 0.2	-27.4 ± 0.2	-30.1 ± 0.3	-31.1 ± 0.3	1.0
P. sylvestris	-24.8 ± 0.3	-25.8 ± 0.2	-25.5 ± 0.2	-25.1 ± 0.1	-29.8 ± 0.3	-31.2 ± 0.2	1.4

4.3.2 $\delta^{18}O_{pollen}$ after chemical treatment

Mean $\delta^{18}O_{pollen}$ values of *B. pendula* (+0.1‰) and *Q. robur* (+1.0‰) are enriched after exposure to KOH, whereas values of all other species are depleted in a range of -0.3‰ (*P. abies*) to -2.6‰ (*A. glutinosa*; Table 4.4; Figure 4.2). The HF treatment leads for *C. avellana* to enriched pollen-isotope values of +0.5‰, whereas the values of *P. abies* (-1.8‰) and *P. sylvestris* (-1.7‰) are depleted. All broad-leaved species have enriched $\delta^{18}O_{pollen}$ values after the treatment with NaClO. The enrichment ranges between +1.1‰ (*C. avellana*) and +3.1‰ (*B. pendula*). NaClO had no measurable effect on *A. glutinosa* $\delta^{18}O_{pollen}$ values (Table 4.4; Figure 4.2). Coniferous $\delta^{18}O_{pollen}$ values (*P. abies*: -1.7‰; *P. sylvestris*: -0.5‰) are depleted as a result of the NaClO treatment. The H_2SO_4-treatment has distinct effects on $\delta^{18}O_{pollen}$. Mean pollen-isotope values of broad-leaved species are depleted in a range of -0.7‰ (*A. glutinosa*) to -5.8‰ (*C. betulus*), whereas coniferous $\delta^{18}O_{pollen}$ values are depleted by -9.7‰ (*P. abies*) and -17.9‰ (*P. sylvestris*), respectively. The depletion of mean $\delta^{18}O_{pollen}$ values after the successive treatment has a broad range between -3.7‰ (*A. glutinosa*) and -19.2‰ (*P. sylvestris*; Table 4.4).

4.3.3 Linear regression analysis

The regression analysis of raw and chemically treated $\delta^{13}C_{pollen}$ values yield linear correlations after the composite analysis of all species for KOH (Adj.$R^2 = 0.79$, p-value <0.0001*), HF (Adj.$R^2 = 0.86$, p-value <0.0001*) and NaClO (Adj.$R^2 = 0.94$, p-value <0.0001*; Figure 4.3). When only broad-leaved species are compared (Figure 4.4), the $\delta^{13}C_{pollen}$ values of raw pollen correlate strongly to KOH (Adj.$R^2 = 0.80$, p-value <0.0001*), H_2SO_4 (Adj.R 2= 0.74, p-value <0.0001*), NaClO (Adj.$R^2 = 0.96$, p-value <0.0001*) and all (Adj.R^2

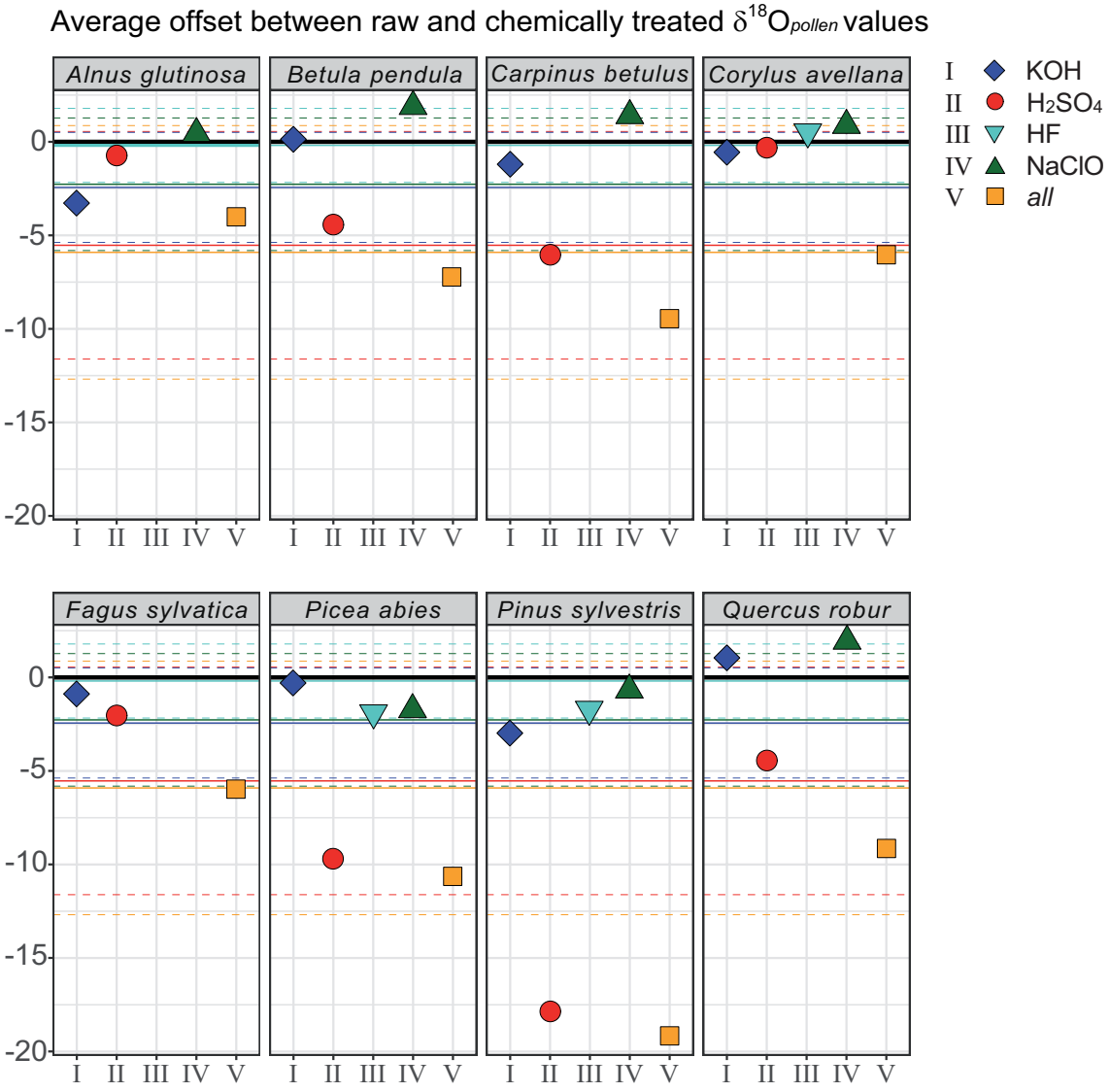

Figure 4.2: Average offset between untreated (raw) and chemically treated $\delta^{18}O_{pollen}$ values (vs. VSMOW). Three pollen samples from individual trees of eight species were treated with four different chemicals (KOH (I), H_2SO_4 (II), HF (III) and NaClO (IV); HF was applied to three species and NaClO is missing for *F. sylvatica*). Three samples each underwent a full chemical treatment procedure (*all* (V)). Coloured symbols indicate the mean value of three repetitions for each species and chemical. Horizontal solid lines show the mean deviation of each chemical for all species compared to the mean isotope values of the raw material. Dashed lines represent the corresponding first standard deviation to the overall mean isotope values for each chemical

= 0.67, p-value <0.0001*). $\delta^{13}C_{pollen}$ of coniferous species yield linear correlations after treatment with HF (Adj.R^2 = 0.93, p-value 0.0012*), NaClO (Adj.R^2 = 0.93, p-value 0.0011*; Figure 4.5) and KOH (Adj.R^2 = 0.92, p-value 0.0017*; Figure 4.5). $\delta^{18}O$ of raw and treated pollen yield linear correlations after the application of KOH (Adj.R^2 = 0.79, p-value <0.0001*), NaClO (Adj.R^2 = 0.71, p-value <0.0001*; Figure 4.3) and HF (Adj.R^2 = 0.86, p-value 0.0002*). $\delta^{18}O$ of raw and treated pollen from broad-leaved trees correlate strongly after a treatment with KOH (Adj.R^2 = 0.86, p-value <0.0001*) and NaClO (Adj.R^2 = 0.89, p-value <0.0001*; Figure 4.4). $\delta^{18}O_{pollen}$ values of raw and treated samples of coniferous species yield a strong linear relationship after the successive treatment all (Adj.R^2 = 0.98, p-value <0.0001*), but also after exposure to NaClO (Adj.R^2 = 0.96, p-value 0.0003), and HF (Adj.R^2 = 0.95, p-value 0.0006; Figure 4.5).

4.4 Discussion

4.4.1 $\delta^{13}C_{pollen}$ after chemical treatments

Chemical treatment alters the stable carbon isotope values of pollen and the amount of the deviation is species- and substance-dependent (Amundson *et al.*, 1997; Loader and Hemming, 2000; Jahren, 2004, Nelson *et al.*, 2006). However, $\delta^{13}C_{pollen}$ values are mostly depleted compared to untreated pollen material (Figure 4.1; Table 4.3). Even though the individual deviation between raw and treated pollen is species-specific for $\delta^{13}C_{pollen}$, the overall response patterns to each chemical reveal similarities (Figure 4.1), which have also been detected for other species (Loader and Hemming, 2000; Jahren, 2004). We assume,

Table 4.4: Mean $\delta^{18}O_{pollen}$ values (expressed in ‰) and standard deviation after chemical treatment with KOH, HF, NaClO, H_2SO_4 and *all* (successive treatment procedure following the protocol of four chemicals applied consecutively; see text). Raw $^{18}O_{pollen}$ values refer to chemically untreated pollen of the same individuals. Isotope ratios are expressed relative to VSMOW for $\delta^{18}O$. Dev. H_2SO_4/*all* refers to the difference between values after treatment solely with H_2SO_4 and after the successive treatment (*all*, expressed in ‰).

Plant species	δ^{18}**O raw**	δ^{18}**O KOH**	δ^{18}**O HF**	δ^{18}**O NaClO**	δ^{18}**O H_2SO_4**	δ^{18}**O all**	**Dev. δ^{18}O: H_2SO_4/all**
A. glutinosa	21.7 ± 0.5	19.1 ± 1.8	–	21.7 ± 0.5	21.0 ± 0.6	18.0 ± 0.8	3.0
B. pendula	24.8 ± 0.2	24.9 ± 0.2	–	27.9 ± 0.1	20.3 ± 0.4	16.9 ± 0.2	3.4
C. betulus	26.4 ± 0.2	24.6 ± 0.3	–	27.9 ± 0.1	20.6 ± 0.1	17.2 ± 0.2	3.4
C. avellana	21.5 ± 0.4	20.6 ± 0.3	22.0 ± 0.3	22.6 ± 0.4	20.7 ± 0.3	16.0 ± 0.2	4.7
F. sylvatica	23.3 ± 0.2	22.2 ± 0.2	–	–	21.5 ± 0.1	17.1 ± 0.4	4.4
Q. robur	27.4 ± 1.0	28.4 ± 0.7	–	29.7 ± 0.5	22.7 ± 0.3	18.3 ± 0.3	4.4
P. abies	24.5 ± 0.8	24.2 ± 0.5	22.7 ± 0.8	22.8 ± 0.2	14.8 ± 0.8	13.9 ± 1.1	0.9
P. sylvestris	30.1 ± 0.5	27.2 ± 0.2	28.4 ± 0.5	29.6 ± 0.2	12.3 ± 0.5	11.0 ± 0.6	1.3

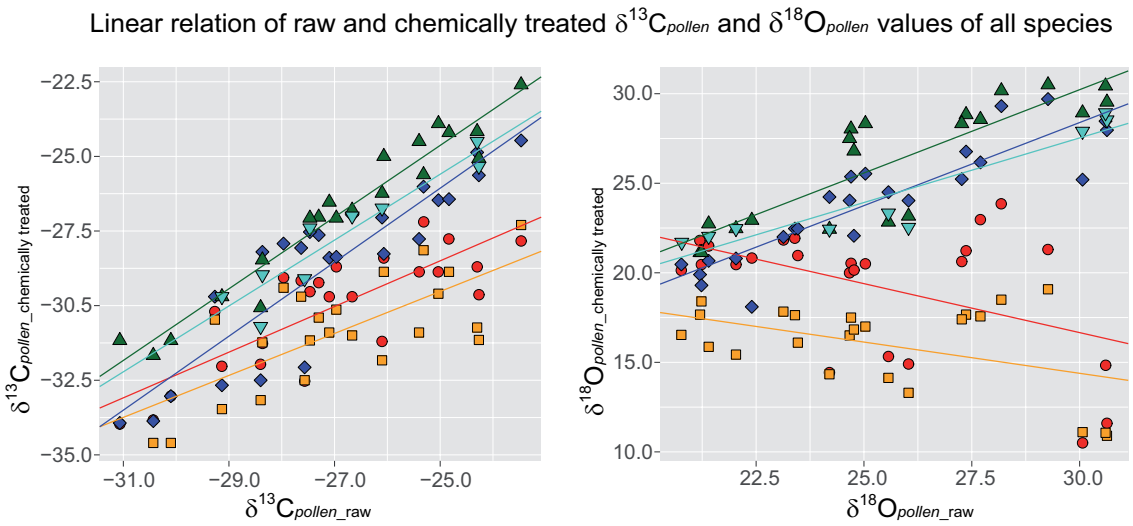

all species		KOH	HF	NaClO	H_2SO_4	*all*
(n indiv.)		(24)	(9)	(20)	(24)	(23)
$\delta^{13}C$	Adj.R^2	0.79	0.86	0.94	0.64	0.48
	p-value	<0.0001*	0.0002*	<0.0001*	<0.0001*	0.0001*
$\delta^{18}O$	Adj.R^2	0.79	0.86	0.71	0.19	0.16
	p-value	<0.0001*	0.0002*	<0.0001*	0.0202*	0.0335*

Figure 4.3: Linear relation of raw and chemically treated pollen-isotopes of all species: $\delta^{13}C_{pollen}$ values (right graph) and $\delta^{18}O_{pollen}$ values (left graph). The table contains the correlation coefficient Adj.R^2 and the probability value (significance level p-value = 0.05) for a linear relation between raw and chemically treated pollen-isotope values of KOH (24 individuals), HF (9 individuals), NaClO (20 individuals), H_2SO_4 (24 individuals) and the successive treatment *all* (23 individuals).

that the influence of the chemicals on pollen is generally comparable, but species-specific pollen wall structure and coating as well as pollen-shape and -size determine the impact.

4.4.2 Impact of KOH, HF and NaClO on $\delta^{13}C_{pollen}$

KOH

Even though the mean depletion of carbon isotope values after KOH exposure varies between -0.3‰ (*F. sylvatica*) and -4.0‰ (*C. avellana*), species react in a similar fashion and therefore the correlation of $\delta^{13}C_{pollen}$ from raw and treated pollen is significant (Figure 4.3). The correlation coefficient is higher, when the species are separated between broad-leaved and coniferous pollen types, because the impact seems determined by shape and size of the pollen, which differ between the respective affiliation (Table 4.1; Figure 4.4 and 4.5). In general, KOH has a bigger impact on species of the family Belulaceae (*A. glutinosa*, *C. betulus*, *C. avellana* and *B. pendula*). Pollen values of Betulaceae species are on average -2.6‰ depleted, whereas the average difference of all other species (*F. sylvatica*, *P. abies*, *P. syvestris* and *Q. robur*) is -0.5‰ (Table 4.3; Figure 4.1). Potassium

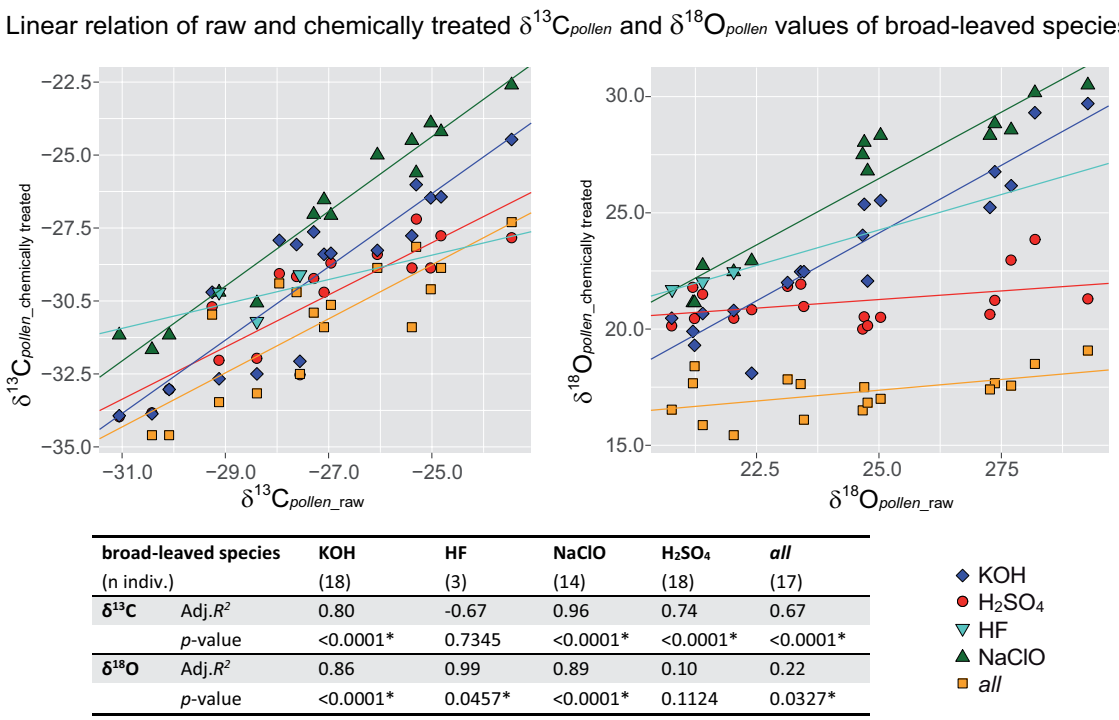

broad-leaved species (n indiv.)		KOH (18)	HF (3)	NaClO (14)	H_2SO_4 (18)	*all* (17)
$\delta^{13}C$	Adj.R^2	0.80	-0.67	0.96	0.74	0.67
	p-value	<0.0001*	0.7345	<0.0001*	<0.0001*	<0.0001*
$\delta^{18}O$	Adj.R^2	0.86	0.99	0.89	0.10	0.22
	p-value	<0.0001*	0.0457*	<0.0001*	0.1124	0.0327*

Figure 4.4: Linear relation of untreated (raw) and chemically treated $\delta^{13}C_{pollen}$ values (right graph) and $\delta^{18}O_{pollen}$ values (left graph) of broad-leaved species. The table contains the correlation coefficient Adj.R^2 and the probability value (significance level p-value = 0.05) for a linear relation between raw and chemically treated pollen-isotope values of KOH (18 individuals), HF (3 individuals), NaClO (14 individuals), H_2SO_4 (18 individuals) and the successive treatment *all* (17 individuals).

hydroxide is not bearing carbon and should thus not affect the $\delta^{13}C$ of sporopollenin, but it may alter the structurally weaker inner pollen wall (Fan *et al.*, 2019) and attack the coating of raw pollen from species of the family Betulaceae more severely, because they may contain derivates of humic acids (Moore *et al.*, 1991). Thus, already decomposed fossil pollen may react differently or significantly less to KOH exposure, but we did not test the direct impact of KOH on fossilised pollen.

HF

Hydrofluoric acid (HF) is widely used to extract pollen from lake sediments (Bennett and Willis, 2002). Even though it has only been tested in protocols containing several chemicals (Jahren, 2004; Nelson *et al.*, 2006), HF is suspected to have generally little influence on the organic structure of pollen (Jahren, 2004). The impact of solely hydrofluoric acid on $\delta^{13}C_{pollen}$ was smallest in comparison to other chemical substances applied in this study ranging between -0.4‰ (*P. abies*) and -1.4‰ (*C. avellana*). Pollen-isotope values of raw and treated samples of all species analysed together correlate with Adj.R^2 = 0.86 (p-value 0.0002*) whereas the three raw and treated $\delta^{13}C_{pollen}$ values of *C. avellana* do not

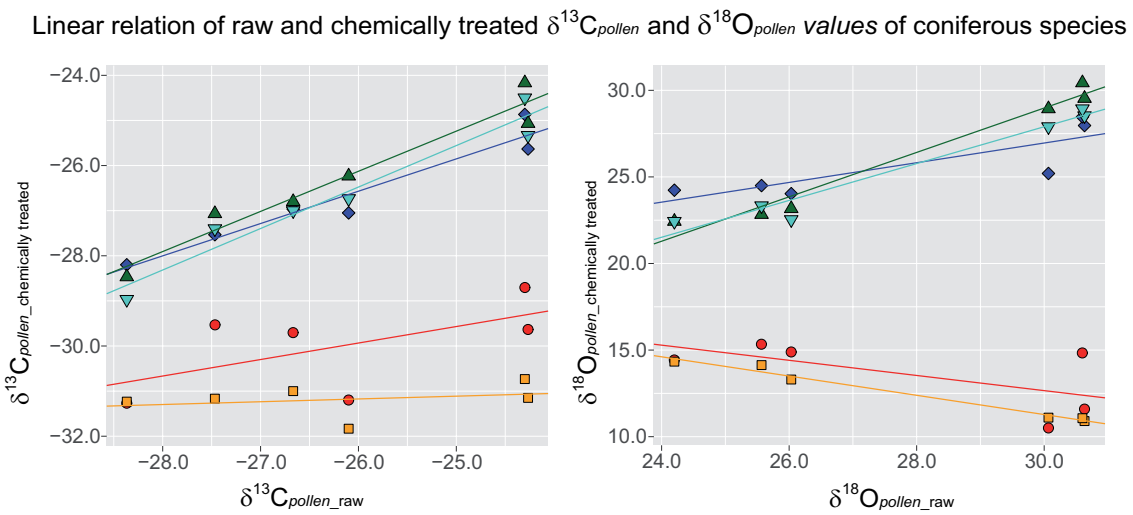

coniferous species (n indiv.)		KOH (6)	HF (6)	NaClO (6)	H_2SO_4 (6)	*all* (6)
$\delta^{13}C$	Adj.R^2	0.92	0.93	0.93	0.20	-0.15
	p-value	0.0017*	0.0012*	0.0011*	0.2094	0.5875
$\delta^{18}O$	Adj.R^2	0.63	0.95	0.96	0.24	0.98
	p-value	0.0374*	0.0006*	0.0003*	0.1831	<0.0001*

Figure 4.5: Linear relation of untreated (raw) and chemically treated $\delta^{13}C_{pollen}$ values (right graph) and $\delta^{18}O_{pollen}$ (left graph) of coniferous species. The table contains the correlation coefficient Adj.R^2 and the probability value (significance level p-value = 0.05) for a linear relation between raw and chemically treated pollen-isotope values of six individuals treated with KOH, HF, NaClO, H_2SO_4 and the successive treatment *all*.

correlate when analysed separately (Adj.R^2 = -0.67, p-value 0.7345; Figure 4.4). Despite small sample size six individuals of coniferous species, raw and treated pollen-isotope values correlate (Adj.R^2 = 0.93, p-value 0.0012*; Figure 4.5).

NaClO

Fossil pollen are used for ^{14}C age dating and the extraction protocols include, among others, HF and NaClO (e.g. Zhou *et al.*, 1997; Fletcher *et al.*, 2017). Even though the individual impact of each chemical has not been tested to date, the age dates Zhou *et al.* (1997) compared to age dates of other material extracted from the sediment core relate to each other and thus ^{14}C does not seem to be influenced markedly by the chemical treatment.

The impact of NaClO on $\delta^{13}C_{pollen}$ varies between +1.0‰ (*B. pendula*) and -1.4‰ (*C. avellana*) but the overall response is similar for most species and thus, raw pollen-isotope values are linearly related to the values after NaClO exposure (Figure 4.1, 4.3, 4.4, 4.5).

4.4.3 Impact of H_2SO_4 on $\delta^{13}C_{pollen}$

Average depletion of $\delta^{13}C_{pollen}$ values after treatment with H_2SO_4 is -3.2‰, but the isotopic shift varies highly between species and with differing pollen characteristics (Figure 4.1; Table 4.1; Table 4.3a). Even though the impact is strong, raw and chemically treated $\delta^{13}C_{pollen}$ values correlate (Adj.$R^2 = 0.64$, p-value <0.0001*; Figure 4.3). A species-specific amount of depletion for the $\delta^{13}C_{pollen}$ values after H_2SO_4 treatment is also shown in other studies (Loader and Hemming, 2000; Nelson *et al.*, 2006; Descolas-Gros and Schölzel, 2007; Nelson, 2012). $\delta^{13}C_{pollen}$ values of herbaceous plants and broad-leaved trees are on average -2.2‰ depleted, ranging between -0.15‰ (pollen of family Asteraceae; Nelson, 2012) and -3.7‰ (grass pollen, Nelson *et al.*, 2006). That is in accordance with the range for broad-leaved trees detected in this study, which is averaging at -2.8‰ (Table 4.3a). Raw and H_2SO_4-treated $\delta^{13}C_{pollen}$ values of board-leaved trees are linearly related with Adj.$R^2 = 0.74$ (p-value <0.0001*; Figure 4.3).

However, the impact of H_2SO_4 on $\delta^{13}C_{pollen}$ of the coniferous tree species *P. sylvestris* is exceptionally high (Table 4.3; Figure 4.1). *Pinus sylvestris* $\delta^{13}C_{pollen}$ are on average -5.0‰ depleted and a comparison of raw and H_2SO_4-treated $\delta^{13}C_{pollen}$ values of coniferous trees yields no linear correlation (Adj.$R^2 = 0.20$, p-value 0.2094; Figure 4.5). Loader and Hemming (2000) detected an average depletion of -2.18‰ for *P. sylvestris* $\delta^{13}C_{pollen}$ after treatment with H_2SO_4 and the comparison of chemically treated and raw pollen yields a high correlation coefficient of $R^2 = 0.93$. A methodological reason for the different offsets between raw and chemically treated $\delta^{13}C_{pollen}$ values of *P. sylvestris* might be the usage of a Whatman microcentrifuge tube with a mesh to extract the pollen from the sulfuric acid by Loader and Hemming (2000). In our study, we slowly diluted the acid with deionized water until the velocity of the sulfuric acid was low enough to extract the pollen via centrifugation. The dilution had a warming effect on the liquid, whose impact on the $\delta^{13}C_{pollen}$ values remain unknown. The same method of slowly diluting the sulfuric acid was used in Bell *et al.* (2017), where a constant and low depletion of -1.5‰ could be found for coniferous *Cedrus atlantica* pollen but no impact of a warming effect is reported. Loader and Hemming (2000) suggest a treatment duration of 8h. Less treatment time left cellulose residues on the pollen, whereas a longer treatment resulted in partly degraded pollen grains. Based on this finding, we settled on a treatment time of 5h and additional constant shaking (Table 4.2). Visual inspection after H_2SO_4 exposure showed no degradation of the pollen and cellulose residues could not be detected after staining the pollen with Safranin and Fast Green (Loader and Hemming, 2000), therefore we can

exclude methodological faults to cause the high offset of -5‰. Descolas-Gros and Schölzel (2007) applied H_2SO_4 for 8h on pollen of different species and measured lower species-specific offsets between -0.91‰ and -1.18‰. Bell *et al.* (2017) treated *C. atlantica* pollen with H_2SO_4 only for 45 minutes without additional stirring or heating, but verified the results of cellulose free pollen grains using the staining technique (Loader and Hemming, 2000) and Nelson *et al.* (2006) applied the sulfuric acid for 2h on grass pollen grains resulting in constant offsets between raw and chemically treated pollen. All treatment durations entailed reliable results for different species. The reason for exceptionally high depletion of the *P. sylvestris* $\delta^{13}C_{pollen}$ values after H_2SO_4 exposure in this study requires further investigations.

Fossil pollen retrieved from lake sediments are at least partly decomposed and the remaining part of the pollen wall is mostly sporopollenin. Thus, the $\delta^{13}C_{pollen}$ of fossil pollen are believed to be isotopically closer to the values of raw pollen treated with sulfuric acid (Table 4.3). However, to enhance the comparability of raw and fossil pollen, a treatment protocol imitating the diagenetic processes without using sulfuric acid may be beneficial (Jahren, 2004).

4.4.4 Impact of successive chemical treatment (*all*) on $\delta^{13}C_{pollen}$

For all species, a successive application of KOH, HF, NaClO and H_2SO_4 caused the highest depletion in $\delta^{13}C_{pollen}$ (between -1.6‰ for *F. sylvatica* and -6.4‰ for *P. sylvestris*). Even though this protocol avoids carbon contaminating chemicals, the overall mean depletion of chemically treated $\delta^{13}C_{pollen}$ in comparison to raw $\delta^{13}C_{pollen}$ is -4.0‰ (Figure 4.1).

In most cases, the successive treatment with four chemicals alters the samples only slightly more than solely treated with H_2SO_4 (Table 4.3). The average additional depletion of $\delta^{13}C_{pollen}$ for the successive treatment is 0.9‰ (range: 0.4‰ to 1.4‰) and the deviation between $\delta^{13}C_{pollen}$ values after applying the full protocol and the samples treated solely with sulphuric acid seems to be related to pollen morphology and family affiliation (Table 4.1 and 4.3a). Thus, application of the full protocol may only in some cases be beneficial to purify lake sediment samples depending on the type of pollen designated for stable isotope analysis. However, linear regression analysis of raw and treated pollen-isotope values of all species reveal with Adj.R^2 = 0.48 a weak correlation for the $\delta^{13}C_{pollen}$ values (p-value 0.0001*; Figure 4.3). Separate analysis of solely broad-leaved species yields a significant Adj.R^2 value of 0.67 (p-value <0.0001*; Figure 4.4), but the analysis of solely coniferous pollen types reveals no correlation (Adj.R^2 = -0.15; p-value 0.5875; Figure 4.5).

4.4.5 $\delta^{18}O_{pollen}$ values after chemical treatment

Chemical treatment affects the $\delta^{18}O_{pollen}$ of all species markedly (Figure 4.2; Table 4.3b). The chemical treatment protocols to purify pollen from lake sediments were created to avoid chemical contamination of the $\delta^{13}C_{pollen}$ and was not adjusted for the application to analyse stable oxygen pollen-isotopes. Hence, the application of chemicals results in some cases in strongly depleted pollen-isotope values compared to the raw pollen-isotopes (Figure 4.2; Table 4.4).

4.4.6 Impact of KOH, HF and NaClO on $\delta^{18}O_{pollen}$

There are no comparable studies on $\delta^{18}O_{pollen}$ after chemical treatment procedures solely with potassium hydroxide (KOH), hydrofluoric acid (HF) and sodium hypochlorite (NaClO) available at the moment. Mean $\delta^{18}O_{pollen}$ values of *B. pendula* (+0.1‰) and *Q. robur* (+1.0‰) are enriched after exposure to KOH, whereas the isotope values of all other species are depleted in a range of -0.3‰ (*P. abies*) to -2.6‰ (*A. glutinosa*; Table 4.4; Figure 4.2). Even though the impact of KOH on $\delta^{18}O_{pollen}$ of different species is inconsistent, isotope values of raw and treated pollen correlate strongly with Adj.$R^2 = 0.79$ (p-value <0.0001*; Figure 4.3). The correlation is even stronger, when only the isotope values of broad-leaved species are compared (Adj.$R^2 = 0.86$, p-value <0.0001*; Figure 4.4), but the $\delta^{18}O_{pollen}$ values of coniferous species yield a weak correlation after the linear regression analysis (Adj.$R^2 = 0.63$, p-value 0.0374). Coniferous pollen have relatively thin pollen wall structures in relation to the size of the pollen and thus may be more vulnerable to chemical treatment. In general, considering species-specific pollen membrane porosity is necessary when chemical substances are applied prior to stable isotope analysis (Loader and Hemming, 2000).

Treatment with hydrofluoric acid leads for the broad-leaved species *C. avellana* to enriched mean $\delta^{18}O_{pollen}$ values of +0.5‰, whereas mean $\delta^{18}O_{pollen}$ values of coniferous species are depleted, both in a similar fashion (*P. abies*: -1.8‰; *P. sylvestris*: -1.7‰; Table 4.4). HF is the only non-oxygen bearing chemical in this protocol, but nonetheless some diagenetic processes affecting the pollen wall occur during chemical exposure. Despite the isotopic changes after treatment, the raw and treated $\delta^{18}O_{pollen}$ values yield strong correlations (Figure 4.3, 4.4, 4.5).

Broad-leaved species have enriched $\delta^{18}O_{pollen}$ values ranging between +1.1‰ (*C. avellana*) and +3.1‰ (*B. pendula*) following treatment with NaClO (Table 4.4, Figure 4.2).

The $\delta^{18}O_{pollen}$ values of raw and treated samples of broad-leaved species correlate with Adj.R^2 = 0.86 (p-value <0.0001*; Figure 4.4). The correlation of coniferous $\delta^{18}O_{pollen}$ values is stronger with Adj.R^2 = 0.96 (p-value 0.0006*; Figure 4.5), even though the pollen-isotopes are depleted as a result of the NaClO treatment (*P. abies*: -1.7‰; *P. sylvestris*: -0.5‰). What exactly causes the different impact on pollen-isotopes except for pollen shape and size remains unknown.

4.4.7 Impact of H_2SO_4 on $\delta^{18}O_{pollen}$

Raw and chemically treated mean $\delta^{18}O_{pollen}$ values of coniferous species deviate strongly after H_2SO_4 exposure (Figure 4.2; Table 4.4). Especially *P. sylvestris* responses to a H_2SO_4-treatment with a depletion of -17.9‰ and also mean $\delta^{18}O_{pollen}$ values of *P. abies* are with -9.7‰ highly depleted. Raw and chemically treated $\delta^{18}O_{pollen}$ values of coniferous pollen are not related with Adj.R^2 = 0.24 (p-value 0.1831; Figure 4.5). Broad-leaved species exhibit a distinctly weaker response to H_2SO_4 exposure. The average depletion of treated $\delta^{18}O_{pollen}$ values compared to raw $\delta^{18}O_{pollen}$ values of broad-leaved species is -3.1‰. The offset varies markedly between species, thus raw and treated $\delta^{18}O_{pollen}$ values are not linearly related (Adj.R^2 = 0.10, p-value 0.1124; Figure 4.5).

A strong response of coniferous pollen to chemical exposure might be caused by the size of the pollen grains and a relatively thin pollen wall, having thus a bigger surface where chemicals can corrode the organic material. This applies in milder form also to *C. betulus* and *Q. robur* pollen (Figure 4.2), which have the biggest pollen amongst the broad-leaved species examined in this study and a relatively thin pollen wall. However, the effect does not seem to be consistent: *Alnus glutinosa*, *Betula pendula* and *Corylus avellana* are almost similar in size and shape (Beug 2004), but the treatment affects *B. pendula* pollen more than *A. glutinosa* and *C. avellana* (Figure 4.2; Table 4.4).

4.4.8 Impact of successive chemical treatment (*all*) on $\delta^{18}O_{pollen}$

Depletion of mean $\delta^{18}O_{pollen}$ values of broad-leaved species after the successive treatment with all chemicals is ranging between -3.7‰ (*A. glutinosa*) and -9.1‰ (*Q. robur*), whereas coniferous species pollen-isotopes are depleted by -10.6‰ (*P. abies*) and -19.2‰ (*P. sylvestris*; Table 4.3b). Despite severe alterations, raw and chemically treated pollen samples of coniferous species correlate strongly with Adj.R^2 = 0.98 (p-value <0.0001*; Figure 4.5), whereas the broad-leaved species yield a low Adj.R^2 value of 0.22 (p-value

0.00327*; Figure 4.4). The successive treatment alters the $\delta^{18}O_{pollen}$ values of broad-leaved trees on average 3.9‰ more than a treatment solely with H_2SO_4. However, the average additional depletion of coniferous species $\delta^{18}O_{pollen}$ is only 1.1‰ (Table 4.4). Thus, applying the full protocol may have an assessable effect on some species, whereas others are severely altered. Applying chemicals prior to stable isotope analysis should generally be considered carefully, depending on the type of pollen and necessities based on the original fossil sample.

4.4.9 $\delta^{13}C_{pollen}$ in relation to $\delta^{18}O_{pollen}$

Species-specific response patterns are generally alike, also when carbon and oxygen pollen-isotope patterns are compared (Figure 4.1 and 4.2). Even though the overall offset is higher for treated $\delta^{18}O_{pollen}$ values, the changes for each species among the different chemicals are almost equal (Figure 4.1 and 4.2). This might be caused by the species-specific pollen wall composition and shape of the pollen grain (Table 4.1). The chemicals can alter the pollen-isotopes only to a certain degree in relation to a species-specific pollen structure and vulnerability. Nevertheless, *Alnus glutinosa* and *Corylus avellana* reveal differing patterns for $\delta^{18}O_{pollen}$ and $\delta^{13}C_{pollen}$ after chemical treatment (Figure 4.1 und 4.2). This might be related to their plant specific time of pollination from January to March which is why this species have generally low baseline values of raw pollen-isotopes (Müller *et al.*, 2020)

4.5 Conclusions

Potassium hydroxide (KOH), hydrofluoric acid (HF) and sodium hypochlorite (NaClO) alter the $\delta^{13}C_{pollen}$ and $\delta^{18}O_{pollen}$ values according to the species affiliation and pollen characteristics. However, all raw and chemically treated pollen yield strong linear correlations and thus, the usage of these chemicals prior to carbon and oxygen stable isotope analysis seems unproblematic. Hence, KOH, HF and NaClO can be used in any protocol applied in palaeoclimate investigations to purify pollen samples without hesitation.

The impact of sulfuric acid (H_2SO_4) is highly species-specific and the offset between raw and chemically treated pollen-isotope values can be as high as 5.0‰ for $\delta^{13}C_{pollen}$ and 17.9‰ for $\delta^{18}O_{pollen}$ (both from *Pinus sylvestris*). Comparison of raw and H_2SO_4-treated $\delta^{13}C_{pollen}$ values of broad-leaved species yield a linear correlation (Adj.$R^2 = 0.74$, p-value <0.0001*), whereas coniferous species react stronger and the impact of H_2SO_4 on the $\delta^{13}C_{pollen}$ values seems rather unpredictable (Adj.$R^2 = 0.20$, p-value 0.2094). Raw and

H_2SO_4-treated $\delta^{18}O_{pollen}$ values are neither related for broad-leaved species, nor coniferous species.

The usage of chemicals is inevitable to extract fossil pollen prior to palaeoclimate investigations. Purification protocols for pollen samples need to be adjusted due to the requirements of the source material. However, the usage of pollen-isotope altering substances should be brought to a minimum and thus, protocols avoiding the usage of sulfuric acid, e.g. a dense media separation technique, may be most promising.

4.6 Acknowledgements

We are thankful to Maike Glos who helped with the sample preparation in the laboratory (Freie Universität Berlin) and Michèle Dinies (Deutsches Archäologisches Institut) and for discussion, support and consultations concerning laboratory methods and completion. This work was financially supported by the Deutsche Forschungsgesellschaft (DFG) under grant 463 number RI 809/33-1.

Chapter 5

Synthesis and Outlook

5.1 Conclusions

This doctoral thesis explores ways and limitations of using the proxy pollen in palaeoclimate investigations. Morphology-based analysis is a well-established method that can easily be applied to investigate past vegetation compositions. If the reconstruction of short-term climate shifts are aimed to be reconstructed, pollen-isotope analysis is a more suitable approach.

A classic morphology-based pollen analysis was performed to identify changes in the composition of the plant community around the Daotang Pond on the northeastern Qinghai-Tibetan Plateau caused by varying dominances in the atmospheric circulation system. A vegetation reconstruction on a 20 year basis provided a rather high-resolution investigation covering the last 1200 years and the pollen data suggested fluctuating strengths of the East Asian Summer Monsoon (EASM) and the Westerly Winds. The climate anomaly of the Medieval Warm Period (CE 850 to 1400) was found to be moist due to frequent EASM precipitation and a prevailing moist microclimate around the Qinghai Lake drainage basin. Three short dry spells within this time period were supported by the pollen data through an increase of the Poaceae pollen abundances and the quantitative interpretation method of the*Artemisia*/Chenopodiaceae ratio. The Little Ice Age (CE 1450 to 1950) is characterised by cold and humid conditions in the Daotang Pond area, although the pollen data also suggested a weaker EASM causing lower summer rainfall amounts during this period. This phenomenon can be explained by reduced evapotranspiration due to the lower temperatures, hence the climate remains moist. But the Qinghai-Tibetan Plateau has since long been used as a pastoral region by nomads and reconstructing prevailing climate traits using pollen assemblages, which reflect severely impacted environments, is

generally error-prone.

The identified limitations of morphology-based palynology can be resolved by pollen-isotope analysis. The predominance of the wind system and local microclimate conditions could be traced more accurately with stable isotope analysis, when sufficient background knowledge is available and pollen-isotope variability as well as the pollen-isotope-environment relation have been thoroughly investigated.

Gaining knowledge about carbon and oxygen isotope variability of pollen and evaluating the specific applicability for nine different tree species was performed to promote pollen-isotope analysis in environmental reconstructions. The results of the study suggested, that pollen-isotope values of modern pollen are mostly determined by their taxonomic affiliation and the geographic location of their sampling. Each species has specific pollen-isotope ranges and patterns, and the $\delta^{13}C_{pollen}$ and $\delta^{18}O_{pollen}$ values reflect gradients between maritime and continental sampling sites. Thus the isotope values represent the geographic setting and local environmental conditions, suggesting that fossil pollen-isotopes can indeed be used to trace past climate change.

A prime advantage of pollen-isotope analysis is the direct response of the plant to the environment. Species-specific pollen-isotope values varied inter-annually on average 1.0‰ for $\delta^{13}C_{pollen}$ and 1.6‰ for $\delta^{18}O_{pollen}$ and therefore high-resolution environmental reconstructions are feasible if pollen are analysed on a yearly basis. Weather can even be traced intra-seasonally by analysing pollen of trees flowering during different periods within one vegetation period. Pollen-isotope values of broad-leaved trees flowering before leaf proliferation had significantly lower $\delta^{13}C_{pollen}$ and $\delta^{18}O_{pollen}$ values than broad-leaved trees flowering later in spring, each reflecting the environmental conditions during pollen formation and maturation. Different sampling position within one tree (lower and higher positions as well as the cardinal directions) accounted for pollen-isotope variability. Up to 3.5‰ difference between cardinal directions were found for $\delta^{13}C_{pollen}$ and 2.1‰ for $\delta^{18}O_{pollen}$. Therefore, the usage of an appropriate minimum amount of pollen for isotope measurements, depending on the species and origin of the sample, is another recommendation that results from the study. Otherwise samples containing mainly pollen from a certain direction are impacted by the position of the flower on the tree leading to inaccurate values which falsify the interpretation of the measured value.

All analysed species were evaluated for specific suitability in future climate studies. Our results advised against using *Acer pseudoplatanus*, because of great fluctuations within the $\delta^{13}C_{pollen}$ and $\delta^{18}O_{pollen}$ values of this species. Other spring-flowering broad-leaved species

can be used to reconstruct environmental traits. *Betula pendula* seems to reflect long-term environmental changes, whereas *Fagus sylvatica* and *Qercus robur* seem equally suitable to evaluate late spring conditions. Both species flowering early in the year, *Alnus glutinosa* and *Corylus avellana*, seem to reflect conditions of the previous winter. However, the pollen wall of *A. glutinosa* is thicker and contains more sporopollenin. Therefore, fewer fossil pollen grains might be needed to gather the minimum amount of carbon and oxygen for isotope measurements. Pollen of the investigated coniferous species *Picea abies* and *Pinus sylvesteris* seem to reflect local environmental conditions equally good, but their isotope offset is on average 3‰ and thus, pollen of both species, which show morphological similarities, need to be separated thoroughly prior to an isotope analysis. The variability of species-specific isotope patterns and ranges emphasizes the need to separate the fossil pollen on the lowest taxonomic level possible.

Advancing the actual application of pollen-isotope analysis requires an evaluation of the impact of chemicals used in purification protocols on the isotope values of the pollen. Purification of samples using potassium hydroxide (KOH) altered the $\delta^{13}C_{pollen}$ and $\delta^{18}O_{pollen}$ values of raw pollen material species-specifically. But the isotope values of raw pollen and the values of the treated pollen were linearly correlated, which lead to the assumption of a stable and thus calculable offset that renders the general usage of KOH in preparations of pollen for palaeoclimate studies unproblematic. The same is valid for a treatment with HF (hydrofluoric acid) and NaClO (sodium hypochlorite). Sulfuric acid (H_2SO_4), which is applied to extract sporopollenin, altered the $\delta^{13}C_{pollen}$ according to the pollen type and taxonomic affiliation. The impact on pollen from broad-leaved species was generally less than the impact on pollen of coniferous species. These findings suggest that the effect of the chemical needs to be tested on the modern analogue for the pollen extracted and measured from fossil samples. The impact of H_2SO_4 on the oxygen isotope values was severe. An application of H_2SO_4 needs to be avoided prior to $\delta^{18}O_{pollen}$ analysis. The development of a chemical treatment protocol for fossil pollen is necessary prior to each study. The protocol can be adjusted according to the requirements of the original sample material and different types of records, and therefore the impact of the chemicals on the pollen-isotope values can be brought to a minimum.

Both approaches that use pollen to reconstruct past environmental conditions have advantages and challenges. Morphology-based quantitative methods are well established and can be executed without detailed knowledge of the present-day vegetation composition. These methods are suitable to gain a solid overview of changes over long time

periods. Pollen-isotope analysis on the other hand even enables seasonal weather reconstructions and can catch short term climate shifts due to the direct physiological response of the plant to environmental conditions that change the isotope ratios within the plant material. However, pollen-isotope analysis is still in the need of further preliminary investigations. Prior to each palaeoclimate study, the modern vegetation composition and pollen-isotope values need to be examined. Additionally, the chemical treatment protocol to extract fossil pollen should be adjusted and tested on modern pollen of the species that will be extracted from the core and investigated isotopically.

5.2 Additional analytical results

More knowledge has been gained within the pollen-isotope research project of the FU Berlin promoting the establishment of pollen-isotope analysis as a regular approach in climate studies. A first attempt to combine and compare the results of a classic morphology-based pollen analysis and pollen-isotope analysis has been conducted as a bachelor thesis by Alena Zippel under the supervision of Carolina Müller (Zippel, 2016: *Rekonstruktion der Vegetationsdynamik im Spätholozän mittels Untersuchung von Pollen aus dem Xingyun See vom Yunnan Plateau, SW-China, und Messungen stabiler Sauerstoff- und Kohlenstoffisotope der Pollen zur Prüfung einer Korrelation beider analytischer Methoden*). Ten pollen samples of a lake sediment core drilled at the Xingyun Lake in SW China in 2014 were analysed morphologically and pollen of 19 samples of the same core were prepared for carbon and oxygen isotope analysis. The samples for the isotope analysis contained *Pinus* pollen, which were extracted with a dense media separation technique and chemically purified prior to the isotope measurements. Additionally, carbon and oxygen isotopes of modern pollen from 30 pine trees, collected in the direct vicinity of the lake, were analysed. The results of the different approaches using pollen in palaeoclimate investigations were compared and a similar climate reconstruction could be recognized for both fossil pollen analyses. However, the isotope analysis revealed an offset between modern and fossil carbon and oxygen pollen material attributable to the chemical impact on the isotope values during laboratory preparation of the fossil pollen. This finding emphasizes the need for further chemical tests on modern and fossil pollen to advance the preparation protocol.

Two additional studies analysing modern pollen collected by bees were part of the same pollen-isotope project of the FU Berlin. Both studies were conducted under the

supervision of Carolina Müller. The first study was done by Fransizka Pritzke in 2015: *Morphological examination and stable isotope analysis of recent bee pollen pellets.* Pollen pellets collected by bees, mostly containing herbaceous pollen, were sampled continuously throughout the sampling season of 2015 at several different settings in Europe (Poland, Belgium and Germany (Potsdam and Templin)). The study was performed to evaluate whether bee pollen pellets are suitable as raw material for isotope analysis and it concludes that measured carbon isotope values reflect the taxonomic assignment and the photosythetic pathway cycle of the host plant. Therefore, if herbaceous fossil pollen are analysed in future studies bee pollen pellets containing pollen of the same species, genus or even family can be used as modern reference material. Additionally, chemical preparation to purify the pollen packages was evaluated in this study and the author advises not to use a chemical extraction method which includes sulfuric acid because it leads to large species-specific offsets within the isotope values.

The second study using bee pollen as reference material was conducted by Hendrik Schultz in 2018: *Correlations between atmospheric conditions, biotic factors and isotopic ratios* $^{13}C/^{12}C$ *und* $^{18}O/^{16}O$ *in pollen exines from bee pollen packages.* He analysed carbon and oxygen isotope values of pollen collected by bees between February and August 2015 from one location in Potsdam, Germany. The aim of this study was to correlate the measured isotope values with weather data from the ongoing season and determine the impact of weather parameters on herbaceous pollen isotopes. The results show that the temperatures of one to four weeks prior to efflorescence affect the δ^{13}C values of herbaceous pollen, whereas only weak correlation between the amount of precipitation and δ^{18}O could be found. All conducted tests of the pollen-isotope-weather-relation contribute very well to the overall aim of the pollen-isotope project of the FU Berlin: advancing the method towards a regular application of pollen-isotopes in climate studies.

5.3 Future perspectives

The combination of both research approaches using fossil pollen, morphology-based pollen analysis and pollen-isotope analysis, could be used as a dual approach towards high-resolution and easy-to-accomplish climate and vegetation reconstructions, covering multiple research questions and the reconstruction of various environmental parameters simultaneously. For example, analysing pollen-isotopes of the Daotang Pond record additional to the already existing palynological study would be beneficial towards a detailed recon-

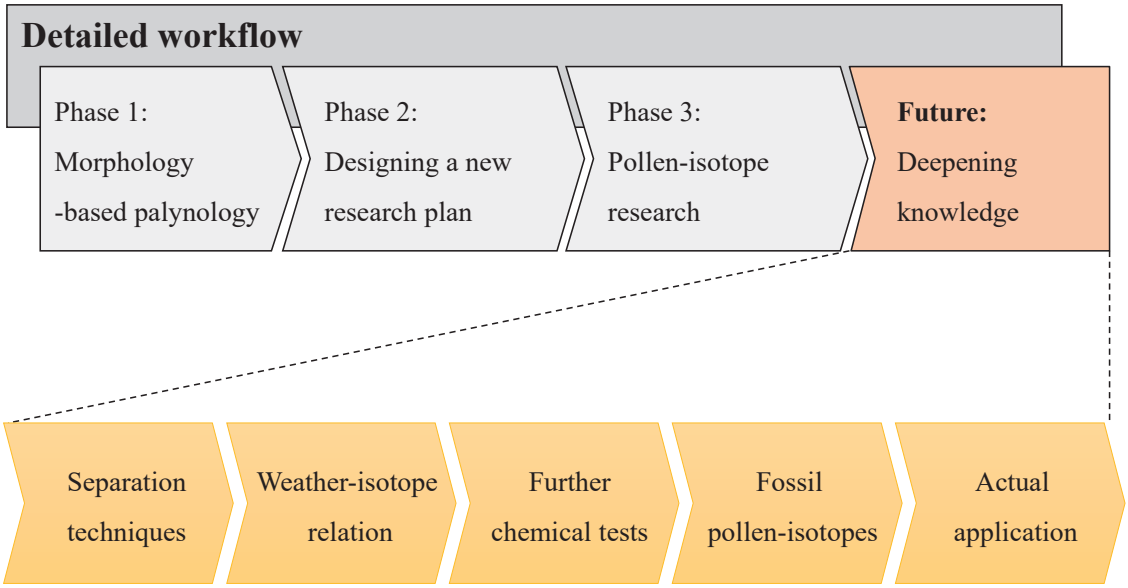

Figure 5.1: Detailed workflow of future research is characterised by deepening of general knowledge about adequate separation techniques to extract and purify pollen samples, the investigation of the relation of pollen-isotope values and weather parameters during the time of pollen formation and maturation. Additionally, isotope-altering chemicals need to be tested on modern a fossil pollen and pollen-isotope values of a fossil pollen record shall be measured and past ecological traits evaluated.

struction of the predominant wind system due to their unique isotope signal when bringing moisture onto the Tibetan Plateau. However, the possibility to choose between the two approaches, depending on the research question and type of original material, is only given when practical and analytical limitations of the second approach are fully explored. As pollen-isotope analysis is a newer method compared to the well-established morphology-based pollen analysis, a thorough assessment of the applicability and limitations of this method is still required. In detail, the following studies are proposed:

1. One of the key priorities lies in advancing the pollen-extraction and purification methods to separate fossil pollen from other material. The separation has to be very precise to extract pollen on the lowest taxonomic level possible. This could be achieved by advancing a density separation method using as little chemicals as possible and additionally by testing flow cytometry as a tool to automatically separate pollen based on cell size and other characteristics.

2. Correlations between the measured carbon and oxygen isotope values of modern pollen and prevailing weather parameters during the time of pollen formation and maturation in the anther can be assessed. The most influential climate factors can be identified for each species and each sampling site in order to evaluate the latitudinal and altitudinal effect on the pollen-isotope values.

3. Another, more detailed, case study using both approaches can be executed. Classic morphology-based pollen analysis can provide an overview of long-term climate and vegetation changes, whereas pollen-isotope analysis can be used to investigate detailed short-term weather parameters, especially during times of climate instability and change.

4. Herbaceous pollen have the advantage, that molecules are directly incorporated into newly built plant material at the beginning of a vegetation period without being mixed with stored molecules, as it can occur in trees or shrubs. Thus, herbaceous pollen display pure climate signals of the ongoing season. The easiest way to gain knowledge about herbaceous pollen-isotope values and variability is by analysing bee pollen packages. The knowledge about herbaceous pollen can contribute to future palaeoclimate studies when either one herbaceous pollen type is extracted or the pollen are sparse and several types have to be measured as one sample. In this case, the proportion of each pollen type can be calculated enabling the interpretation of the isotope value of the bulk sample.

Bibliography

Ahas R, Aasa A, Menzel A, Fedotova VG, Scheifinger H (2002). Changes in European spring phenology. *International Journal of Climatology* 22: 1727–1738.

Amundson R, Evett RR, Jahren AH, Bartolome J (1997). Stable carbon isotope composition of Poaceae pollen and its potential in paleovegetational reconstructions. *Review of Palaeobotany and Palynology* 99: 17–24.

An CB, Feng ZD, Barton L (2006). Dry or humid? Mid-Holocene humidity changes in arid and semi-arid China. *Quaternary Science Reviews* 25: 351–361.

An ZS, Colman SM, Zhou W, Li X, Brown ET *et al.* (2012). Interplay between the Westerlies and Asian monsoon recorded in Lake Qinghai sediments since 32 ka. *Scientific Reports* 2: DOI: 10.1038/srep00619.

An ZS, Porter SC, Kutzbach JE, Wu XH, Wang SM *et al.* (2000). Asynchronous Holocene optimum of the East Asian monsoon. *Quaternary Science Reviews* 19: 743–762.

Archetti M, Richardson AD, O'Keefe J, Delpierre N (2013). Predicting climate change impacts on the amount and duration of autumn colors in a New England forest. *PLoS One* 8: e57373.

Baker NR. Photosynthesis and the Environment. *Springer*, November 1996.

Bao Y, Bräuning A, Shi YF (2003). Late Holocene temperature fluctuations on the Tibetan Plateau. *Quaternary Science Reviews* 22: 2335–2344.

Barbour MM and Farquhar GD (2000). Relative humidity- and ABA-induced variation in carbon and oxygen isotope ratios of cotton leaves. *Plant Cell Environment* 23: 473–485.

Bell BA, Fletcher WJ, Cornelissen HL, Campbell JF, Ryan P *et al.* (2019). Stable carbon isotope analysis on fossil *Cedrus* pollen shows summer aridification in Morocco during the last 5000 years. *Journal of Quaternary Science* 34: 323–332.

Bell BA, Fletcher WJ, Ryan P, Grant H, Ilmen R *et al.* (2017). Stable carbon isotope analysis of *Cedrus atlantica* pollen as an indicator of moisture availability. *Review of Palaeobotany and Palynology* 244: 128–139.

Bell BA (2018). Advancing the application of analytical techniques in the biological chemistry of sporopollenin: Towards novel plant physiological tracers in quaternary Palynology. Dissertation. The University of Manchester (United Kingdom).

Bennett KD and Birks HJB (1990). Postglacial history of alder (*Alnus glutinosa* (L.; Gaertn.) in the British Isles. *Journal of Quaternary Science* 5: 123–133.

Bennett KD and Willis KJ (2002). Pollen. In *Tracking environmental change using lake sediments*: 5–32. *Springer*, Dordrecht.

Beug HJ (2004). Leitfaden der Pollenbestimmung für Mitteleuropa und angrenzende Gebiete. Stuttgart: *Gustav Fischer Verlag.*

Bezrukova EV, Tarasov PE, Solovieva N, Krivonogov SK, Riedel F (2010). Last glacial–interglacial vegetation and environmental dynamics in southern Siberia: Chronology, forcing and feedbacks. *Palaeogeography, Palaeoclimatology, Palaeoecology* 296: 185–198.

Birks HJB and Birks HH (1980). Quaternary palaeoecology. London: *E. Arnold.*

Blackmore S, Wortley AH, Skvarla JJ, Rowley JR (2007). Pollen wall development in flowering plants. *New Phytologist* 174: 483–498.

Bräuning A and Mantwill B (2004). Summer temperature and summer monsoon history on the Tibetan plateau during the last 400 years recorded by tree rings. *Geophysical Research Letters* 31: DOI: 10.1029/2004GL020793.

Brett DW (1964). The inflorescence of *Fagus* and *Castanea*, and the evolution of the cupules of the Fagaceae. *New Phytologist* 63: 96–118.

Brooks J and Shaw G (1978). Sporopollenin: a review of its chemistry, palaeochemistry and geochemistry. *Grana* 17: 91–97.

Burk RL and Stuiver M (1981). Oxygen isotope ratios in trees reflect mean annual temperature and humidity. *Science* 211: 1417–1419.

Cerling TE (1999). Paleorecords of C4 plants and ecosystems. In C4 Plant Biology, R.F. Sage and R.K. *Monson, Academic Press*: 445–469.

Chang C, Pan Y, Sun Y (1989). The tectonic evolution of the Qinghai-Tibet Plateau: A review. In: Sengor AMC (ed.) Tectonic evolution of the Tethyan Region. London, *Kluwer Academic Publishers*: 415–476.

Cheddadi R, Vendramin GG, Litt T, François L, Kageyama M *et al.* (2006). Imprints of glacial refugia in the modern genetic diversity of *Pinus sylvestris*. *Global Ecology and Biogeography* 15: 271–282.

Chen FH, Chen JH, Holmes J, Boomer I, Austin P *et al.* (2010). Moisture changes over the last millennium in arid central Asia: a review, synthesis and comparison with monsoon region. *Quaternary Science Reviews* 29: 1055–1068.

Chen FH, Yu ZC, Yang ML, Ito E, Wang SM *et al.* (2008). Holocene moisture evolution in arid central Asia and its out-of-phase relationship with Asian monsoon history. *Quaternary Science Reviews* 27: 351–364.

Chen JH, Chen FH, Zhang EL, Brooks SJ, Zhou AF *et al.* (2009). A 1000-year chironomid-based salinity reconstruction from varved sediments of Sugan Lake, Qaidam Basin, arid Northwest China, and its palaeoclimatic significance. *Chinese Science Bulletin* 50: 3749–3759.

Chesson LA, Tipple BJ, Erkkila BR, Cerling TE, Ehleringer JR (2011). B-HIVE: Beeswax hydrogen isotopes as validation of environment. Part I: Bulk honey and honeycomb stable isotope analysis. *Food chemistry* 125: 576–581.

Chesson LA, Tipple BJ, Erkkila BR, Ehleringer JR (2013). Hydrogen and oxygen stable isotope analysis of pollen collected from honey. *Grana* 52: 305–315.

Chuine I, Belmonte J, Mignot A (2000). A modelling analysis of the genetic variation of phenology between tree populations. *Journal of Ecology* 88: 561–570.

Clift PD and Plumb AR (2008). The Asian Monsoon: Causes, History and Effects. *Cambridge University Press* Vol. 288, Cambridge, UK.

Colman SM, Yu S, An Z, Shen J, Henderson ACG (2007). Late Cenozoic climate changes in China's western interior: A review of research on Lake Qinghai and comparison with other records. *Quaternary Science Reviews* 26: 2281–2300.

Cook ER, Esper J, D'Arrigo RD (2004). Extra-tropical Northern Hemisphere land temperature variability over the past 1000 years. *Quaternary Science Reviews* 23: 2063–2074.

Cour P, Zheng Z, Duzer D, Calleja M, Yao Z (1999). Vegetational and climatic significance of modern pollen rain in northwestern Tibet. *Review of Palaeobotany and Palynology* 104: 183–204.

Črepinšek Z, Štampar F, Kajfež-Bogataj L, Solar A (2012). The response of *Corylus avellana* (L.) phenology to rising temperature in north-eastern Slovenia. *International Journal of Biometeorology* 56: 681–694.

Datta R, Chamusco KC, Chourey PS (2002). Starch biosynthesis during pollen maturation is associated with altered patterns of gene expression in maize. *Plant Physiology* 130: 1645–1656.

Dawson TE, Mambelli S, Plamboeck AH, Templer PH, Tu KP (2002). Stable isotopes in plant ecology. *Annual Review of Ecology, Evolution and Systematics* 33: 507–559.

Delcourt HR and Delcourt PA (1985). Comparison of taxon calibrations, modern analogue techniques, and forest-stand simulation models for the quantitative reconstruction of past vegetation. *Earth Surface Processes and Landforms* 10: 293–304.

Demske D, Tarasov PE, Nakagawa T (2013). Atlas of pollen, spores and further non-pollen palynomorphs recorded in the glacial-interglacial late Quaternary sediments of Lake Suigetsu, central Japan. *Quaternary International* 290: 164–238.

Demske D and Mischke S (2003). Palynological investigation of a Holocene profile section from the Palaeo-Gaxun-Nur-Basin. *Chinese Science Bulletin* 48: 1418–1422.

Descolas-Gros C and Schölzel C (2007). Stable isotope ratios of carbon and nitrogen

in pollen grains in order to characterize plant functional groups and photosynthetic pathway types. *New Phytologist* 176: 390–401.

Dickinson HG, Bell PR (1976). The changes in the tapetum of Pinus banksiana accompanying formation and maturation of the pollen. *Annals of Botany* 40: 1101–1109.

Dongmann G, Nürnberg HW, Förstel H, Wagener K (1974). On the enrichment of H_2O^{18} in the leaves of transpiring plants. *Radiation and Environmental Biophysics* 11: 41–52.

Ducousso A, Michaud H, Lumaret R (1993). Reproduction and gene flow in the genus *Quercus* L. *Annales des sciences forestières* 50: 91–106.

Ehleringer JR, Cerling TE, Helliker BR (1997). C4 photosynthesis, atmospheric CO_2, and climate. *Oecologia* 112: 285–299.

Ehleringer JR and Dawson TE (1992). Water uptake by plants: perspectives from stable isotope composition. *Plant, Cell and Environment* 15: 1073–1082.

El-Moslimany AP (1990). Ecological significance of common nonarboreal pollen: Examples from drylands of the Middle East. *Review of Palaeobotany and Palynology* 64: 343–350.

Erdman G (1969). Handbook of palynology. An introduction of the study of pollen grains and spores. *Macmillan Pub Co.*, New York.

Faegri K, Kaland PE, Krzywinski K (1989). Textbook of pollen analysis (No. Ed. 4). *John Wiley and Sons Ltd*, New York.

Fan TF, Potroz MG, Tan EL, Ibrahim MS, Miyako E *et al.* (2019). Species-specific biodegradation of sporopollenin-based microcapsules. *Scientific reports* 9: 1–13.

Fang K, Wang Y, Yu T, Lingyun Z, Baluska F *et al.* (2008) Isolation of de exined polled and cytological studies of the pollen intines of *Pinus bungeana* Zucc. Ex Endl. and *Picea wilsonii* Mast. *Flora* 203: 332–340.

Farquhar GD, Ehleringer JR, Hubick KT (1989). Carbon isotope discrimination and photosynthesis. *Annual review of plant physiology and plant molecular biology* 40: 503–537.

Farquhar GD, Cernusak LA, Barnes B (2007). Heavy Water Fractionation during Transpiration. *Plant physiology* 143: 11–18.

Farquhar GD and Gan KS (2003). On the progressive enrichment of the oxygen isotopic composition of water along a leaf. *Plant, Cell and Environment* 26: 801–819.

Flanagan LB and Farquhar GD (2014). Variation in the carbon and oxygen isotope composition of plant biomass and its relationship to water-use efficiency at the leaf-and ecosystem-scales in a northern Great Plains grassland. *Plant, Cell and Environment* 37: 425–438.

Fletcher WJ, Zielhofer C, Mischke S, Bryant C, Xu X *et al.* (2017). AMS radiocarbon dating of pollen concentrates in a karstic lake system. *Quaternary Geochronology* 39: 112–123.

Fraser WT, Watson JS, Sephton MA, Lomax BH, Harrington G *et al.* (2014). Changes in spore chemistry and appearance with increasing maturity. *Review of Palaeobotany and Palynology* 201: 41–46.

Gallinat AS, Primack RB, Wagner DL (2015). Autumn, the neglected season in climate change research. *Trends in Ecology and Evolution* 30: 169–176.

Gasse F, Arnold M, Fontes JC, Fort M, Gilbert E *et al.* (1991). A 13,000-year climate record from western Tibet. *Nature* 353: 742–745.

Gaudinski JB, Torn MS, Riley WJ, Swanston C, Trumbore SE *et al.* (2009). Use of stored carbon reserves in growth of temperate tree roots and leaf buds: analyses using radiocarbon measurements and modeling. *Global Change Biology* 15: 992–1014.

George E, Seith B, Schaeffer C, Marschner H (1997). Responses of *Picea*, *Pinus* and *Pseudotsuga* roots to heterogeneous nutrient distribution in soil. *Tree Physiology* 17: 39–45.

Gernet J (1997). Die Chinesische Welt. *Suhrkamp*, Frankfurt am Main.

Gessler A, Ferrio JP, Hommel R, Treydte K, Werner RA *et al.* (2014). Stable isotopes in tree rings: towards a mechanistic understanding of isotope fractionation and mixing processes from the leaves to the wood. *Tree Physiology* 34: 796–818.

Graham HV, Patzkowsky ME, Wing SL, Parker GG, Fogel ML *et al.* (2014). Isotopic characteristics of canopies in simulated leaf assemblages. *Geochimica et Cosmochimica Acta* 144: 82–95.

Griener KW, Nelson DM, Warny S (2013). Declining moisture availability on the Antarctic Peninsula during the Late Eocene. *Palaeogeography, palaeoclimatology, palaeoecology* 383: 72–78.

Grimm EC (2011). Coniss: a Fortran 77 program for stratigraphically constrained cluster analysis by the method of incremental sum of squares. *Computers and Geosciences* 13: 13–55.

He Y, Zhao C, Wang Z, Wang H, Song M *et al.* (2013). Late Holocene coupled moisture and temperature changes on the northern Tibetan Plateau. *Quaternary Science Reviews* 80: 47–57.

Helle G and Schleser GH (2004). Beyond CO_2-fixation by Rubisco–an interpretation of $^{13}C/^{12}C$ variations in tree rings from novel intra-seasonal studies on broad-leaf trees. *Plant, Cell and Environment* 27: 367–380.

Henderson ACG, Holmes JA, Zhang JW, Leng MJ, Carvalho LR (2003). A carbon- and oxygen-isotope record of recent environmental change from Qinghai Lake, NE Tibetan Plateau. *Chinese Science Bulletin* 48: 1463–1468.

Henderson ACG and Holmes JA (2009). Palaeolimnological evidence for environmental change over the past millennium from Lake Qinghai sediments: A review and future research prospective. *Quaternary International* 194: 134–147.

Henderson ACG, Holmes JA, Leng MJ (2010). Late Holocene isotope hydrology of Lake Qinghai, NE Tibetan Plateau: effective moisture variability and atmospheric circulation changes. *Quaternary Science Reviews* 29: 2215–2223.

Herzschuh U (2006). Palaeo-moisture evolution in monsoonal Central Asia during the last 50,000 years. *Quaternary Science Reviews* 25: 163–178.

Herzschuh U, Tarasov P, Wünnemann B, Hartmann K (2004). Holocene vegetation and climate of the Alashan Plateau, NW China, reconstructed from pollen data. *Palaeogeography, Palaeoclimatology, Palaeoecology* 211: 1–17.

Herzschuh U, Winter K, Wünnemann B, Li S (2006). A general cooling trend on the central Tibetan Plateau throughout the Holocene recorded by the Lake Zigetang pollen spectra. *Quaternary International* 154: 113–121.

Hoefs J (2009). Stable Isotope Geochemistry. *Springer*, Germany.

Hosner D, Wagner M, Tarasov PE, Chen, X, Leipe C (2016). Spatiotemporal distribution patterns of archaeological sites in China during the Neolithic and Bronze Age: An overview. *The Holocene* 26: 1576–1593.

Hou JZ, D'Andrea WJ, Liu ZH (2012). The influence of ^{14}C reservoir age on interpretation of paleolimnological records from the Tibetan Plateau. *Quaternary Science Reviews* 48: 67–79.

Hou X (2001). Vegetation atlas of China. *Scientific Press*, Beijing.

Huang JG and Zhang QB (2007). Tree rings and climate for the last 680 years in Wulan area of northeastern Qinghai-Tibetan Plateau. *Climate Change* 80: 369–377.

Hultine KR and Marshall JD (2000). Altitude trends in conifer leaf morphology and stable carbon isotope composition. *Oecologia* 123: 32–40.

Ingestad T (1979). Mineral nutrient requirements of *Pinus silvestris* and *Picea abies* seedlings. *Physiologia Plantarum* 45: 373–380.

Jahren AH (2004). The carbon stable isotope composition of pollen. *Review of Palaeobotany and Palynology* 132: 291–313.

Jarzen DM and Nichols DJ (1996). Pollen. In *Palynology: principles and applications*. American Association of Stratigraphic Palynologists Foundation, Salt Lake City, Utah: 261–291.

Ji JF, Shen J, Balsam W, Chen J, Liu LW *et al.* (2005). Asian monsoon oscillations in the northeastern Qinghai-Tibet Plateau since the late glacial as interpreted from visible reflectance of Lake Qinghai. *Earth and Planetary Science Letters* 233: 61–70.

Jiang H, Shevenell A, Yu S, Xu H, Mao X (2015). Decadal-to centennial-scale East Asian summer monsoon variability during the Medieval Climate Anomaly reconstructed from an eastern Tibet lacustrine sequence. *Journal of Paleolimnology* 54: 205–222.

Jones PD, Briffa KR, Osborn TJ, Lough JM, Van Ommen TD, *et al.* (2009). High-resolution palaeoclimatology of the last millennium: a review of current status and future prospects. *Holocene* 19: 3–49.

Kamenik C, Van der Knaap WO, Van Leeuwen JF, Goslar T (2009). Pollen/climate calibration based on a near-annual peat sequence from the Swiss Alps. *Journal of Quaternary Science* 24: 529–546.

Kampstra P (2008). Beanplot: A Boxplot Alternative for Visual Comparison of Distributions. *Journal of Statistical Software* 28: 1–9.

Kikuzawa K (1995). Leaf phenology as an optimal strategy for carbon gain in plants. *Canadian Journal of Botany* 73: 158–163.

King DC, Schubert BA, Jahren AH (2012). Practical considerations for the use of pollen δ^{13}C value as a paleoclimate indicator. *Rapid Communication in Mass Spectrometry* 26: 2165–2172.

Körner C, Farquhar GD, Wong SC (1991). Carbon isotope discrimination by plants follows latitudinal and altitudinal trends. *Oecologia* 88: 30–40.

Kramer K (1996). Phenology and growth of European trees in relation to climate change. *University of Wageningen Press*, Netherlands.

Krizo M and Slobodnik B (1997). Changes in the size of pollen grains and structure of the tapetal layer in *Betula pendula* (Roth) during the maturation of pollen. *Bulletin of the Polish Acadamy of Sciences* 45: 2–4.

Kuang A and Musgrave ME (1996). Dynamics of vegetative cytoplasm during generative cell formation and pollen maturation in *Arabidopsis thaliana*. *Protoplasma* 194: 81–90.

Kumar K, Rajagopalan B, Cane M (1999). On the weakening relationship between the Indian Monsoon and ENSO. *Science* 284: 2156–2159.

Kupila-Ahvenniemi S, Pihakaski S (1966). Qualitative study on the nucleic acids in the microsporangiate strobilus primordia and the spur shoot primordia of the dormant Scotch Pine. *Annales Botanici Fennici* SOCIETAS ZOOLOGICA BOTANICA FENNICA VANAMO: 117–122.

Kürschner H, Herzschuh U, Wagner D (2005). Phytosociological studies in the north-eastern Tibetan Plateau (NW China) – A first contribution to the subalpine scrub and alpine meadow vegetation. *Botanische Jahrbücher für Systematik* 126: 273–315.

Lancaster J (1990). Carbon-13 fractionation in carbon dioxide emitted diurnally from soils and vegetation at ten sites on the North-America continent. (Dissertation). University of San Diego. *Univ. Microfilms International* Ann Arbor: No. 9024008.

Leavitt SW and Long A (1984). Sampling strategy for stable carbon isotope analysis of tree rings in pine. *Nature* 311: 145–147.

Leavitt SW and Long A (1986). Stable-carbon isotope variability in tree foliage and wood. *The Ecological Society of America* 67: 1002–1010.

Leavitt SW (2010). Tree-ring C–H–O isotope variability and sampling. *Science of the Total Environment* 408: 5244–5253.

Leipe C, Demske D, Tarasov PE, HIMPAC Project Members (2014). A Holocene pollen record from the northwestern Himalayan lake Tso Moriri: Implications for palaeoclimatic and archaeological research. *Quaternary International* 348: 93-112.

Lejoly-Gabriel M and Leuschner RM (1983). Comparison of air-borne pollen at Louvain-la-Neuve (Belgium) and Basel (Switzerland) during 1979 and 1980. *Grana* 22: 59–64.

Li FS, Phyo P, Jacobowitz J, Hong M, Weng JK (2019). The molecular structure of plant sporopollenin. *Nature plants* 5: 41–46.

Li J, Ilvonen L, Xu Q, Ni J, Jin L *et al.* (2016). East Asian summer monsoon precipitation variations in China over the last 9500 years: A comparison of pollen-based reconstructions and model simulations. *Holocene* 26: 592–602.

Liu B, Jin H, Sun Z, Miao Y, Su Z *et al.* (2014). Evidence of Holocene millennial-scale climatic change from Gonghe Basin peat deposit, northeastern Qinghai-Tibet Plateau. *Journal of Arid Environments* 106: 1–10.

Liu KB, Yao Z, Thompson LG (1998). A pollen record of Holocene climatic changes from the Dunde ice cap, Qinghai-Tibetan Plateau. *Geology* 26: 135–138.

Liu XJ, Lai Z, Madsen D, Zeng F (2015). Last deglacial and Holocene lake level variations of Qinghai Lake, north-eastern Qinghai–Tibetan Plateau. *Journal of Quaternary Science* 30: 245–257.

Liu XQ, Shen J, Wang SM, Yang XD, Tong GB *et al.* (2002). A 16000-year pollen record of Qinghai Lake and its paleo-climate and paleoenvironment. *Chinese Science Bulletin* 47: 1931–1936.

Liu Y, An ZS, Linderholm HW, Chen DL, Song HM *et al.* (2009). Annual temperatures during the last 2485 years in the mid-eastern Tibetan Plateau inferred from tree rings. *Science in China, Series D: Earth Sciences* 52: 348–359.

Loader NJ and Hemming DL (2000). Preparation of pollen for stable carbon isotope analyses. *Chemical Geology* 165: 339–344.

Loader NJ and Hemming DL (2002). Stable isotope analysis of pollen as a palaeoindicator-Methodological considerations and future challenges. *No. IAEA-CSP–13/P.*

Loader NJ and Hemming DL (2001). Spatial variation in pollen δ^{13}C correlates with temperature and seasonal development timing. *Holocene* 11: 587–592.

Loader NJ and Hemming DL (2004). The stable isotope analysis of pollen as an indicator of terrestrial palaeoenvironmental change: a review of progress and recent developments. *Quaternary Science Reviews* 23: 893–900.

Lockheart MJ, Van Bergen PF, Evershed R (1997). Variations in the stable carbon isotope compositions of individual lipids from the leave of modern angiosperms: implications for the study of higher land plant-derived sedimentary organic matter. *Organic Geochemistry* 26: 137–153.

Loescher WH, McCamant T, Keller JD (1990). Carbohydrate reserves, translocation, and storage in woody plant roots. *Horticultural Science* 25: 274–281.

Luomajoki A (1986). Timing of microsporogenesis in trees with reference to climatic adaptation: a review. *Acta Forestalia Fennica* 196: Article ID 7642.

Marquez J, Seoane-Camba JA, Suarez-Cervera M (1997). The role of the intine and cytoplasm in the activation and germination processes of Poaceae pollen grains. *Grana* 36: 328–342.

McCarroll D and Loader NJ (2004). Stable isotopes in tree rings. *Quaternary Science Reviews* 23: 771–801.

McVean DN (1953). *Alnus glutinosa* (L.) Gaertn. *Journal of Ecology* 41: 447–466.

Michelot A, Simard S, Rathgeber C, Dufrêne E, Damesin C (2012). Comparing the intra-annual wood formation of three European species (*Fagus sylvatica*, *Quercus petraea* and *Pinus sylvestris*) as related to leaf phenology and non-structural carbohydrate dynamics. *Tree Physiology* 32: 1033–1045.

Miehe G, Miehe S, Bach K, Nölling J, Hansbach J *et al.* (2011). Plant communities of central Tibetan pastures in the Alpine Steppe/*Kobresia pygmaea* ecotone. *Journal of Arid Environments* 75: 711–723.

Miehe G, Miehe S, Kaiser K, Liu JQ, Zhao XQ (2008). Status and dynamics of the *Kobresia pygmaea* ecosystem on the Tibetan Plateau. *AMBIO: A Journal of Human Environments* 37: 272–279.

Mikhael A, Jurcic K, Schneider C, Carr D, Fisher GL *et al.* (2019). Demystifying and Unravelling the Factual Molecular Structure of the Biopolymer Sporopollenin. *ChemRxiv*. Preprint. DOI: doi.org/10.26434/chemrxiv.10059860.v1

Mischke S, Herzschuh U, Zhang C, Bloemendal J, Riedel F (2005). A Late Quaternary lake record from the Qilian Mountains (NW China): lake level and salinity changes inferred from sediment properties and ostracod assemblages. *Global and Planetary Change* 46: 337–359.

Moore PD, Webb JA, Collinson ME (1991) Pollen Analysis. *Blackwell Scientific Publications*, London, England.

Morecroft MD and Roberts JM (1999). Photosynthesis and stomatal conductance of mature canopy oak (*Quercus robur*) and sycamore (*Acer pseudoplatanus*) trees throughout the growing season. *Functional Ecology* 13: 332–342.

Morecroft MD, Stokes VJ, Morison JIL (2003). Seasonal changes in the photosynthetic capacity of canopy oak (*Quercus robur*) leaves: the impact of slow development on annual carbon uptake. *International Journal of Biometeorology* 47: 221–226.

Müller C, Hethke M, Riedel F, Helle G (2020). Inter- and intra- tree variability of carbon and oxygen stable isotope ratios of modern pollen from nine European tree species. *PLoS ONE* 15(6):e0234315 (doi.org/10.1371/journal.pone.0234315).

Müller C (2017). Bi-decadal climate reconstruction derived from a 1200-year long pollen record from the NE Qinghai-Tibet Plateau and its implications for discussion of the late Holocene environmental dynamics. *Quaternary International* 444: 1–10.

Myszkowska D, Jenner B, Puc M, Stach A, Nowak M *et al.* (2010). Spatial variations in the dynamics of the *Alnus* and *Corylus* pollen seasons in Poland. *Aerobiology* 26: 209–221.

Nelson DM (2012). Carbon isotopic composition of *Ambrosia* and *Artemisia* pollen: assessment of a C3-plant paleophysiological indicator. *New Phytologist* 195: 787–793.

Nelson DM, Hu FS, Michener RH (2006). Stable-carbon isotope composition of Poaceae pollen: an assessment for reconstructing C3 and C4 grass abundance. *Holocene* 16: 819–825.

Nelson DM, Hu FS, Scholes DR, Joshi N, Pearson A (2008). Using SPIRAL (Single Pollen Isotope Ratio AnaLysis) to estimate C3- and C4-grass abundance in the paleorecord. *Earth and Planetary Science Letters* 269: 11–16.

Nelson DM (2012). Carbon isotopic composition of *Ambrosia* and *Artemisia* pollen: assessment of a C3-plant paleophysiological indicator. *New Phytologist* 195: 787–793.

New M, Lister D, Hulme M, Makin I (2002). A high-resolution data set of surface climate over global land areas. *Climate Research* 21: 1–25.

O'Leary MH (1988). Carbon isotopes in photosynthesis. *Bioscience* 38: 328–336.

Panagos P, Van Liedekerke M, Jones A, Montanarella L (2012). European Soil Data Centre: Response to European policy support and public data requirements. *Land Use Policy* 29: 329–338.

Paul C, Skrzypek G, Forizs I (2007). Normalization of Measured Stable Isotopic Compositions to Isotope Reference Scales – a Review. *Rapid Communication in Mass Spectrometry* 21: 3000–3014.

Paulsen DE, Li HC, Ku TL (2003). Climate variability in central China over the last 1270 years revealed by high-resolution stalagmite records. *Quaternary Science Reviews* 22: 691–701.

Pearcy RW and John Ehleringer (1984). Comparative ecophysiology of C3 and C4 plants. *Plant, Cell and Environment* 7: 1–13.

Piao SL, Ciais P, Friedlingstein P, Peylin P, Reichstein M, *et al.* (2008). Net carbon dioxide losses of northern ecosystems in response to autumn warming. *Nature* 451: 49–52.

Pritzke F (2015). Morphological examination and stable isotope analysis of recent bee pollen pellets (Bachelor's Thesis). Humboldt-Universität Berlin, Germany.

Prentice C, Guiot J, Huntley B, Jolly D, Cheddadi R (1996). Reconstructing biomes from palaeoecological data: a general method and its application to European pollen data at 0 and 6 ka. *Climate Dynamics* 12: 185–194.

Pu Y, Nace T, Meyers PA, Zhang H, Wang Y *et al.* (2013). Paleoclimate changes of the last 1000yrs on the eastern Qinghai–Tibetan Plateau recorded by elemental, isotopic, and molecular organic matter proxies in sediment from glacial Lake Ximencuo. *Palaeogeography, Palaeoclimatology, Palaeoecology* 380: 39–53.

Putnam AE, Putnam DE, Andreu-Hayles L, Cook ER, Palmer JG *et al.* (2016). Little Ice Age wetting of interior Asian deserts and the rise of the Mongol Empire. *Quaternary Science Reviews* 131: 33–50.

R Core Team (2017). R: A Language and Environment for Statistical Computing. https://www.R-project.org/

Ramsey CB, Dee M, Lee S, Nakagawa T, Staff R (2010). Developments in the calibration and modelling of radiocarbon dates. *Radiocarbon* 52: 953–961.

Reille M (1992). Pollen et spores d'Europe et d'Afrique du Nord. *Laboratoire de Botanique historique et Palynologie*, Marseille.

Reille M (1995). Pollen et spores d'Europe et d'Afrique du nord, supplement 1. *Laboratoire de Botanique historique et Palynologie*, Marseille.

Reille M (1998). Pollen et spores d'Europe et d'Afrique du nord, supplement 2. *Laboratoire de Botanique historique et Palynologie*, Marseille.

Reimer PJ, Baillie MGL, Bard E, Bayliss A, Beck JW *et al.* (2009). IntCal09 and Marine09 radiocarbon age calibration curves, 0-50,000 years cal BP. *Radiocarbon* 51: 1111–1150.

Richardson AD, Carbone MS, Keenan TF, Czimczik CI, Hollinger DY *et al.* (2013). Seasonal dynamics and age of stemwood nonstructural carbohydrates in temperate forest trees. *New Phytologist* 197: 850–861.

Rötzer T and Chmielewski FM (2001). Phenological maps of Europe. *Climate Research* 18: 249–257.

Rowley JR, Skvarla JJ, Walles B (2000). Microsporogenesis in *Pinus sylvestris* L. VIII. Tapetal and late pollen grain development. *Plant Systematics and Evolution* 225: 201–224.

RStudio Team. RStudio: Integrated Development for R. RStudio, Inc., Boston 2015; MA URL http://www.rstudio.com/.

Saurer M, Borella S, Leuenberger M (1997). δ^{18}O of tree rings of beech (*Fagus silvatica*) as a record of δ^{18}O of the growing season precipitation. *Tellus B* 49: 80–92.

Saurer M, Siegenthaler U, Schweingruber FH (1995). The climate-carbon isotope relationship in tree rings and the significance of site conditions. *Tellus B* 47: 320–330.

Saurer M and Siegenthaler U (1989). $^{13}C/^{12}C$ isotope ratios in trees are sensitive to relative humidity. *Dendrochronologia* 7: 9–13.

Scheifinger H, Menzel A, Koch E, Peter C, Ahas R (2002). Atmospheric mechanisms governing the spatial and temporal variability of phenological phases in central Europe. *International Journal of Climatology* 22: 1739–1755.

Schleser GH (1999). $^{13}C/^{12}C$ in growth rings and leaves: carbon distribution in trees. In: *Fossil plants and spores: modern techniques.* London: Geological Society 306–309.

Schönwiese C (2013). Klimaänderungen: Daten, Analysen, Prognosen. *Springer-Verlag*, Germany.

Schultz H (2018). Zusammenhänge zwischen atmosphärischen Bedingungen, biotischer Faktoren und den Isotopenverhältnissen $^{13}C/^{12}C$ und $^{18}O/^{16}O$ in Pollenexinen aus Bienenpollenpaketen (Master's Thesis). Humboldt-Universität Berlin, Germany.

Schuster C, Kirchner M, Jakobi G, Menzel A (2014). Frequency of inversions affects senescence phenology of *Acer pseudoplatanus* and *Fagus sylvatica*. *International Journal of Biometeorology* 58: 485–498.

Schwarz DM (2016). A Stable Isotope Investigation Of Pollen From Pinery Provincial Park, Southwestern Ontario, Canada. The University of Western Ontario. *Electronic Thesis and Dissertation Repository*: 4254.

Seppä H and Bennett KD (2003). Quaternary pollen analysis: recent progress in palaeoecology and palaeoclimatology. *Progress in Physical Geography* 27: 548–579.

Shao X, Xu Y, Yin ZY, Liang E, Zhu H *et al.* (2010). Climatic implications of a 3585-year tree-ring width chronology from the northeastern Qinghai-Tibetan Plateau. *Quaternary Science Reviews* 29: 2111–2122.

Sheppard PR, Tarasov PE, Graumlich LJ, Heussner KU, Wagner M *et al.* (2004). Annual precipitation since 515 BC reconstructed from living and fossil juniper growth of northeastern Qinghai Province, China. *Climate Dynamics* 23: 869–881.

Shi Y, Yao T, Yang B (1999). Decadal climatic variations recorded in Guliya ice core and comparison with the historical documentary data from East China during the last 2000 years. *Science in China Series D, Earth Science* 42: 91–100.

Sparks TH and Carey PD (1995). The responses of species to climate over two centuries: an analysis of the Marsham phenological record, 1736-1947. *Journal of Ecology* 83: 321–329.

Speer J (2010). Fundamentals of Tree Ring Research. *University of Arizona Press*, USA.

Stach A, Emberlin J, Smith M, Adams-Groom B, Myszkowska D (2008). Factors that determine the severity of *Betula* spp. pollen seasons in Poland (Poznań and Krakow) and the United Kingdom (Worcester and London). *International Journal of Biometeorology* 52: 311–321.

Stairs GR (1964). Effects of chronic and acute gamma irradiation of male flower buds and mature pollen in *Quercus*. *Forest Science* 10: 397–409.

Stanley RG and Linskens HF (2012). Pollen: biology biochemistry management. *Springer Science and Business Media*.

Steinhilber F, Abreu JA, Beer J, Brunner I, Christl M *et al.* (2012). 9,400 years of cosmic radiation and solar activity from ice cores and tree rings. *PNAS* 109: 5967–5971.

Taft L, Wiechert U, Riedel F, Weynell M, Zhang HC (2012). Sub-seasonal oxygen and carbon isotope variations in shells of modern *Radix* sp. (Gastropoda) from the Tibetan Plateau: potential of a new archive for palaeoclimatic studies. *Quaternary Science Reviews* 34: 44–56.

Taft L, Wiechert U, Zhang H, Lei G, Mischke S *et al.* (2013). Oxygen and carbon isotope patterns archived in shells of the aquatic gastropod Radix: Hydrologic and climatic signals across the Tibetan Plateau in submonthly resolution. *Quaternary International* 291: 282–298.

Thompson L, Yao T, Davis ME, Henderson KA, Mosley-Thompson E *et al.* (1997). Tropical climate instability: The last glacial cycle from a Qinghai-Tibetan ice core. *Science* 276: 1821–1825.

Thompson LG, Mosley-Thompson E, Davis ME, Bolzan J, Dai J *et al.* (1990). Glacial stage ice-core records from the subtropical Dunde ice cap, China. *Annals of Glaciology* 14: 288–297.

Tian F, Herzschuh U, Dallmeyer A, Xu Q, Mischke S *et al.* (2013). Environmental variability in the monsoon–westerlies transition zone during the last 1200 years: lake sediment analyses from central Mongolia and supra–regional synthesis. *Quaternary Science Reviews* 73: 31–47.

Traverse A (2007). Paleopalynology. Vol. 28. *Springer Science and Business Media*.

Treydte K, Schleser GH, Schweingruber FH, Winiger M (2001). The climatic significance of δ^{13}C in subalpine spruces (Lötschental, Swiss Alps) a case study with respect to altitude, exposure and soil moisture. *Tellus B* 53: 593–611.

Urban MA, Nelson DM, Jiménez-Moreno G, Hu FS (2016). Carbon isotope analyses reveal relatively high abundance of C4 grasses during early–middle Miocene in southwestern Europe. *Palaeogeography, Palaeoclimatology, Palaeoecology* 443: 10–17.

Urban MA, Nelson DM, Kelly R, Ibrahim T, Dietze M *et al.* (2013). A hierarchical Bayesian approach to the classification of C3 and C4 grass pollen based on SPIRAL δ^{13}C data. *Geochimica et Cosmochimica Acta* 121: 168–176.

Van Campo E, Cour P, Hang SX (1996). Holocene environmental changes in Bangong Co basin (Western Tibet). Part 2: the pollen record. *Palaeogeography, Palaeoclimatology, Palaeoecology* 120: 49-63.

van der Sleen P, Zuidema PA, Pons TL (2017). Stable isotopes in tropical tree rings: theory, methods and applications. *Functional Ecology* 31: 1674–1689.

van Roij L, Sluijs A, Laks JJ, Reichart GJ (2017). Stable carbon isotope analyses of nanogram quantities of particulate organic carbon (pollen) with laser ablation nano combustion gas chromatography/isotope ratio mass spectrometry. *Rapid Communication in Mass Spectrometry* 31: 47–58.

Vitasse Y, Delzon S, Dufrêne E, Pontailler JY, Louvet JM *et al.* (2009a). Leaf phenology sensitivity to temperature in European trees: Do within-species populations exhibit similar responses? *Agricultural and Forest Meteorology* 149: 735–744.

Vitasse Y, Porté AJ, Kremer A, Michalet R, Delzon S (2009b). Responses of canopy duration to temperature changes in four temperate tree species: relative contributions of spring and autumn leaf phenology. *Oecologia* 161: 187–198.

Walcroft AS, Silvester WB, Whitehead D, Kelliher FM (1997). Seasonal changes in stable carbon isotope ratios within annual rings of Pinus radiata reflect environmental regulation of growth processes. *Functional Plant Biology* 24: 57–68.

Wang N, Yao T, Thompson LG, Henderson KA, Davis ME (2002). Evidence for cold events in the early Holocene from the Guliya ice core, Tibetan Plateau, China. *Chinese Science Bulletin* 47: 1422–1427.

Wang R, Zhang Y, Wünnemann B, Biskaborn BK, Yin H *et al.* (2015). Linkages between Quaternary climate change and sedimentary processes in Hala

Lake, northern Tibetan Plateau, China. *Journal of Asian Earth Sciences* 107: 140–150.

Wang X, Liang T, Xie H, Huang X, Lin H (2016). Climate-driven changes in grassland vegetation, snow cover, and lake water of the Qinghai Lake basin. *Journal of Applied Remote Sensing* 10: DOI: 10.1117/1.JRS.10.036017.

Warren CR, McGrath JF, Adams MA (2001). Water availability and carbon isotope discrimination in conifers. *Oecologia* 127: 476–486.

Webb EA and Longstaffe FJ (2000). The oxygen isotopic compositions of silica phytoliths and plant water in grasses: implications for the study of paleoclimate. *Geochimica et Cosmochimica Acta* 64: 767-780.

Weninger B and Jöris O (2008). A ^{14}C age calibration curve for the last 60ka: the Greenland-Hulu U/Th timescale and its impact on understanding the Middle to Upper Paleolithic transition in Western Eurasia. *Journal of Human Evolution* 55: 772-781.

Weninger B, Jöris O, Danzeglocke U (2015). CalPal-2007. Cologne Radiocarbon Calibration and Palaeoclimate Research Package. http://www.calpal.de/(accessed 13.09.15).

Wernicke J, Grießinger J, Hochreuther P, Bräuning A (2015). Variability of summer humidity during the past 800 years on the eastern Tibetan Plateau inferred from δ^{18}O of tree-ring cellulose. *Climate of the Past* 11: 327–337.

Wertmann P, Tarasov PE, Wagner M (2016). Sogdian careers and families in 6-7th century northern China: case study of the Shi family based on archaeological finds and epitaph inscriptions. *The History of the Family* 21: 103–135.

Wiermann R, Gubatz S (1992). Pollen wall and sporopollenin. *International Review of Cytology* 140: 35–72.

Wilczek AM, Burghardt LT, Cobb AR, Cooper MD, Welch SM *et al.* (2010). Genetic and physiological bases for phenological responses to current and predicted climates. *Philosophical Transactions of the Royal Society B: Biological Sciences* 365: 3129–3147.

Willis CG, Ruhfel B, Primack R B, Miller-Rushing AJ, Davis CC (2008). Phylogenetic patterns of species loss in Thoreau's woods are driven by climate change. *PNAS* 105: 17029–17033.

Wilson AT, Grinsted MJ (1977). $^{12}C/^{13}C$ in cellulose and lignin as palaeothermometers. *Nature*, 265: 133-135.

Wischnewski J, Herzschuh U, Rühland KM, Bräuning A, Mischke S *et al.* (2014). Recent ecological responses to climate variability and human impacts in the Nianbaoyeze Mountains (eastern Tibetan Plateau) inferred from pollen, diatom and tree-ring data. *Journal of Paleolimnology* 52: 287-302.

Wischnewski J, Mischke S, Wang Y, Herzschuh U (2011). Reconstructing climate variability on the northeastern Tibetan Plateau since the last Lateglacial – a multi-proxy, dual-site approach comparing terrestrial and aquatic signals. *Quaternary Science Reviews* 30: 82–97.

Xu H, Ai L, Tan L, An Z (2006). Stable isotopes in bulk carbonates and organic matter in recent sediments of Lake Qinghai and their climatic implications. *Chemical Geology* 235: 262–275.

Xu H, Hou Z, An Z, Liu X, Dong J (2010). Major ion chemistry of waters in Lake Qinghai catchments, NE Qinghai-Tibet plateau, China. *Quaternary International* 212: 35–43.

Xu H, Hou ZH, Ai L, Tan LC (2007). Precipitation at Lake Qinghai, NE Qinghai–Tibet Plateau, and its relation to Asian summer monsoons on decadal/interdecadal scales during the past 500 years. *Palaeogeography, Palaeoclimatology, Palaeoecology* 254: 541–549.

Xu H, Liu X, Hou Z (2008). Temperature variations at Lake Qinghai on decadal scales and the possible relation to solar activities. *Journal of Atmospheric and Solar-Terrestrial Physics* 70: 138–144.

Yan D, Wünnemann B, Hu Y, Frenzel P, Zhang Y *et al.* (2017). Wetland evolution in the Qinghai Lake area, China, in response to hydrodynamic and eolian processes during the past 1100 years. *Quarternary Science Reviews* 162: 42–59.

Yang B, Braeuning A, Johnson RK, Shi YF (2002). General characteristics of temperature variation in China during the last two millennia. *Geophysical Research*

Letters 29: DOI: 10.1029/2001GL014485.

Yang B, Bräuning A, Liu J, Davis ME, Yajun S (2009a). Temperature changes on the Tibetan Plateau during the past 600 years inferred from ice cores and tree rings. *Global and Planetary Change* 69: 71–78.

Yang B, Qin C, Wang J, He M, Melvin TM *et al.* (2014). A 3,500-year tree-ring record of annual precipitation on the northeastern Tibetan Plateau. *PNAS* 111: 2903–2908.

Yang B, Wang J, Bräuning A, Dong Z, Esper J (2009b). Late Holocene climatic and environmental changes in arid central Asia. *Quaternary International* 194: 68–78.

Yao T, Duan K, Xu B, Wang N, Guo X *et al.* (2008). Precipitation record since AD 1600 from ice cores on the central Tibetan Plateau. *Climate of the Past* 4: 175–180.

Yao T, Shi Y, Thompson LG (1997). High resolution record of paleoclimate since the Little Ice Age from the Tibetan ice cores. *Quaternary International* 37: 19–23.

Yao T, Thompson LG, Qin D, Tian L, Jiao K *et al.* (1996). Variations in temperature and precipitation in the last 2000a on the Xizang Plateau, Guliya ice core record. *Science in China, Series D: Earth Sciences* 39: 426–433.

Yapp CJ and Epstein S (1982). A reexamination of cellulose carbon-bound hydrogen D measurements and some factors affecting plant-water D/H relationships. *Geochimica et Cosmochimica Acta* 46: 955–965.

Yu G, Tang L, Yang X, Ke X, Harrison SP (2001). Modern pollen samples from alpine vegetation on the Tibetan Plateau. *Global Ecology and Biogeography* 10: 503–519.

Yu JQ and Kelts KR (2002). Abrupt changes in climatic conditions across the late-glacial/Holocene transition on the N. E. Tibet-Qinghai Plateau: evidence from Lake Qinghai, China. *Journal of Paleolimnology* 28: 195–206.

Zan J, Fang X, Yan M, Zhang W, Zhang Z (2015). Magnetic variations in surface soils in the NE Tibetan Plateau indicating the climatic boundary between the

Westerly and East Asian summer monsoon regimes in NW China. *Global and Planetary Change* 130: 1–6.

Zhang E, Shen J, Wang S, Yin Y, Zhu Y *et al.* (2004). Quantitative reconstruction of the paleosalinity at Qinghai Lake in the past 900 years. *Chinese Science Bulletin* 49: 730–734.

Zhang JW, Chen FH, Holmes JA, Li H, Guo XY *et al.* (2011). Holocene monsoon climate documented by oxygen and carbon isotopes from lake sediments and peat bogs in China: a review and synthesis. *Quaternary Science Reviews* 30: 1973–1987.

Zhang P, Cheng H, Edwards RL, Chen F, Wang Y *et al.* (2008). A test of climate, sun, and culture relationships from an 1810-year Chinese cave record. *Science* 322: 940–942.

Zhang QB, Cheng GD, Yao TD, Kang XC, Huang JG (2003). A 2,326-year tree-ring record of climate variability on the northeastern Qinghai-Tibetan Plateau. *Geophysical Research Letters* 30, 14. DOI: 10.1029/2003GL017425.

Zhou WJ, Donahue D, Jull AJT (1997). Radiocarbon AMS dating of pollen concentrated from eolian sediments: implications for monsoon climate change since the late Quaternary. *Radiocarbon* 39: 19–26.

Zippel A (2016). Rekonstruktion der Vegetationsdynamik im Spätholozän mittels Untersuchung von Pollen aus dem Xingyun See vom Yunnan Plateau, SW-China, und Messungen stabiler Sauerstoff- und Kohlenstoffisotope der Pollen zur Prüfung einer Korrelation beider analytischer Methoden (Bachelor's Thesis). Universität Potsdam, Germany.

Appendix A

A.1 Supplementary material to the manuscripts

Supplementary data associated with manuscript 1 and 2 are available in the Open Access information system PANGAEA (Table A.1). Supplementary Information of manuscript 2 containing detailed results of the stepwise regression analysis for the influence of environmental factors on $\delta^{13}C_{pollen}$ and $\delta^{18}O_{pollen}$ is available online at the open source journal Plos One (Table A.1).

Additional information about the ^{14}C age dating of Daotang Pond samples (manuscript 1) and the generated age model dased on the carbon 14 dates are given in Table A.2 and Figure A.1. Given are intervals of calendar age, where the true ages of the samples encompass with the probability of ca. 68% and ca. 95%. The calibration was made with the OxCal software, OxCal v4.1.5 (Ramsey *et al.*, 2010) and additionally atmospheric data from Reimer *et al.* (2009).

Measured $\delta^{13}C_{pollen}$ and $\delta^{18}O_{pollen}$ values of chemically treated modern pollen material of eight tree species compiled for manuscript 3 are listed in Table A.3. This data is supplementary material for the publication and will be freely availiable upon acceptance of the manuscript by the *Journal of Quarternay Sciences*.

Table A.1: Details of the availiability of supplementary date of manuscript 1 and 2 (MS no. I and MS no. II). Supplementary information of manuscript 2 is availiable at Plos One, the pollen counts of Daotang Pond record (manuscript 1) and the results of the pollen-isototope measurements for manuscript 2 are deposited at the online databse PANGEA.

Chapter	**Data**	**Availability (digital object identifier)**
2 (MS no. I)	Pollen counts of the Daotang Pond record	doi.pangaea.de/10.1594/PANGAEA.919329
3 (MS no. II)	S1, stepwise regression analysis, $\delta^{13}C$	doi.org/10.1371/journal.pone.0234315.s001
3 (MS no. II)	S2, stepwise regression analysis, $\delta^{18}O$	doi.org/10.1371/journal.pone.0234315.s002
3 (MS no. II)	Results of the pollen-isotope measurements	doi.org/10.1594/PANGAEA.910977

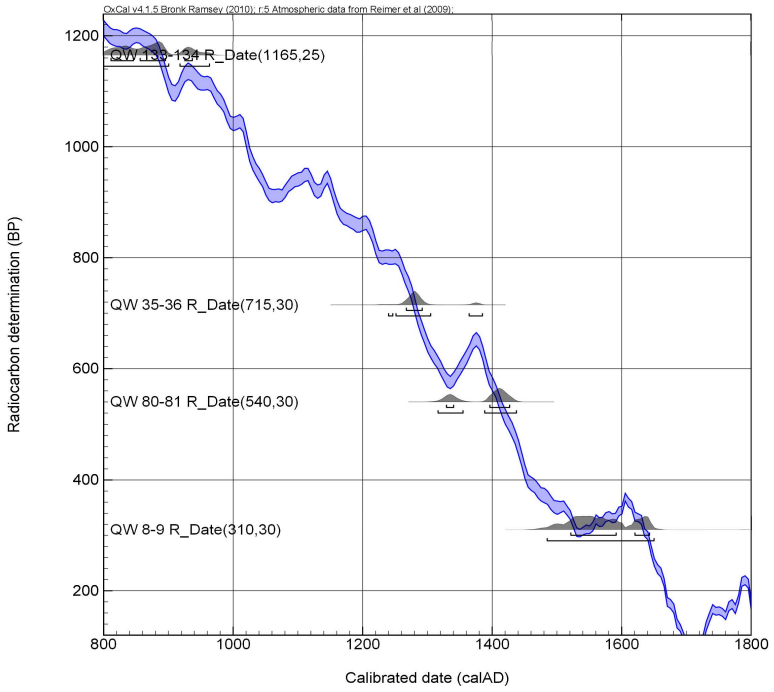

Figure A.1: Comparison of the radiocarbon determination (BP) and the calibrated date (calCE) of four ^{14}C dated samples of the Daotang Pond record. The calibration was made with the OxCal software, OxCal v4.1.5 (Ramsey *et al.*, 2010) and additionally atmospheric data from Reimer *et al.* (2009).

Table A.2: ^{14}C dates of four age dated samples of the Daotang Pond record. Given are intervals of calendar age, where the true ages of the samples encompass with the probability of ca. 68% and ca. 95%. The calibration was made with the OxCal software, OxCal v4.1.5 (Ramsey *et al.*, 2010) and additionally atmospheric data from Reimer *et al.* (2009).

Sample name	**Lab. no.**	**Age ^{14}C**	**68.2% probability**	**95.4% probability**
QW 8-9	Poz-58700	310 ± 30 BP	1521 CE (51.8%) 1591 CE 1620 CE (16.4%) 1643 CE	1485 CE (95.4%) 1650 CE
QW 35-36	Poz-58703	715 ± 25 BP	1270 CE (68.2%) 1290 CE	1259 CE (91.9%) 1299 CE 1370 CE (3.5%) 1380 CE
QW 80-81	Poz-58701	540 ± 25 BP	1331 CE (9.1%) 1338 CE 1397 CE (59.1%) 1426 CE	1320 CE (24.5%) 1351 CE 1390 CE (70.9%) 1435 CE
QW 133-134	Poz-58702	1165 ± 25 BP	782 CE (4.3%) 789 CE 811 CE (23.4%) 846 CE 856 CE (33.2%) 895 CE 925 CE (7.3%) 937 CE	777 CE (77.5%) 900 CE 918 CE (17.9%) 963 CE

Table A.3: Detailed sample list including the species, sample ID and location of sampling (longitude, latitude and altitude). The chemical formula (chem. formula) refers to the treatment of the pollen. Most samples were measured with three repititions (Rep. no). The $\delta^{13}C_{pollen}$ and $\delta^{18}O_{pollen}$ values of chemically treated modern pollen are normalised after Paul *et al.* (2007).

Species	Sample ID	Latitude	Longitude	Altitude (m a.s.l.)	Chem. formula	Rep. no	δ^{13}C (‰)	δ^{18}O (‰)
Alnus glutinosa	ARD3_Alder11	49.74229	05.67883	405	*all*	1	-34.8	17.2
Alnus glutinosa	ARD3_Alder11	49.74229	05.67883	405	*all*	2	-34.3	18.0
Alnus glutinosa	ARD3_Alder11	49.74229	05.67883	405	*all*	3	-34.7	17.8
Alnus glutinosa	ARD3_Alder11	49.74229	05.67883	405	H_2SO_4	1	-34.0	21.6
Alnus glutinosa	ARD3_Alder11	49.74229	05.67883	405	H_2SO_4	2	-34.0	22.6
Alnus glutinosa	ARD3_Alder11	49.74229	05.67883	405	H_2SO_4	3	-33.5	21.2
Alnus glutinosa	ARD3_Alder11	49.74229	05.67883	405	KOH	1	-33.6	20.1
Alnus glutinosa	ARD3_Alder11	49.74229	05.67883	405	KOH	2	-34.3	19.9
Alnus glutinosa	ARD3_Alder11	49.74229	05.67883	405	KOH	3	-33.7	19.7
Alnus glutinosa	ARD3_Alder11	49.74229	05.67883	405	NaClO	1	-31.7	21.3
Alnus glutinosa	ARD3_Alder11	49.74229	05.67883	405	NaClO	2	-32.0	21.0
Alnus glutinosa	ARD3_Alder11	49.74229	05.67883	405	NaClO	3	-31.3	21.1
Alnus glutinosa	ARD3_Alder11	49.74229	05.67883	405	raw	1	-30.7	21.7
Alnus glutinosa	ARD3_Alder11	49.74229	05.67883	405	raw	2	-30.3	20.9
Alnus glutinosa	ARD3_Alder11	49.74229	05.67883	405	raw	3	-30.3	21.0
Alnus glutinosa	ARD3_Alder15	49.74182	05.67972	390	H_2SO_4	1	-34.7	20.6
Alnus glutinosa	ARD3_Alder15	49.74182	05.67972	390	H_2SO_4	2	-33.9	21.0
Alnus glutinosa	ARD3_Alder15	49.74182	05.67972	390	H_2SO_4	3	-33.3	20.9
Alnus glutinosa	ARD3_Alder15	49.74182	05.67972	390	KOH	1	-34.1	20.3
Alnus glutinosa	ARD3_Alder15	49.74182	05.67972	390	KOH	2	-31.2	21.5
Alnus glutinosa	ARD3_Alder15	49.74182	05.67972	390	KOH	3	-36.5	12.5
Alnus glutinosa	ARD3_Alder15	49.74182	05.67972	390	NaClO	1	-31.1	23.5
Alnus glutinosa	ARD3_Alder15	49.74182	05.67972	390	NaClO	2	-31.5	22.6
Alnus glutinosa	ARD3_Alder15	49.74182	05.67972	390	NaClO	3	-30.9	22.7
Alnus glutinosa	ARD3_Alder15	49.74182	05.67972	390	raw	1	-31.0	22.0
Alnus glutinosa	ARD3_Alder15	49.74182	05.67972	390	raw	2	-31.0	22.4
Alnus glutinosa	ARD3_Alder15	49.74182	05.67972	390	raw	3	-31.2	22.8
Alnus glutinosa	ARD3_Alder20	49.75604	05.66175	430	*all*	1	-35.1	17.0
Alnus glutinosa	ARD3_Alder20	49.75604	05.66175	430	*all*	2	-34.5	19.0
Alnus glutinosa	ARD3_Alder20	49.75604	05.66175	430	*all*	3	-34.2	19.2
Alnus glutinosa	ARD3_Alder20	49.75604	05.66175	430	H_2SO_4	1	-33.9	19.9
Alnus glutinosa	ARD3_Alder20	49.75604	05.66175	430	H_2SO_4	2	-32.3	21.0
Alnus glutinosa	ARD3_Alder20	49.75604	05.66175	430	KOH	1	-33.6	19.7
Alnus glutinosa	ARD3_Alder20	49.75604	05.66175	430	KOH	2	-33.8	19.0
Alnus glutinosa	ARD3_Alder20	49.75604	05.66175	430	KOH	3	-31.7	19.2
Alnus glutinosa	ARD3_Alder20	49.75604	05.66175	430	NaClO	1	-31.1	22.1
Alnus glutinosa	ARD3_Alder20	49.75604	05.66175	430	NaClO	2	-31.2	20.8
Alnus glutinosa	ARD3_Alder20	49.75604	05.66175	430	NaClO	3	-31.2	20.5
Alnus glutinosa	ARD3_Alder20	49.75604	05.66175	430	raw	1	-30.1	21.4
Alnus glutinosa	ARD3_Alder20	49.75604	05.66175	430	raw	2	-30.0	21.4
Alnus glutinosa	ARD3_Alder20	49.75604	05.66175	430	raw	3	-30.2	20.9
Betula pendula	ARD4_Bet12	49.83259	05.65819	454	*all*	1	-27.2	17.4
Betula pendula	ARD4_Bet12	49.83259	05.65819	454	*all*	2	-27.3	17.6
Betula pendula	ARD4_Bet12	49.83259	05.65819	454	*all*	3	-27.4	17.5
Betula pendula	ARD4_Bet12	49.83259	05.65819	454	H_2SO_4	1	-28.1	20.8
Betula pendula	ARD4_Bet12	49.83259	05.65819	454	H_2SO_4	2	-27.8	20.3
Betula pendula	ARD4_Bet12	49.83259	05.65819	454	H_2SO_4	3	-27.6	20.5
Betula pendula	ARD4_Bet12	49.83259	05.65819	454	KOH	1	-24.4	25.4
Betula pendula	ARD4_Bet12	49.83259	05.65819	454	KOH	2	-24.2	25.6
Betula pendula	ARD4_Bet12	49.83259	05.65819	454	KOH	3	-24.8	25.1
Betula pendula	ARD4_Bet12	49.83259	05.65819	454	NaClO	1	-22.7	28.0
Betula pendula	ARD4_Bet12	49.83259	05.65819	454	NaClO	2	-22.6	28.1
Betula pendula	ARD4_Bet12	49.83259	05.65819	454	NaClO	3	-22.5	28.0
Betula pendula	ARD4_Bet12	49.83259	05.65819	454	raw	1	-23.4	24.6
Betula pendula	ARD4_Bet12	49.83259	05.65819	454	raw	2	-23.6	24.9
Betula pendula	ARD4_Bet12	49.83259	05.65819	454	raw	3	-23.4	24.6
Betula pendula	ARD4_Bet15	49.83259	05.65819	454	*all*	1	-29.5	17.2
Betula pendula	ARD4_Bet15	49.83259	05.65819	454	*all*	2	-29.3	16.9

Continued on next page

Species	Sample ID	Latitude	Longitude	Altitude (m a.s.l.)	Chemical formula	Rep. no	$\delta^{13}C$ (‰)	$\delta^{18}O$ (‰)
Betula pendula	ARD4_Bet15	49.83259	05.65819	454	*all*	3	-30.0	16.9
Betula pendula	ARD4_Bet15	49.83259	05.65819	454	H_2SO_4	1	-28.4	20.1
Betula pendula	ARD4_Bet15	49.83259	05.65819	454	H_2SO_4	2	-29.1	20.7
Betula pendula	ARD4_Bet15	49.83259	05.65819	454	H_2SO_4	3	-29.1	20.7
Betula pendula	ARD4_Bet15	49.83259	05.65819	454	KOH	1	-26.3	25.6
Betula pendula	ARD4_Bet15	49.83259	05.65819	454	KOH	2	-26.6	25.3
Betula pendula	ARD4_Bet15	49.83259	05.65819	454	KOH	3	-26.5	25.7
Betula pendula	ARD4_Bet15	49.83259	05.65819	454	NaClO	1	-24.0	28.3
Betula pendula	ARD4_Bet15	49.83259	05.65819	454	NaClO	2	-23.7	28.3
Betula pendula	ARD4_Bet15	49.83259	05.65819	454	NaClO	3	-24.0	28.4
Betula pendula	ARD4_Bet15	49.83259	05.65819	454	raw	1	-25.0	24.8
Betula pendula	ARD4_Bet15	49.83259	05.65819	454	raw	2	-24.9	25.1
Betula pendula	ARD4_Bet15	49.83259	05.65819	454	raw	3	-25.2	25.2
Betula pendula	ARD4_Bet5	49.83263	05.66144	462	*all*	1	-30.9	16.3
Betula pendula	ARD4_Bet5	49.83263	05.66144	462	*all*	2	-30.8	16.3
Betula pendula	ARD4_Bet5	49.83263	05.66144	462	*all*	3	-31.0	16.9
Betula pendula	ARD4_Bet5	49.83263	05.66144	462	H_2SO_4	1	-28.6	19.8
Betula pendula	ARD4_Bet5	49.83263	05.66144	462	H_2SO_4	2	-29.0	20.6
Betula pendula	ARD4_Bet5	49.83263	05.66144	462	H_2SO_4	3	-29.0	19.6
Betula pendula	ARD4_Bet5	49.83263	05.66144	462	KOH	1	-27.7	24.0
Betula pendula	ARD4_Bet5	49.83263	05.66144	462	KOH	2	-27.8	23.9
Betula pendula	ARD4_Bet5	49.83263	05.66144	462	KOH	3	-27.8	24.2
Betula pendula	ARD4_Bet5	49.83263	05.66144	462	NaClO	1	-24.5	27.3
Betula pendula	ARD4_Bet5	49.83263	05.66144	462	NaClO	2	-24.5	27.6
Betula pendula	ARD4_Bet5	49.83263	05.66144	462	NaClO	3	-24.5	27.6
Betula pendula	ARD4_Bet5	49.83263	05.66144	462	raw	1	-25.5	24.6
Betula pendula	ARD4_Bet5	49.83263	05.66144	462	raw	2	-25.2	24.6
Betula pendula	ARD4_Bet5	49.83263	05.66144	462	raw	3	-25.5	24.8
Carpinus betulus	Ste1_Carp1	49.86620	10.53169	444	*all*	1	-30.7	17.6
Carpinus betulus	Ste1_Carp1	49.86620	10.53169	444	*all*	2	-31.0	17.8
Carpinus betulus	Ste1_Carp1	49.86620	10.53169	444	*all*	3	-31.0	17.6
Carpinus betulus	Ste1_Carp1	49.86620	10.53169	444	H_2SO_4	1	-29.7	21.5
Carpinus betulus	Ste1_Carp1	49.86620	10.53169	444	H_2SO_4	2	-29.9	21.3
Carpinus betulus	Ste1_Carp1	49.86620	10.53169	444	H_2SO_4	3	-29.5	20.9
Carpinus betulus	Ste1_Carp1	49.86620	10.53169	444	KOH	1	-28.4	26.9
Carpinus betulus	Ste1_Carp1	49.86620	10.53169	444	KOH	2	-28.1	27.0
Carpinus betulus	Ste1_Carp1	49.86620	10.53169	444	KOH	3	-28.7	26.4
Carpinus betulus	Ste1_Carp1	49.86620	10.53169	444	NaClO	1	-26.6	28.7
Carpinus betulus	Ste1_Carp1	49.86620	10.53169	444	NaClO	2	-26.2	28.9
Carpinus betulus	Ste1_Carp1	49.86620	10.53169	444	NaClO	3	-26.8	28.9
Carpinus betulus	Ste1_Carp1	49.86620	10.53169	444	raw	1	-27.3	27.6
Carpinus betulus	Ste1_Carp1	49.86620	10.53169	444	raw	2	-26.9	27.1
Carpinus betulus	Ste1_Carp1	49.86620	10.53169	444	raw	3	-27.1	27.4
Carpinus betulus	Ste1_Carp6	49.86331	10.53318	436	*all*	1	-28.8	17.6
Carpinus betulus	Ste1_Carp6	49.86331	10.53318	436	*all*	2	-28.7	17.2
Carpinus betulus	Ste1_Carp6	49.86331	10.53318	436	*all*	3	-29.1	17.4
Carpinus betulus	Ste1_Carp6	49.86331	10.53318	436	H_2SO_4	1	-27.3	20.6
Carpinus betulus	Ste1_Carp6	49.86331	10.53318	436	H_2SO_4	2	-28.4	20.7
Carpinus betulus	Ste1_Carp6	49.86331	10.53318	436	H_2SO_4	3	-27.6	20.6
Carpinus betulus	Ste1_Carp6	49.86331	10.53318	436	KOH	1	-26.8	25.2
Carpinus betulus	Ste1_Carp6	49.86331	10.53318	436	KOH	2	-26.2	25.4
Carpinus betulus	Ste1_Carp6	49.86331	10.53318	436	KOH	3	-26.3	25.1
Carpinus betulus	Ste1_Carp6	49.86331	10.53318	436	NaClO	1	-24.1	28.2
Carpinus betulus	Ste1_Carp6	49.86331	10.53318	436	NaClO	2	-24.3	28.5
Carpinus betulus	Ste1_Carp6	49.86331	10.53318	436	NaClO	3	-24.2	28.3
Carpinus betulus	Ste1_Carp6	49.86331	10.53318	436	raw	1	-24.9	27.4
Carpinus betulus	Ste1_Carp6	49.86331	10.53318	436	raw	2	-24.8	27.3
Carpinus betulus	Ste1_Carp6	49.86331	10.53318	436	raw	3	-24.8	27.1
Carpinus betulus	Ste1_Carp7	49.85999	10.52233	385	*all*	1	-28.8	17.0
Carpinus betulus	Ste1_Carp7	49.85999	10.52233	385	*all*	2	-29.3	16.6
Carpinus betulus	Ste1_Carp7	49.85999	10.52233	385	*all*	3	-28.5	16.9
Carpinus betulus	Ste1_Carp7	49.85999	10.52233	385	H_2SO_4	1	-28.4	20.2
Carpinus betulus	Ste1_Carp7	49.85999	10.52233	385	H_2SO_4	2	-28.4	20.1
Carpinus betulus	Ste1_Carp7	49.85999	10.52233	385	KOH	1	-28.5	21.7

Continued on next page

Species	Sample ID	Latitude	Longitude	Altitude (m a.s.l.)	Chemical formula	Rep. no	$\delta^{13}C$ (‰)	$\delta^{18}O$ (‰)
Carpinus betulus	Ste1_Carp7	49.85999	10.52233	385	KOH	2	-28.2	22.3
Carpinus betulus	Ste1_Carp7	49.85999	10.52233	385	KOH	3	-28.1	22.2
Carpinus betulus	Ste1_Carp7	49.85999	10.52233	385	NaClO	1	-24.9	26.7
Carpinus betulus	Ste1_Carp7	49.85999	10.52233	385	NaClO	2	-25.2	26.8
Carpinus betulus	Ste1_Carp7	49.85999	10.52233	385	NaClO	3	-24.9	26.9
Carpinus betulus	Ste1_Carp7	49.85999	10.52233	385	raw	1	-26.0	24.7
Carpinus betulus	Ste1_Carp7	49.85999	10.52233	385	raw	2	-26.2	24.7
Carpinus betulus	Ste1_Carp7	49.85999	10.52233	385	raw	3	-26.0	24.9
Corylus avellana	ARD3_Hazel18	49.78055	05.69954	431	*all*	1	-33.5	15.5
Corylus avellana	ARD3_Hazel18	49.78055	05.69954	431	*all*	2	-33.4	15.5
Corylus avellana	ARD3_Hazel18	49.78055	05.69954	431	*all*	3	-33.5	15.3
Corylus avellana	ARD3_Hazel18	49.78055	05.69954	431	H_2SO_4	1	-31.2	20.9
Corylus avellana	ARD3_Hazel18	49.78055	05.69954	431	H_2SO_4	2	-32.5	20.5
Corylus avellana	ARD3_Hazel18	49.78055	05.69954	431	H_2SO_4	3	-32.4	20.0
Corylus avellana	ARD3_Hazel18	49.78055	05.69954	431	HF	1	-29.6	23.0
Corylus avellana	ARD3_Hazel18	49.78055	05.69954	431	HF	2	-29.7	22.4
Corylus avellana	ARD3_Hazel18	49.78055	05.69954	431	HF	3	-29.8	22.0
Corylus avellana	ARD3_Hazel18	49.78055	05.69954	431	KOH	1	-32.4	20.2
Corylus avellana	ARD3_Hazel18	49.78055	05.69954	431	KOH	2	-32.9	21.2
Corylus avellana	ARD3_Hazel18	49.78055	05.69954	431	KOH	3	-32.7	21.0
Corylus avellana	ARD3_Hazel18	49.78055	05.69954	431	NaClO	1	-29.5	22.8
Corylus avellana	ARD3_Hazel18	49.78055	05.69954	431	NaClO	2	-29.9	22.4
Corylus avellana	ARD3_Hazel18	49.78055	05.69954	431	NaClO	3	-29.7	22.2
Corylus avellana	ARD3_Hazel18	49.78055	05.69954	431	raw	1	-29.5	22.3
Corylus avellana	ARD3_Hazel18	49.78055	05.69954	431	raw	2	-29.0	21.8
Corylus avellana	ARD3_Hazel18	49.78055	05.69954	431	raw	3	-28.9	22.0
Corylus avellana	ARD3_Hazel4	49.75593	05.66205	420	*all*	1	-33.0	16.1
Corylus avellana	ARD3_Hazel4	49.75593	05.66205	420	*all*	2	-33.4	15.8
Corylus avellana	ARD3_Hazel4	49.75593	05.66205	420	*all*	3	-33.1	15.7
Corylus avellana	ARD3_Hazel4	49.75593	05.66205	420	H_2SO_4	1	-30.7	21.8
Corylus avellana	ARD3_Hazel4	49.75593	05.66205	420	H_2SO_4	2	-33.3	21.3
Corylus avellana	ARD3_Hazel4	49.75593	05.66205	420	H_2SO_4	3	-31.9	21.4
Corylus avellana	ARD3_Hazel4	49.75593	05.66205	420	HF	1	-30.6	22.0
Corylus avellana	ARD3_Hazel4	49.75593	05.66205	420	HF	2	-31.0	22.2
Corylus avellana	ARD3_Hazel4	49.75593	05.66205	420	HF	3	-30.5	21.9
Corylus avellana	ARD3_Hazel4	49.75593	05.66205	420	KOH	1	-32.7	20.6
Corylus avellana	ARD3_Hazel4	49.75593	05.66205	420	KOH	2	-32.1	20.8
Corylus avellana	ARD3_Hazel4	49.75593	05.66205	420	KOH	3	-32.7	20.6
Corylus avellana	ARD3_Hazel4	49.75593	05.66205	420	NaClO	1	-30.1	23.3
Corylus avellana	ARD3_Hazel4	49.75593	05.66205	420	NaClO	2	-30.0	22.3
Corylus avellana	ARD3_Hazel4	49.75593	05.66205	420	NaClO	3	-30.1	22.6
Corylus avellana	ARD3_Hazel4	49.75593	05.66205	420	raw	1	-28.5	21.3
Corylus avellana	ARD3_Hazel4	49.75593	05.66205	420	raw	2	-28.4	21.7
Corylus avellana	ARD3_Hazel4	49.75593	05.66205	420	raw	3	-28.3	21.2
Corylus avellana	ARD3_Hazel6	49.74008	05.68151	411	*all*	1	-32.4	16.4
Corylus avellana	ARD3_Hazel6	49.74008	05.68151	411	*all*	2	-32.5	16.5
Corylus avellana	ARD3_Hazel6	49.74008	05.68151	411	*all*	3	-32.6	16.7
Corylus avellana	ARD3_Hazel6	49.74008	05.68151	411	H_2SO_4	1	-32.5	20.0
Corylus avellana	ARD3_Hazel6	49.74008	05.68151	411	H_2SO_4	2	-32.5	20.1
Corylus avellana	ARD3_Hazel6	49.74008	05.68151	411	H_2SO_4	3	-32.6	20.3
Corylus avellana	ARD3_Hazel6	49.74008	05.68151	411	HF	1	-28.6	21.8
Corylus avellana	ARD3_Hazel6	49.74008	05.68151	411	HF	2	-29.5	21.5
Corylus avellana	ARD3_Hazel6	49.74008	05.68151	411	HF	3	-29.2	21.8
Corylus avellana	ARD3_Hazel6	49.74008	05.68151	411	KOH	1	-32.0	20.5
Corylus avellana	ARD3_Hazel6	49.74008	05.68151	411	KOH	2	-32.2	20.3
Corylus avellana	ARD3_Hazel6	49.74008	05.68151	411	KOH	3	-32.0	20.6
Corylus avellana	ARD3_Hazel6	49.74008	05.68151	411	raw	1	-27.4	20.5
Corylus avellana	ARD3_Hazel6	49.74008	05.68151	411	raw	2	-27.7	20.7
Corylus avellana	ARD3_Hazel6	49.74008	05.68151	411	raw	3	-27.6	21.1
Fagus sylvatica	ARD4_Fagus5	49.74115	05.67451	404	*all*	1	-29.4	17.0
Fagus sylvatica	ARD4_Fagus5	49.74115	05.67451	404	*all*	2	-29.5	17.7
Fagus sylvatica	ARD4_Fagus5	49.74115	05.67451	404	*all*	3	-29.3	18.2
Fagus sylvatica	ARD4_Fagus5	49.74115	05.67451	404	H_2SO_4	1	-29.6	21.9
Fagus sylvatica	ARD4_Fagus5	49.74115	05.67451	404	H_2SO_4	2	-28.9	22.0

Continued on next page

Species	Sample ID	Latitude	Longitude	Altitude (m a.s.l.)	Chemical formula	Rep. no	δ^{13}C (‰)	δ^{18}O (‰)
Fagus sylvatica	ARD4_Fagus5	49.74115	05.67451	404	H_2SO_4	3	-28.7	21.9
Fagus sylvatica	ARD4_Fagus5	49.74115	05.67451	404	KOH	1	-28.1	22.2
Fagus sylvatica	ARD4_Fagus5	49.74115	05.67451	404	KOH	2	-27.8	22.6
Fagus sylvatica	ARD4_Fagus5	49.74115	05.67451	404	KOH	3	-28.0	22.4
Fagus sylvatica	ARD4_Fagus5	49.74115	05.67451	404	raw	1	-27.9	23.8
Fagus sylvatica	ARD4_Fagus5	49.74115	05.67451	404	raw	2	-28.0	23.2
Fagus sylvatica	ARD4_Fagus5	49.74115	05.67451	404	raw	3	-28.0	23.2
Fagus sylvatica	ARD4_Fagus7	49.74140	05.67621	402	*all*	1	-30.5	18.2
Fagus sylvatica	ARD4_Fagus7	49.74140	05.67621	402	*all*	2	-30.5	17.4
Fagus sylvatica	ARD4_Fagus7	49.74140	05.67621	402	*all*	3	-30.4	17.9
Fagus sylvatica	ARD4_Fagus7	49.74140	05.67621	402	H_2SO_4	1	-30.8	21.7
Fagus sylvatica	ARD4_Fagus7	49.74140	05.67621	402	H_2SO_4	2	-30.5	21.7
Fagus sylvatica	ARD4_Fagus7	49.74140	05.67621	402	H_2SO_4	3	-29.3	22.1
Fagus sylvatica	ARD4_Fagus7	49.74140	05.67621	402	KOH	1	-29.4	22.1
Fagus sylvatica	ARD4_Fagus7	49.74140	05.67621	402	KOH	2	-29.8	21.9
Fagus sylvatica	ARD4_Fagus7	49.74140	05.67621	402	KOH	3	-29.9	22.0
Fagus sylvatica	ARD4_Fagus7	49.74140	05.67621	402	raw	1	-29.4	23.1
Fagus sylvatica	ARD4_Fagus7	49.74140	05.67621	402	raw	2	-29.3	23.2
Fagus sylvatica	ARD4_Fagus7	49.74140	05.67621	402	raw	3	-29.1	23.1
Fagus sylvatica	ARD4_Fagus8	49.74140	05.67621	402	*all*	1	-29.7	16.4
Fagus sylvatica	ARD4_Fagus8	49.74140	05.67621	402	*all*	2	-29.5	15.9
Fagus sylvatica	ARD4_Fagus8	49.74140	05.67621	402	*all*	3	-29.9	16.0
Fagus sylvatica	ARD4_Fagus8	49.74140	05.67621	402	H_2SO_4	1	-29.0	20.9
Fagus sylvatica	ARD4_Fagus8	49.74140	05.67621	402	H_2SO_4	2	-29.1	21.1
Fagus sylvatica	ARD4_Fagus8	49.74140	05.67621	402	H_2SO_4	3	-29.4	20.9
Fagus sylvatica	ARD4_Fagus8	49.74140	05.67621	402	KOH	1	-28.0	22.8
Fagus sylvatica	ARD4_Fagus8	49.74140	05.67621	402	KOH	2	-28.1	22.4
Fagus sylvatica	ARD4_Fagus8	49.74140	05.67621	402	KOH	3	-28.1	22.2
Fagus sylvatica	ARD4_Fagus8	49.74140	05.67621	402	raw	1	-27.5	23.6
Fagus sylvatica	ARD4_Fagus8	49.74140	05.67621	402	raw	2	-27.9	23.3
Fagus sylvatica	ARD4_Fagus8	49.74140	05.67621	402	raw	3	-27.5	23.5
Picea abies	ARD4_Picea10	49.74501	05.68633	394	*all*	1	-31.1	15.6
Picea abies	ARD4_Picea10	49.74501	05.68633	394	*all*	2	-31.1	13.1
Picea abies	ARD4_Picea10	49.74501	05.68633	394	*all*	3	-31.3	13.7
Picea abies	ARD4_Picea10	49.74501	05.68633	394	H_2SO_4	1	-29.3	15.9
Picea abies	ARD4_Picea10	49.74501	05.68633	394	H_2SO_4	2	-30.1	14.7
Picea abies	ARD4_Picea10	49.74501	05.68633	394	H_2SO_4	3	-29.2	15.4
Picea abies	ARD4_Picea10	49.74501	05.68633	394	HF	1	-27.6	22.7
Picea abies	ARD4_Picea10	49.74501	05.68633	394	HF	2	-27.2	23.2
Picea abies	ARD4_Picea10	49.74501	05.68633	394	HF	3	-27.4	24.1
Picea abies	ARD4_Picea10	49.74501	05.68633	394	KOH	1	-27.6	24.4
Picea abies	ARD4_Picea10	49.74501	05.68633	394	KOH	2	-27.3	24.7
Picea abies	ARD4_Picea10	49.74501	05.68633	394	KOH	3	-27.7	24.4
Picea abies	ARD4_Picea10	49.74501	05.68633	394	NaClO	1	-27.0	22.8
Picea abies	ARD4_Picea10	49.74501	05.68633	394	NaClO	2	-27.2	22.8
Picea abies	ARD4_Picea10	49.74501	05.68633	394	NaClO	3	-27.0	22.9
Picea abies	ARD4_Picea10	49.74501	05.68633	394	raw	1	-27.3	25.8
Picea abies	ARD4_Picea10	49.74501	05.68633	394	raw	2	-27.3	25.6
Picea abies	ARD4_Picea10	49.74501	05.68633	394	raw	3	-27.8	25.3
Picea abies	ARD4_Picea11	49.74501	05.68633	394	*all*	1	-30.9	13.9
Picea abies	ARD4_Picea11	49.74501	05.68633	394	*all*	2	-31.2	12.8
Picea abies	ARD4_Picea11	49.74501	05.68633	394	*all*	3	-30.9	13.2
Picea abies	ARD4_Picea11	49.74501	05.68633	394	H_2SO_4	1	-29.4	15.7
Picea abies	ARD4_Picea11	49.74501	05.68633	394	H_2SO_4	2	-29.8	14.6
Picea abies	ARD4_Picea11	49.74501	05.68633	394	H_2SO_4	3	-29.9	14.4
Picea abies	ARD4_Picea11	49.74501	05.68633	394	HF	1	-27.1	22.2
Picea abies	ARD4_Picea11	49.74501	05.68633	394	HF	2	-26.7	22.4
Picea abies	ARD4_Picea11	49.74501	05.68633	394	HF	3	-27.2	23.0
Picea abies	ARD4_Picea11	49.74501	05.68633	394	KOH	1	-27.1	23.9
Picea abies	ARD4_Picea11	49.74501	05.68633	394	KOH	2	-26.8	24.3
Picea abies	ARD4_Picea11	49.74501	05.68633	394	KOH	3	-27.0	23.9
Picea abies	ARD4_Picea11	49.74501	05.68633	394	NaClO	1	-26.9	23.3
Picea abies	ARD4_Picea11	49.74501	05.68633	394	NaClO	2	-26.9	23.0
Picea abies	ARD4_Picea11	49.74501	05.68633	394	NaClO	3	-26.6	23.2

Continued on next page

Species	Sample ID	Latitude	Longitude	Altitude (m a.s.l.)	Chemical formula	Rep. no	$\delta^{13}C$ (‰)	$\delta^{18}O$ (‰)
Picea abies	ARD4_Picea11	49.74501	05.68633	394	raw	1	-26.8	26.0
Picea abies	ARD4_Picea11	49.74501	05.68633	394	raw	2	-26.7	26.1
Picea abies	ARD4_Picea11	49.74501	05.68633	394	raw	3	-26.5	26.0
Picea abies	ARD4_Picea9	49.74303	05.68061	400	*all*	1	-30.9	16.1
Picea abies	ARD4_Picea9	49.74303	05.68061	400	*all*	2	-31.0	13.2
Picea abies	ARD4_Picea9	49.74303	05.68061	400	*all*	3	-31.8	13.7
Picea abies	ARD4_Picea9	49.74303	05.68061	400	H_2SO_4	1	-31.2	15.5
Picea abies	ARD4_Picea9	49.74303	05.68061	400	H_2SO_4	2	-31.2	14.0
Picea abies	ARD4_Picea9	49.74303	05.68061	400	H_2SO_4	3	-31.4	13.8
Picea abies	ARD4_Picea9	49.74303	05.68061	400	HF	1	-29.3	21.2
Picea abies	ARD4_Picea9	49.74303	05.68061	400	HF	2	-28.7	23.5
Picea abies	ARD4_Picea9	49.74303	05.68061	400	HF	3	-28.9	22.6
Picea abies	ARD4_Picea9	49.74303	05.68061	400	KOH	1	-28.4	23.6
Picea abies	ARD4_Picea9	49.74303	05.68061	400	KOH	2	-28.2	23.8
Picea abies	ARD4_Picea9	49.74303	05.68061	400	KOH	3	-28.0	25.3
Picea abies	ARD4_Picea9	49.74303	05.68061	400	NaClO	1	-28.6	22.2
Picea abies	ARD4_Picea9	49.74303	05.68061	400	NaClO	2	-28.6	22.2
Picea abies	ARD4_Picea9	49.74303	05.68061	400	NaClO	3	-28.2	22.9
Picea abies	ARD4_Picea9	49.74303	05.68061	400	raw	1	-28.7	24.3
Picea abies	ARD4_Picea9	49.74303	05.68061	400	raw	2	-28.3	24.3
Picea abies	ARD4_Picea9	49.74303	05.68061	400	raw	3	-28.1	24.0
Pinus sylvestris	ARD4_Pine10	50.06328	04.76259	252	*all*	1	-31.6	11.6
Pinus sylvestris	ARD4_Pine10	50.06328	04.76259	252	*all*	2	-32.1	10.7
Pinus sylvestris	ARD4_Pine10	50.06328	04.76259	252	*all*	3	-31.8	11.0
Pinus sylvestris	ARD4_Pine10	50.06328	04.76259	252	H_2SO_4	1	-31.3	11.0
Pinus sylvestris	ARD4_Pine10	50.06328	04.76259	252	H_2SO_4	2	-31.2	10.1
Pinus sylvestris	ARD4_Pine10	50.06328	04.76259	252	H_2SO_4	3	-31.1	10.4
Pinus sylvestris	ARD4_Pine10	50.06328	04.76259	252	HF	1	-26.9	27.6
Pinus sylvestris	ARD4_Pine10	50.06328	04.76259	252	HF	2	-26.6	28.2
Pinus sylvestris	ARD4_Pine10	50.06328	04.76259	252	HF	3	-26.7	27.9
Pinus sylvestris	ARD4_Pine10	50.06328	04.76259	252	KOH	1	-26.9	25.3
Pinus sylvestris	ARD4_Pine10	50.06328	04.76259	252	KOH	2	-27.2	25.1
Pinus sylvestris	ARD4_Pine10	50.06328	04.76259	252	NaClO	1	-26.4	28.9
Pinus sylvestris	ARD4_Pine10	50.06328	04.76259	252	NaClO	2	-26.1	29.0
Pinus sylvestris	ARD4_Pine10	50.06328	04.76259	252	NaClO	3	-26.2	28.9
Pinus sylvestris	ARD4_Pine10	50.06328	04.76259	252	raw	1	-26.2	30.0
Pinus sylvestris	ARD4_Pine10	50.06328	04.76259	252	raw	2	-26.1	30.1
Pinus sylvestris	ARD4_Pine10	50.06328	04.76259	252	raw	3	-26.0	30.1
Pinus sylvestris	ARD4_Pine14	50.06322	04.76239	252	*all*	1	-30.9	11.6
Pinus sylvestris	ARD4_Pine14	50.06322	04.76239	252	*all*	2	-31.4	10.2
Pinus sylvestris	ARD4_Pine14	50.06322	04.76239	252	H_2SO_4	1	-29.6	12.0
Pinus sylvestris	ARD4_Pine14	50.06322	04.76239	252	H_2SO_4	2	-30.3	11.0
Pinus sylvestris	ARD4_Pine14	50.06322	04.76239	252	H_2SO_4	3	-29.0	11.8
Pinus sylvestris	ARD4_Pine14	50.06322	04.76239	252	HF	1	-25.4	28.3
Pinus sylvestris	ARD4_Pine14	50.06322	04.76239	252	HF	2	-25.4	28.7
Pinus sylvestris	ARD4_Pine14	50.06322	04.76239	252	HF	3	-25.2	28.6
Pinus sylvestris	ARD4_Pine14	50.06322	04.76239	252	KOH	1	-25.6	28.1
Pinus sylvestris	ARD4_Pine14	50.06322	04.76239	252	KOH	2	-25.8	28.0
Pinus sylvestris	ARD4_Pine14	50.06322	04.76239	252	KOH	3	-25.5	27.8
Pinus sylvestris	ARD4_Pine14	50.06322	04.76239	252	NaClO	1	-25.0	29.4
Pinus sylvestris	ARD4_Pine14	50.06322	04.76239	252	NaClO	2	-25.0	29.7
Pinus sylvestris	ARD4_Pine14	50.06322	04.76239	252	NaClO	3	-25.2	29.5
Pinus sylvestris	ARD4_Pine14	50.06322	04.76239	252	raw	1	-25.2	30.0
Pinus sylvestris	ARD4_Pine14	50.06322	04.76239	252	raw	2	-24.0	30.3
Pinus sylvestris	ARD4_Pine14	50.06322	04.76239	252	raw	3	-23.6	31.6
Pinus sylvestris	ARD4_Pine9	50.06328	04.76259	252	*all*	1	-30.7	11.5
Pinus sylvestris	ARD4_Pine9	50.06328	04.76259	252	*all*	2	-30.7	10.7
Pinus sylvestris	ARD4_Pine9	50.06328	04.76259	252	*all*	3	-30.8	11.0
Pinus sylvestris	ARD4_Pine9	50.06328	04.76259	252	H_2SO_4	1	-28.8	15.2
Pinus sylvestris	ARD4_Pine9	50.06328	04.76259	252	H_2SO_4	2	-28.6	14.9
Pinus sylvestris	ARD4_Pine9	50.06328	04.76259	252	H_2SO_4	3	-28.7	14.4
Pinus sylvestris	ARD4_Pine9	50.06328	04.76259	252	HF	1	-24.6	28.0
Pinus sylvestris	ARD4_Pine9	50.06328	04.76259	252	HF	2	-24.6	29.7
Pinus sylvestris	ARD4_Pine9	50.06328	04.76259	252	HF	3	-24.3	29.1

Continued on next page

Species	Sample ID	Latitude	Longitude	Altitude (m a.s.l.)	Chemical formula	Rep. no	δ^{13}C (‰)	δ^{18}O (‰)
Pinus sylvestris	ARD4_Pine9	50.06328	04.76259	252	KOH	1	-25.0	28.7
Pinus sylvestris	ARD4_Pine9	50.06328	04.76259	252	KOH	2	-24.8	28.4
Pinus sylvestris	ARD4_Pine9	50.06328	04.76259	252	KOH	3	-24.8	28.3
Pinus sylvestris	ARD4_Pine9	50.06328	04.76259	252	NaClO	1	-24.0	30.2
Pinus sylvestris	ARD4_Pine9	50.06328	04.76259	252	NaClO	2	-24.3	30.5
Pinus sylvestris	ARD4_Pine9	50.06328	04.76259	252	NaClO	3	-24.2	30.6
Pinus sylvestris	ARD4_Pine9	50.06328	04.76259	252	raw	1	-24.3	30.6
Pinus sylvestris	ARD4_Pine9	50.06328	04.76259	252	raw	2	-24.5	30.5
Pinus sylvestris	ARD4_Pine9	50.06328	04.76259	252	raw	3	-24.1	30.8
Quercus robur	ARD4_Quercus13	49.74303	05.68061	400	*all*	1	-28.1	18.1
Quercus robur	ARD4_Quercus13	49.74303	05.68061	400	*all*	2	-28.3	18.4
Quercus robur	ARD4_Quercus13	49.74303	05.68061	400	*all*	3	-28.0	18.7
Quercus robur	ARD4_Quercus13	49.74303	05.68061	400	H_2SO_4	1	-27.6	23.9
Quercus robur	ARD4_Quercus13	49.74303	05.68061	400	H_2SO_4	2	-27.3	23.7
Quercus robur	ARD4_Quercus13	49.74303	05.68061	400	H_2SO_4	3	-27.0	24.0
Quercus robur	ARD4_Quercus13	49.74303	05.68061	400	KOH	1	-25.1	29.5
Quercus robur	ARD4_Quercus13	49.74303	05.68061	400	KOH	2	-25.9	29.3
Quercus robur	ARD4_Quercus13	49.74303	05.68061	400	KOH	3	-26.2	29.3
Quercus robur	ARD4_Quercus13	49.74303	05.68061	400	NaClO	1	-25.3	30.3
Quercus robur	ARD4_Quercus13	49.74303	05.68061	400	NaClO	2	-25.5	29.5
Quercus robur	ARD4_Quercus13	49.74303	05.68061	400	NaClO	3	-25.8	30.8
Quercus robur	ARD4_Quercus13	49.74303	05.68061	400	raw	1	-25.7	25.2
Quercus robur	ARD4_Quercus13	49.74303	05.68061	400	raw	2	-25.1	28.5
Quercus robur	ARD4_Quercus13	49.74303	05.68061	400	raw	3	-25.5	28.1
Quercus robur	ARD4_Quercus15	49.73832	05.66935	381	*all*	1	-30.8	18.5
Quercus robur	ARD4_Quercus15	49.73832	05.66935	381	*all*	2	-30.1	19.0
Quercus robur	ARD4_Quercus15	49.73832	05.66935	381	*all*	3	-30.6	19.3
Quercus robur	ARD4_Quercus15	49.73832	05.66935	381	H_2SO_4	1	-29.1	21.3
Quercus robur	ARD4_Quercus15	49.73832	05.66935	381	H_2SO_4	2	-29.6	21.8
Quercus robur	ARD4_Quercus15	49.73832	05.66935	381	H_2SO_4	3	-29.0	20.8
Quercus robur	ARD4_Quercus15	49.73832	05.66935	381	KOH	1	-27.9	29.1
Quercus robur	ARD4_Quercus15	49.73832	05.66935	381	KOH	2	-27.5	30.2
Quercus robur	ARD4_Quercus15	49.73832	05.66935	381	KOH	3	-27.5	29.8
Quercus robur	ARD4_Quercus15	49.73832	05.66935	381	NaClO	1	-26.9	30.3
Quercus robur	ARD4_Quercus15	49.73832	05.66935	381	NaClO	2	-27.1	30.7
Quercus robur	ARD4_Quercus15	49.73832	05.66935	381	NaClO	3	-27.1	30.5
Quercus robur	ARD4_Quercus15	49.73832	05.66935	381	raw	1	-27.3	29.5
Quercus robur	ARD4_Quercus15	49.73832	05.66935	381	raw	2	-27.2	29.1
Quercus robur	ARD4_Quercus15	49.73832	05.66935	381	raw	3	-27.4	29.2
Quercus robur	ARD4_Quercus6	50.06114	04.75692	242	*all*	1	-30.0	17.6
Quercus robur	ARD4_Quercus6	50.06114	04.75692	242	*all*	2	-30.2	17.6
Quercus robur	ARD4_Quercus6	50.06114	04.75692	242	*all*	3	-30.2	17.5
Quercus robur	ARD4_Quercus6	50.06114	04.75692	242	H_2SO_4	1	-29.0	23.3
Quercus robur	ARD4_Quercus6	50.06114	04.75692	242	H_2SO_4	2	-28.7	22.9
Quercus robur	ARD4_Quercus6	50.06114	04.75692	242	H_2SO_4	3	-28.4	22.7
Quercus robur	ARD4_Quercus6	50.06114	04.75692	242	KOH	1	-29.0	25.2
Quercus robur	ARD4_Quercus6	50.06114	04.75692	242	KOH	2	-27.4	27.7
Quercus robur	ARD4_Quercus6	50.06114	04.75692	242	KOH	3	-28.7	25.6
Quercus robur	ARD4_Quercus6	50.06114	04.75692	242	NaClO	1	-26.9	28.4
Quercus robur	ARD4_Quercus6	50.06114	04.75692	242	NaClO	2	-27.4	28.1
Quercus robur	ARD4_Quercus6	50.06114	04.75692	242	NaClO	3	-26.9	29.2
Quercus robur	ARD4_Quercus6	50.06114	04.75692	242	raw	1	-27.0	27.5
Quercus robur	ARD4_Quercus6	50.06114	04.75692	242	raw	2	-26.7	27.8
Quercus robur	ARD4_Quercus6	50.06114	04.75692	242	raw	3	-27.2	27.8

A.2 List of publications

A.2.1 Journal articles

C. Müller, J. Hennig, F. Riedel, G. Helle (2020). Quantifying the impact of chemicals on stable carbon and oxygen isotope values of raw pollen. *Journal of Quaternary Science* (under review)

C. Müller, M. Hethke, F. Riedel, G. Helle (2020). Inter- and intra-tree variability of carbon and oxygen stable isotope ratios of modern pollen from nine European tree species. *PLoS ONE* 15(6): e0234315. https://doi.org/10.1371/journal.pone.0234315

C. Müller (2017). Bi-decadal climate reconstruction derived from a 1200-year long pollen record from the NE Qinghai-Tibet Plateau and its implications for discussion of the late Holocene environmental dynamics. *Quarternary International* 444: 1-10. https://doi.org/10.1016/j.quaint.2017.05.058

G. Stauch, P. Schulte, A. Ramisch, K. Hartmann, D. Hülle, G. Lockot, B. Diekmann, V. Nottebaum, **C. Müller**, B. Wünnemann, D. Yan, F. Lehmkuhl (2017). Landscape and climate on the northern Tibetan Plateau during the late Quaternary. *Geomorphology* 286: 78-92. https://doi.org/10.1016/j.geomorph.2017.03.008

C. Müller and H. Kürschner (2014). Phytosociological and palynological studies of alpine steppe communities on the northern Tibetan Plateau, Qinghai Province, China. *Feddes Repertorium* 124: 122-138. https://doi.org/10.1002/fedr.201400006

A.2.2 Abstracts for conference presentations

C. Müller, F. Riedel, G. Helle: "Inter- and intra-tree variability of carbon and oxygen stable isotope ratios of modern pollen from nine European tree species" - EGU Conference, Vienna. 03.-08. May, 2020

C. Müller, P. Tarasov, B. Wünnemann, F. Riedel: "High-resolution climate reconstruction derived from a 1200-year long pollen record from the NE Qinghai Tibetan Plateau and its implications for discussion of the late Holocene environmental dynamics." - INQUA Conference, Nagoya. 26. July – 02. August, 2015

A.3 Curriculum Vitae

Due to data protection regulations, the curriculum vitae is not included in the online version of this doctoral thesis.

A.4 Declaration

I hereby certify that this doctoral thesis is written and composed by myself without using sources other than indicated in the text and reference list. This work has not been previously submitted to the Freie Universität or elsewhere.

Carolina Müller Berlin, June 2020